

NEW METHODOLOGY FOR MEASURING SEMANTIC FUNCTIONAL SIMILARITY BASED ON BIDIRECTIONAL INTEGRATION

By

Jong Cheol Jeong

Submitted to the graduate degree program in Bioengineering and the Graduate Faculty of the University of Kansas in partial fulfillment of the requirements for the degree of Doctor of Philosophy.

Chairperson Bo Luo

Co-chairperson Xue-wen Chen

Arvin Agah

Jerzy Grzymala-Busse

Jun Huan

Wonpil Im

Date Defended: April 12, 2013

The Dissertation Committee for Jong Cheol Jeong
certifies that this is the approved version of the following dissertation:

**NEW METHODOLOGY FOR MEASURING
SEMANTIC FUNCTIONAL SIMILARITY BASED
ON BIDIRECTIONAL INTEGRATION**

Chairperson Bo Luo

Co-chairperson Xue-wen Chen

Date approved: April 12, 2013

Abstract

1.2 billion users in facebook, 17 million articles in Wikipedia, and 190 million tweets per day have demanded significant increase of information processing through Internet in recent years. Similarly life sciences and bioinformatics also have faced issues of processing *Big data* due to the explosion of publicly available genomic information resulted from the Human Genome Project (HGP) and the increasing usage of high throughput technology. HGP was completed in 2003 and resulted in identifying 20,000-25,000 genes in human DNA and determining the sequences of three billion human base pairs. The information requires huge amount of data storage and becomes difficult to process using on-hand database management tools or traditional data processing applications. This thesis introduces new method, Biological and Statistical Mean (BSM) score to calculate functional similarity between gene products (GPs) that can help to extract biologically relevant and statistically robust information from large-scale biomedical, genomic and proteomic data sources. BSM score is defined by 16 different scoring matrices derived from principles of multi-view learning in machine learning algorithm and five different databases including Gene Ontology, UniProt, SCOP, CATH, and KUPS. The proposed method also shows how diverse databases and principles in machine learning theory can be integrated into a simple scoring function, and how the simple concept can give significant impact on the studies in biomedical and human life sciences. The comprehensive evaluations and performance comparisons with other conventional methods show that BSM score clearly outperforms other methods in terms of sensitivity of clustering similarity functional groups and coverage of identifying related genes. As a part of potential applications handling large amount of diverse data sources in medical domain, this thesis introduces similarity-based drug target identification and disease networks using BSM scores. Application of BSM score is freely available through <http://www.ittc.ku.edu/chenlab/goal/>

Acknowledgement

I would like to gratefully and sincerely thank my advisor, Professor Xue-wen Chen, for his effective guidance and encouragement that he has given me during my graduate studies at University of Kansas. I thank Prof. Arvin Agah and Jerzy Grzymala-Busse for spending their valuable times to review my dissertation and give great advices. I also appreciate Dr. Bo Luo to help me figuring out the issues during the preparation of my defense. I thank Prof. Jun Huan. He has always given valuable advices whenever I asked him, and no matter what they are. I also thank Prof. Wonpil Im who has helped me opening my eyes in new exciting research area and given excellent advices on finding my new career.

I would especially like to thank my parents, Jaewook Jeong and Sungim Lee. Without their unconditional love and support for my entire life, nothing has been possible. I also appreciate the patience and love from my families including Haeyoung Jeong, Haeja Jeong, and my nephews and nieces.

I also thank my father and mother in law, Jaeyoung Kim and Bokja Yang and brother and sister in law, Jongchang Kim, Eunok Kim, and Eunkyung Kim.

Most importantly, I truly give my deepest thanks to my wife Eunmi Kim. During this journey, her support, encouragement, patience and eternal love and devotion are the actual source of my endeavor and endurance. I know it is not enough just say thank to her, but I do know that she understands what I am thinking and what I really want to say to her as she always did.

I thank my two sons, Jayden Geonu Jeong and Joshua Myeongu Jeong although they may need several more years to read what I have written in this page. They are the source of my happiness and the most glorious and precious gift in my life. They make me laugh all the times.

Finally, I appreciate my brother Jongdae Jeong who had been waiting for long time to hear the success of my PhD defense. Although we cannot talk and see each other anymore, I know he must be happy at the beyond the sky and keep watching me with smile.

A portion of this work was supported by the US National Science Foundation Award (IIS-0644366). The opinions, findings, or conclusions in this report are those of the authors and do not necessarily reflect the views of the National Science Foundation.

TABLE OF CONTENTS

1	Introduction.....	1
1.1	Motivation.....	1
2	Background studies.....	5
2.1	Introductions on functional similarity	5
2.1.1	Referring GO graph vs. experimental data	5
2.1.2	Weight sources	6
2.1.3	Node vs. Edge based methods.....	7
2.1.4	Similarity from a pair vs. a group.....	8
2.2	Current issues.....	10
2.3	Conventional methods	26
3	Methodology	31
3.1	Principals of proposed method	31
3.2	Biological and statistical mean score	33
3.2.1	The reference score, R_{scr}.....	35
3.2.2	The graph-based score, G_{scr}.....	38
3.2.3	Calculating the similarity between Gene Products.....	40
3.2.4	Theoretical relevance of R_{scr}.....	43
4	Experiments and results.....	56
4.1	Experiment I: measuring functional correlation	56
4.1.1	Dataset.....	56
4.1.2	Similarity measurements.....	56
4.1.3	Results	59
4.2	Experiment II: measuring clustering performances	66
4.2.1	Dataset.....	66
4.2.2	Results	67
4.3	Experiment III: identifying new disease related genes	94
4.3.1	Dataset.....	94
4.3.2	Results	94
4.4	Experiment IV: drawing disease network.....	103
4.4.1	Dataset.....	103
4.4.2	Results	103

5 Gene Ontology Analysis Layer (GOAL)	109
5.1 Introduction	109
5.2 Input	112
5.3 Output	112
5.4 Submenus	113
6 Conclusion and future works	115
Supplementary materials	117
[S-1] Statistics of root shared GO terms and GPs	117
[S-2] GPs containing root shared GO terms I.....	120
[S-3] GPs containing root shared GO terms II.....	141
[S-4] PPI pairs having root-shared GOterms	143
[S-5] GPs containing root shared GO terms III.....	144
[S-6] PPI pairs having root-shared GO terms.....	148
[S-7] Statistical significance of BSM score.....	149
[S-8] SCOP domains used in experiments	157
[S-9] 25 species used for creating phylogenetic profiles.....	209
[S-10] Analysis on domain clusters	210
[S-11] OMIM dataset.....	227
References	241

LIST OF FIGURES

Figure 2.1 Number of annotated GPs along with the time line of released versions.	13
Figure 2.2 Number of annotated GPs with five model organisms.	14
Figure 2.3 Difference in the number of annotated GPs	15
Figure 2.4 GO term associations toward GPs.....	18
Figure 2.5 Statistics of GO terms in GO categories based on the released dates.	23
Figure 2.6 Distributions of GO term and leaf nodes at different depth levels.	24
Figure 3.1 Visualization of variables in G_{scr}	34
Figure 3.2 Visualization of a score matrix and its similarity equation.....	38
Figure 3.3 Tendencies of G_{scr}	39
Figure 3.4 Visualization of calculating similarity of GPs.	41
Figure 3.5 Visualization of proposed method.	42
Figure 3.6 Heat map of 16 score matrices.	44
Figure 3.7 The visualization of correlation coefficient derived from score matrices within CATH.	47
Figure 3.8 The visualization of correlation coefficient derived from score matrices within SCOP	47
Figure 3.9 The visualization of correlation coefficient between CATH and SCOP.....	49
Figure 3.10 Relative occurrences of GO term with original accumulated array.	50
Figure 3.11 Relative occurrences of GO term with PPI-based accumulated array.....	51
Figure 3.12 Relative occurrences of GO term with binary array.....	53
Figure 4.1 The tendency of domain similarity among three categories.....	60
Figure 4.2 Correlation measurements based on BSM score.	63
Figure 4.3 Correlation measurements with Ye and Schlicker's method.	64

Figure 4.4 Correlation measurements with Resnik and Lin's method.	64
Figure 4.5 Correlation measurements with Gentleman and Jiang's method.....	65
Figure 4.6 Comparing precisions among clusters.....	68
Figure 4.7 Comparing false clusters.	69
Figure 4.8 Comparing number of clusters.....	70
Figure 4.9 Analysis of statistical distributions.	72
Figure 4.10 Analysis of statistical distributions.....	73
Figure 4.11 Analysis of statistical distributions.	74
Figure 4.12 Tendency of clusters upon nodes and edges.	75
Figure 4.13 Tendency of clusters upon clusters and highest false class family clusters.	76
Figure 4.14 Tendency of clusters upon highest false super family clusters and family clusters..	77
Figure 4.15 Tendency of precision upon class family and super family.	78
Figure 4.16 Tendency of precision upon family and of coverage upon class family.	79
Figure 4.17 Tendency of coverage upon super family and family.....	80
Figure 4.18 Distributions of score in mixed clusters.	81
Figure 4.19 Analysis of mixed families of FA:47241, FA:54293, and FA:56301.....	84
Figure 4.20 Analysis of mixed families of FA:50514 and FA:52744.....	85
Figure 4.21 Analysis of mixed families of FA:52130 and FA:54002.....	86
Figure 4.22 Analysis of mixed families of FA:159031, 55000, 52081, 52314, 54576, and 50105.	87
Figure 4.23 Analysis of mixed families of FA:89743 and FA:110671.....	88
Figure 4.24 Analysis of mixed families of FA:51070 and FA:53057.....	89
Figure 4.25 Analysis of mixed families of FA:64311 and FA:69044.....	90
Figure 4.26 Analysis of mixed families of FA:48246 and FA:48440.....	91
Figure 4.27 Analysis of mixed families of FA:69560 and FA:117688.....	92

Figure 4.28 OMIM network generated by different methods.	95
Figure 4.29 New disease related genes identified by BSM score.....	100
Figure 4.30 Disease Similarity Network created by BSM score.....	104
Figure 5.1 GOAL schematic diagram.	114

LIST OF TABLES

Table 3.1 Comparing scores and biological significance of GO pairs	55
Table 4.1 Disease-related genes identified by BSM score.....	97
Table 4.2 Disease-related genes identified by conventional methods.	98
Table 5.1 Comparing GOAL and other existing services.....	110

LIST OF EQUATIONS

(Equation 2-1).....	26
(Equation 2-2).....	26
(Equation 2-3).....	27
(Equation 2-4).....	27
(Equation 2-5).....	28
(Equation 2-6).....	29
(Equation 2-7).....	29
(Equation 2-8).....	30
(Equation 3-1).....	33
(Equation 3-2).....	38
(Equation 3-3).....	38
(Equation 3-4).....	40
(Equation 3-5).....	46
(Equation 4-1).....	57
(Equation 4-2).....	66

1 Introduction

1.1 Motivation

Measuring similarities among genes and gene products (GPs) are neither a new nor special issue in current genomics and proteomics anymore, but this issue could be the one of the issues having longest history in modern computational biology or bioinformatics. Indeed, this issue is continuously evolved in different manners and to give motivation to produce new technologies. For example, the technology of measuring sequence similarity is evolved from pair-wise sequence alignment [1-4] to multiple sequence alignment [5-13]. Methods for measuring secondary and higher structural similarity keeps evolving and improving their algorithms [14-22]. In spite of existing numerous technologies in similarity issue shown above, new aspect of measuring similarities are continuously introduced such as similarity in chemical structure [23-25] or in activity across cell lines [26-30]. By considering this phenomenon, a question naturally arises: “*what makes this issue getting important and having such immortal lifecycle in its evolution?*” The reasons should be varied from study to study, but the one of the most inevitable reasons would be the strong relation to making pipelines among diverse data sources. This has been particularly important after initiating and finishing the human genome project (HGP) and increasing usage of high throughput technology. HGP was completed in 2003 and resulted in identifying 20,000-25,000 genes in human DNA and determining the sequences of three billion human base pairs. The information requires huge amount of data storage and becomes difficult to process using on-hand database management tools or traditional data processing applications. This introduces many issues in diverse areas. For example, biologists

and medical scientists have been faced problems of retrieving relevant data that are required to conduct researches on their purpose such that identifying new discovery is not trivial question any more due do requiring exploring huge amount of data and big scales of data which make difficult to manual analysis (e.g. identifying functional modules from microarray data). Another importance can be found in relations of treating disease or more precisely, designing new drugs or making drugs safer by identifying the relationships of molecular mechanisms or functions in cellular life [26, 31-40]. In fact, reports show that developing a new drug requires average of \$800 million and 12 years [41-43] and the drug approvals from Biotech industry are about 45% and 95% of failures are from phase III [44]. Studies on deceased subjects showed that 3.5% of subjects were suspected to have died from fatal adverse drug reactions (ADRs) [45] and more than 7% of patients are suffered from adverse drug reactions [46]. Indeed, the percentage of patients who suffers from ADRs is significantly increased up to 33% with elderly patients [47]. This implies that adverse drug reactions and delay of clinical trials are often caused by the insufficient information about characteristics of proteins or their interactions; therefore, if successfully controlled drug targets or proteins having enriched information obtained from real clinical trials are identified as functional neighbors of unknown or newly discovered disease related genes or GPs in a specific level, both the risk of ADRs and the cost of developing new treatments should be significantly reduced. Although modern sequence similarity-based methods have devoted for improving identification of biomarkers for diagnosis, disease activity assessment or prognosis [48-50], studies show that their devotion toward actual drug discovery is very disappointing [39, 40, 51, 52] due to the lack of relations between drug targets and biological validations and leads bottle neck problem in drug validation [38, 39, 53]. To narrow down the gaps between identified novel drug targets and their validations, alternative approaches

are emerged for helping the discovery of new types of drug targets such that instead of discovering breakthrough drug targets, the ones similar to the well known targets are identified, so that the risk of failure on target/drug validation can be reduced by recycling the information derived from previous information gathered from clinical trials [26, 54-57]. As a consequence of these efforts, studies measuring functional relations among potential drug targets are of interest since defining closeness between proteins can be directly used for identifying and validating the drug targets by comparing the known functions of targets instead of implied from homology-based methods derived from sequence or structure similarity. In other words, this type of approach compares real factors proved by actual experiments including wet-laboratory works but not predictions. Recently more direct approach measuring functional similarity among genes and their products are introduced by using GO graph structure and/or information content (IC) of GO aspect [58-76]. GO [77] is a dictionary of biological terms describing molecular function, biological process and cellular component of gene with controlled vocabulary. Although adequateness and limitations of GO terms are somewhat controversial [78], there are several reasons that the issues of GO-based functional similarity is considered to be more important than other methods. First, GO functional terms are defined by several sources including wet-laboratory works; therefore, by using GO annotation implies integrating multiple data sources and gives more sophisticated and specified information about the relations on protein functions. Second, the multiple data sources can be purified by controlling the hierachal relations of terms and the evidence of providing functions known as GO evidence code. Third, compared to Enzyme Commission (EC) number, GO provides a unique and most advanced form of a bridge between different biological communities by providing system level interpretations of biological data. Finally, GO database itself provides both data repository of genes and GPs and

attributes across species and databases, so this makes easy to integrate and get the information of genes and GPs from wide range of data sources. These unique and outstanding features/roles of GO itself and increasing demands on development of new tools to make connections between identifying new drug targets and their validations have encouraged me to build a new method measuring functional similarity. Indeed, this study has found that conventional methods often neglect and makes pointless aims on their algorithms and evaluations. It often happens due to the lack of guidelines for developing and evaluating GO-based semantic similarity measurements, regardless of introducing new measurements. Therefore, this paper introduces new semantic functional similarity methods together with proposing novel guidelines on developing and evaluating GO-based methods. At the same time, this study also shows that the proposed method defining functional similarity between genes or GPs can be easily extended to make pipelines used for exploring and retrieving information from diverse sources or existing networks.

2 Background studies

2.1 Introductions on functional similarity

Functional similarity methods can be briefly categorized into four different groups: i) present/absence of embedding GO graph, ii) the sources of the defining weights, iii) the location of weights (i.e, node/edge-based weights and calculating distance or similarity), and iv) the number of target terms (i.e, a pair of GO terms vs. a group of GO terms).

2.1.1 Referring GO graph vs. experimental data

Conventional methods for measuring functional similarity often use the topology of GO graph [63, 67, 74, 79] due to the simplicity of defining problems and broad support of GO functional annotations from wide range of existing databases. By limiting the scope of protein function inside domains of GO topology, this automatically narrows down the problems of measuring semantic similarity into defining the distance between GO terms appeared in GO graph. Indeed GO functional terms of GPs are widely supported by well known databases including UniProt [80] and EMBL [81]; therefore, by adapting GO, the given problems can be much simpler and conveniently reformulated. Compared to GO-based methods, some methods are referring external experimental data such as protein-protein interaction networks, microarray, and sequence or phylogenetic profiles to define similarities or differences of GPs in their own purposes: identifying functional modules [82-84], analyzing experimental results [68, 85-88] and predicting protein functions [30, 76, 89].

2.1.2 Weight sources

Methods for measuring GO-based semantic similarity can be grouped into three categories based on the source of defining their weight: the number of GPs associated with a GO term, the hierarchical relations of GO terms and integration of multiple sources. Resnik [90] defines the weight based on IC by considering the number of annotated GPs, and variations in this approach have been applied into several different methods including Lin [91] and Tao *et al.* [79] which normalized Resnik's score, Couto *et al.* [63, 64] which considered multiple ancestor nodes, Schlicker *et al.* [58, 59] which combined Resnik and Lin's method, and IntelliGO [66] which considered the weight of GO evidence code. Although IC-based weighting schemes are one of the most popular approaches to define functional similarity, the principle itself has inevitable defects on specific GO terms having no annotated GPs and/or the root node as their common ancestor. The details on these issues are discussed in the section of *current issues*. Besides these defects, biased [92] annotations and containing errors [93, 94] in GPs are also problematic although GO itself is systemically designed and more consistent among different released versions. Due to the systematic approach to build a graph structure and more conserved domains of GO terms compared to GPs, some methods are measuring the semantic functional similarity by using statistics of GO topology. Wu *et al.* [74] used the number of shared nodes existed in the path of two GO terms as the similarity score. simUI [95] defines GO similarity of two GO terms by using the ratio between shared nodes and total unique number of nodes in GO graph and can be considered as normalized version of Wu *et al.* Other studies integrating both approaches and external data sources have been studied as well. Lerman and Shakhnovich [62] and del Pozo *et al.* [65] defined the weight of edges based on the co-occurrence of domain between a pair of nodes from SCOP [96] and InterPro [97] respectively. Jiang and Conrath [98]

defined the weight of an edge by integrating its depth and local density and the difference of IC between parent and child nodes. XOA [72, 99, 100] compares similarity scores calculated by multiple methods including Resnik, Jiang, Lin and Bodenreider's method and takes the maximum similarity among them.

2.1.3 Node vs. Edge based methods

The topology of GO requires two critical elements, nodes and edges to get a final graph structure in which the nodes correspond to the GO terms and edges denote the links between child and parent nodes. Due to the graph structure of considered as a specialized characteristic in GO, methods are often focused on weighting either nodes or edges, and for convenience, it now is called node and edge based methods respectively. The principle of node-based method is that similar GO term pairs are likely to be correlated with their associations or expressions of annotated genes or GPs. Node-based methods often define GO similarity as the average weight of common ancestors of which two GO terms share their ancestor GO terms or the weight of the nearest common ancestor (NCA) which is one of the furthest common ancestor terms from the root node, so this type of method focuses on defining the weight of individual node. Resnik, Lin, Cuoto, simUI, Bodenreider and Schlicker's method can be grouped into node-based methods. Edge based methods define the weight of edges directly connecting two GO nodes. More precisely, this type of methods defined the weight of edges that connect child and parent nodes, so that the weight of edge can be directly used for defining similarity or used for calculating distance or similarity of two GO terms by exploring the path of two GO terms. The idea behind edge-based method is that the child nodes are more important than parent nodes due to the characteristics of hierarchical structure in GO (i.e, the lower terms which are far from the root node give more information than terms located close to root node since the deeper term describes

the more specific functions of GPs), so the edges closer to leaf nodes has higher weights than edges closer to the root node. simLP [95] defines similarity between two GO terms by measuring the depth of the longest shared path from the root node (GO:0003674, ‘molecular_function’). Ye *et al.* [101] and Pekar [102] introduced normalized version of simLP. RSS [75] defined similarity by combining relative depth and normalized common path coverage. Wang *et al.* [73] introduced propagated bottom-up weighting scheme to define the weight of edges such that a fixed initial weight of the edge between a leaf node and its direct parent is first defined. The weight of rest edges are calculated by multiplying the fixed initial weight to the weight of an edge associated with directly connected child node of the target edge, so the initial weight is propagated from the edge associated with the leaf node to all the way toward the root node. Some methods can be located in between as integrating both node and edge-based approaches. For example, IntelliGO [66] can be considered as extended version of simLP multiplied by a coefficient calculated from the number of annotated GPs.

2.1.4 Similarity from a pair vs. a group

Although the main stream of the methods in measuring functional similarity is focused on measuring semantic similarity based on GO, studies specially give more attentions on two distinct tasks: measuring semantic similarity for a pair of GO terms or GPs. Most of conventional methods are more focused on GO term similarity including the works from Resnik [90], Lin [91], Gentleman (i.e, simLP and simUI) [95], Ye [101], Jiang [98], Bodenreider [84], Schlikcer [59], and Wu [74]. This type of methods does not explicitly define the way to define GP similarity or tend to ignore similarity between GPs. This happens because these methods are often originated from different purposes like natural language processing (NLP) or information retrieval, so these methods are often biased toward solving problems in information theory rather

than the biological targets. Thus identifying functional modules and predicting protein functions in which the real problems are often required dealing with GPs are conventionally ignored. Compared to the methods emphasizing the similarity between GO terms, some methods are relatively more focusing on GP similarity. The simplest method measuring a pair of GP similarity is counting the number of GO term matches [29] or its normalized version [71]. Similarity scores averaged on all against all GO terms and their variations are also introduced [61, 66, 72, 99, 100, 103]. More sophisticate versions of matching score based on Hausdorff distance [104] and its variations is also applied [62, 65, 73, 79]. Some methods directly define GP similarity by identifying a most specific GO term pair having the minimum number of annotated GPs [67] or co-expressed microarray data [29, 87].

2.2 Current issues

So far it has been reviewed above, there is no single rule that can categorize one from another. On the other hand, this may imply that current methods are fully specified and diverse enough to be used for clinical trials or practical studies. However, in reality, conventional methods measuring functional similarity is rarely found in practical studies including drug design and its related studies. In fact, approaches using single experiment or dataset are often preferred such as microarray data or PPI networks rather than GO-based methods in which multiple experimental verifications are often required to annotate the functions of GPs. During the research on this topic, only few case studies of GO-based functional similarity measurement has been found: evaluating the similarity of GO or GP itself [105] and analyzing gene expression data [106]. This low usage of conventional methods implies two important criticisms about the method at current stage: i) the conventional methods are not mature enough to be applied yet, and ii) some points in overall design of current methods are not suitable or possibly misled in practical points of view. The first criticism may be too broad and unclear, so let's consider the following facts that the functional annotations of a protein are defined by multiple experiments or screenings. In other words, why the methods relying on the annotations identified with various experiments are considered less confidant or rarely used? One of the reasons can be found from their contradicted performances reported in various studies [61, 64, 68, 70, 87, 106, 107], so this unreliable performances make end users difficult to choose it or less confident on using conventional methods. Therefore, the meaning of ‘immature’ in the first critique can be redefined as insufficient general performances containing low quality and inconsistent performance of the existing methods. One of assumptions which cause this problem is the lack of guidelines of validation procedures since most evaluations are conducted with the task

independent general approaches; therefore although the validation or testing data are derived from various types of sources and problem domains such as functional predictions [79, 108], human interactive vision analysis [73], common cellular pathways [66, 103, 109], sharing functional domains [63, 64, 66], text mining [84] and sequence similarity [59, 69, 70, 72, 100], these approaches often require over simplified assumptions without clarifying biological relevancies. For example, majority of evaluations is conducted based on the assumption that sequence similarity and functional similarities are proportional. However, the studies showed that identifying the functional similarity between two GPs by using sequence similarity alone is not enough, and the relations between functional similarity and sequences similarities are not necessarily to be proportional but more likely to be correlated [62, 92, 93, 110-112]. By considering the fact that most conventional methods treat the problem of functional similarity without reflecting the ultimate goals or clarifying the definition in evaluation process, most validation methods are not suitable for revealing the task specific true powers. Therefore, through this study, I propose specific guidelines of evaluation process that increase the intuitive interpretation of similarity scores through comprehensive evaluation processes including comparisons of structure, phylogenetic profile and sequence similarity and biological/topological clusters. Although validation processes take important role to decide the performance of the GO-based functional similarity measurements, the fundamental theory consisting of methods would be more crucial to define their performance and biological relevancies. Some conventional methods often derive their theoretical background from natural language processing (NLP) without serious consideration of the differences. There are two distinct differences between biological processes and NLP. First the dictionary used in NLP is believed to be fully discovered and their relations are implicitly assumed to be finite and fully specified. Second,

documents in NLP are assumed to be completely known and time-invariant [113] while annotated GPs are highly biased and time variant. In contrast to NLP, my belief about the role of a gene or GP in cellular life is still accumulating and evolving, so even if GO exists, the terms and relations are neither finite nor fully specified. For example, the majority of methods employ the information content (IC) as their major distributor to define functional similarity [58, 59, 61, 63, 64, 66, 72, 79, 90, 91, 98-100] which is calculated by the ratio between the number of overall GPs and the number of GPs directly annotated by a specific GO term. However, IC itself can be highly biased due to the uncompleted genome and interest of studies toward specific species and genomes. To make matters worse, the biased data does not guarantee to reflect the true distribution of gene or GPs in nature; therefore, although IC-based method works well in NLP, it does not guarantee its promising performances in biological point of view. To check out the tendency of growing annotated GPs, all released versions of gene ontology database have downloaded through GO data repository (<http://archive.geneontology.org/>), and calculated the statistics of annotated GPs.

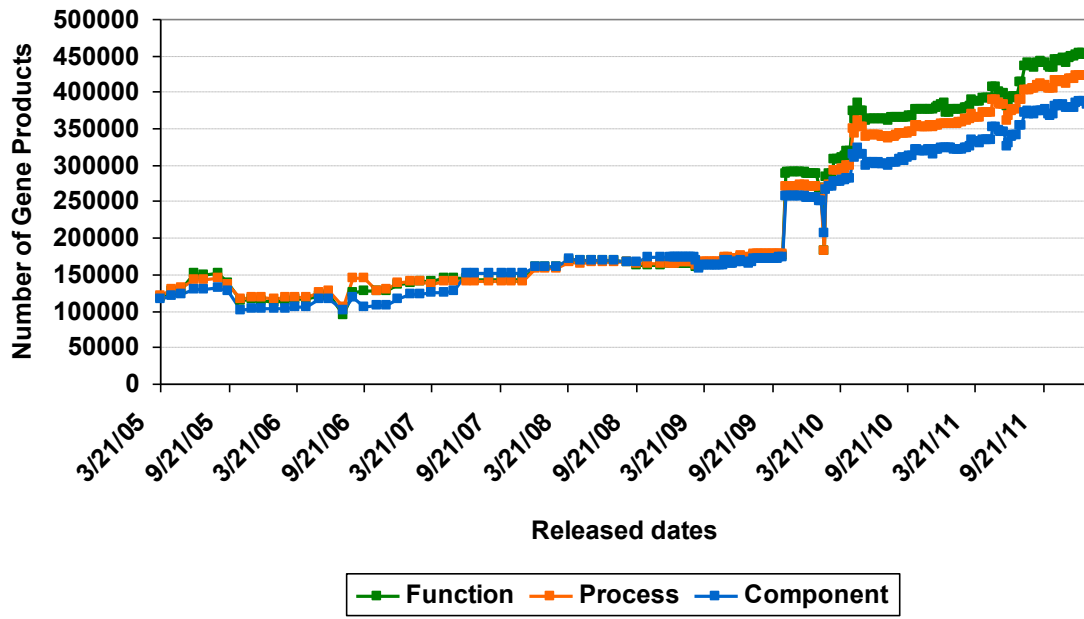


Figure 2.1 Number of annotated GPs along with the time line of released versions.

This graph shows the number of annotated GPs from March 2005 to January 2012.

Figure 2.1 shows an interesting point that even if by considering annotated GPs alone, the distributions of GPs belonging to timelines are varied widely. Indeed, by comparing Figure 2.1 and 2, the significant biased distributions in GPs are observed such that overall number of GPs in Figure 2.1 is dramatically increased at around September 2009 but Fly and Yeast do not show significant changes at this period. More interestingly, overall annotated GPs in Figure 2.1 are significantly decreased at around March 2010 but in Figure 2.2, Bacteria only have similar pattern observed in overall annotated GPs at Figure 2.1.

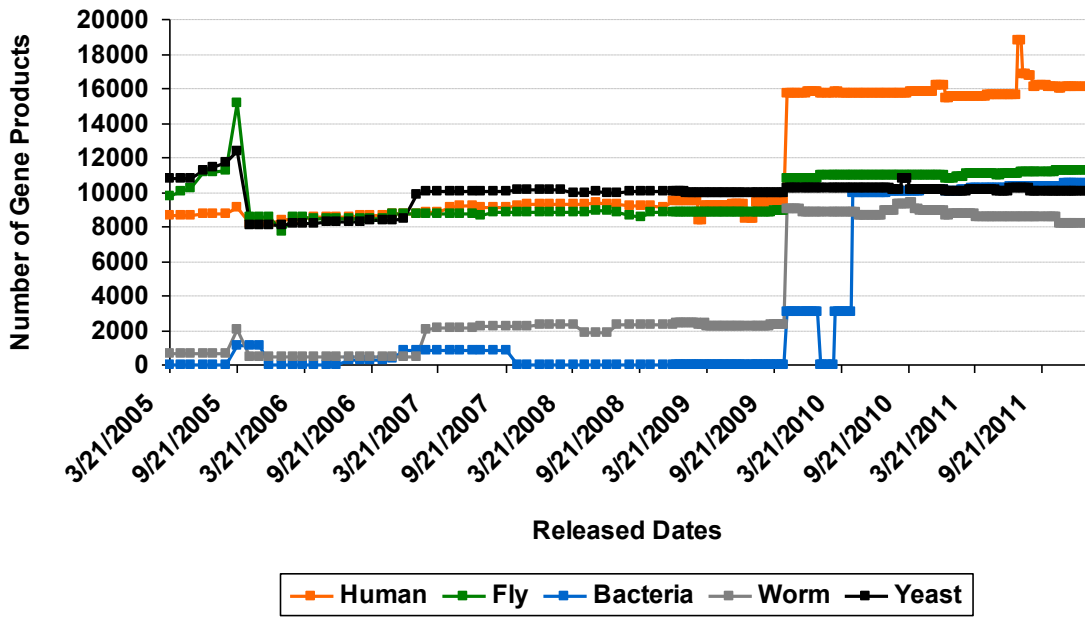


Figure 2.2 Number of annotated GPs with five model organisms.

The model organisms consist of seven species: *Homo sapiens* (Human), *Drosophila melanogaster* (Fruit fly), *Escherichia coli* (Bacteria), *Caenorhabditis briggsae* (Worm), *Caenorhabditis elegans* (Worm), *Saccharomyces cerevisiae* (Baker's yeast), and *Schizosaccharomyces pombe* (Fission yeast).

These biased and contradicted distributions of GPs shows that IC-based method is not suitable for defining the weight of individual node since the biased distributions are directly affecting the frequency of GO annotations which actually is the most critical information to define functional similarity in most cases. However, there is no such evidence that these biased distributions actually reflect the true nature of functional relations, especially by considering the gaps between the numbers of known sequences and annotated GPs which can be referred by Figure 2.3; therefore, the lack of biological connections between the results from biased IC and actual functional similarity increase the uncertainty of reflecting true nature of functional relations. Indeed, this fact also contradict the commonly used assumptions in NLP, documents are completely known and time-invariant [113].

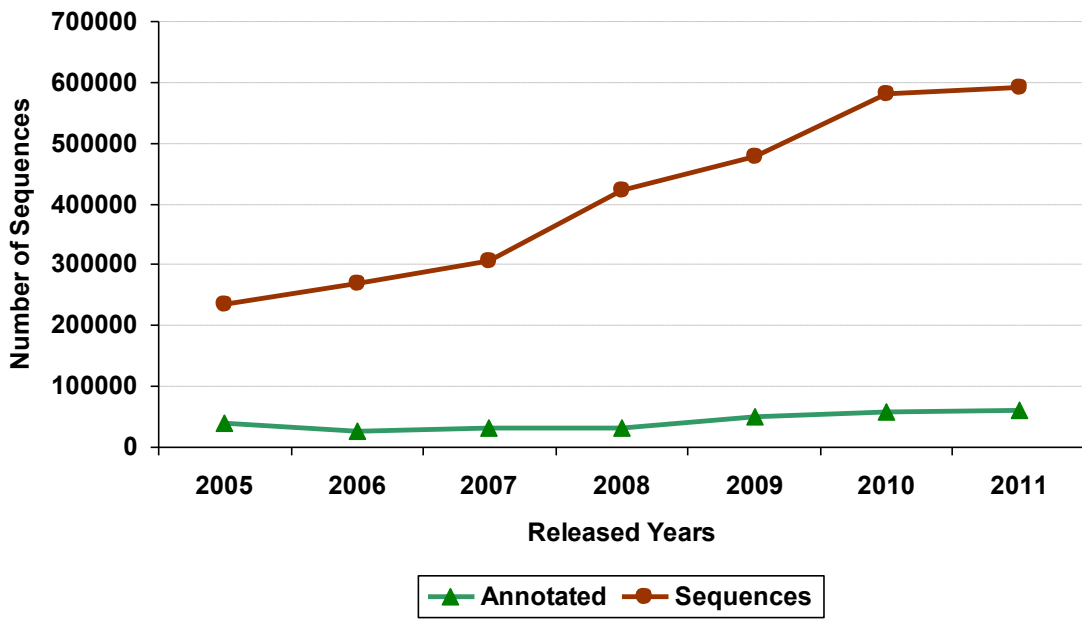


Figure 2.3 Difference in the number of annotated GPs

The five model organisms and known sequences are retrieved from SwissProt (<ftp://ftp.uniprot.org/pub/databases/uniprot/>)

Besides biological uncertainty of IC and time-variant characteristics of GO, two more problems should be considered when information theory is considered as significant contributor to define functional similarity: i) GPs with no annotation and ii) root shared GO terms. When this study started, GO database released at April 2011 was first used as the master database of this research. The database shows that total 9833 functional GO terms exist, and among them 820 GO terms are obsolete, so 9013 GO terms are actually used. Since most methods derived from information theory use IC as a part of their critical information to define functional similarity, it is interesting to see the distributions of GPs at individual GO terms. Surprisingly any related studies on this issue have not been found. Although most studies use IC as a part of critical scoring functions to define functional similarity, the fundamental sources of this score, (i.e. the distributions of GPs) have not been reported yet. Simple statistics shows that 2479 GO terms out of 9013 GO terms do

not have any associated GPs which is about 28% of total GO terms, so 6534 out of 9013 GO terms are actually meaningful terms in IC-based methods. 153 out of 2479 GO terms are not leaf nodes having at least a child node. These non-leaf nodes without any annotated GPs are corresponding to 6% of all GO terms having no annotated GPs. In other words, 28% of GO terms cannot calculate their functional similarity. This is a serious defect on IC-based methods but no study has been claimed on this issue. These GO terms with no annotated GPs give inevitable restrictions on related studies including but not limited in protein function predictions and identifying functional modules. This may be considered as minor problem in most cases since no annotation means that there is no existing reference data, so why GO terms having no GPs have to be considered? They do not exist, so there is no reason to calculate functional similarity for these terms. However, this is not true, since none existing annotation does not necessarily mean that there is no gene product exists, since the GO terms and annotated GPs are not simultaneously updated and reflected into the database, so these terms are still needed especially for discovering new functions of already annotated GPs. Therefore, the inability of calculating IC should be considered as the limitations of IC-based methods. Figure 2.4 shows another interesting point such that 3,679 GO terms are associated with less than 50 GPs which are 56% of entire meaningful GO terms (i.e. $6534 = 9,013 - 2,479$) depicted as a green diagonal bar. By considering less than five annotated GPs which are associated with a green diagonal bar, 26% of entire meaningful GO terms are falling into this range. In other words, more than half of GO terms control functional similarity with less than 50 GPs and majority of them are distributed to measuring functional similarity with less than five GPs. Is it enough to represent the nature of functional similarity with less than five GPs? As discussed previously, what if the biased distributions of GPs are considered together with this small sample issue? The uncertainty of the

relationship between IC and functional similarity must be increased significantly. The other critical problem in IC-based method can be found when the nearest common ancestors (NCA) are considered together [59, 79, 90, 91]. A *shadow problem* is one of the typical issues caused in conventional methods such that the specificity (i.e, how specific they are – the GO terms located in lower/deeper graph is considered to have more specific information about the function of a GP) of individual GO terms is not contributed to the calculation of GO term similarity by ignoring the influence of terms located below the NCA [64, 91]. In contrast to shadow problem, a *shallow problem* is also reported as significant defects in Jiang [98] and Lin's [91] method. For example, if two sets of GO term pairs having same depth are considered, it is possible that a pair of which the NCA is located near the root node has higher similarity score than the other pair of which the NCA of this pair is located far away from the root node due to the biased distributions of annotated GPs [73, 87] although based on human perspectives, NCA located near the root of the ontology (more general term) should be more significantly penalized than the pair with NCA located far away from the root of the ontology (more specific term).

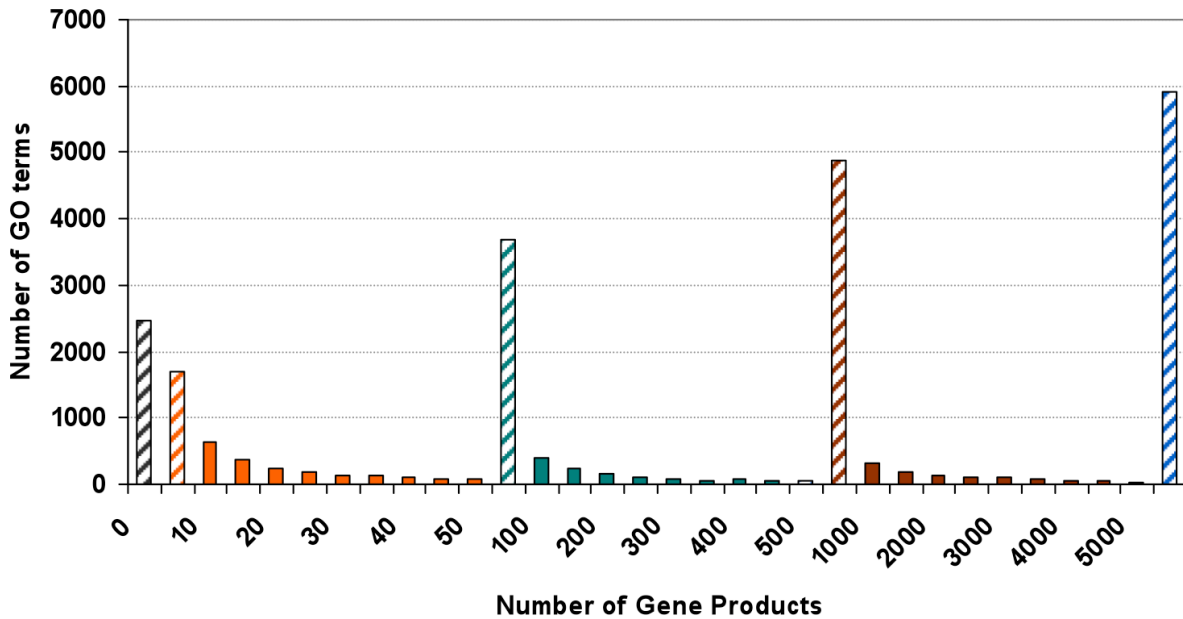


Figure 2.4 GO term associations toward GPs.

Bars with diagonal lines show the number of accumulated gene product. 5927/5000 denotes that there are 5927 GO terms which have less than 5000 annotated GPs. Bars having solid colors show the corresponding number of GO terms based on the given range of GPs. GO terms with no annotation (2479/0) are excluded from other statistics in this graph (i.e. they are not accumulated to calculate bars with diagonal stripes).

Besides these known problems, more general and critical problems of IC-based methods are also found such that IC is calculated by the ratio between the number of overall GPs and the number of GPs annotated by a specific GO term; therefore, if the nearest common ancestor (NCA) is considered, the functional similarity of two GO terms having NCA with root node always has nil similarity which means there is no functional similarity between two GO terms. By considering 9,013 GO terms, all possible pairs among them are 40,621,591 pairs, and all possible pairs have been searched to find their NCAs by identifying the common paths through cluster machine with 264 nodes for 12 days and the results show that 20,986,023 pairs which are 52% of all possible

GO pairs have their NCA as a root node. This result shows that methods derived from IC and NCA-based methods cannot distinct the differences of GO terms or can mislead the results for more than half of all possible GO term pairs. Indeed, these pairs with nil similarity are highly problematic since they lead biologically irrelevant statistical point of view by treating all root-shared pairs as having same similarity or distance. In other words, more than half of GO-term pairs are treated as exactly same. Therefore, consequently, these equally scored root-shared terms are propagated toward measuring the functional similarity/distance between two GPs as proportionally penalizing the similarity score based on the number of nil GO similarity pairs in two GPs. However, just by considering a simple well known biological fact of fusion genes in which two different genes having different functions can develop new functions, nil similarity of root shared GO terms biologically does not make any sense. To check out the biological relevance of using IC and NCA-based method, protein-protein interaction (PPI) pairs associated with root shared GO terms are investigated from KUPS, the PPI database which contains manually curated PPIs retrieved from IntAct, MINT, and HPRD [114]. To enforce the significance of contributing root-shared terms toward PPIs, individual GPs containing a pair of root-shared GO term pairs are randomly retrieved. Once GPs annotated with at least a pair of root-shared GO terms are retrieved, the relationships of nominated GPs are figured out through PPI networks in KUPS. This ensures that root-shared same GO annotation pairs associated with retrieved PPIs are significantly contributed toward triggering protein bindings. Some of findings from these retrieved GPs are of interest. For example, ribonuclease III activity (GO:0004525) and metal ion binding (GO:0046872) are shared by root-node molecular function (GO:0003674) and retrieves all 53 GPs from UniProt which contain both GO:0004525 and GO0046872). These GPs are all associated with ‘dicer-like endoribonuclease’ proteins which cleave the

phosphodiester bond within a polynucleotide chain and lead double-stranded RNA (dsRNA) and pre-microRNA (miRNA) into short double-stranded RNA fragments called small interfering RNA (siRNA). As expected from their names, these enzymes share EC 3.1.26.- which corresponds to ‘ribonuclease’. Indeed, they also share a cofactor which is ‘magnesium or manganese’. By considering the significant functional similarity and large amount of retrieved GPs, it is stunning that the root-shared GO term GO:0004525 and GO:0046872 are only terms shared by 53 GPs consisted with 516 GO terms. In short, co-occurrence of GO terms, GO:0004525 and GO:0046872, should not be neglected or equally treated with other root-shared terms since ribonuclease III activity (GO:0004525) and metal ion binding (GO:0046872) are necessary GO terms which describe the functions and cofactors of the groups of nominated GPs. Indeed, they are the only GO terms shared by all retrieved GPs which are all dicer-like endoribonuclease and have same or similar biological functions together with cofactors. Therefore, IC and NCA-based methods which always treat root-shared GO terms equally are not suitable to identify groups of GPs having strong agreement on root-shared GO terms. For more details about statistics of root-shared GO terms, biological functions, cofactors and others please refer supplement material [S-1,2]. The second example is more interesting such that ribose phosphate diphosphokinase activity (GO:0004749) and Identical protein binding (GO:0042802) are root-shared GO terms commonly found in four ribose-phosphate pyrophosphokinase proteins and a phosphoribosyl pyrophosphate synthase-associated protein. Similar to the previous example, these GPs share EC 2.7.6.1 except Phosphoribosyl pyrophosphate synthase-associated protein (Q14558). As shown in protein names and EC, their biological functions are same such that they are involved in nucleotide, histidine, and tryptophan biosynthesis and active in heteromultimeric complexes with other 5-phosphoribose 1-diphosphate synthesis. Q14558 plays

a negative regulatory role in 5-phosphoribose 1-diphosphate synthesis; therefore, all retrieved GPs are related with regulatory of 5-phosphoribose 1-diphosphate synthesis. In contrast to previous example, all retrieved GPs consist of PPI networks including isolated self-binding of Q14558. These functional similarity and binding affinity are also considered as important facts that root-shared GO terms should be carefully treated when GO or GP similarities are measured (for more details about biological functions, cofactors and others please refer supplement material [S-3,4]). The third example is even more interesting compared to previous two examples. In this example, instead of considering a pair of root-shared GO terms, triplet root-shared GO terms are considered. The fact that increasing the number of root-shared GO terms can increase the significance of GP similarity influenced by root-shared GO terms shows that equally treating or ignoring the root-shared GO terms in calculating GO or GP similarity is biologically not relevant. In this example, total four GPs are retrieved from UniProt of which each GP is annotated with three GO terms and others. Three GO terms, which is the triplet of root-shared GO terms associated with retrieved GPs, are GO:0004716, GO:0046982, and GO:0005524 which are ‘receptor signaling protein tyrosine kinase activity’, ‘Protein heterodimerization activity’, and ‘ATP binding’ respectively. Same as previous two examples, retrieved GPs share EC number and protein name which are 2.7.10.1 and ‘receptor tyrosine-protein kinase’ correspondingly. All pairs are root-shared relations except GO:0046982 and GO:000552 which is shared by ‘binding’ (GO:0005488) which is direct child of root term and often neglected by IC and NCA-based method as well. By considering the fact that all retrieved GPs are protein tyrosine kinase, they are part of several cell surface receptor complexes and need a coreceptor for ligand binding which activates several signaling cascades to trigger appropriate cellular responses. Besides sharing EC number, biological function and catalytic

activity, the similarity of quaternary structure, homo-and/or heterodimerization of EGFR, ERBB2, ERBB3 or ERBB4 and significant PPIs existing among retrieved GPs also shows that the root-shared triplet GO terms are essential for defining a group of biologically similar GPs (for more details about biological functions, cofactors and others please refer supplement material [S-5,6]). More statistics on root-shared GO terms and associated GPs and PPIs can be found in [S-1~6].

In contrast to node-based methods, edge based methods often take advantage on several issues especially when the topology of GO graph is applied rather than relying on annotated GPs: i) stabilized or completed GO terms which deliver positive impact to the assumptions of time-invariant and completeness of data, ii) relaxed conditions of GO terms associated with no annotated GPs and root-shared terms, and iii) reduced risk of biased sources. Figure 2.5 shows the changes of GO terms based on released versions. Compared to Figure 2.1, the graph is more stabilized although the terms associated with biological process are continuously increased. Indeed, edge-based methods often rely on GO term itself, so issues related to annotated GPs can be ignored. However, edge-based methods often assume that similarity of unit edges (i.e, between child and parent node) is same. In other words, relations between any pair of parent and child node have a same distribution or proportional to the depth of the node or edge, so no matter what GO terms are given, they would have exactly same similarity if they have same depth.

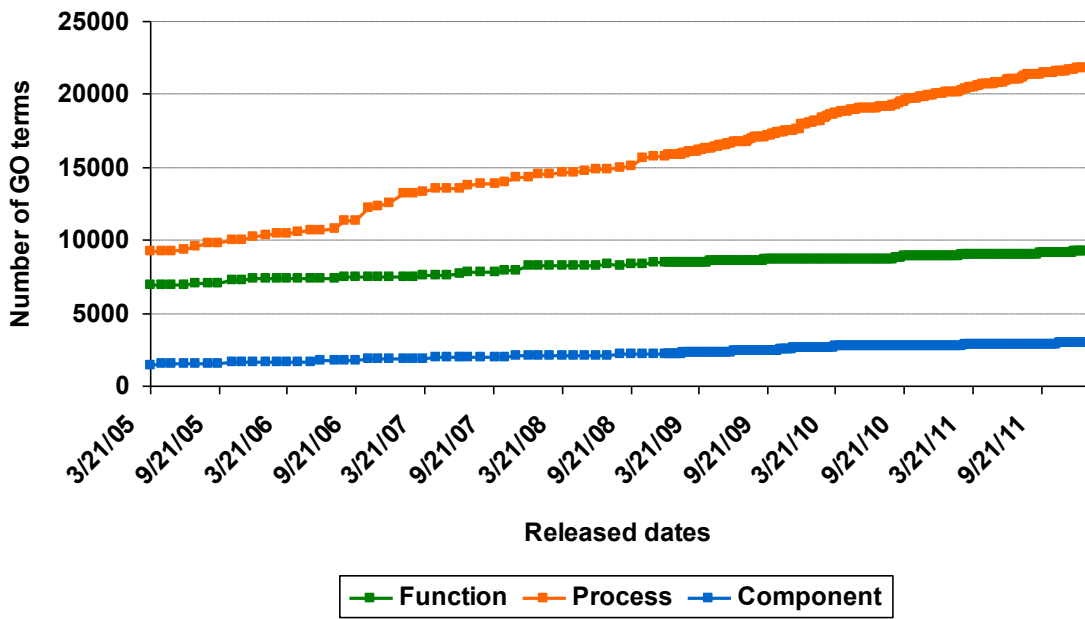


Figure 2.5 Statistics of GO terms in GO categories based on the released dates.

Function (green dots in the middle) denotes molecular function, Process (orange dots on the top) denotes biological process, and Component (blue dots at the bottom) denotes cellular component in gene ontology category.

However, this assumption ignores fidelity of cellular life in which some proteins or functions have distinct associations compared to others as having high specificity and low affinity of their relations [115-117]. Besides the fidelity, specificity of GO terms should be considered as well. Figure 2.6 shows the distributions of GO terms at each level or depth. In the context the depth and level of a GO term are treated to be same. Level 1 or depth 1 denotes the root node, the most general term. As the depth is getting deeper and the levels are getting higher by increasing the number, they are further away from the root node and have more specific information about the function of a GP. In the graph, each level consists of two different types of GO terms: leaf nodes and others. Leaf nodes are the most specific GO term of a current GO version, and others are less specific GO terms than leaf nodes.

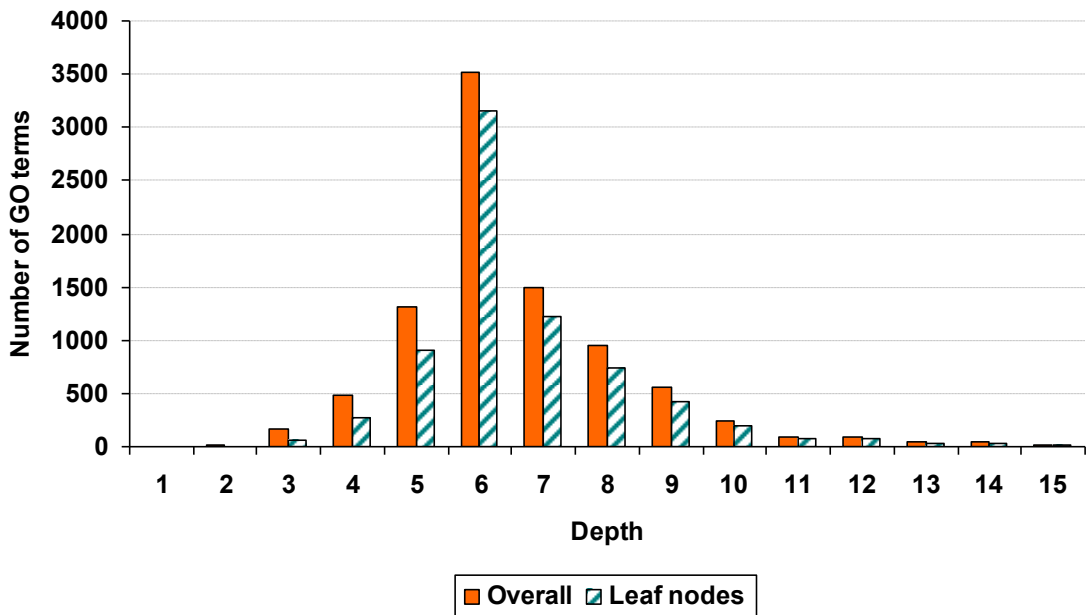


Figure 2.6 Distributions of GO term and leaf nodes at different depth levels.

The ‘overall’ denoted as orange bars consist of all GO terms which pass the corresponding depth (i.e., horizontal axis) to get their maximum depth (i.e., leaf node). Leaf nodes consist of GO terms having no child nodes. The overall statistics shows that more than 72% of GO terms consist of leaf nodes.

This shows that the depth of GO term is not enough to reflect the significance of information at the given GO term. For example, let us consider that the distance/depth between two GO term pairs are same, and one pair is from depth 6 but both of them are not the leaf node. In contrast to this pair, the other pair is from depth 6 but both of them are leaf nodes. Intuitively, the later case should receive higher similarity score if the specificity/detail of GO term is considered. In summary, there are several issues being considered to design methods of measuring GO-based functional similarity: i) biased distributions of annotated GPs, ii) complete and time-invariant assumptions of GPs, iii) shadow & shallow problem, iv) nil similarity on root-shared GO terms, v) validations upon lack of specific aims, vi) considering similarity score from GO terms having no annotated GPs and vii) the assumption of uniform distance between parent and child nodes.

Besides these critical issues, the range of the score also has to be considered. For example, non-normalized score in which the score is ranged from 0 to ∞ makes difficult to identify the significance of scores. So far it has been discussed that conventional methods have several pitfalls in their theoretical background and algorithms including intuitively and biologically irrelevant assumptions and validation methods. To overcome these pitfalls, new method to measure functional similarity based on gene ontology functional terms are proposed. The proposed method has several distinct features compared to conventional methods: i) having a broad definition of functional similarity by integrating biologically and statistically specified relations among GPs including co-occurrence in PPIs, structural similarity in functional modules, and geometrical distance in GO instead of focusing only on the relations of GO terms in GO graph, ii) reducing the noise effects caused by biased datasets, iii) evaluating the method with strictly designed procedure by considering both GO and GP similarity and iv) validating the methods with comprehensive datasets and biological and biomedical points of view. The details of proposed method can be found in method section.

2.3 Conventional methods

For the evaluation purposes, six conventional methods are compared to the proposed method. The brief introduction of each method is described below.

Resnik's [90] method uses Information Content (IC) of Nearest Common Ancestor (NCA), which is the closest node from leaf nodes or the farthest node from the root node shared by two GO terms, as the functional similarity of two GO terms. The final score is negative logarithm of the ratio between the number of annotated GPs corresponding to NCA of two GO terms, go_i and go_j , and total number of GPs associated with molecular function. The equation is defined by

$$\begin{aligned} simResnik(go_i, go_j) &= -\log(p(NCA)) \\ \text{where } p(NCA) &= \frac{\# \text{ of GPs associated with NCA of } go_i \text{ and } go_j}{\# \text{ of GPs associated with root node}} \end{aligned} \quad (\text{Equation 2-1})$$

The range of Resnik's similarity, $simResnik(\cdot)$ is a value greater than and equal to zero. Due to the unlimited range of maximum score, defining the relative significance of similarity score directly from the provided scoring scale is not trivial; therefore, the score is normalized between 0 and 1 by using maximum and minimum value of the observation. The equation of normalization is following

$$GO_{norm}(go_i, go_j) = \frac{GO_{sim}(go_i, go_j) - min(GO_{sim}(\cdot))}{max(GO_{sim}(\cdot)) - min(GO_{sim}(\cdot))} \quad (\text{Equation 2-2})$$

GO_{norm} denotes normalized GO term similarity for two GO terms, go_i and go_j . $GO_{sim}(\cdot)$ denotes all observed GO term similarity calculated by conventional methods. $GO_{sim}(go_i, go_j)$ calculates GO term similarity between go_i and go_j . In short, the given normalization function transforms

original value to relative values ranged from 0 to 1 which corresponds to the minimum and maximum value of all observed GO term similarity scores.

To overcome the difficulty of interpreting significance of GO term similarity resulted in non-normalized Resnik's score, Lin introduced normalized version of Resnik's method while avoiding the shadow problems also caused in Resnik's method [91]. The *shadow problem* is caused by directly using NCA-based scoring scheme. In Resnik's method, any pairs of GO term similarity can be same if their NCAs are the same. In other words, by focusing on NCA only, Resnik's method ignores the specificity or details of GO terms that can be interpreted as the distance between NCA and leaf nodes. The equation of Lin's method is defined below.

$$simLin(go_i, go_j) = \frac{2 \times \sum_{k=\text{root}}^{\text{NCA}} w_k}{\sum_{n=\text{root}}^{go_i} w_n + \sum_{m=\text{root}}^{go_j} w_m} \quad (\text{Equation 2-3})$$

In this equation the weight of each node is defined by IC similar to Resnik's method.

$$w = -\log(p(c))$$

$$\text{where } p(c) = \frac{\# \text{ of GPs associated with current GO term}}{\# \text{ of GPs associated with root node}} \quad (\text{Equation 2-4})$$

The equation shows that Lin's method can be defined as ratio between the summation of ICs belonging to the path from root node to NCA and the summation of ICs belonging to the path from root node to target nodes. Although the *shadow problem* can be avoided as considering both the specificity of NCA and leaf nodes, a new problem, *shallow problem* arises in this case. There are two factors which directly affect this problem: score scheme focusing on the ratios only and the biased distribution of annotated GPs. Ratio is not necessary to reflect true

specificity of GO terms since this only considers relative difference of two distances. Indeed, the annotated GPs are not necessarily to be evenly distributed to individual functional term. Therefore, these two factors can cause such situation that a pair of GO terms having both NCA and leaf nodes closer to root node has higher similarity score than a GO term pair having both NCA and leaf nodes far away from the root node.

Schlicker *et al.* [58, 59] introduced the combination of Resnik and Lin's method. The equation is defined by

$$simSchlicker(go_i, go_j) = \frac{2 \cdot \log p(NCA)}{\log p(go_i) + \log p(go_j)} \cdot (1 - p(NCA)) \quad (\text{Equation 2-5})$$

In the equation, $p(go_i)$ and $p(go_j)$ are the probability of two GO terms, go_i and go_j calculated by the number of annotated GPs, and $p(NCA)$ is the probability of their NCA. Therefore, the left and right term corresponds to Lin and Resnik's method respectively. This score is designed to be decreased when $p(NCA)$ is increased. In other words, the specificity of NCA defines the final GO similarity score by rewarding or penalizing the score made at NCA.

As an edge-based method, Jiang method [98] is also used for comparison. Jiang's method is different from others in two categories. First instead of focusing on nodes, Jiang's method uses weighted edges by using the density of parent terms in GO graph. Second this method calculates semantic distance rather than similarity by measuring distance of two GO terms based on the space of GO graph. The equation of this method is defined below.

$$diffJiang(go_i, go_j) = \sum_{i \in min[path(go_i, go_j)]} w_i$$

$$w_i = w(c, p)$$

$$= \left(\beta + (1 - \beta) \frac{\bar{E}}{E(p)} \right) \cdot \left(\frac{d(p) + 1}{d(p)} \right)^\alpha \cdot (IC(c) - IC(p)) \cdot T(c, p)$$

(Equation 2-6)

To make comprehensive comparisons, Gentleman's method [95] which is also known as simUI are also included in performance evaluation. In this equation, w_i denotes the weight of i^{th} edge which is one of edges connecting two GO terms go_i and go_j with shortest distance, $i \in min[path(go_i, go_j)]$. The weight of each edges is defined between a child node and its direct parent node, $w(c,p)$. $E(p)$ denotes the number of edges from a parent node to its direct child nodes, and for convenience, it now is called a density of parent node. \bar{E} denotes average density in entire GO graph. $d(p)$ denotes depth of parent node and $IC(c)$ and $IC(p)$ are the information content (IC) at child node and parent node respectively and can be calculated same as Resnik's method. $T(c,p)$ is a link relation factor (i.e. ‘is-a’ and ‘part-of’ relation) and set to 1 for all relations. α and β are parameters to control the significance between depth and density factors. The optimal value 0.5 and 0.3 suggested in original paper are used as the default value of α and β respectively. The range of Jiang's distance is greater and equal to zero, so the observed values are normalized by Equation 2-2. simUI uses the number of GO terms to calculate the similarity of GO terms instead of using IC based on the number of GPs. The equation is defined in Equation 2-7.

$$simUI(go_i, go_j) = \frac{2 \times |path(root, NCA)|}{|path(root, go_i) \cup path(root, go_j)|}$$

(Equation 2-7)

The similarity score is defined by ratio between the number of GO terms belonging to the path from root node to NCA $|path(root, NCA)|$ and the number of GO terms resulted in the union of all nodes belonging to the path from root node to each of GO terms, go_i and go_j , $|path(root, go_i) \cup path(root, go_j)|$. The equation looks similar to Lin's method. Indeed, due to the lack of considering GO term specificity, the *shallow problem* observed in Lin's method is also detected in Gentleman's method. The range of similarity score is between 0 and 1.

Ye's method [101] is also considered in the experiments. Compared to other conventional method this method more focuses on the specificity of GO terms by directly adapting the relative depth of NCA into its similarity function.

$$simYe(go_i, go_j) = \frac{depth(NCA) - min[depth(\cdot)]}{max[depth(\cdot)] - min[depth(\cdot)]} \quad (\text{Equation 2-8})$$

The final value of the Equation 2-8 is normalized depth of NCA, $depth(NCA)$ defined by two GO terms, go_i and go_j . The normalization is derived from maximum and minimum depth of entire functional GO terms in GO graph which corresponds to $\max[depth(\cdot)]$ and $\min[depth(\cdot)]$ respectively; therefore, the range of similarity score is between 0 and 1.

3 Methodology

3.1 Principals of proposed method

Biological and Statistical Mean (BSM) score is designed to integrate biological facts derived from protein domains and PPI networks and statistical significance derived from GO graph structure. To derive biologically relevant scores, two commonly believed biological facts are used: i) if GPs and genes share functional domains then they have similar functions and ii) interacting protein pairs tend to have similar function. To maximize the statistical significance of GO graph, two principals are derived from the hierarchical structure of GO term relations and information theory such that the score is intentionally designed to give higher score for GO terms located closer to leaf node or further away from root nodes, and the score is penalized for the terms have many siblings or edges between parent child nodes. The definition of functional similarity applied in the proposed method also can be explained as an integration of two different approaches toward identifying functional relations of GPs. Briefly speaking, conventional methods can be categorized into two groups either top-down or bottom-up approaches. However, both of them have intrinsic and reciprocal drawbacks. Top-down methods are favorable for evaluating or calculating GP similarity by directly analyzing the consequences of various genetic tests [29, 76, 87] or interactions between GPs [118]. These top-down approaches only consider direct consequences of an experiment or association observed from GPs having multiple functions. However, gathering data for targeted genes or GPs are neither always possible nor reliable due to limited amount of available sources and biased/inconsistent datasets [93, 110-112, 119]. Although some of top-down methods use the GO based scoring scheme [62, 65] before directly calculating the similarity of specific GPs, this type of method has two significant

drawbacks: i) it requires additional datasets, and it is not always possible to get relevant datasets for the given task ii) acquired dataset can be biased toward species and case histories; therefore, this can mislead and/or confuse the human interpretations toward relationships of functional terms (e.g. parent and child relations in GO term may not be observed or can be under/over estimated). In contrast to top-down approach, bottom-up approaches evaluate functional similarity by comparing predefined individual functions of GPs. Indeed, most of GO based methods are categorized into bottom-up approach, and this type of methods can bypass the pitfalls in top-down approach by referring multiple evidences projected into GO terms. However, biological relevance toward measuring GP similarity is somewhat questionable due to unrevealed relations of different functional branches in GO topology. In other words, GO itself does not define any functional priority or precedence among functional terms to bring the final consequences or reactions from sets of GO functional terms in a GP or a group of GPs; therefore, top-down and bottom-up approaches have reciprocal relations on their drawbacks and advantages. To get the advantages of both methods while minimizing drawbacks, a bidirectional method is proposed. The proposed method integrates both top-down and bottom-up approaches. To reduce and minimize the noise effects in top-down approach, the principles of multi view learning [120, 121] is applied by projecting independent observations into an integrated probabilistic distribution.

3.2 Biological and statistical mean score

The definition of functional similarity governed by the proposed method is from the consideration of biological relations identified from experimentally supported evidences and the topological similarity of GO terms referred from graphical structure of GO database. This new paradigm of functional similarity is refined and integrated in a new scoring function defined in the Equation 3-1. In the equation, GO_{sim} consists of two distinct terms: reference score R_{scr} and gene ontology graph-based score G_{scr} .

$$BSM_{sim}(t_1, t_2) = \alpha \cdot R_{scr} + \beta \cdot G_{scr}$$

$$= \alpha \cdot (M_{scr}(t_1, t_2)) + \beta \cdot \exp\left(-\frac{1}{1 - \frac{Ep}{E_{max}}}\right)^{\left(1 - \frac{d_{NCA}}{d_{max}}\right)}$$
(Equation 3-1)

The function GO_{sim} requires two parameters, t_1 and t_2 which are the pair of targeted gene ontology (GO) functional terms of which their semantic similarity is expected to be measured. R_{scr} and G_{scr} denote reference score. R_{scr} is derived from external data sources, and G_{scr} is derived from GO graph-based score in which the score is calculated from the topology of GO. α and β are real values by satisfying $\alpha+\beta=1$ to define a weight for reference and GO graph based score correspondingly. For the experiments equal contribution $\alpha=0.5$ and $\beta=0.5$ are used, so the contribution of R_{scr} and G_{scr} toward final functional similarity score is equal. As shown in Equation 3-1, R_{scr} is directly calculated from M_{scr} which is a score matrix derived from SCOP and CATH database. The details of creating score matrix, M_{scr} are described in following section. In contrast to R_{scr} , G_{scr} is consisting of four variables: d_{NCA} denotes the depth of NCA, and Ep denotes the number of edges between the parents of nearest common ancestor (NCA) of two GO

functional terms and their corresponding child nodes; therefore Ep can be easily calculated by counting the number of siblings of NCA. d_{max} and E_{max} are the maximum depth and number of edges in the given problem respectively. The values of these variables can be calculated from two different manners by considering either entire GO graph or local path only. To help better understanding the equations, variables used in the graph-based score are graphically visualized in Figure 3.1.

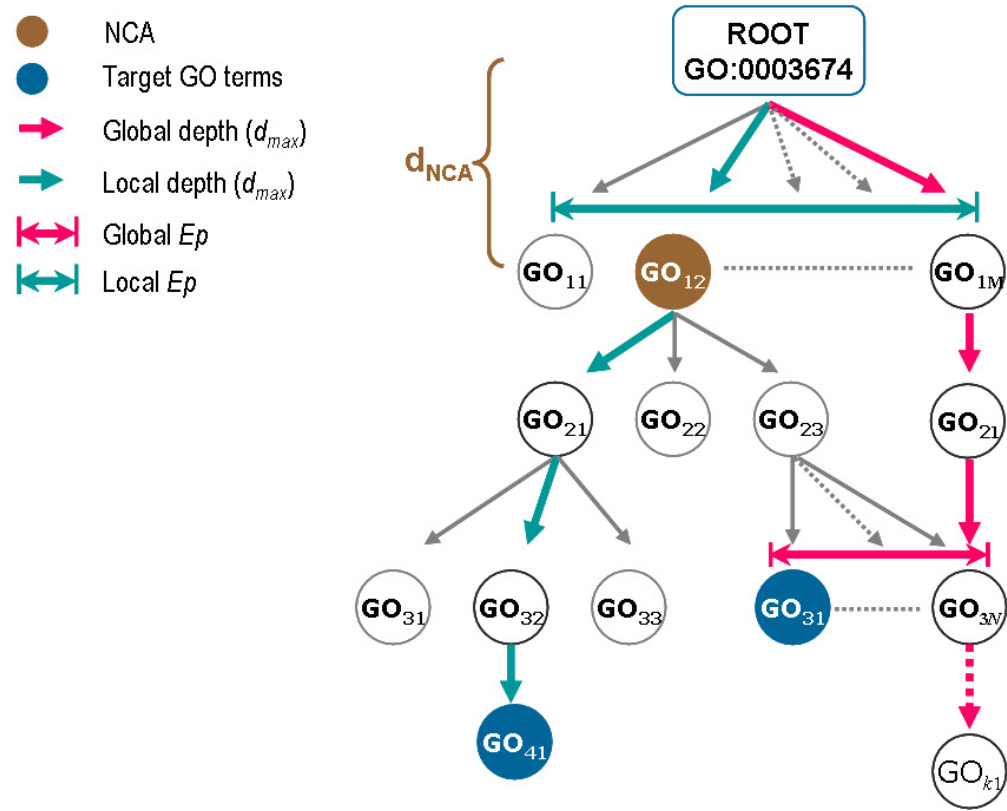


Figure 3.1 Visualization of variables in G_{scr} .

Global and local are defined as maximum values found by considering entire GO graph or local path toward target nodes respectively. In this graph, the first digit in GO index denotes the depth of a GO term and the second digit denotes the order of edges belonging to a parent node. For example, GO_{12} is nearest common ancestor of two target GO terms, GO_{41} and GO_{31} . This node is located at depth 1 and second child (i.e., next to GO_{11}) of ROOT node. In practice, there is no such an order, so this index is only used for counting total number of child nodes of the target node. With this example, the *global* $d_{max}=k$ and *local* $d_{max}=4$. By using same approach both *global* and *local* E_{max} and Ep are N and M respectively where $N > M$.

In short, the rationale of the given equation is that the score of GO functional similarity should reflect both affinity of biological interactions among GPs and systemic significance of functional relations, thus such scores can provide a standard tool for analyzing associations of GPs under functional similarities and associations. Consequently this method can help elucidating and translating the relations of cellular functions in high throughput way without human interaction. The details of each score term will be further described below together with more detailed principles and algorithms.

3.2.1 The reference score, R_{scr}

The reference score described here shows a general procedure to calculate R_{scr} from diverse databases, and it is not necessarily limited on specific databases. R_{scr} requires at least two different databases which contain information about functions of domains, genes or GPs since the principles of multi view learning show that a high consensus of independent hypotheses or observations results in a low generalization error [120, 121]. In order to meet specified requirements, two different protein structure classification databases, SCOP [122] and CATH [123] are considered as two independent views. Creating R_{scr} or more precisely M_{scr} in Equation 3-1 requires several steps of procedures.

Step one, downloading and parsing databases: SCOP 1.75 (<http://scop.mrc-lmb.cam.ac.uk/scop/parse/>) and CATH 3.4 (<http://release.cathdb.info/v3.4.0/>) are downloaded and then each database is parsed to extract required information. Domain and homologous super family are retrieved from SCOP and CATH respectively to extract a group of proteins having high conservation on evolutionary and functional relationships. From this

filtering step, 10,214 domains and 2,549 homologous super families are retrieved from SCOP and CATH respectively.

Step two, identifying associated proteins and mapping identification: R_{scr} is based on the assumption that closely related functions share the patterns of domains being present or absent on genes or GPs. Studies show that this assumption is biologically relevant. For example, Bodenreider *et al.* [84] used the same assumption to identify dependence relations among three different groups of GO, molecular function, cellular component, and biological process by projecting annotations from five different databases into a vector space, Yu *et al.* [76] annotated target genes by selecting GO terms associated with highly correlated reference genes with target gene in microarray data, and del Pozo *et al.* [65] defined GO similarity by using co-occurrence of GO terms upon the annotations of InterPro databases [124]. Once domains are retrieved upon this assumption, associated GPs are retrieved by referring PDB [125] names in each database. To get the annotations of PDB structure, the retrieved PDB IDs are mapped into UniProt [80] accession number.

Step three, generating score matrix (M_{scr}) from the occurrences of GO annotation by projecting them into multiple views: Annotations of proteins containing domains defined by SCOP and CATH are retrieved from UniProt. The occurrences of annotations are accumulated into the array of score matrix consisting with all domains and functional GO terms. The matrix filled with the occurrence of exact annotations is now called Original Direct Annotation (ODA). To make multiple views, diverse observations are applied. First, Hierarchical topology of GO database is applied such that an annotation is tagged in the score matrix then all ancestor nodes belonging to the target nodes (i.e. from the target node to root node) are also counted as current occurrences. This hierarchical annotation is called Original Hierarchical Annotation (OHA). To

generate more generalized view, protein-protein interaction (PPI) networks are considered. The applied PPIs are derived from KUPS [114] which is public databases consisting with manually curated PPIs derived from three PPI data bases, IntAct, MINT, and HPRD. Annotations of both target proteins associated with a domain and their direct PPIs are simultaneously tagged into a score matrix since it is well known that two proteins tend to have same function if they interact each other. This now is called PPI-based Direct Annotation (PDA). By using same approach creating OHA, PPI-based Hierarchical Annotation (PHA) is also produced by including direct interacting pairs in PPI network as current occurrences. Therefore, each protein structure classification database can produce four score matrix, ODA, OHA, PDA, and PHA, and this is resulted in total eight score matrix from both SCOP and CATH. Finally, more views are introduced by using binary projection of all existing views. Instead of counting the occurrences, these views only checks whether a GO term is appeared or not. In short, above all eight score matrix is converted into simple binary value such that if an array has equal or greater than an occurrence then the associated occurrence is projected into 1 in binary views and otherwise 0. Therefore, total 16 score matrices are created and they are all used for calculating R_{scr} .

Final step, calculating GO similarity, R_{scr} from 16 score matrices: The final R_{scr} is the average of cosine similarities calculated from 16 scoring matrices. The equation of cosine similarity is defined below together with graphical descriptions of score matrix at Figure 3.2. GO_1 and GO_2 are targeted two functional GO terms for which their semantic functional similarity is calculated. \mathbf{GO}_1 and \mathbf{GO}_2 are two column vectors in a scoring matrix associated with occurrence of domains. Due to the property of the cosine function, the values are ranged from 0 to 1 in which 0 means no similarity and 1 means exact match.

$$GO_{sim}(GO_1, GO_2) = \cos\theta(GO_1, GO_2)$$

$$= \frac{GO_1 \cdot GO_2}{\|GO_1\| \times \|GO_2\|}$$

(Equation 3-2)

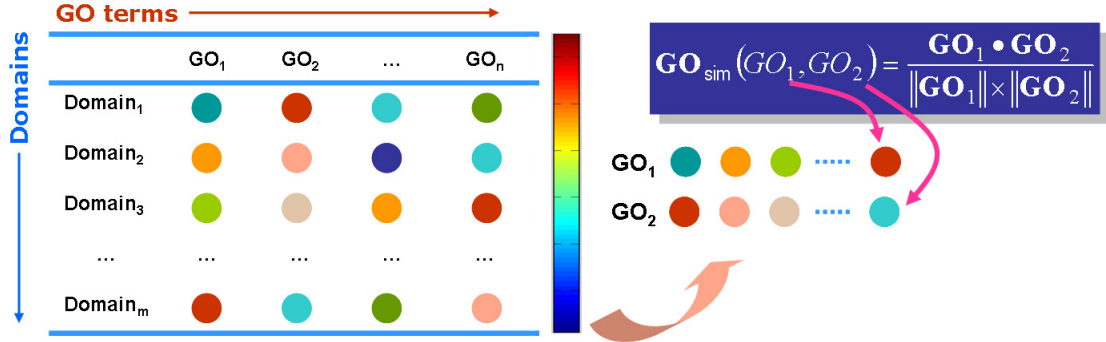


Figure 3.2 Visualization of a score matrix and its similarity equation.

Each row consists of domains defined by SCOP or CATH and each column consists of all known functional GO terms. Colored circle represents the frequency of occurrences corresponding to domains and GO terms. Assume that the intensity of color is proportional to the frequency of occurrences (i.e. blue is lowest and red is highest). Each column vector of GO terms is fed into cosine similarity function, and the result is defined as semantic similarity between two GO terms.

3.2.2 The graph-based score, G_{scr}

The principle of graph-based score is to reflect the specificity of GO terms into their similarity measurements. To accomplish this aim, the specificity of a GO term pair is scaled by projecting both the depth of a node and certainty of a path into an equation. Four variables, Ep , d_{NCA} , E_{max} and d_{max} are introduced and the complete equation is defined below.

$$G_{scr} = \exp\left(-\frac{1}{1 - \frac{Ep}{E_{max}}}\right)^{\left(1 - \frac{d_{NCA}}{d_{max}}\right)}$$

(Equation 3-3)

In Equation 3-3, E_p and d_{NCA} are representing number of siblings and depth of NCA and used for defining certainty and depth respectively. The weight of certainty and depth toward the specificity is relative to their maximum values, E_{max} and d_{max} . Thus these values can be defined in two different scopes, local and global. Local maximum indicates the maximum number of siblings or depth that belongs to the paths from root node to the leaf node that contains the target node. Global maximum results from exploring all possible paths associated with molecular functions in GO graph. The equations are designed to return higher score when the path is simpler and the depth is deeper which are corresponding to more distinctive and specific functional terms respectively. To see the effects of each variable, let's separate the equation into two terms: certainty term containing E_p and specificity term containing d_{NCA} . To get a high score from the given equation, the value of certainty term needs to be increased and specificity term should be decreased. Therefore, in order to increase the certainty term, the number of siblings of NCA should be small. In contrast to certainty term, the depth of NCA should be increased to increase the specificity term.

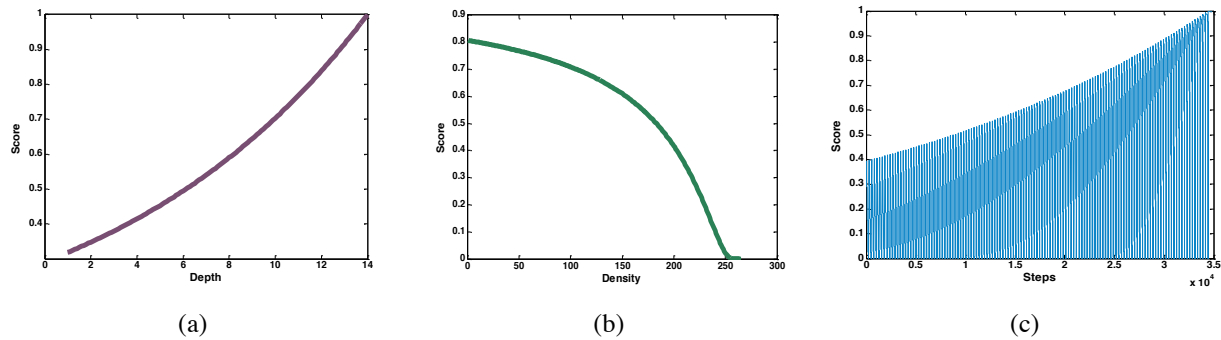


Figure 3.3 Tendencies of G_{scr} .

(a) the tendency of G_{scr} by increasing the depth of d_{NCA} (b) the tendency of G_{scr} by increasing the density of E_p (c) overall tendency of G_{scr} which is normalized score between 0 and 1

In short, the equation results high score when the number of siblings of NCA, E_p is small and the depth of NCA, d_{NCA} is deeper or getting closer to the leaf node. The visualization of G_{scr} tendency is shown in Figure 3.3 Two major scoring schemes, R_{scr} and G_{scr} , used in the proposed method have been introduced, and these scores represent top-down and bottom-up methods respectively; therefore, through weighted integration by using two more variable α and β , the proposed method, bidirectional integration is completed.

3.2.3 Calculating the similarity between Gene Products

In reality, calculating similarity score between individual GO terms is practically not much useful since most functions in GPs are described with more than a single GO term; therefore, additional metric is required for measuring similarity between groups of GO terms or GPs. To calculate the similarity of GPs, enhanced version of Hausdorff metric is used in this study by averaging the normalized Hausdorff metric. Similar approaches have been used for other studies as well [61, 62, 65, 73]. The equation is defined by

$$Hd(GP_1, GP_2) = \frac{1}{2} \left(\sqrt{\frac{1}{|GP_1|} \sum_{x_i \in GP_1} [GO_{sim}(x_i, GP_2)]^2} + \sqrt{\frac{1}{|GP_2|} \sum_{x_i \in GP_2} [GO_{sim}(x_i, GP_1)]^2} \right)$$

(Equation 3-4)

where $GO_{sim}(x, GP_i) = \max_{y \in GP_i} GO_{sim}(x, y), i = 1, 2$

The Hausdorff metric between two GPs, GP_1 and GP_2 are defined by $Hd(GP_1, GP_2)$. This function averages two normalized similarity scores derived from reciprocal directions, from GP_1 to GP_2 and vice versa. $|GP_1|$ and $|GP_2|$ denotes the number of GO terms associated with two GPs,

GP_1 and GP_2 respectively. $GO_{sim}(\cdot)$ refers any method that can measure the similarity between two GO terms. However, it should be careful when the final score is calculated since the final score is purely depends on the GO_{sim} whether it measures similarity or distance. If GO_{sim} measures similarity then the final score should be based on the maximum score, but if distance is measured then it should be based on minimum score at each GO term. To give better understand on this metric, details are described with graphical representation.

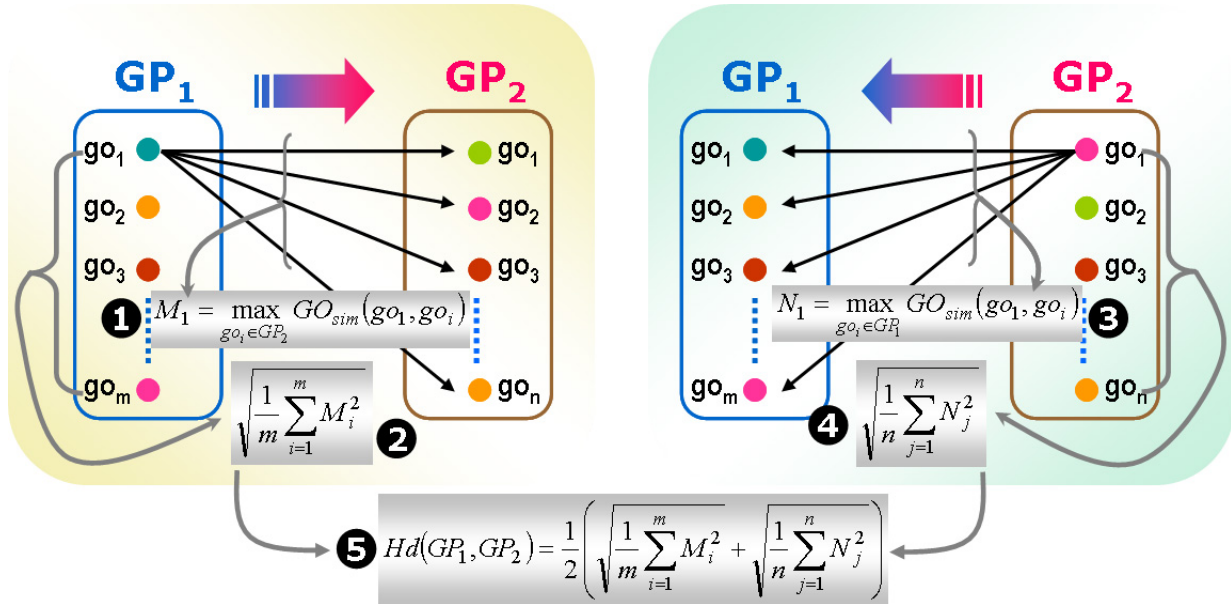


Figure 3.4 Visualization of calculating similarity of GPs.

- Identifying maximum (minimum) similarity (distance) between one of the GO terms in GP_1 against all GO terms in GP_2 .
- normalizing maximum similarity.
- and 4) reproducing 1) and 2) with opposite direction respectively.
- the final Hausdorff score is the average of normalized similarity.

So far, overall procedures of the proposed method from measuring a pair of GO term to GP similarity have been introduced. In summary the proposed method integrates five different databases, GO, UniProt, KUPS, CATH and SCOP to reflect broad range of biological factors into functional similarity.

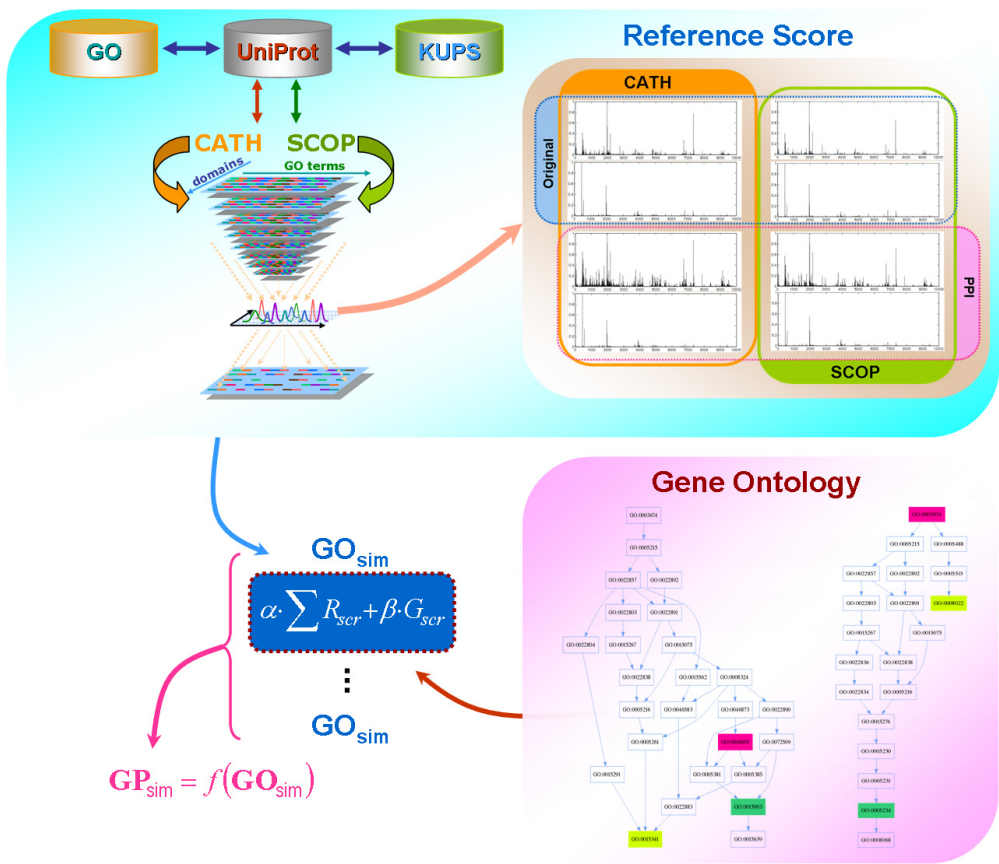


Figure 3.5 Visualization of proposed method.

To the clockwise, first image shows the way to create R_{scr} which integrates five databases by mapping and retrieving information among GO, Uniprot, KUPS, CATH and SCOP. The initial score matrix is composed of annotation occurrences upon domains defined by CATH and SCOP. As producing multiple views, diverse score matrices are derived such as referring annotations from PPIs, hierarchical annotations and binary projections. The second Figure shows the distribution of annotations in different score matrix: left (orange) and right (green) show two databases, CATH and SCOP respectively, and top (blue) and bottom (PPI) show the distribution of scores whether PPI pairs are considered or not. These distributions only show the occurrences of annotation, but actual score matrices contains more views by projecting all scores into binary conditions based on appearance and absence of GP occurrences; therefore, this makes total 16 different score matrices. The third Figure shows examples of GO graphs in which the light green and green are a pair of target GO terms, and pink node denotes their NCA. This information is fed into equation 3-3 and resulted in G_{scr} . The last Figure shows that the final score of semantic similarity between GO terms are made by the summation of weighted R_{scr} and G_{scr} . Finally the GP similarity is defined by a function of individual GO similarity which is defined in equation 3-4

To reduce the generalization error or bias effects, the principles of multi-view learning is adapted such that observed factors are projected into diverse spectrums of data distribution as multiple views. Both integration in wide range of biological factors and systematically designed algorithm, which helps to reduce generalization error, guarantee that the proposed method can effectively handle the problems of measuring functional similarity. The visualization of proposed method is shown in Figure 3.5.

3.2.4 Theoretical relevance of R_{scr}

The reference score, R_{scr} has two main purposes: giving a metric of GO terms shared by the root node and reducing general errors caused by single dataset. As mentioned above, 52% of GO term pairs out of all possible pairs of currently existing GO terms are shared by root node. This means conventional methods defining similarity based on the location of nearest common ancestor (NCA) will give nil similarity for these pairs or treat them as having exactly same similarity. Defining them as either nil similarity or same similarity does not seem like biologically reasonable, especially by considering the facts that more than half of GO term pairs are shared by root node and most of GPs have multiple GO terms. The semantic similarity of proposed method calculates root-shared GO terms with following assumption. Two GO terms are close if two GO terms tend to be co-annotated by GPs having same functional domains and/or their interacting partners since GO terms are designed for describing the function of GPs; therefore, if the function of two GPs are similar each other then their functional terms should be similar as well. In fact, it is well known that if two proteins interact each other then they tend to have similar functions [126-128].

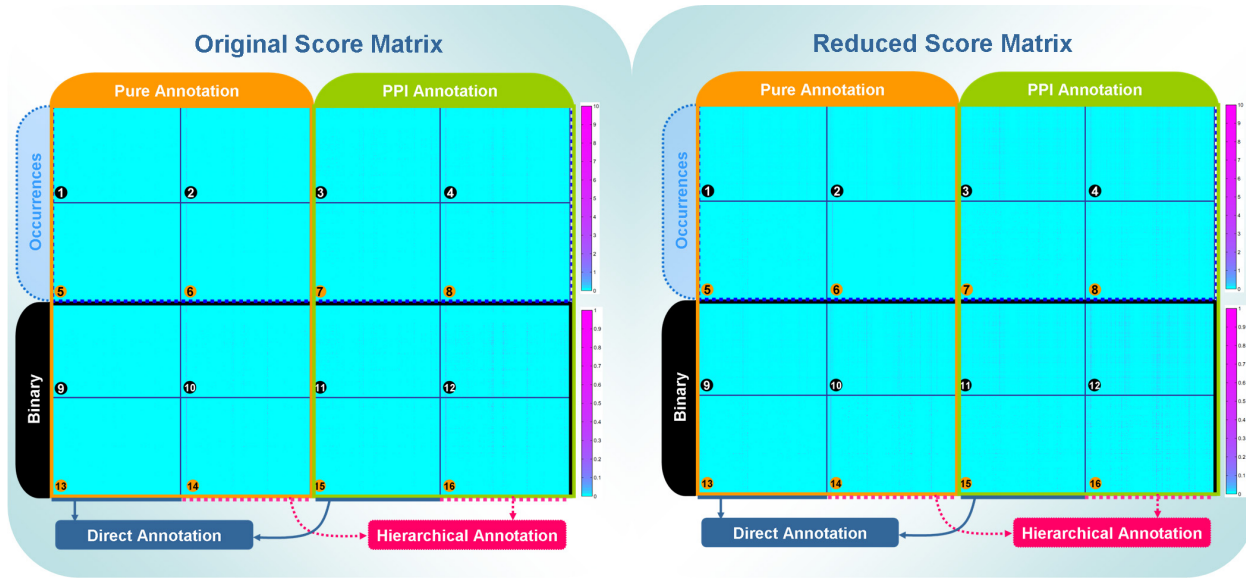


Figure 3.6 Heat map of 16 score matrices.

The left image, ‘original score matrix’ is the actual matrix that used for calculating R_{scr} and the right image, ‘reduced score matrix’ is heat maps to get better resolution of correlation significance by eliminating columns and rows with all zero elements. The black circle numberings depicted in the each of left bottom of score matrices indicate score matrices derived from CATH and the orange circle numberings depicted in the left bottom of rest score matrices are corresponding to score matrices derived from SCOP. Upper two rows denoted as “occurrences” in 16 score matrices are created by occurrences of GO terms at each domain. Bottom two rows denoted as “Binary” in 16 score matrices are obtained by projecting occurrences into binary value (i.e, one or zero) based on their presence and absence respectively. First two columns denoted as “Pure Annotation” of 16 score matrices are calculated by relying on the annotations of GPs considering corresponding functional domains only. Rest two columns denoted as “PPI Annotation” among 16 score matrices are extended versions of the first two columns by considering corresponding functional domains and all GPs containing the domains while they appear in integrated PPI database (i.e, KUPS). First and third column denoted as “Direct Annotation” counts the occurrence of annotations with exact GO terms. Second and fourth column denoted as “Hierarchical Annotation” counts the occurrence of annotations by including all ancestors of the target GO term derived from hierarchical structure of GO.

To incorporate this assumption into the proposed similarity score, multiple score matrices are designed which are derived from two domain structure databases SCOP [129] and CATH [123], and manually curated comprehensive protein-protein interaction networks, KUPS [130]. The final score matrices are completed by projecting the initial score matrix into statistically different

views. The final score measuring similarity between two GO terms is made by integrating these multiple views or observations; thus the final score represents the high consensus of multiple observations. In fact, similar approach is already well known in machine learning area as a multi-view learning which is known to reduce generalization error [120, 121]. The actual distributions and relationships among 16 score matrices are depicted from Figure 3.6~9. In Figure 3.6, figures show the heat map of the actual 16 matrices. Each column of the matrices corresponds to all functional GO terms in GO database and each row corresponds to the domains. The numbers in black and orange circles denote CATH and SCOP database respectively. The domains are from two different databases. Thus, these score matrices are created independently. Since the original score matrix is too sparse to visualize differences in a small figure, reduced score matrix is also shown in the right image at Figure 3.6 Reduced score matrices are drawn by eliminating columns and rows of which elements of either columns or rows do not have any associated GPs. These figures show that the patterns of score matrices derived from two different databases are similar to each other. In other words, the pattern of GO terms annotated by GPs having similar domains is conserved even if it is derived from different domain databases. This implies that the similarity of patterns between two GO terms can be used for defining the functional relations between two GO terms since their patterns are derived from functional domains. To check out the distributions of domains upon GO terms, simple statistics are conducted such that the correlations among the normalized distribution of annotated GPs along with GO terms are calculated. Let's assume that a score matrix is composed of m by n matrix. Here m corresponds to the number of domains, and n corresponds to the number of GO terms in GO database and then the normalized distributions of GO terms are defined by $\mathbf{G} =$

$[f(G_1), f(G_2), \dots, f(G_n)]$ in which $f(G_i)$ denotes the normalized value of G_i ($i=1,\dots,n$). The equation is defined below.

$$G_i = \sum_{d=1}^m g_{d,i} \quad i = 1 \dots n$$

$$f(G_i) = \frac{G_i - \min(\mathbf{G})}{\max(\mathbf{G}) - \min(\mathbf{G})} \quad (\text{Equation 3-5})$$

Here $g_{d,i}$ denotes the value corresponding to d^{th} row and i^{th} column of a score matrix; therefore, this equation shows the relative distributions of domains belonging to GO terms at the given matrix. To check out relations within and between score matrices, correlations of normalized distributions are calculated. For the convenience, each of 16 score matrices is named as following: original direct annotation (ODA), original hierarchical annotation (OHA), PPI direct annotation (PDA), PPI hierarchical annotation (PHA), binary original direct annotation (bODA), binary original hierarchical annotation (bOHA), binary PPI direct annotation (bPDA), and binary PPI hierarchical annotation (bPHA) in which *original* and *PPI* denotes that GO term occurrences are counted by using GPs having target domains only or including direct interacting pairs of the GPs respectively. *Direct* and *Hierarchical* annotation denotes whether the occurrences of GO terms are counted by using an exact match or including all ancestor nodes respectively. More precisely, in Figure 3.6, the name of individual matrix is given as: ODA, OHA, PDA, PHA, bODA, bOHA, bPDA, bPHA of which the name is corresponding to the order of numbers from 1 to 4 and from 9 to 12 for CATH and from 5 to 8 and 13-16 for SCOP.

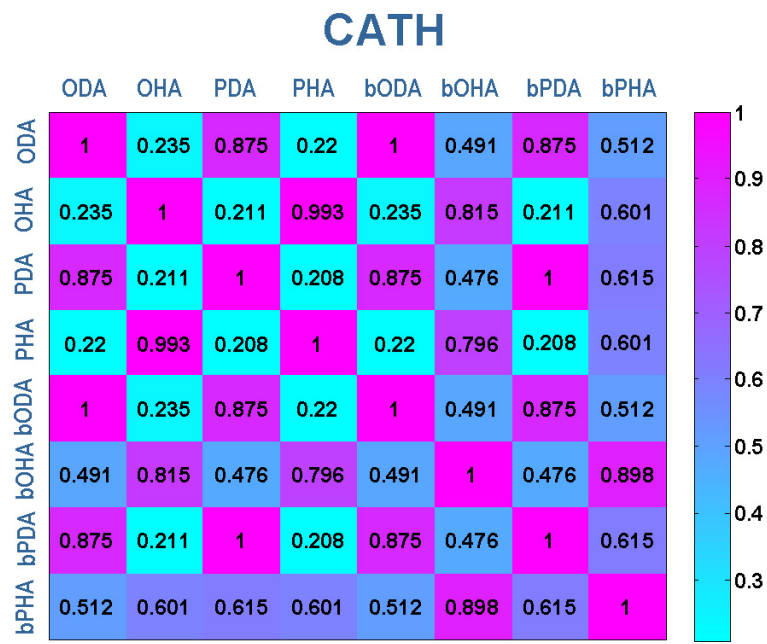


Figure 3.7 The visualization of correlation coefficient derived from score matrices within CATH.

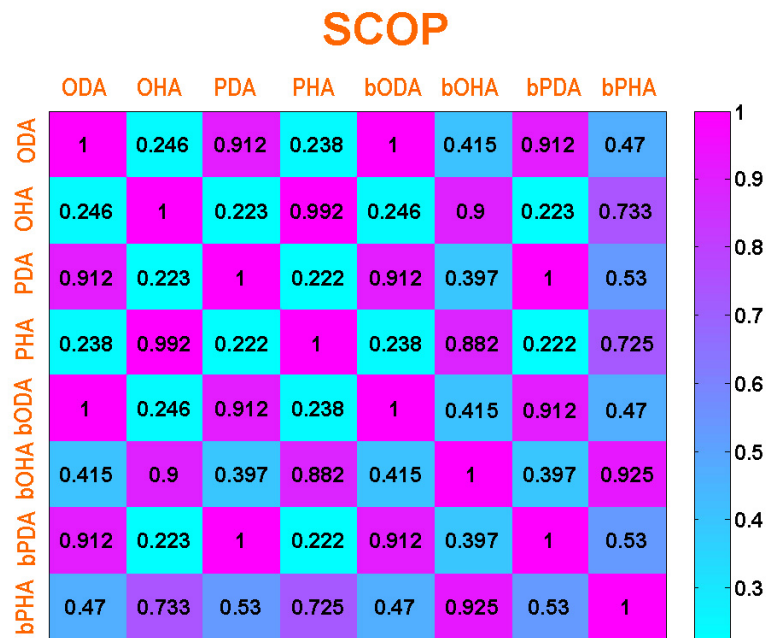


Figure 3.8 The visualization of correlation coefficient derived from score matrices within SCOP

Figure 3.7 and 3.8 show the correlations within score matrices derived from CATH and SCOP respectively. Each of heat maps clearly shows that homologous scoring schemes conserve high correlation. For example, no matter what databases are referred, direct annotations are highly correlated with any types of direct annotations and similarly the patterns of hierarchical annotations are also high correlated each other. Interestingly the binary-based score matrices also conserve similar patterns with the ones in occurrence-based score matrices. However, compared to the occurrence-based score matrices, their correlations are rather smoothly distributed by increasing the correlation between homologous annotations and decreasing the correlation between heterologous annotations such that the correlation within direct annotations or hierarchical annotations are increased but the correlation between direct and hierarchical annotation are decreased. Thus these two different scoring schemes give positive effects on reducing the noises or biased observations by increasing the number of views. The correlations between two independent databases, CATH and SCOP are also calculated, and the results are shown in Figure 3.9. The patterns of correlated relations between CATH and SCOP are very similar to the ones calculated from within the individual databases. The overall statistics show that the distributions of GPs associated with individual GO terms in multiple matrices are highly conserved, so this should results in reductions of biased and noise effect; thus this implies that the power of co-annotations categorized at same functional domains can be used for robust similarity measurement of two GO terms.

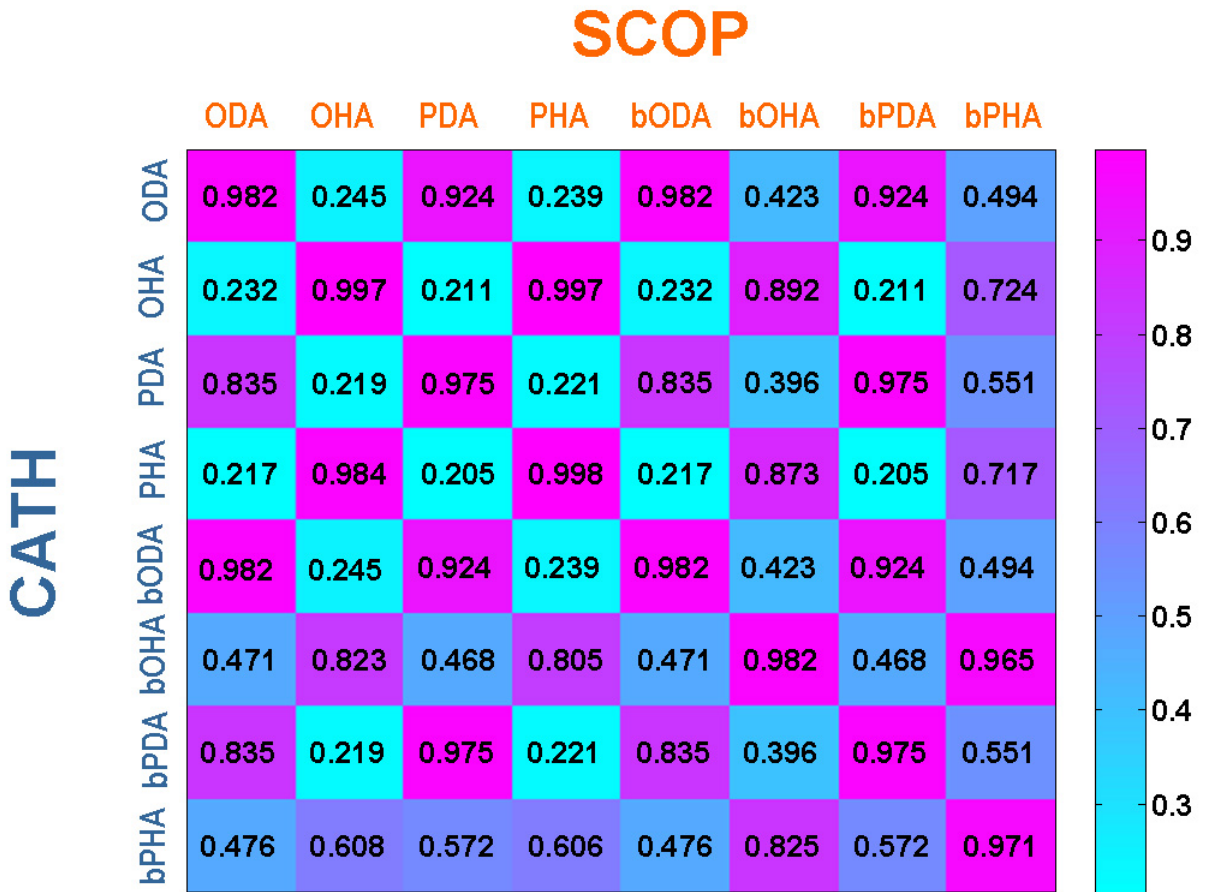


Figure 3.9 The visualization of correlation coefficient between CATH and SCOP.

For the convenience, the names of 16 score matrices are given as following in the rest of this article: original direct annotation (ODA), original hierarchical annotation (OHA), PPI direct annotation (PDA), and PPI hierarchical annotation (PHA) from CATH and SCOP. In addition, the occurrences in all eight score matrices are projected into binary space which checks whether each array of score matrices are present or absent. At each term, *Original* and *PPI* denotes that GO term occurrences are counted by using GPs having target domains only or including direct interacting pairs of the GPs respectively. *Direct* and *Hierarchical* annotation denotes whether either using an exact match or including all ancestor nodes respectively to count the occurrences of GO terms. More precisely, numbers from 1 to 4 and from 9 to 12 are derived from CATH, and numbers from 5 to 8 and from 13 to 16 are derived from SCOP. The numbers in each group (i.e. CATH and SCOP) can be denoted with original direct annotation (ODA), original hierarchical annotation (OHA), PPI direct annotation (PDA), PPI hierarchical annotation (PHA), binary original direct annotation (bODA), binary original hierarchical annotation (bOHA), binary PPI direct annotation (bPDA), and binary PPI hierarchical annotation (bPHA) as corresponding to the order of numbers.

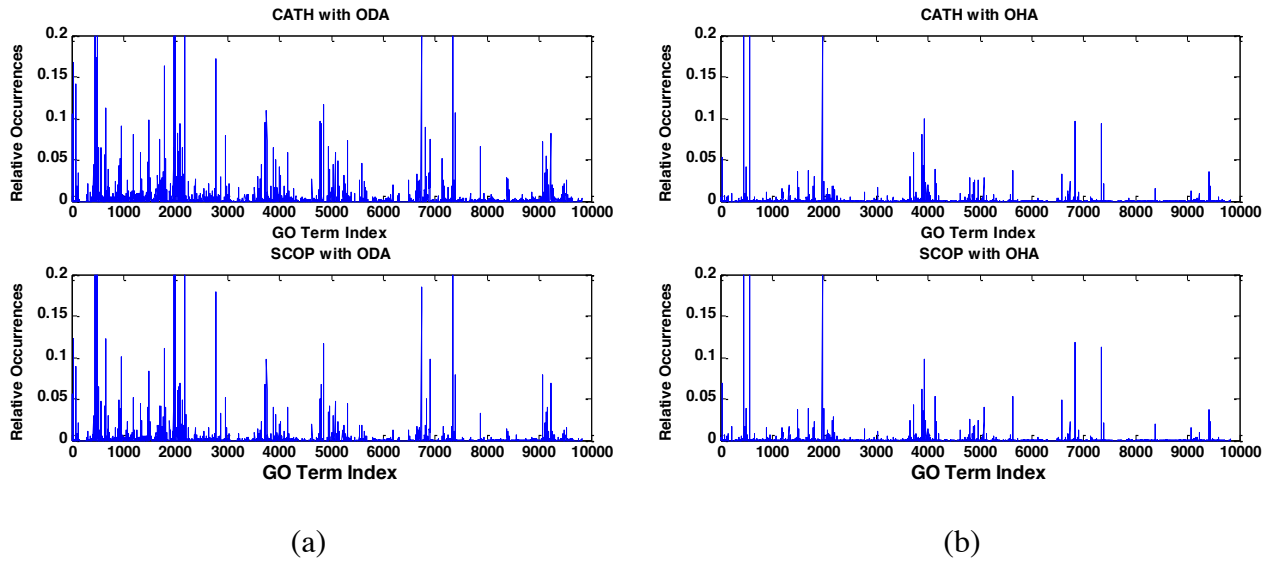


Figure 3.10 Relative occurrences of GO term with original accumulated array.

The number of occurrences is sequentially increased if a new occurrence is detected at the previously counted array corresponding to same domains and GO terms. Relative occurrences are calculated by the ratio between each corresponding occurrence and the maximum occurrence at the score matrix. In order to emphasize the differences between score matrices, the relative occurrences smaller than 0.2 are magnified (i.e, the relative occurrences, greater than 0.2 are not fully depicted (a) First row, the histogram of original direct annotation (ODA) from CATH and second row, the histogram of ODA from SCOP. (b) First row, the histogram of original hierarchical annotation (OHA) from CATH and second row, the histogram OHA from SCOP.

Figure 3.10~13 are provided for visualizing comparisons among normalized distributions of individual score matrices derived from occurrences and binary. Due to the significant difference between maximum and minimum number of GP occurrences, the figures used cut-off value of 0.2. In the graphs the horizontal axis denotes the index of total 9,833 GO functional terms, and vertical axis denotes *relative occurrences* calculated by the ratio between each corresponding occurrence and the maximum occurrence at the score matrix.

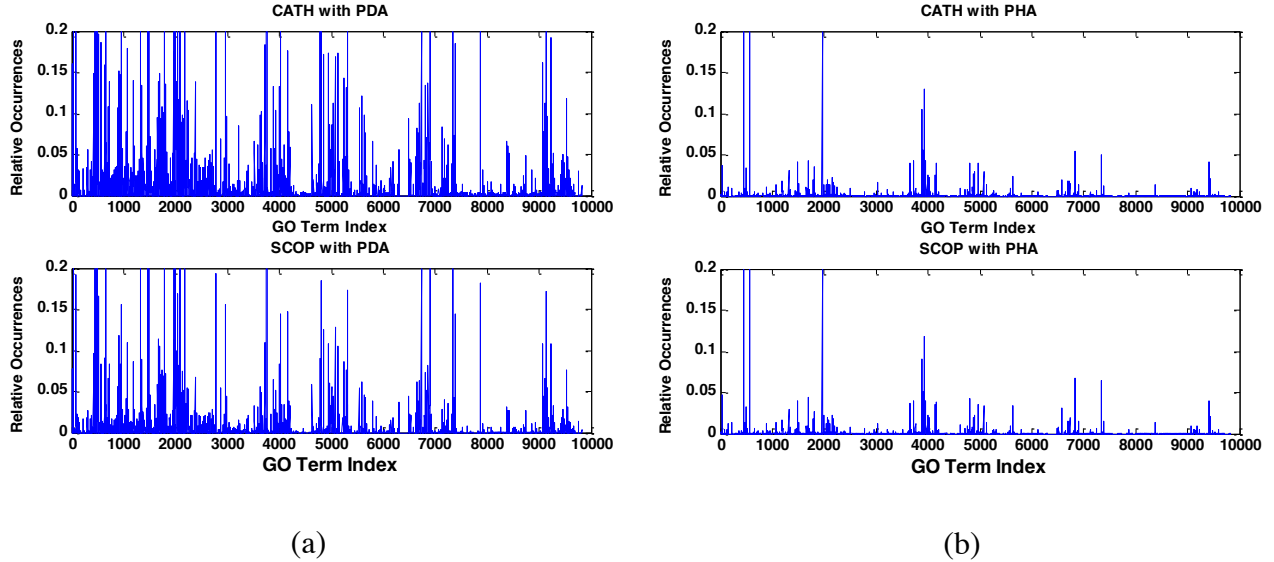


Figure 3.11 Relative occurrences of GO term with PPI-based accumulated array.

(a) First row, the histogram of PPI direct annotation (PDA) from CATH and second row, the histogram PDA from SCOP. (b) First row, the histogram of PPI hierarchical annotation (PHA) from CATH and second row, the histogram PHA from SCOP. *Original* and *PPI* denotes that GO term occurrences are counted by using GPs having target domains only or including direct interacting pairs of the GPs respectively. *Direct* and *Hierarchical* annotation denotes whether the occurrences of GO terms are counted by using an exact match or including all ancestor nodes of the target GO term respectively.

Figure 3.10 (a) compared relative occurrences between CATH and SCOP upon ODA which correspond to the top and bottom of the figure. Although there are subtle differences, for example, the picks around 7,000 and 9,000 have different numbers and shapes, overall patterns look very similar each other; thus this results in high correlation as shown in Figure 3.9 (i.e. 0.982). Rest of figures, Figure 3.10 (b) and Figure 3.11 (a) and (b) also shows similar patterns. Low correlation or dissimilar patterns can be identified by comparing heterogeneous matrices. Comparing PDA from CATH and PHA from SCOP, which are located in Figure 3.11 (a) and (b) respectively, could be one of the examples to figure out the differences between two figures such that the density of picks are clearly noticeable to shows the differences. In fact, their correlations

are denoted relatively low and can be found in Figure 3.9 (i.e. 0.205). OHA from CATH and PDA from SCOP which are located in the Figure 3.10 (b) and Figure 3.11 (a) respectively also show the clear difference of patterns between two matrices. As expected, their correlation is relatively low and can be found in Figure 3-9 (i.e. 0.211). Binary version of Figure 3.10 and 11 are depicted in Figure 3.12 and 13. Indeed, compared to direct annotation, the patterns of the hierarchical annotation between binary and occurrence-based scoring matrix show significant difference. As expected and described before, the patterns are more evenly distributed in hierarchical annotations in binary-based score matrix. This implies that binary-based scoring scheme helps to make uniform distribution by emphasizing the fidelity or specific functions in cellular life while fading the weight of general GO terms located in higher level (i.e, closer to root GO term). In other words, under the consideration of hierarchical annotations, broader terms have higher occurrences than specific term since the general terms are counted redundantly while their descendent terms are counted. However, binary based-scoring matrix does not rely on the occurrence of annotation, but it only considers the status of appearance or absence. The consequence of binary-based scoring matrix can be easily found in Figure 3.7~9 where correlations in heterogeneous binary-based score (e.g, correlation between bODA and bOHA is 0.491, 0.415 and 0.423 in Figure 3.7, 8 and 9 respectively) is higher than correlations in occurrence-based heterogeneous matrices (e.g, correlation between ODA and OHA is 0.235, 0.246 and 0.245 in Figure 3.7, 8 and 9 respectively). It is of interest to analyze the relations between the final score of proposed method and R_{scr} only. For the analysis, 50 GO terms having R_{scr} score greater than 0.5 are randomly selected to ensure that the final score is derived from both R_{scr} and G_{scr} . The second column in table 1 shows that R_{scr} is likely to give higher score for ‘tight’ relations of which NCA and two GO terms have parent and child relationship.

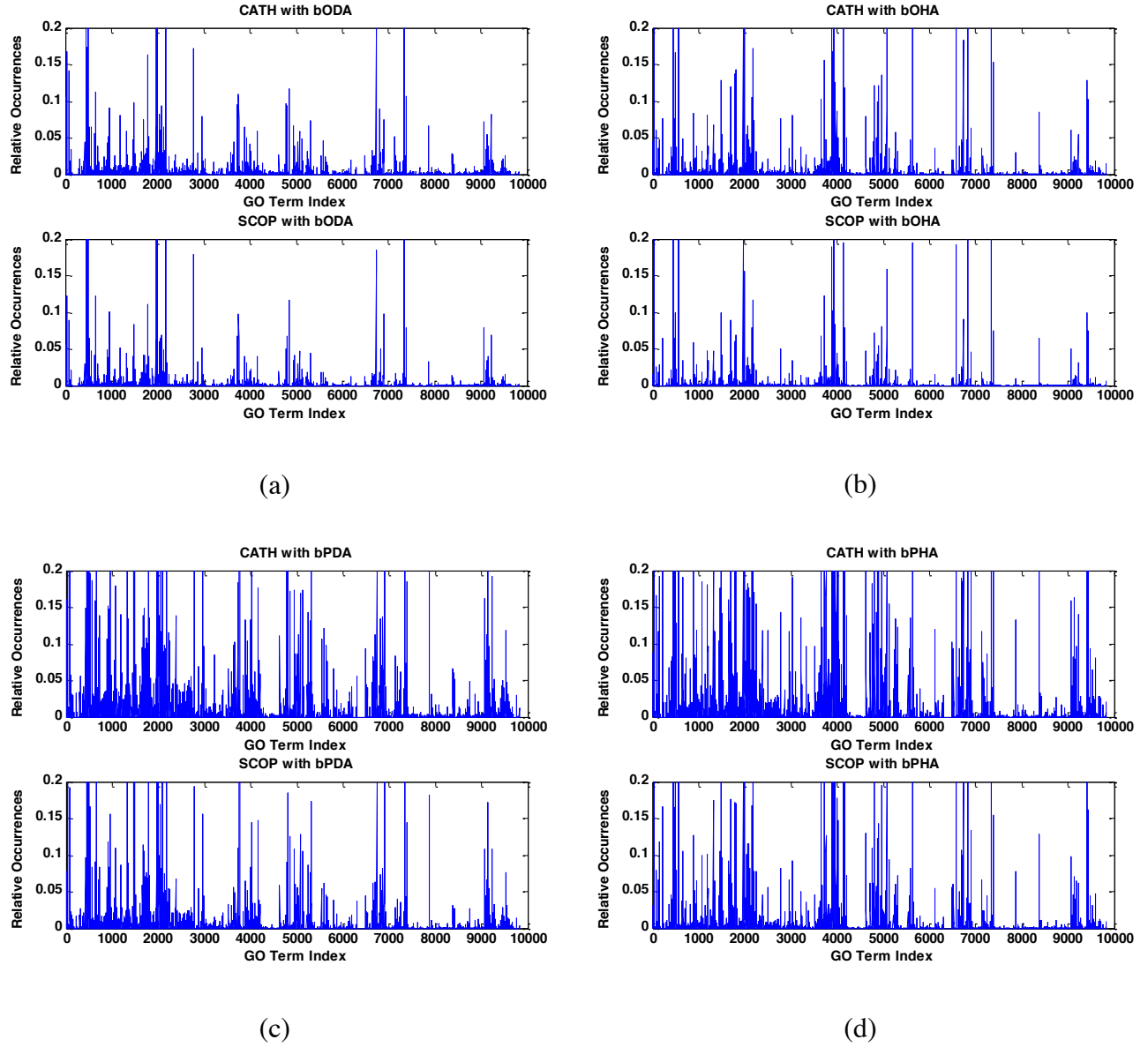


Figure 3.12 Relative occurrences of GO term with binary array.

The number of occurrences are denoted as 1 or zero if corresponding array is present or absent respectively. In order to emphasize the differences between score matrices, the relative occurrences smaller than 0.2 are magnified (i.e., the maximum value shown in the graph is limited to less than and equal to 0.2). (a) First row, the histogram of binary original direct annotation (bODA) from CATH and second row, the histogram of bODA from SCOP. (b) First row, the histogram of binary original hierarchical annotation (bOHA) from CATH and second row, the histogram bOHA from SCOP. (c) First row, the histogram of binary PPI direct annotation (bPDA) from CATH and second row, the histogram bPDA from SCOP. (d) First row, the histogram of binary PPI hierarchical annotation (bPHA) from CATH and second row, the histogram bPHA from SCOP.

This seems very reasonable since they actually have same parent and indeed, they are the most specific term in their path. To see the details of the results please refer supplement material [S-7]. To evaluate biological relevance of R_{scr} , simple statistics of annotated GPs in UniProt is conducted, and the results are shown in Table 3.1. In this table 1st column shows the average score of GO term pairs in a category. 2nd and 4th columns show average number of GPs annotated by ‘either’ or ‘both’ of GO term pairs in a category respectively. 3rd and 5th columns show the average number of GPs having an interaction partner among the GPs in 2nd and 4th column respectively. As an intuitive comparison, 1st column shows that R_{scr} is somewhat proportional to the geometric similarity: the closer distance the higher score. 2nd column shows the difference between R_{scr} and IC-based score since IC-based method penalizes GO terms associated higher number of GPs. Indeed, the problems of penalty policy in IC-based method can be also observed from 1st, 2nd and 4th columns since the order of intuitive score and IC-based score are contradicted such that the direction of scores goes opposition direction. In other words, ‘tight’ should have higher score than ‘root’ under the intuitive comparison, but by considering the characteristics of IC-based method in which the higher number of GPs has lower score, IC-based methods relatively give higher score to ‘root’ and lower score to ‘tight’ relations. This intuitive contradiction of IC-based methods is also reported by Wang et al. [73]. The 3rd and 5th columns show very interesting point and support that the root-shared pairs having relatively high score are not from random selection. As shown in the 3rd and 5th columns at the table, the higher score should be from the effect of considering interacting partners in PPI networks since their annotated GPs are relatively high affinity to be interact. In short, this brief statistic experiment shows that R_{scr} tends to reflect both intuitive and biological relations into its scoring scheme by giving positive feedback toward GO terms having high number of GPs co-annotated and

involved in PPIs. This also shows the significant different between the proposed method and conventional IC-based methods in which all root-shared GO terms are considered as either same or nil similarity.

Table 3.1 Comparing scores and biological significance of GO pairs

❶ Average reference score (R_{scr}) ❷ Average number of GPs annotated by a GO term in each category for which total number of GPs annotated by GO terms in the given category is divided by total number of GO terms in the given category ❸ Average number of GPs including direct interaction partners of GPs annotated by one of GO terms in the target GO term pairs at the given category ❹ average number of GPs annotated by both GO terms consisting a pair of GO terms at each category ❺ average number of GPs which is interacting and annotated by both GO terms consisting a target GO term pair at each category. In category, *Tight* denotes direct parent-child relations between both GO terms and their NCA. *Root* denotes NCA of a GO pair is the root node. *Loose* denotes all GO pairs except *Tight* and *Root* relations

Category	❶	❷	❸	❹	❺
Tight (17)	0.69	56.94	0.70	10.94	0.11
Loose (26)	0.68	29.92	0.76	2.42	0.23
Root (7)	0.66	23.85	0.85	2.14	0.42
Overall (50)	0.68	38.26	0.76	5.28	0.22

4 Experiments and results

4.1 Experiment I: measuring functional correlation

4.1.1 Dataset

To evaluate the performances of the proposed method and other conventional methods, similarity scores calculated from SCOP domain similarities are compared. To get the annotations of each domain in SCOP, high-quality truly domain-centric GO annotations are downloaded from Superfamily DB (<http://supfam.cs.bris.ac.uk>) [131] and parsed and integrated into our local database to retrieve the information later. Based on the annotation of SCOP domain at family level, total 2,690 unique domains are retrieved. 44 out of 2,690 domains are annotated with non-existing GO terms in current GO DB, so these domains are eliminated from the list. Finally total 2,646 domains are obtained from SCOP; therefore, total 3,501,981 all possible pairs of SCOP domains are used for experiments. The list of SCOP domains used in the experiments are attached in supplementary material [S-8].

4.1.2 Similarity measurements

To evaluate methods, four different similarity scores are compared to functional similarities calculated by the proposed method and six conventional methods. Four different similarity score is derived from three categories: sequence, phylogenetic profile and structure similarity. Once all similarity scores are calculated, all scores are grouped into 50 bins based on target similarity. For example, similarity scores calculated by BSM score are grouped into 50 bins from 0 to 1, and then the scores, which are calculated from sequence, phylogenetic profile and structure similarity, corresponding to domain pairs associated with each bin is averaged.

Sequence similarity: sequence similarity is one of the most popular methods identifying the inheritance of homology [132] and homologous proteins are likely to share their functions although several limitations have been reported [94, 111, 133, 134]; therefore this leads the assumption that sequence similarity and functional similarity tend to be correlated. To get the sequence similarity, all SCOP domain sequences are downloaded from ASTRAL [135] (<http://astral.berkeley.edu/>), and sequence similarity of all possible pairs of domains are calculated by BLAST program with default parameters [136] (<http://blast.ncbi.nlm.nih.gov>).

Phylogenetic profile similarity: the rational behind phylogenetic profiles are from the hypothesis that functionally linked proteins are evolved in a correlation fashion; therefore the homologs of functionally related proteins can be found in the same subset of organisms [137]. The phylogenetic profiles are created by checking whether the homologs of proteins are present or absent in a same organism. To create phylogenetic profiles, psiBLAST searches homologs of target proteins against proteins from 25 fully sequenced genomes (see supplementary material [S-9]) with e-value less than 10^{-10} . The similarity of phylogenetic profiles between domains is calculated by mutual information (MI) as following:

$$MI(x,y) = \sum_{x=0}^1 \sum_{y=0}^1 p(x,y) \cdot \log \left[\frac{p(x,y)}{p(x) \cdot p(y)} \right] \quad (\text{Equation 4-1})$$

where $x \in \mathbf{x}$ and $y \in \mathbf{y}$

Here, \mathbf{x} and \mathbf{y} denote two vectors of phylogenetic profiles associated with any pairs of two domains. x and y are elements of two vectors correspondingly. $p(x,y)$ is a joint probability of two domains derived from four possible states of occurrences in which 0 states absence and 1 denotes

presence. $p(x)$ and $p(y)$ describe the probability of absence and presence of corresponding domains.

Structural similarity: the knowledge of protein structures often provides a crucial insight of protein function. Indeed, protein structure is known as more conserved than sequence in evolutionary process[138]; therefore, this implies that the structural similarity can represent the functional relations between two proteins. To increase the relevance of measuring structural similarity, two different structural alignments are used: TM-align [22] and Dali [139]. Corresponding programs are downloaded from <http://zhanglab.ccmb.med.umich.edu/TM-align/> and <http://ekhidna.biocenter.helsinki.fi> respectively. The similarity scores are calculated by 3,501,981 all possible pairs of domains on cluster machine.

4.1.3 Results

To compare the performance between the proposed method and other conventional methods, the tendency of domain similarity is analyzed. The hypothesis in this experiment is that if genes or GPs are functionally similar, then their structure, sequence, and phylogenetic profiles tend to be similar each other. For example, if a pair of GP similarity is close to 1 which corresponds to exact match or closely related each other, then structure, sequence, and phylogenetic profile could be identical or very similar each other as well. This hypothesis is commonly used in many studies although the hypothesis has not been comprehensively verified yet [58, 59, 61, 62, 65, 69, 70, 72, 99, 100]. Therefore, this hypothesis should be verified before further experiments proceed. To do this, similarity relations among three categories are compared, and the results are shown in Figure 4.1.

The details about experimental procedures are described in method section. Figure 4.1 shows tendency of domain similarity based on the score calculated by TM-align (TM), Dali (DALI), phylogenetic profile (PHY), and sequence alignment (SEQ). To help the visual comparison, fitted graph is also drawn through each method, and prefix ‘*fit*’ is added in front of each method to identify fitted graph from the graphs derived from actual similarity scores. Graphs show overall similarity scores derived from three different categories are likely to be correlated.

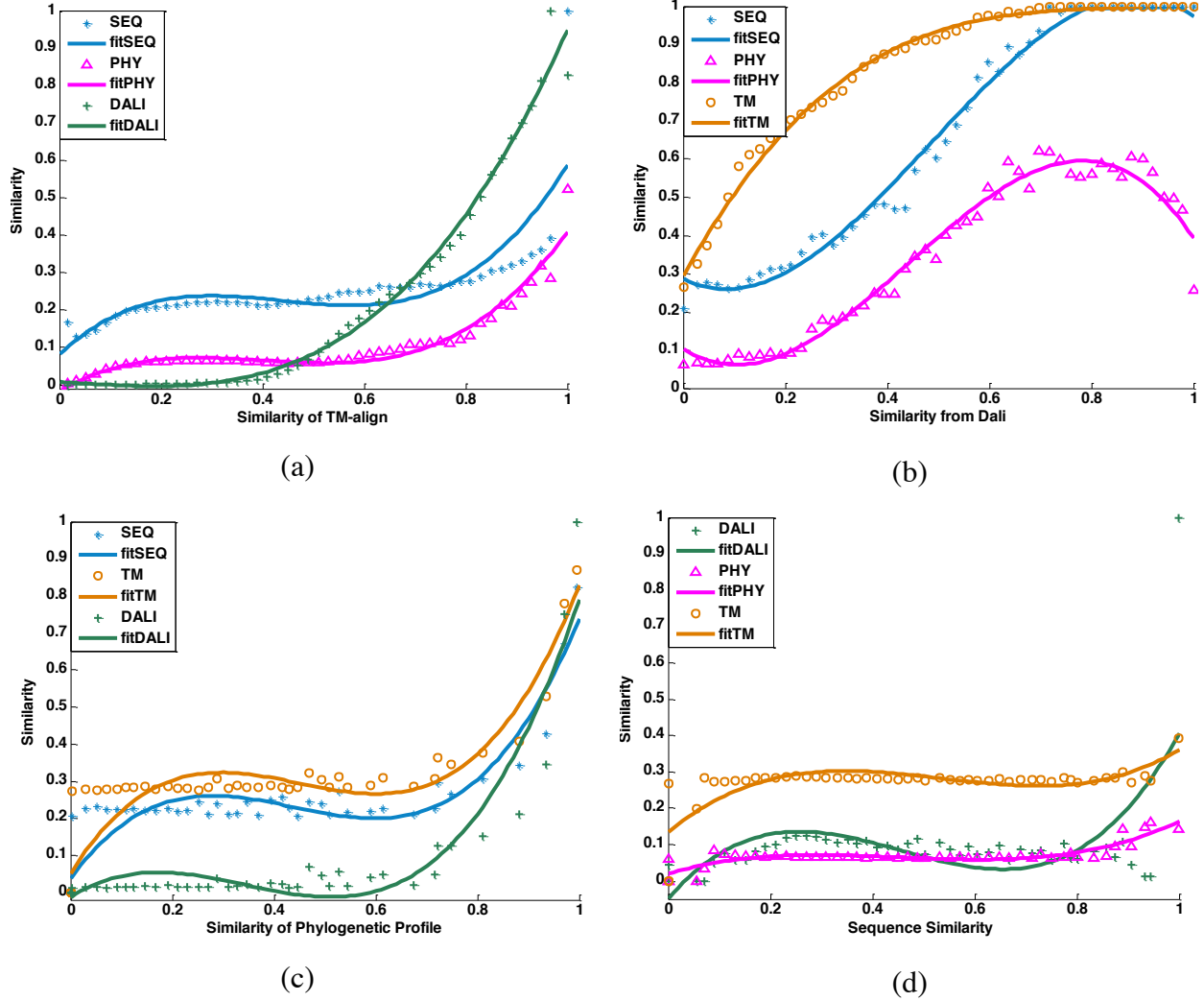


Figure 4.1 The tendency of domain similarity among three categories.

Structure(TM-align and DALI), sequence (SEQ), and phylogenetic (PHY) profile. Horizontal axis denotes similarity score based on one of four methods (i.e, TM-align, DALI, SEQ, and PHY), and vertical axis denotes similarity score for rest of methods. (a) and (b) the tendency of domain similarity based on structure similarity calculated by TM-align and Dali respectively. (c) the tendency of domain similarity based on phylogenetic profile. (d) the tendency of domain similarity based on sequence similarity.

However, as observed in Figure 4.1, their correlations are not exactly proportional to each other.

More precisely, in Figure 4.1 (a), there is stationary area from 0.2 to 0.5 in TM similarity, and strong correlation is observed at higher than structure similarity 0.6. In Figure 4.1 (b), Dali shows very clear correlation between 0.2 and 0.8. However, when zero similarity considering the

most left bottom of each graph at Dali (i.e, Figure 4.1 (b)) is compared to same part of all others, Dali's initial graphs show higher similarity score than those of others (i.e. SEQ and PHY stays around 0.3 and others stay around 0.1). This shows lower Dali score is somewhat chaotic and unreliable. Indeed, when Dali reaches more than structural similarity 0.8, TM-align and sequence similarities are convergent, and phylogenetic profile similarity is dropped significantly. This mismatched tendency shows that higher similarity score of Dali does not guarantee to make agreement on different characteristics of similarity. The tendency of graphs derived from phylogenetic profile in Figure 4.1 (c) and from TM-align in Figure 4.1 (a) show very similar patterns. In contrast to others, Figure 4.1 (d) shows sequence similarity requires very high similarity to observe similarities such that the correlations among three categories are only observed at high similarity degree (i.e. greater than 0.8). However, this result is not that surprising and can be found in previous studies such that the results show finding similar GPs often requires high sequence similarity [49, 50, 140]. Indeed, unreliable performances of sequence similarity toward identifying functional similarity also have been reported [39, 40, 51, 52]. The unreliable sequence similarity itself is not a major concern in this study. The actual problem is that most conventional methods identifying functional similarity have been verified their methods by using sequence similarity only or heavily focusing on the results from sequence similarity to emphasize the performance of proposed methods [59, 61, 65, 69, 71, 72]. Besides showing the relations of sequence similarity toward other similarity scores, as a guidance of evaluation, it is strongly recommended to use multiple measure measurements to verify the rational of the similarity measurement methods. Overall results show that correlations do exist among three categories of similarity measurements although there exist some specific tendencies of which they are not exactly proportional between similarity scores and functional similarity,

but with certain degree or range they do show clear correlations. Indeed, due to the existence of difference tendencies along with different range of similarity score, it is challenge to find such method that makes agreement on correlations among three different categories. In other words, the tendency of all agreement on correlation can be used for one of evaluation criteria to judge similarity methods as a statistical point of view. By following the proposed evaluation criteria and upon the verification of correlation tendency among three categories, conventional methods and proposed methods are compared, and results are shown in Figure 4.2~5. Horizontal and vertical axis in Figure 4.2~5 is similarity score derived from the given method and criteria measurements derived from three different categories respectively. Figure 4.2 and 4.3 are the proposed method, BSM score and Ye's method respectively and show similar patterns of similarity graph along with different criteria. The differences between two graphs are that Ye's method is somewhat looks like shrunken version of the proposed method. In fact, the range of score in Ye's methods is between 0 and 0.5. This happens due to the effect of normalization process in which the depth of NCA is normalized by maximum depth of entire graph. In contrast to Ye's method, the proposed method has score range between 0 and 1. More interestingly, the graphs shown in the proposed method (Figure 4.2) are very similar to those of TM-align in Figure 4.1 (a). By considering the fact that no structural information is used, it is stunning that *the proposed method can derive the result as similar as the ones derived from structural information*

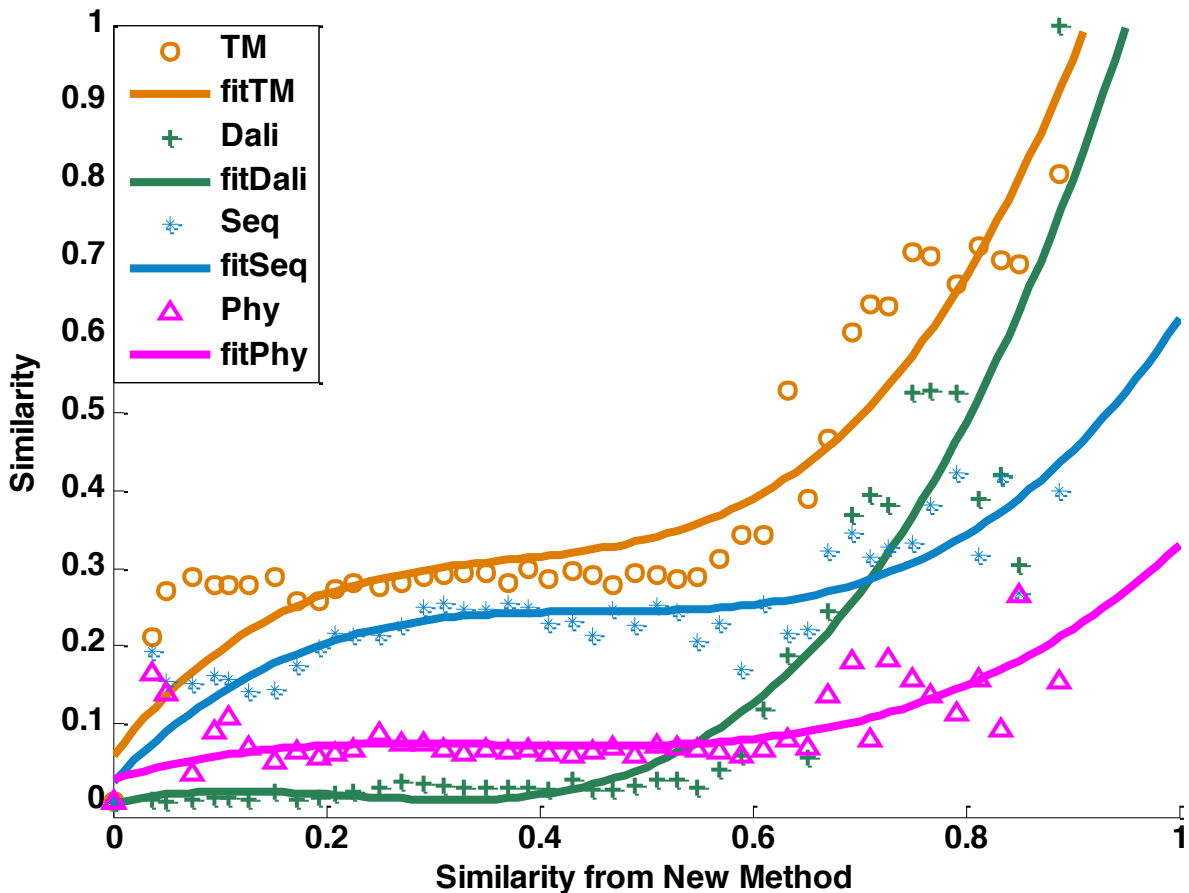


Figure 4.2 Correlation measurements based on BSM score.

Comparing tendency of similarity score based on structural, sequence, and phylogenetic similarity based on BSM score. To get the structural similarity two well-known alignments are used TM-align and Dali which are denoted as TM and Dali respectively. For the sequence similarity, pair-wise alignments are conducted and denoted as Seq. Phylogenetic profile similarity is denoted as Phy. To help reading the graph, fitted graph is also drawn and identified by adding prefix ‘fit’ in front of each method. Horizontal axis denotes functional similarity calculated by corresponding methods, and vertical axis denotes similarity score derived from three categories (i.e. structure, sequence, and phylogenetic profile)

Especially, by considering the facts that the number of annotated GPs without having structure information is much higher than the number of GPs with known structures [141], the potential usage of this method and its performance is very significant in the current stage of in-silico method for identifying protein functions.

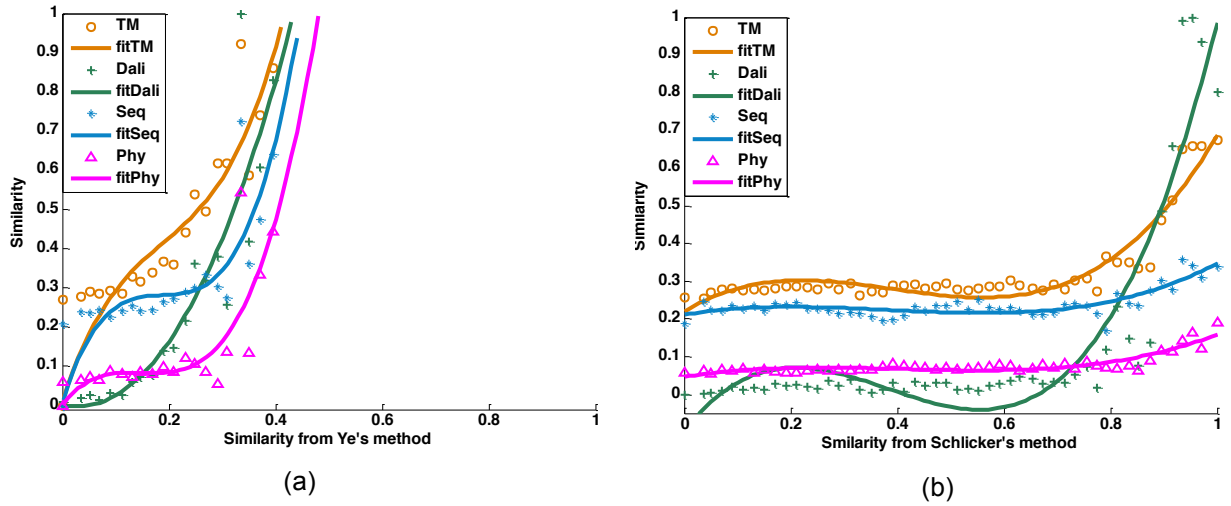


Figure 4.3 Correlation measurements with Ye and Schlicker's method.

Comparing tendency of similarity score based on structural, sequence, and phylogenetic similarity based on (a) Ye and (b) Schlicker's method.

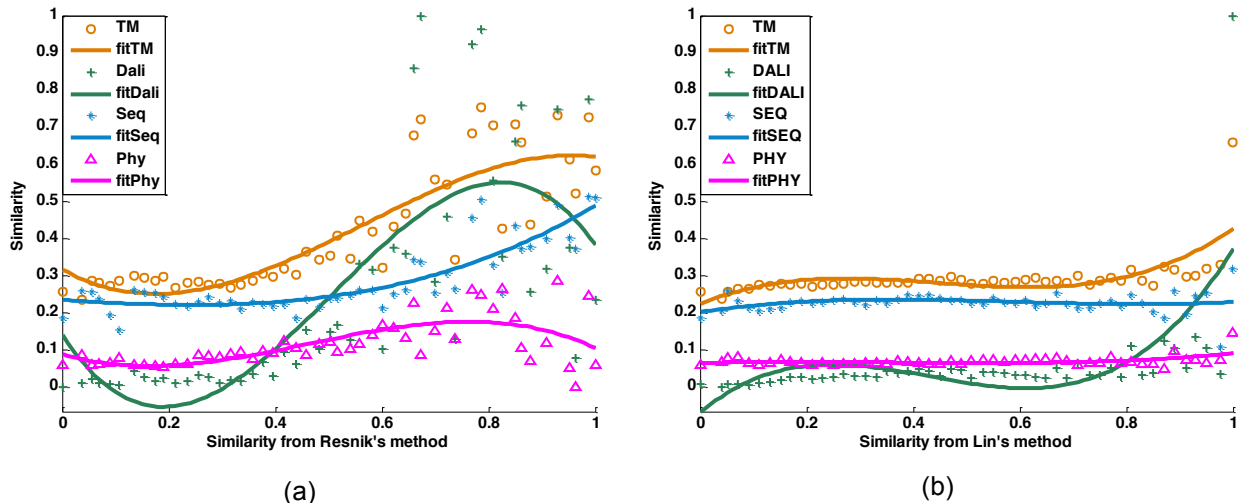


Figure 4.4 Correlation measurements with Resnik and Lin's method.

Comparing tendency of similarity score based on structural, sequence, and phylogenetic similarity based on (a) Resnik and (b) Lin's method.

In other words, this result shows the high possibility that the proposed method can devote identifying similar genes or GPs as accurate as structure based methods such as TM-align and DALI do. In fact, based on proposed criteria that the better similarity measurement tools should

bring the high agreement on correlations among three different similarity measurements, the evaluation shows that TM-align and the proposed method clearly outperform Dali.

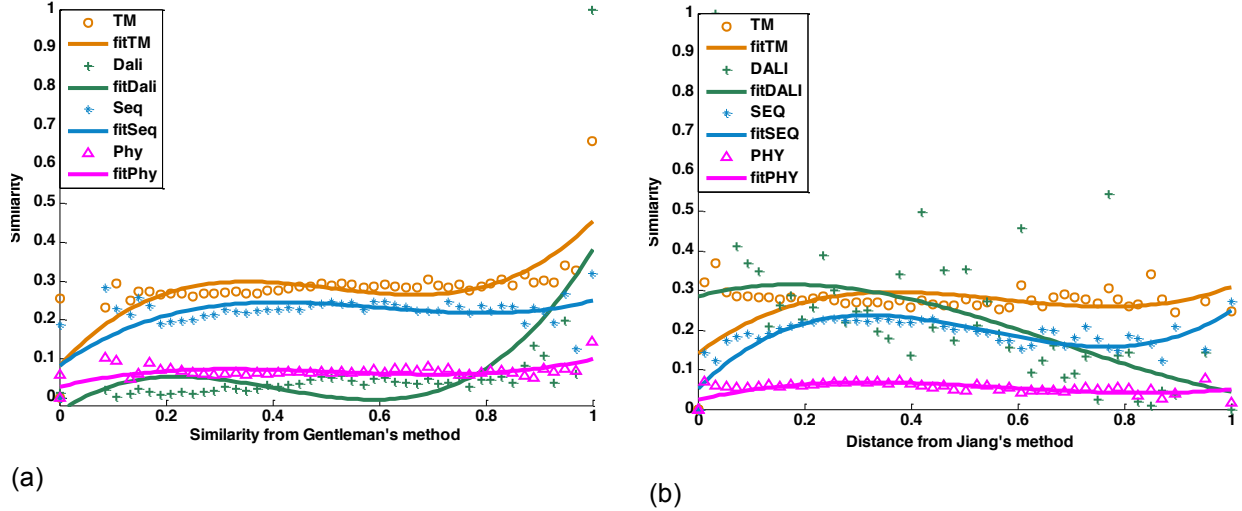


Figure 4.5 Correlation measurements with Gentleman and Jiang's method.

Comparing tendency of similarity score based on structural, sequence, and phylogenetic similarity based on (a) Gentleman and (b) Jiang's method.

Except the proposed method and Ye's method, all other methods are failed to make agreement on the tendency of similarity with others. Interestingly, violations of Dali on similarity tendency are observed across all methods except the proposed method and Ye's method such that in figures 4.3~5, the score range from 0.2 to 0.6, Dali score is anti-proportional to the scores derived from Schlicker, Lin, and Gentleman's methods. Resnik's method in Figure 4.4 (a) show two anti-proportional area: from 0 to 0.2 and from 0.8 to 1.0. Lin, Gentleman and Jiang's method which are Figure 4.4 (b), 4.5 (a), and 4.5 (b) respectively show similar tendency. Interestingly, their patterns are more likely to be the patterns derived from sequence similarity shown in Figure 4.1-(d) in which the similarity is mostly flat along with criteria similarities.

4.2 Experiment II: measuring clustering performances

4.2.1 Dataset

It is well known that proteins in SCOP classification at superfamily level tend to have common evolutionary origins and functional features. Indeed, the family level which is more specific level than superfamily has even more significant relations in terms of protein functions [62, 96]. Therefore, the given assumption is that proteins in same family category should be out expressed in similarity networks based on the score of functional similarity calculated by proposed method and other conventional methods since proteins in same SCOP family level has more functionally similar than protein in other family level. In similarity network each node corresponds to SCOP domain and edges correspond to the score of functional similarity. To emphasize the expression level or distinction between different family levels, threshold value is introduced such that the threshold value is considered as functional similarity score that can isolate one family group from others. In other words, threshold value is defined by changing the similarity score until the network reaches maximum number of clusters or highest precision depending on evaluation criteria. The maximum number of clusters is defined by counting total number of clusters in the network with a threshold value that produces the highest number of isolated clusters. The precision is defined as below.

$$precision = \frac{\# \text{ of misclustered edges}}{\text{total } \# \text{ of edges in a network}} \quad (\text{Equation 4-2})$$

Mis-clustered edges are defined as minority edges in a cluster. In other words, the majority edges belonging to a certain SCOP family is considered as a member of the true cluster.

4.2.2 Results

Upon the results of correlation comparisons, the BSM score and Ye's method do not show clear difference. In fact, both to them work very well, especially compared to the method requiring structure information (i.e. TM-align). To analyze the difference between the proposed method and others, the second evaluations are designed and conducted. The hypothesis of this evaluation is that if groups of functionally similar domains are known, then good similarity analyzer could group them together with certain range of similarity. This type of method is well known in machine learning area as clustering methods or unsupervised learning, but the difference between conventional clustering methods and this experiment is that in the given problem, the clusters are already known, so by comparing the results of clusters made by different methods and known clusters, performances and their differences among different algorithms can be compared. To compare the clustering performances of conventional methods and proposed method, all 2646 domains in SCOP databases are used as testing data such that the functional similarity of all possible combinations of SCOP domains (i.e. 3,501,517 domain pairs) are calculated by each similarity method including the proposed method. Once all similarity score is calculated, the threshold of similarity score for each method is adjusted until it reaches the best performance to which either it has maximum number of clusters or highest average precision. Figure 4.6 shows the maximum precision of each methods. In this result, both proposed method (NEW) and Ye's method reached maximum precision 1.0. However, by considering the similarity score 0.75 (75%) and 1.0 (100%), the proposed method has reached maximum precision in earlier stage.

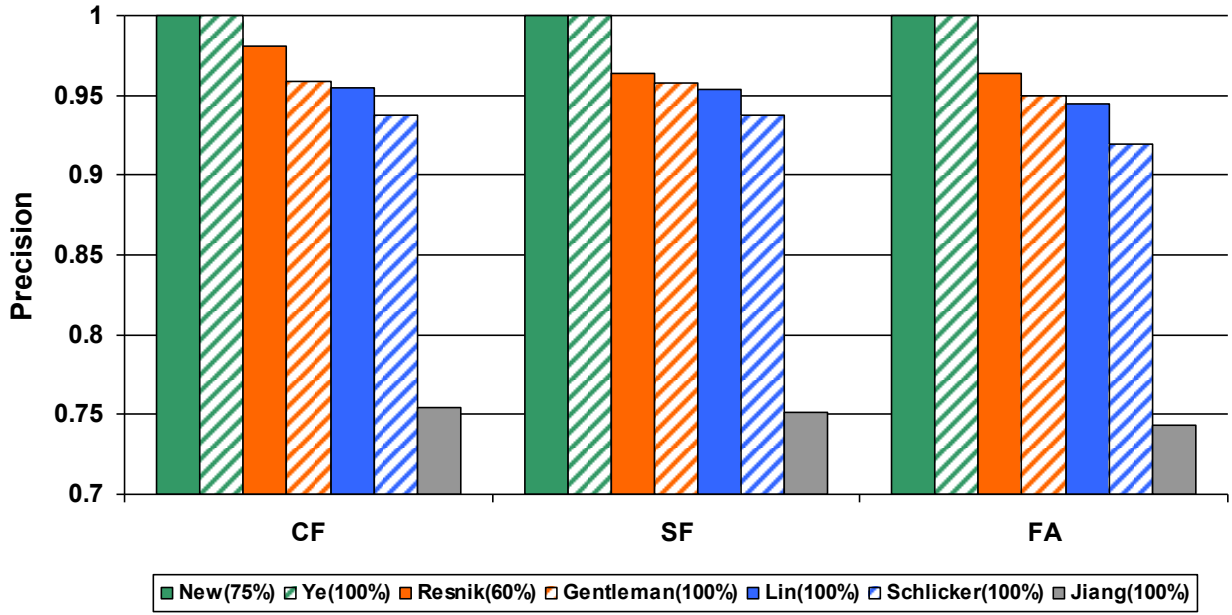


Figure 4.6 Comparing precisions among clusters.

The threshold to functional similarity score is changed until individual method reaches the best clustering performance at each criterion. Maximum precision of each method according to three different levels of domain family in SCOP classification: Class family (CF), Superfamily (SF) and Family (FA) in which the order corresponds to the broad classification to the most specific classification in SCOP definition. The values in parenthesis denote threshold rate.

Figure 4.7 shows the number of mixed domains. As expected, the proposed method and Ye's method do not have any mixed domains since both of them were reached 100% precision as shown in Figure 4.6. By considering the number of clusters between the proposed method and Ye's method as shown in Figure 4.8, the difference between the proposed method and Ye's method are very clear such that the proposed method outperforms Ye's method more than 20 folds with this criterion. Although Gentleman's method and Lin's method have better or similar performance upon the consideration of number of clusters, by considering the precision and number of mixed domains shown in Figure 4.6 and 4.7, their errors are far exceeded those of

BSM score. Therefore, by considering all three criteria, BSM score clearly outperforms all other conventional methods.

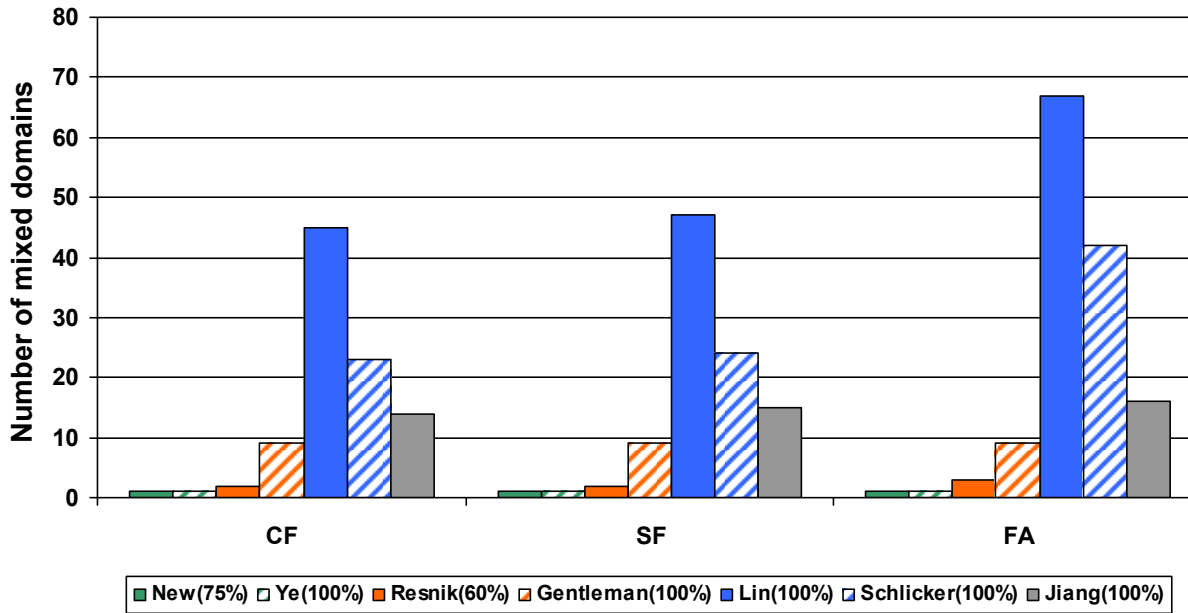


Figure 4.7 Comparing false clusters.

The threshold to functional similarity score is changed until individual method reaches the best clustering performance at each criterion. The average number of mixed domain families along with three different levels in SCOP classification: Class family (CF), Superfamily (SF) and Family (FA). The values in parenthesis denotes threshold rate.

Figure 4.8 shows the difference of the average number of clusters made by certain threshold among the methods such that with 70% of similarity rate, the proposed method clearly outperforms others, and with average above 70% of similarity rate, the proposed method, Gentleman, Lin, and Schlicker's method are comparative. This inconsistent result shows very interesting and critical point of view to define the balance between human cognition and the significance of score reflecting GP relations. Problems originated from normalized and

non-normalized scores are already discussed [64, 91], and although they share the same concept of human cognition at the level of interpreting the score, they show clear difference by considering the gaps between the score significance at algorithm level and user's expectation. In other words, what does the meaning of 70% similarity in each method? Are they can be considered as significant in terms of their functional relations? If the human cognition and the score significance were involved, the evaluation criteria would be more complicated. Unfortunately no study has been conducted on this issue, so as best of my knowledge believe this is the first time to claim the significance of human cognition at reported scores as important evaluation criteria.

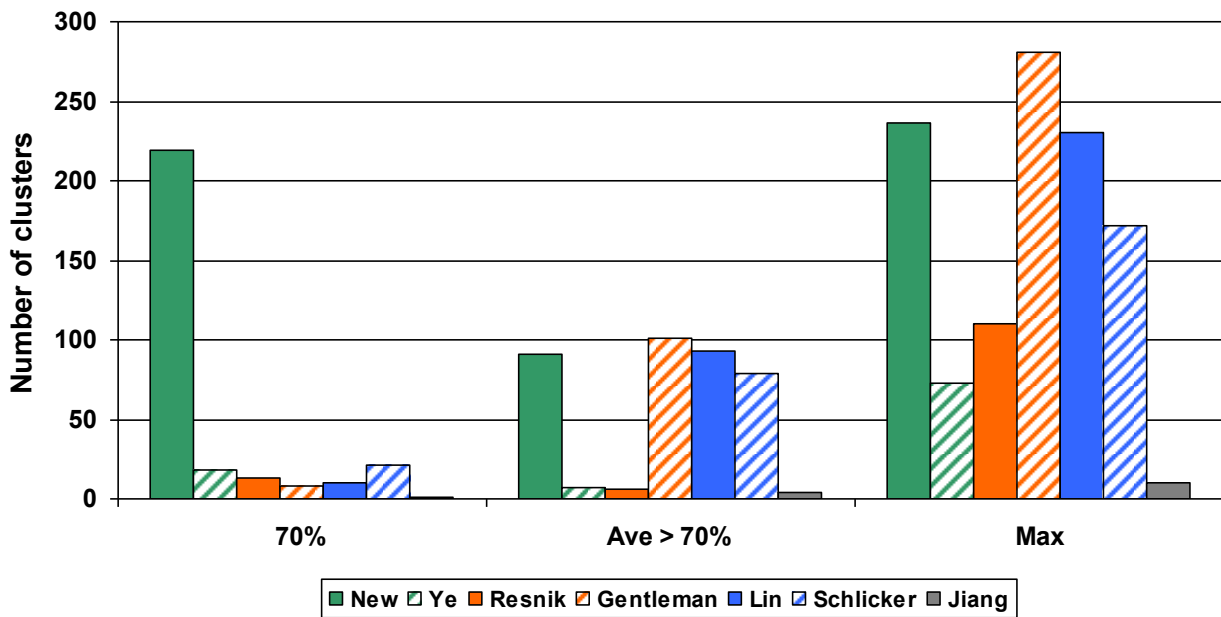


Figure 4.8 Comparing number of clusters.

The threshold to functional similarity score is changed until individual method reaches the best clustering performance at each criterion. Number of clusters identified by the given method with specific threshold range such that the first group of graphs is drawn with 70% of threshold, next group is drawn by averaging the identified number of clusters greater than 70% and the final group is shown to compare the maximum number of identified clusters.

Let's come back to the Figure 4.8, as shown in this figure, the proposed method, Ye and Resnik's methods shows smaller number of clusters by increasing the number similarity rate. In fact, the proposed method reached the maximum number of clusters on 65% similarity rate. Compared to these methods, Gentleman, Lin, Schlicker, and Jiang's method increase the number of cluster while increasing the similarity rate. Indeed, they reached the maximum number of clusters with 100% similarity. Two problems can be found in this result: i) they define the GPs in each cluster with exactly same similarity rate (i.e, 100% similarity) and ii) some of clusters consist of more than two domain families which show that even if GPs in a cluster have 100% similarities, this does not mean they function exact same although user's expectations are often considering 100% similarities are exact same or extremely similar. Indeed, the second group (i.e, Gentleman, Lin, Schlicker, and Jiang's method) would fail to further distinct GPs in a same cluster in such case they cannot narrow down potential neighboring gene or GPs to identify drug targets, so their contributions on this purpose could significantly reduced or limited. The more significant problem is that the question of how the score should be interpreted? Although 100% similarity rate is somewhat reliable as shown in the result, by considering the similarity rate 100% in general or as definition of their maximum similarity, the score does not match the results or user's expectation, which should be exact same genes or GPs. More directly, what does meaning of less than 100% similarity, and what is the significance of these scores that contribute identifying genes or GP similarity as a human cognition point of view? Although the question is very important since this can directly affects interpreting the results and can be propagated to making final decision of the essay or application, the answer is not easy due to the lack of guidelines in this issue. In order to answer this question, this issue is applied to one of criteria in performance evaluation. As shown in the results of precision, the results of proposed method

could be reliable if it reaches higher than 70% similarity. Indeed, the 100% similarity score will not be produced unless two GPs are consisted with exactly same GO terms. Therefore, as a human cognition point of view, the proposed method is only satisfied since Ye and Resnik's method have relatively high chance to produce maximum similarity score for GPs having different GO terms with same depth or the same number of annotated GPs.

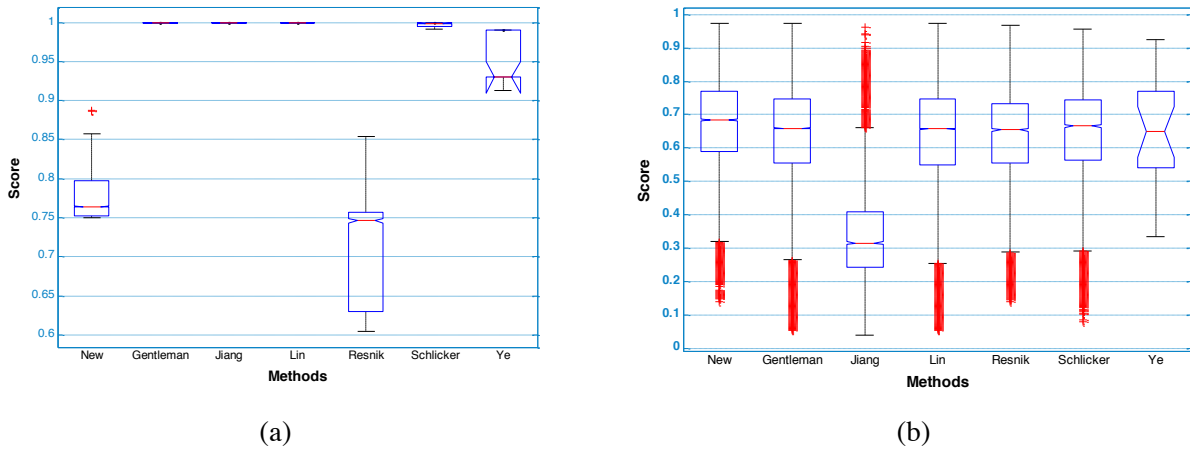


Figure 4.9 Analysis of statistical distributions.

Analyzing statistical distributions of similarity score based on three categories (i.e. structure, sequence, phylogenetic profile). The distributions are calculated from each clusters made by SCOP domains with maximum precision. Corresponding similarity rates are NEW 75%, Ye 100%, Resnik 60%, Gentleman 100%, Lin 100%, Schlicker 100% and Jiang 100%. (a) the distribution of GP similarity scores at the highest precision (b) the distribution of structural similarity calculated by TM-align at highest precision.

To analyze the clustering tendency, the distributions of five different base similarity measurements inside clusters are considered. Figure 4.9 (a) shows the distributions of GP similarity at the highest precision, and the proposed method and Resnik's method have lower similarity score than other methods. Interestingly the range of GP similarity at the proposed method is relatively larger than Gentleman, Jiang, Lin, and Schlicker's method and smaller than Resnik and Ye's method. It is important to have lower score with reaching the highest precision

since this gives more opportunity to further investigate the relations of inside clusters. In other words, BSM score is capable of identifying more specific relations within a cluster while maintaining stabilizing the range of human cognition. Therefore, based on two criteria, possibility of further investigation and the significance of similarity score at human cognition, BSM score clearly outperforms other methods.

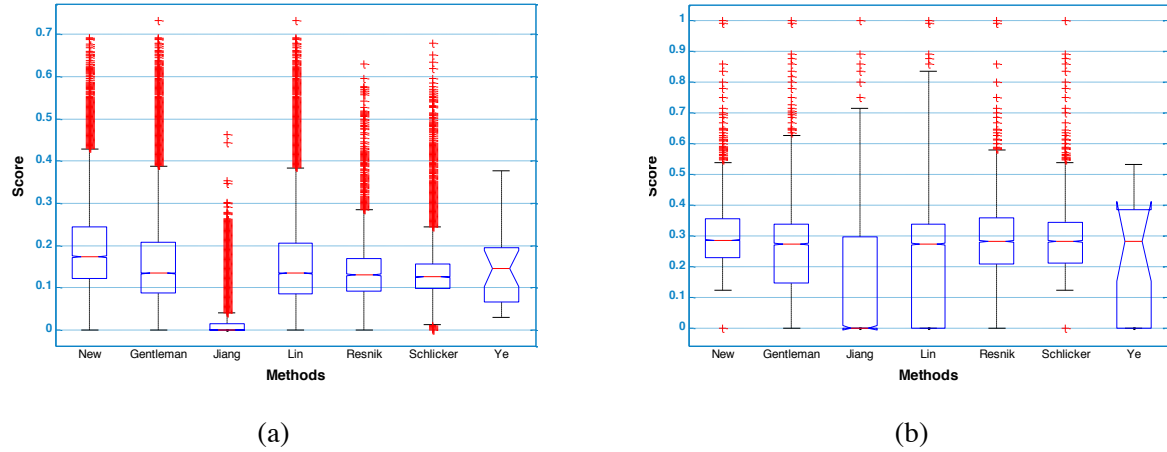


Figure 4.10 Analysis of statistical distributions.

Analyzing statistical distributions of similarity score based on three categories (i.e. structure, sequence, phylogenetic profile). The distributions are calculated from each clusters made by SCOP domains with maximum precision. Corresponding similarity rates are NEW 75%, Ye 100%, Resnik 60%, Gentleman 100%, Lin 100%, Schlicker 100% and Jiang 100%. (a) the distribution of structural similarity calculated by DALI at highest precision. (b) the distribution of sequence similarity at highest precision.

Figure 4.9 (b) and 4.10 (a) show the distribution of structural similarity at the highest precision calculated by TM-align and Dali respectively. With TM-align, although all methods tend to have high structural similarity, the proposed method and Ye's method slightly have higher structural similarity than others. The results from Dali make better discrimination the proposed method and others although their similarity score is lower than TM-align. The lower structural similarity is also observed in Figure 4.1 (b) and 4.4 (a). More importantly, the difference between proposed

method and Ye's method is much clear. The sequence similarity in Figure 4.10 (b) shows that the proposed method, Resnik and Schlicker's method have relatively higher and denser sequence similarity than others.

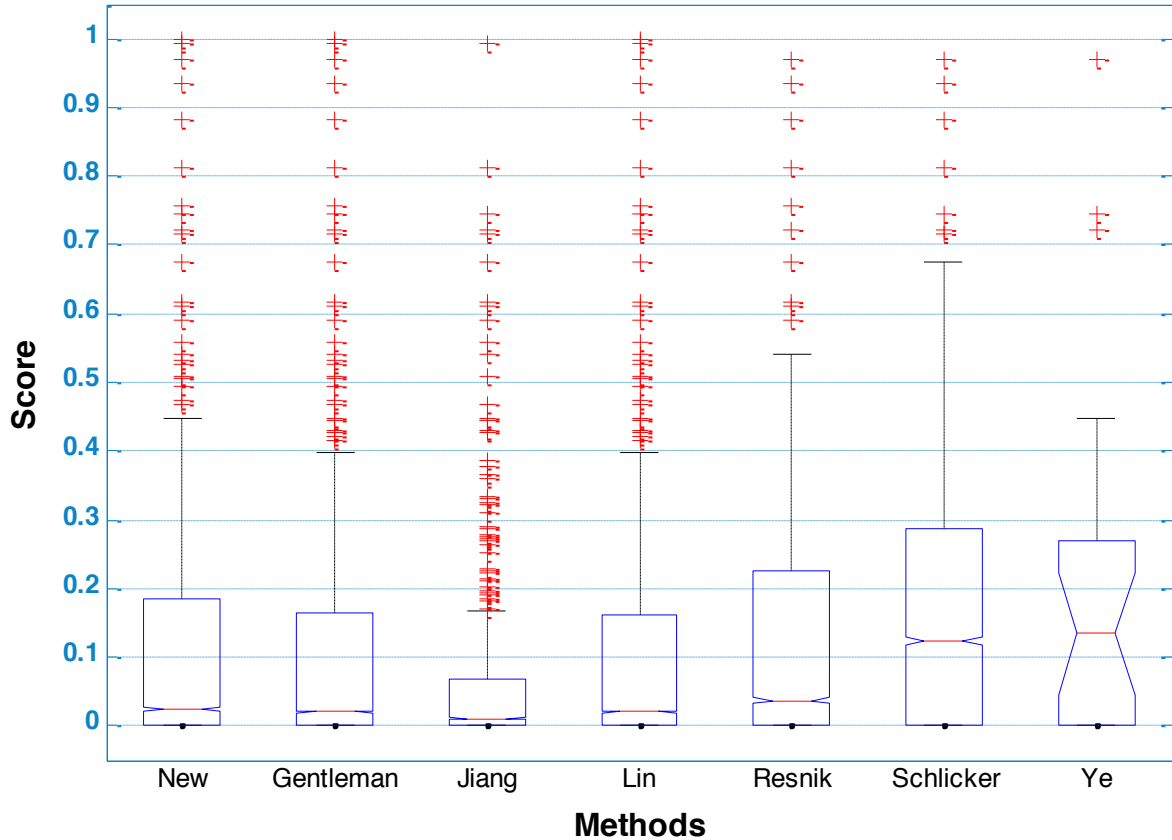


Figure 4.11 Analysis of statistical distributions.

Analyzing statistical distributions of similarity score based on three categories (i.e. structure, sequence, phylogenetic profile). The distributions are calculated from each clusters made by SCOP domains with maximum precision. Corresponding similarity rates are NEW 75%, Ye 100%, Resnik 60%, Gentleman 100%, Lin 100%, Schlicker 100% and Jiang 100%. the distribution of phylogenetic profile similarity at the highest precision.

Although the results of phylogenetic profile similarity shown in Figure 4.11 shows that Schlicker and Ye's method have slightly higher profile similarity score than others, by considering outliers and the upper and lower quartile, the difference of phylogenetic profile similarity distributions is

not significant. In short, the proposed method outperforms other methods at several criteria: the ability of discriminating specific relations with high precision, providing stabilized significance of similarity score at human cognition level, and relatively higher structural and sequence similarity.

To get the broad spectrum of clustering tendency, the changes of clusters are further analyzed by continuously increasing the threshold of similarity score of each method.

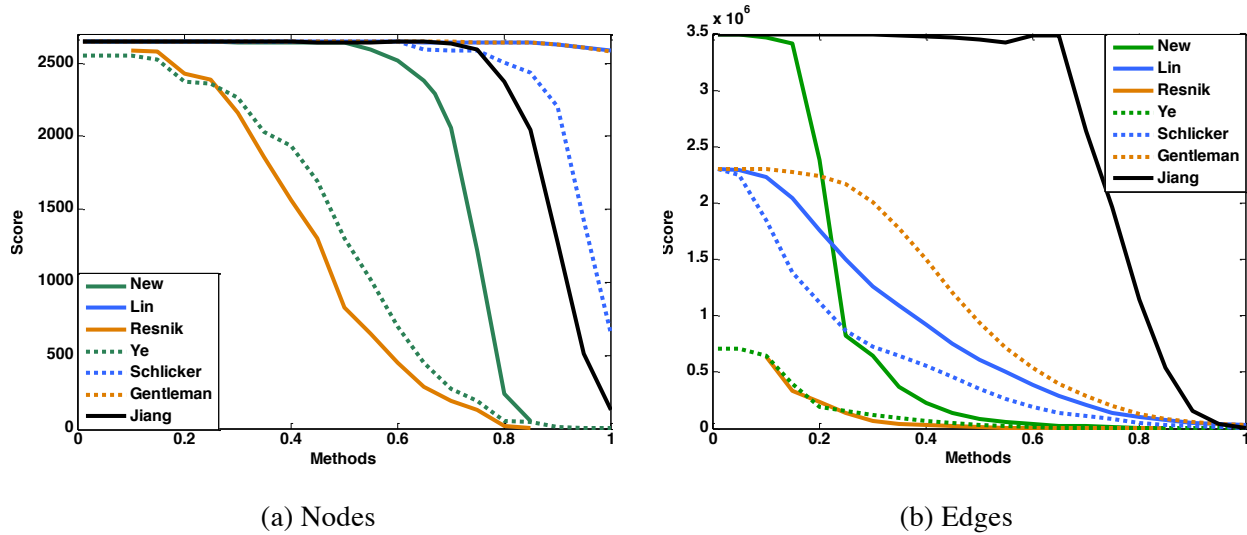


Figure 4.12 Tendency of clusters upon nodes and edges.

Analyzing the tendency of clusters while changing the threshold of similarity score defined by individual methods. Horizontal axis denotes the threshold of similarity score, and vertical axis denotes score of each category. (a) *Nodes* are the individual domains in clusters at the given threshold. (b) *Edges* are the relations connecting two nodes in clusters at the given threshold. In SCOP classification, class-family, super-family, and family is ordered list from broader to the more specific classification level.

The graph *Nodes* in Figure 4.12 (a) shows that all methods dramatically decrease the number of nodes at a certain threshold except Lin and gentleman's method which do not show significant changes in the number of nodes. For example, the proposed method has significant decrease of the number of nodes at the threshold value around 0.7, but Lin's and Gentleman's method stays

at same number as the proposed method has at similarity score around 0.7. In contrast to node changes, the patterns of *edge* changes in Lin and Gentleman's method are similar to others.

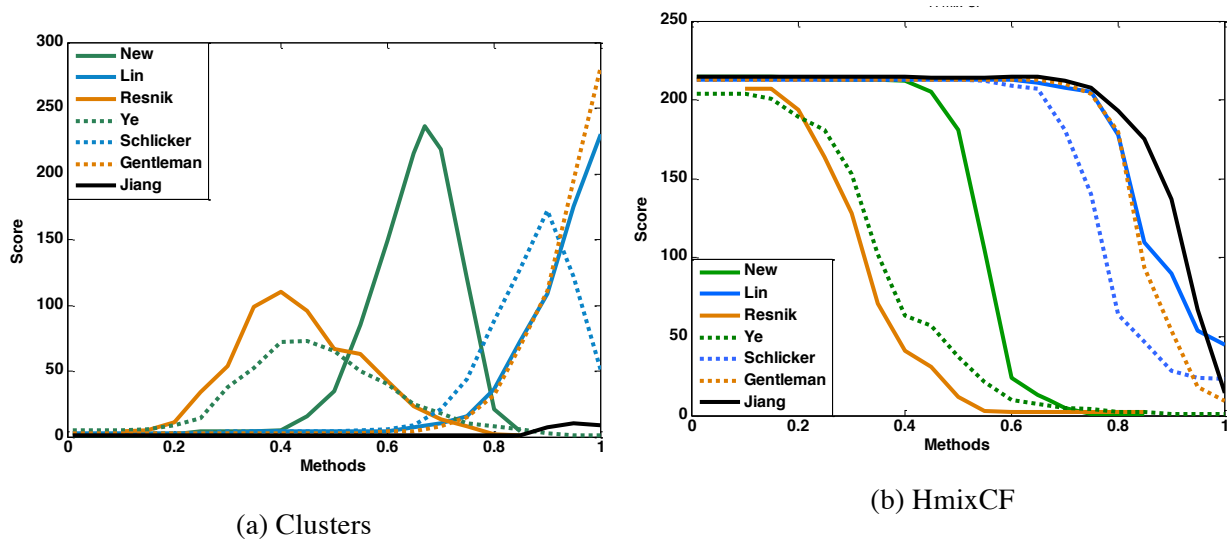


Figure 4.13 Tendency of clusters upon clusters and highest false class family clusters.

Analyzing the tendency of clusters while changing the threshold of similarity score defined by individual methods. Horizontal axis denotes the threshold of similarity score, and vertical axis denotes score of each category. (a) Clusters are the total number of isolated groups at the given threshold. (b) HmixCF denotes the highest number of misclassified edges among all clusters at the level of 'class-family' in SCOP classification. In SCOP classification, class-family, super-family, and family is ordered list from broader to the more specific classification level.

The patterns of *cluster* changes show Lin and Gentleman's reaches the highest number of clusters with the proposed method, but their patterns are different from others such that they only have the ascent of graph and descent does not exist. Indeed, overall graphs from *Nodes*, *Edges*, and *Clusters* show that clusters made by Lin and Gentleman's method have relatively sparse relations than others. These characteristics of Lin and Gentleman's method imply that their methods are not favorable for identifying specific relations at higher similarity score. Indeed, this can be problematic when identifying the threshold of trust level is required.

Figure 4.13 (b), 4.14, 4.15, and 4.16 (a) are measuring the highest number of edges in mixed clusters and precision at three different classification levels: class-family, super-family, and family which are Figure 4.13 (b) HmixCF, 4.14 (a) HmixSF, 4.14 (b) HmixFA, 4.15 (a) precCF, 4.15 (b) precSF, and 4.16 (a) precFA respectively.

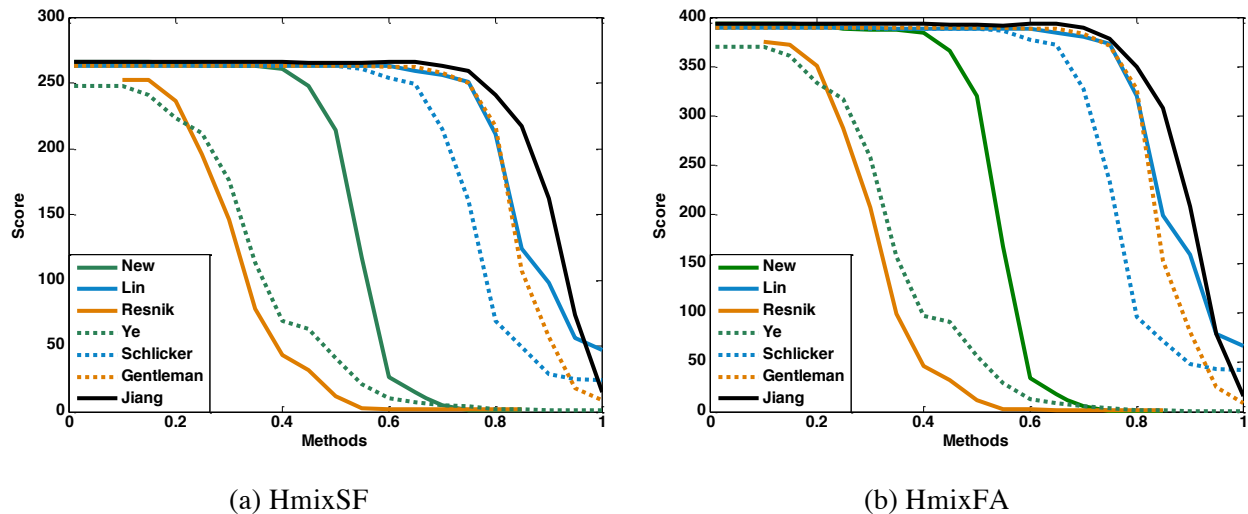


Figure 4.14 Tendency of clusters upon highest false super family clusters and family clusters.

Analyzing the tendency of clusters while changing the threshold of similarity score defined by individual methods. Horizontal axis denotes the threshold of similarity score, and vertical axis denotes score of each category. (a) *HmixSF* denotes the highest number of misclassified edges among all clusters at the level of ‘super-family’ in SCOP classification. (b) *HmixFA* denotes the highest number of misclassified edges among all clusters at the level of ‘family’ in SCOP classification. In SCOP classification, class-family, super-family, and family is ordered list from broader to the more specific classification level.

Ideal similarity analyzer should have high correlation between similarity score and corresponding precisions, and inverse correlation between similarity score and the number of misclassified GP pairs. More precisely, if the similarity analyzer is practically useful then it should give clear relations between significance of scores and functional similarity such that if

the score is getting higher then the precision should be same or getting higher by eliminating unrelated gene or GPs, and the number of misclassified GP pairs should be decreased.

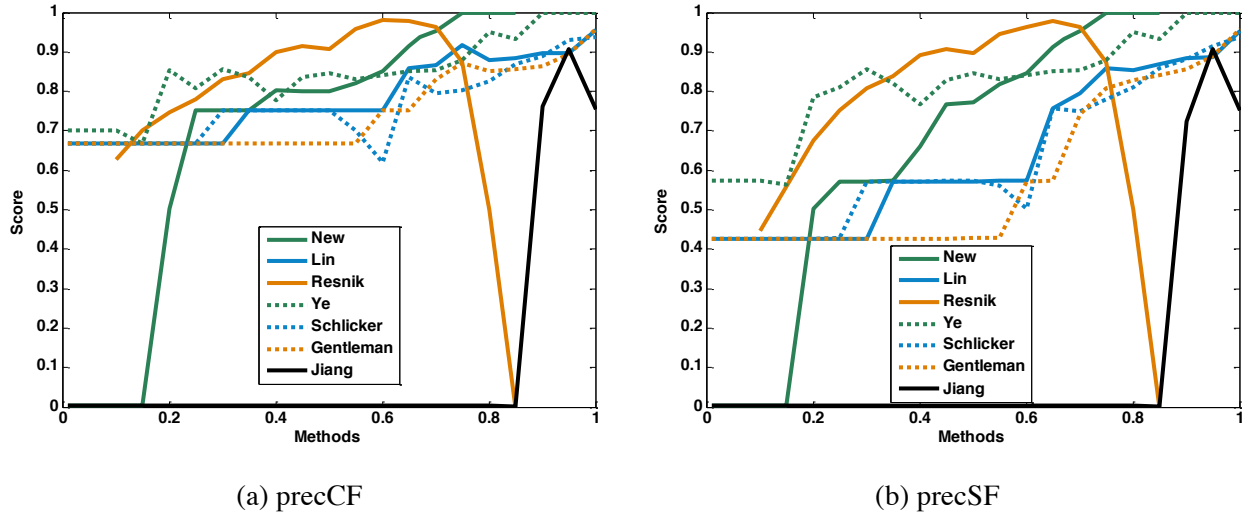


Figure 4.15 Tendency of precision upon class family and super family.

Analyzing the tendency of clusters while changing the threshold of similarity score defined by individual methods. Horizontal axis denotes the threshold of similarity score, and vertical axis denotes score of each category. (a) *precCF* denotes an averaged precision from all clusters at the level of 'class-family' in SCOP classification. (b) *precSF* denotes an averaged precision from all clusters at the level of super-family in SCOP classification. In SCOP classification, class-family, super-family, and family is ordered list from broader to the more specific classification level.

Figures based on precision which are Figure 4.15 and 4.16 (a) show that all methods decrease the number of misclassified GPs while increasing the similarity score, but Lin, Gentleman, Schlicker, and Jiang's methods do not reached to get complete clusters of which all GP pairs are correctly clustered. Interestingly the patterns of mixed domain families are almost conserved along with different levels of domain families although the number of misclassified GP pairs is increased as narrowing down to domain families. This implies that each method has its own confidence level for similarity score, and the confidence level must be conserved for all different levels of domain families while preserving smallest number of misclassified GP pairs.

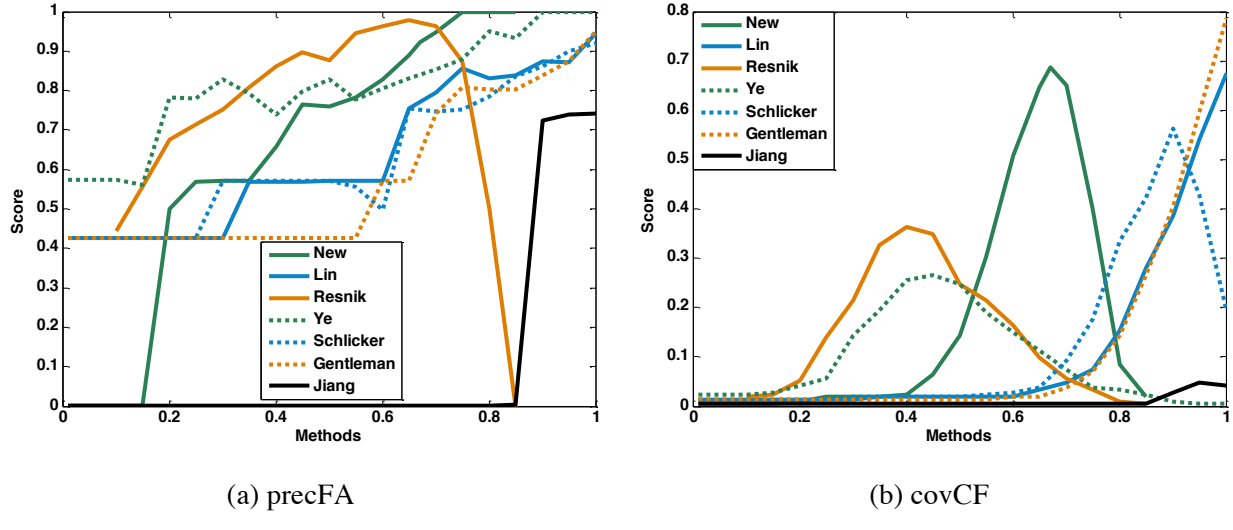


Figure 4.16 Tendency of precision upon family and of coverage upon class family.

Analyzing the tendency of clusters while changing the threshold of similarity score defined by individual methods. Horizontal axis denotes the threshold of similarity score, and vertical axis denotes score of each category. (a) *precFA* denotes an averaged precision from all clusters at the level of ‘family’ in SCOP classification. (b) *covCF* denotes an averaged coverage from all clusters at the level of class-family in SCOP classification. In SCOP classification, class-family, super-family, and family is ordered list from broader to the more specific classification level.

To make a better comparison and get clearer picture of confidence range, let’s look closer into the precision graphs. These precision graphs show that the proposed method only has strong correlations along with precision score. For example, Lin and Gentleman’s method decrease their precision by increasing the similarity score from 0.7 to 0.8. Resnik’s method shows dramatic changes of precision after the threshold similarity 0.7; this happens since the clusters made with higher similarity scores are composed with small number of GP pairs and almost all of them are mixed with more than two domain families. Rest of methods, Ye, Schlicker, and Jiang’s method, are even more fluctuated. These results show that the proposed method is well characterized with

its confidence rate and similarity score by preserving consistent correlation between precision and similarity score.

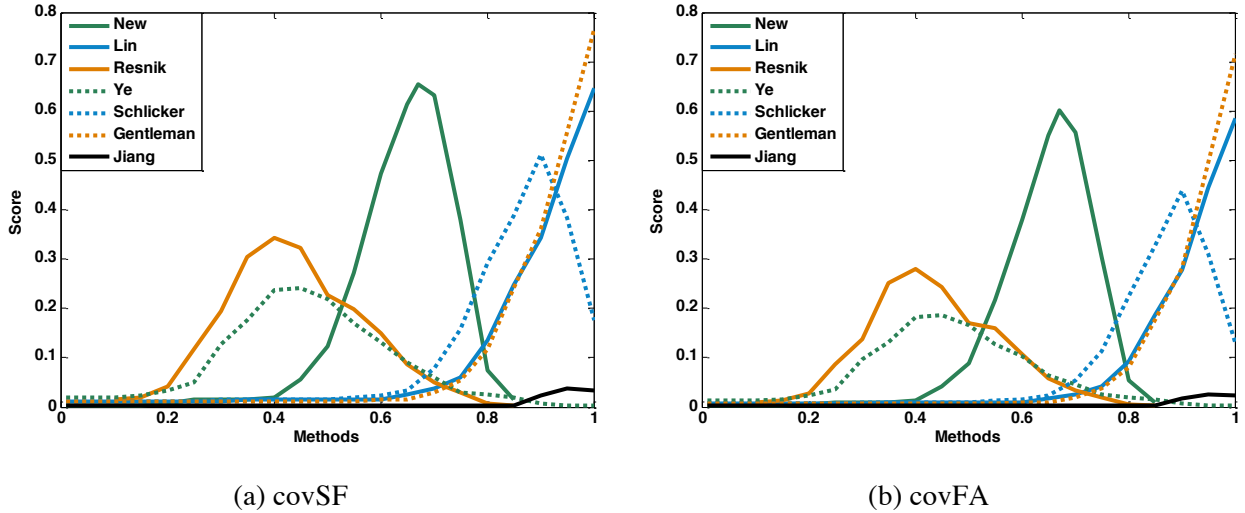


Figure 4.17 Tendency of coverage upon super family and family.

Analyzing the tendency of clusters while changing the threshold of similarity score defined by individual methods. Horizontal axis denotes the threshold of similarity score, and vertical axis denotes score of each category. (a) covSF denotes an averaged coverage of clusters from all clusters at the level of ‘super-family’ in SCOP classification. (b) covFA denotes an averaged coverage from all clusters at the level of ‘family’ in SCOP classification. In SCOP classification, class-family, super-family, and family is ordered list from broader to the more specific classification level.

Figure 4.16 (b) and 4.17 show mean coverage of clusters defined by each method. Every method shows same tendency that broader definition of domain family has the higher coverage. BSM score has obtained one of the highest coverage along with Lin and Gentleman's method.

So far, the results show that the proposed method outperforms conventional methods, and some of methods are compatible to the proposed method. However, the details of differences are still unclear. To further explore on this issue, the direction of investigation is switched to approaching opposite way, such that instead of analyzing successfully classified clusters, mixed clusters are analyzed to understand the behavior of similarity methods. In order to get mixed

clusters, the threshold of the BSM score is set to 0.7 which is corresponding to the second highest precision of the method (i.e, the score 0.75 reached 100% precision). Ye's method has too small number of GPs at 95% similarity score which corresponds to the second highest precision of this method.

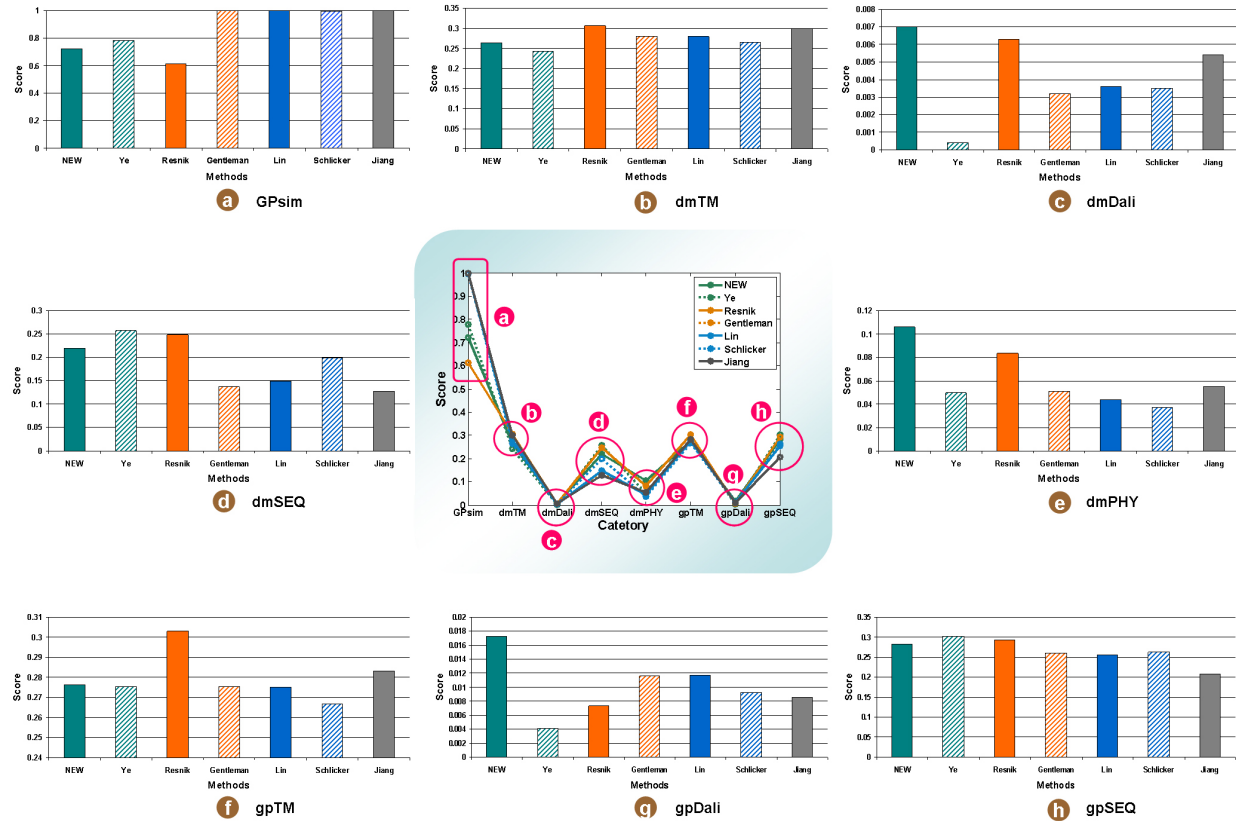


Figure 4.18 Distributions of score in mixed clusters.

The graphs are drawn by analyzing clusters consisting with mixed domain families. Horizontal and vertical axis of each graph show the name of methods involved in this experiments and corresponding scores respectively. The graph in the center highlighted with green background shows the overall patterns of measurement. Each dot in this Figure is enlarged corresponding to their alphabetic index. (a) GPsim: Averaged similarity score calculated by each method (b) dmTM: averaged domain similarity calculated by TM-align (c) dmDali: averaged domain similarity calculated by Dali (d) dmSEQ: averaged sequence similarity of SCOP domain (e) dmPHY: averaged phylogenetic profile similarity of SCOP domain (f) gpTM: averaged GP similarity calculated by TM-align (g) gpDali: averaged GP similarity calculated by Dali (h) gpSEQ: averaged sequence similarity of GPs.

Therefore, to get statistically meaningful number of GPs, the threshold is reduced to 75% similarity. All other methods are obtained with their highest precision since they did not reach the 100% precision. As discussed previously, Figure 4.18 (a) shows that Gentleman, Lin, schlicker and Jiang are not suitable for identifying closely related domains from others since the similarity score of mixed clusters already reaches its maximum score. In Figure 4.18 (b) and (c), although all methods show that misclassified GP pairs have relatively lower structure similarity than majority ones which are shown in Figure 4.9 (b) and 4.10 (a), except Jiang's method which relatively conserved than others. BSM score and Resink's methods are relatively higher similarity on both TM and DALI. Figure 4.18 (d) shows that New, Ye and Resnik's methods tend to conserver the sequence similarity similar with majority ones sown in Figure 4.10 (b). Figure 4.18 (e) shows that the phylogenetic profile similarity in mixed clusters have maintained slightly higher score than average of majority ones, especially for BSM score and Resinik's method. Overall scores of mixed clusters show that domains clustered by proposed method and Resnik's method are closely related by the means of three similarity criteria. To understand relations between domain and GPs, GPs containing each domain are retrieved from SCOP, and corresponding structure and sequence information are downloaded from PDB. The structure similarity of these GPs calculated by TM-align shows that Resnik and Jiang's method obtain higher score than others while the proposed method remains as similar as others. However, Dali shows different results such that BSM score has relatively higher score than others. The sequence similarity shown in Figure 4.18 (h) show that New, Ye, and Resnik's method get relatively higher score. Overall results from examining mixed clusters, BSM score and Resnik's method constantly show that the mixed class has strong relations of the remaining clusters.

However, by considering all comparisons including correlations of similarity score against to structure, sequence, and phylogenetic profile scores, precision and coverage of clusters, and statistics on pure and mixed clusters, the proposed method constantly outperforms all other methods although some methods show compatible performance at certain experiment. More importantly, analyzing the results obtained from mixed clusters shows that misclassified domains in a mixed cluster has somewhat strong relations to other dominant domains since their similarities cannot be distinct from majority domains by structure, sequence and phylogenetic profile similarity. Therefore, it is of great interest to figure out the biological relations between minor and majority domains in a cluster defined by the proposed method.

Analyzing clusters with mixed SCOP families: As continuous analysis on mixed clusters defined by the proposed methods, the relations between heterogeneous SCOP families defined by proposed method are investigated. To get the mixed clusters, similarity score 0.7 is used as similarity threshold. Figure 4.19 shows a cluster consisting with three different families: *Ferritin* (47241), *2Fe-2S ferredoxin-related* (54293), and *purple acid phosphatase-like* (56301) in which the numbers in parenthesis correspond to *sunid* in SCOP classification. *Ferritin* is one of the major non-heme iron storage proteins in animals, plants, and microorganisms [142, 143]. It consists of a mineral core of hydrated ferric oxide, and a multi-subunit protein shell which encloses the former and assures its solubility in an aqueous environment. Purple acid phosphatases (PAPs) are ubiquitous binuclear metal-containing acid hydrolases characterized by their acidic pH optima and their intense purple color due to a TyrO-to-FeIII charge-transfer transition [143].

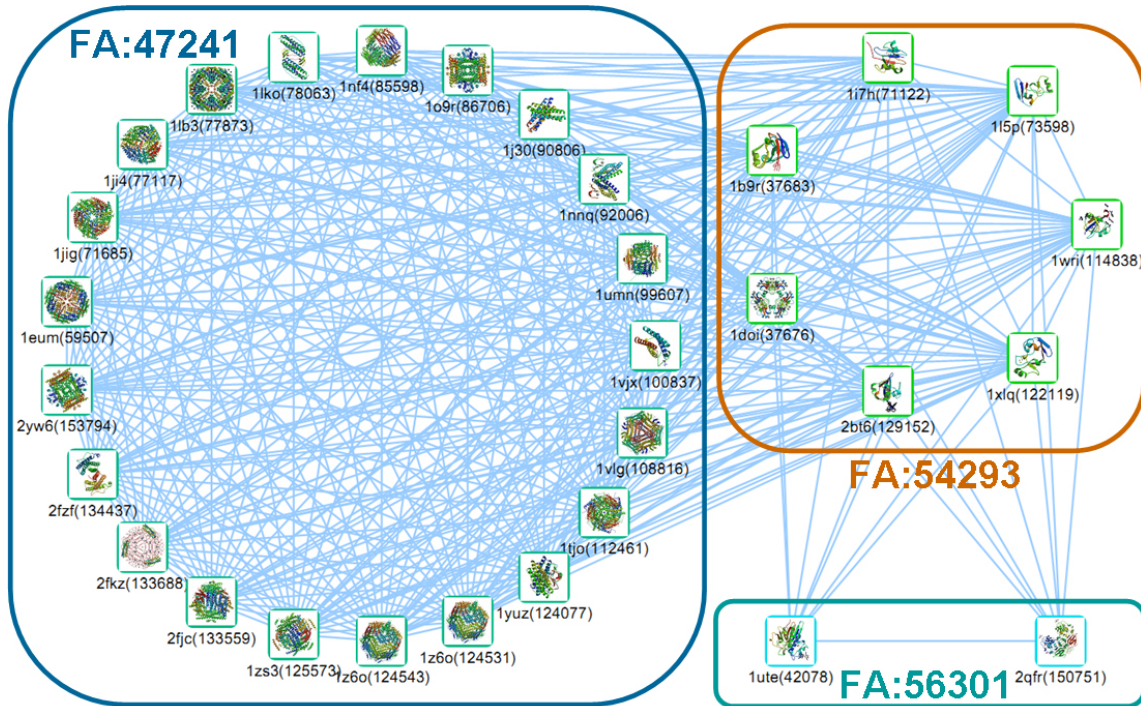


Figure 4.19 Analysis of mixed families of FA:47241, FA:54293, and FA:56301.

Analyzing relations of mixed SCOP families defined by the proposed method with 70% similarity. The numbers in parenthesis correspond to sunid in SCOP classification. 1UTE and 2QFR are associated with FA:56301 which is Purple acid phosphatase-like. 1B9R, 1I7H, 1L5P, 1WRI, 1XLQ, 2BT6, and 1DOI are associated with FA:54293 which is 2Fe-2S ferredoxin-related. All others are associated with FA:47241 which is Ferritin.

Therefore, it seems 2Fe-2S ferredoxin makes strong relation between Ferritin and Purple acid phosphatases by the roles of electron-transfer carriers and donors since 2Fe-2S ferredoxins function as electron carriers in the photosynthetic electron transport chain and as electron donors to various cellular proteins [144]. In hydroxylating bacterial dioxygenase systems, they serve as intermediate electron-transfer carriers between reductase flavoproteins and oxygenase [145].

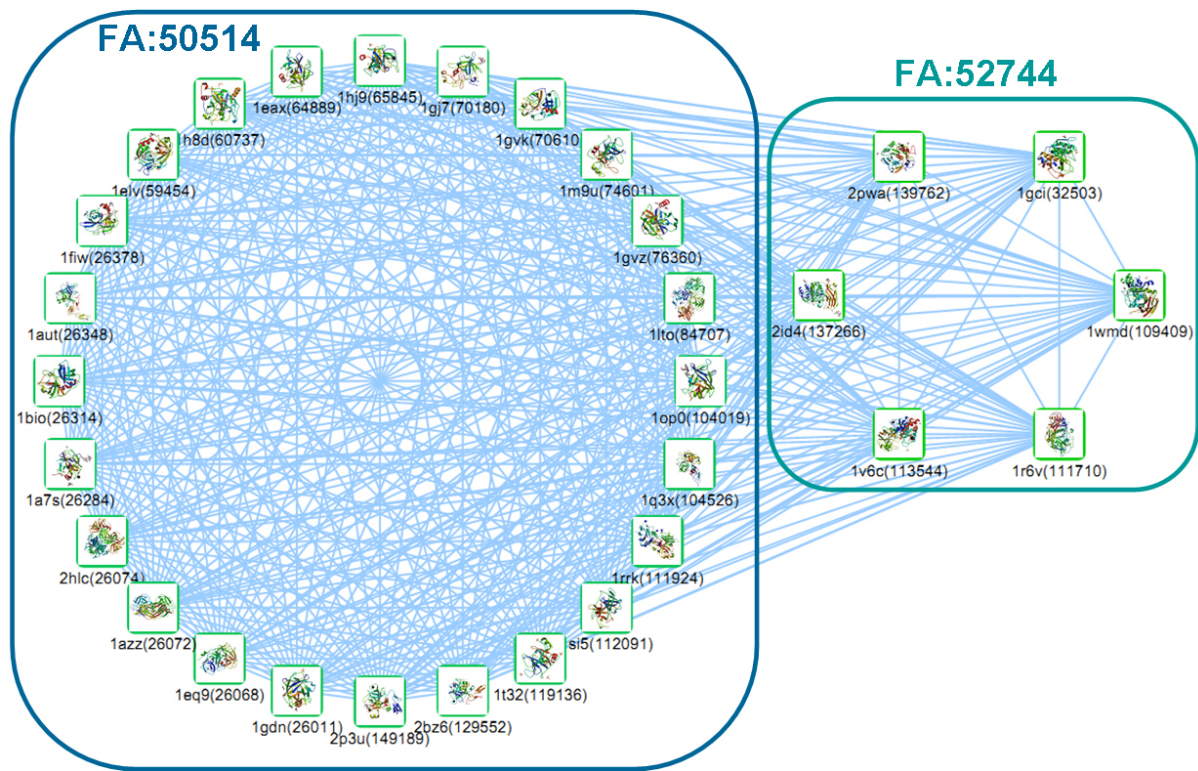


Figure 4.20 Analysis of mixed families of FA:50514 and FA:52744.

Analyzing relations of mixed SCOP families defined by the proposed method with 70% similarity. The numbers in parenthesis correspond to sunid in SCOP classification. 2PWA, 1GCI, 1WMD, 1R6V, 1V6C, and 2ID4 are associated with FA:52744 which is Subtilases family and all others are associated with FA:50514 which is Eukaryotic proteases family.

Figure 4.20 shows a cluster consisting with two different families: *Eukaryotic protease* (50514) and *Subtilases* (52744). Two families are clearly related to their functional roles such that *Subtilases* are a family of subtilisin-like serine proteases and *Eukaryotic protease* is also protease found specially in *Eukaryotic*. This means both of them are enzymes related to hydrolysis of the peptide bonds in proteins although serine is serving as the nucleophilic amino acid at the active site [146] and more widespread so that this can be found in eubacteria, archaebacteria, eukaryotes and viruses [147].

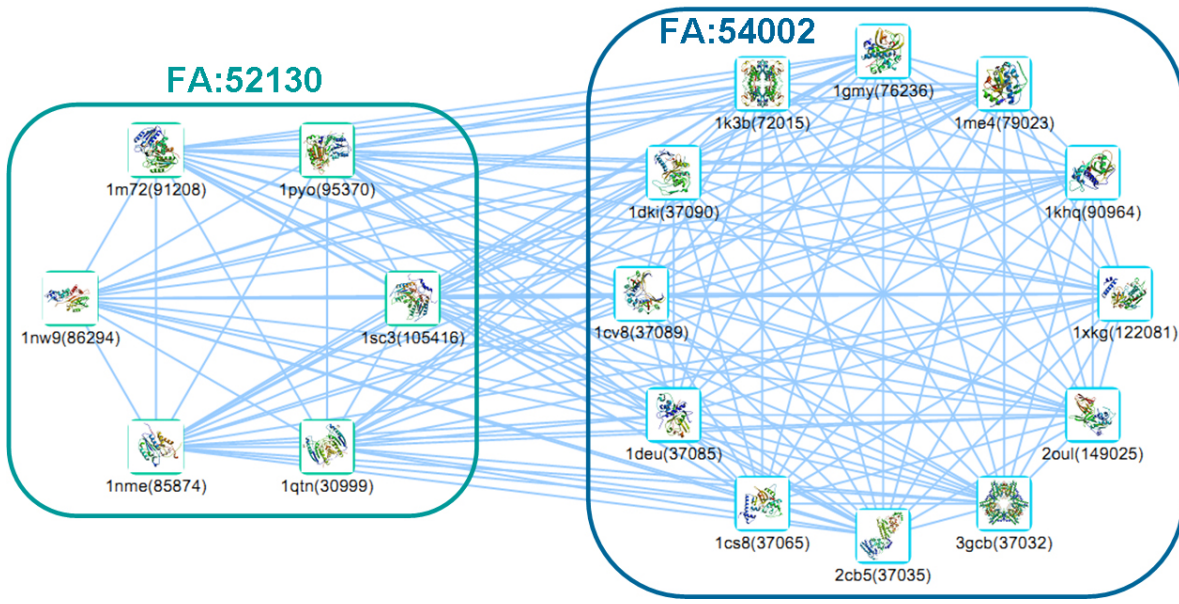


Figure 4.21 Analysis of mixed families of FA:52130 and FA:54002.

Analyzing relations of mixed SCOP families defined by the proposed method with 70% similarity. The numbers in parenthesis correspond to sunid in SCOP classification. 1M72, 1PYO, 1SC3, 1QTN, 1NME, and 1NW9 are associated with FA:52130 which is Caspase catalytic domain family and all others are associated with FA:54002 which is Papain-like family.

Figure 4.21 shows a cluster consisting with two different SCOP families: *Caspase catalytic domain* (52130) and *Papain-like* (54002). These two families are closely related to apoptosis which is known as programmed cell death and immunization such that Caspases are a family of cysteine proteases that play essential roles in apoptosis, necrosis, and inflammation [148], and Papain is involved in deprotonation of Cys-25 by His-159 and known to cleave the Fc which is crystallisable portion of antibodies from the Fab which is antigen-binding portion [149].

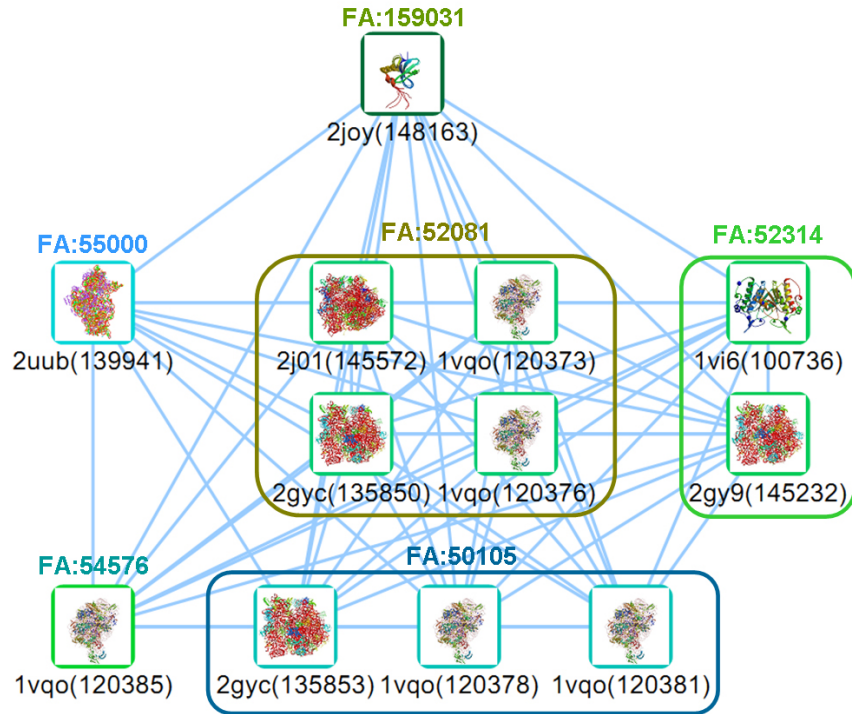


Figure 4.22 Analysis of mixed families of FA:159031, 55000, 52081, 52314, 54576, and 50105.

Analyzing relations of mixed SCOP families defined by the proposed method with 70% similarity. The numbers in parenthesis correspond to sunid in SCOP classification. 2JOY is associated with FA:159031 which is Ribosomal protein L14e. 2UUB is associated with FA:55000 which is Ribosomal protein S10. 1VQO (suid:120385) is associated with FA:54576 which is Ribosomal protein L31e. 1VI6 and 2GY9 are associated with FA:52314 which is Ribosomal protein S2. 2GYC and two 1VQOs consisting of sunid 120378 and 120381 are associated with FA:50105 which is Ribosomal proteins L24p and L21e. 2J01, 1VQO (sunid: 120373, 120376), and 2GYC are associated with FA:52081 which is Ribosomal proteins L15p and L18e.

Figure 4.22 shows a cluster consisting with six different families: Ribosomal protein L14e (159031), Ribosomal proteins L24p (50105), Ribosomal protein S10 (55000), Ribosomal protein L31e (54576), Ribosomal protein S2 (52314), and Ribosomal proteins L15p and L18e (52081). As appeared in their names, they are the ribosomal proteins that make up ribosomal subunits involved in cellular process of translation. Indeed, Ribosomal protein L14e (159031) and Ribosomal proteins L24p (50105) are the subgroup of super-family, translation proteins SH3-like domain (50104).

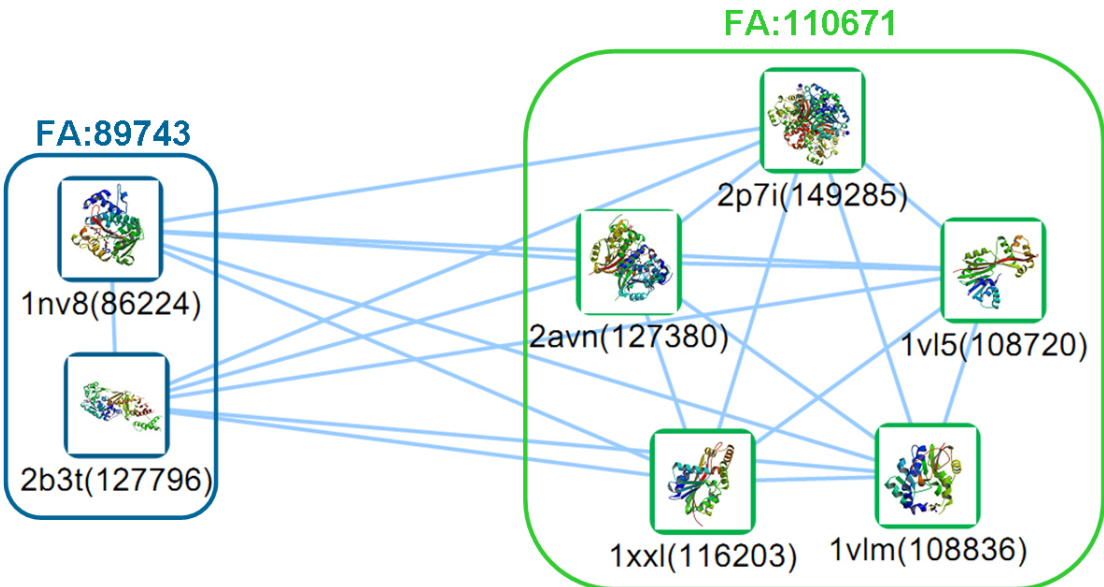


Figure 4.23 Analysis of mixed families of FA:89743 and FA:110671.

Analyzing relations of mixed SCOP families defined by the proposed method with 70% similarity. 1NV8 and 2B3T are associated with FA:89743 which is N5-glutamine methyltransferase, HemK family and all others are associated with FA:110671 which is UbiE/COQ5 methyltransferase family.

Figure 4.23 shows a cluster consisting with two different families: *N5-glutamine methyltransferase, HemK* (89743) and *UbiE/COQ5 methyltransferase* (110671). As shown in their names, both of them are a *methyltransferase* which also known as a methylase and transfers a methyl group from a donor to an acceptor [150]. Indeed, they are the subgroup of superfamily *S-adenosyl-L-methionine-dependent methyltransferases* (53335) which is found primarily in bacteria.

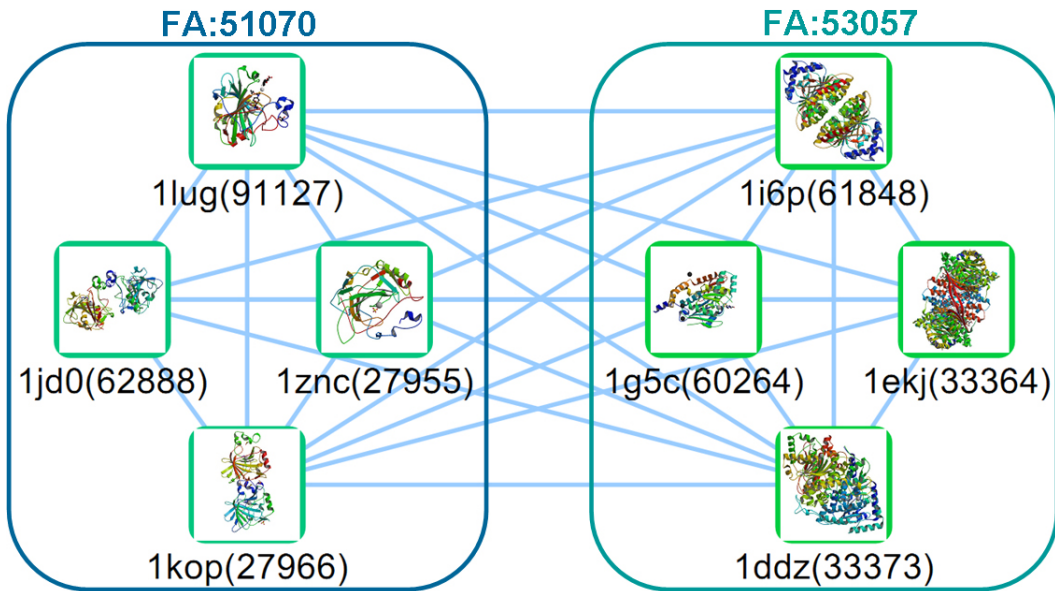


Figure 4.24 Analysis of mixed families of FA:51070 and FA:53057.

Analyzing relations of mixed SCOP families defined by the proposed method with 70% similarity. 1JD0, 1KOP, 1LUG, and 1ZNC are associated with FA:51070 which is Carbonic anhydrase family and all others are associated with FA:53057 which is beta-carbonic anhydrase, cab family.

Figure 4.24 shows a cluster consisting with two different families: *Carbonic anhydrase* (51070) and *beta-carbonic anhydrase, cab* (53057). As shown in their names, both of them are the *carbonic anhydrases* which form a family of enzymes that catalyze the rapid interconversion of carbon dioxide and water to protons and bicarbonate which is also known as hydrogen carbonate, an intermediate form in the deprotonation of carbonic acid [151].

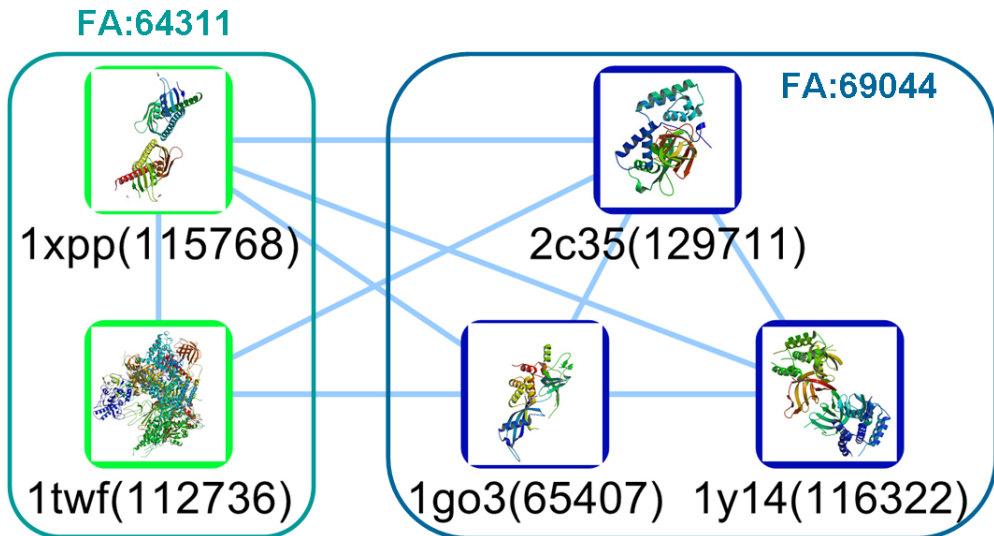


Figure 4.25 Analysis of mixed families of FA:64311 and FA:69044.

Analyzing relations of mixed SCOP families defined by the proposed method with 70% similarity. 1XPP and 1TWF are associated with FA:64311 which is RBP11/RpoL and all others are associated with FA:69044 which is RNA polymerase II subunit RBP4 (RpoF).

Figure 4.25 shows a cluster consisting with two different families: *RBP11/RpoL* (64311) and *RNA polymerase II subunit RBP4 (RpoF)* (69044). These two different families are closely related as the subunit of retinol-binding proteins (*RBP*) which are carrier proteins that bind retinol, and retinol plays a crucial role in the growth and differentiation of various body tissues [152]. Indeed, they also share the functions of RNA polymerases as subunit of DNA-directed RNA polymerases which are responsible for the polymerisation of ribonucleotides that produces RNA [153].

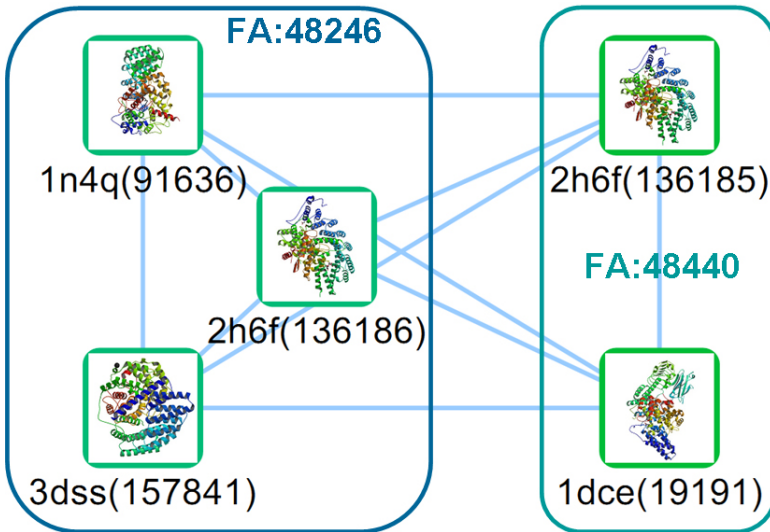


Figure 4.26 Analysis of mixed families of FA:48246 and FA:48440.

Analyzing relations of mixed SCOP families defined by the proposed method with 70% similarity. 2H6F and 1DCE are associated with FA:48440 which is Protein prenyltransferase and all others are associated with FA:48246 which is Protein prenyltransferases.

Figure 4.26 shows a cluster consisting with two different families: *protein prenyltransferase* (48440) and *protein prenyltransferases* (48246). As shown in their names, both families function as prenyltransferases which are a class of enzymes that transfer allylic prenyl groups to acceptor molecules [154].

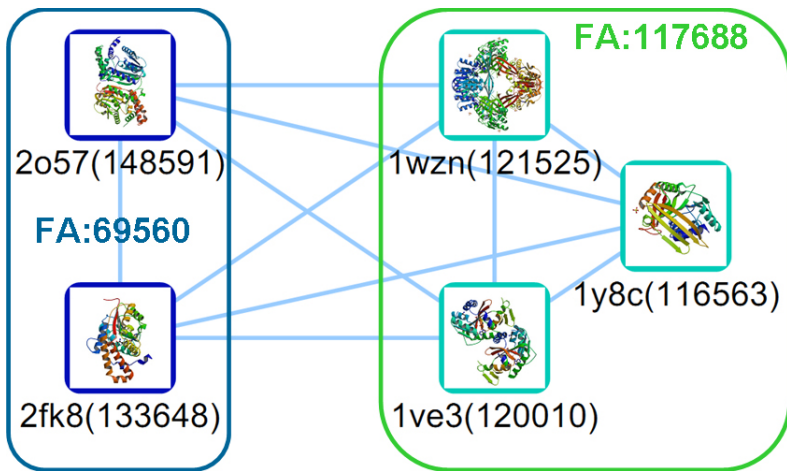


Figure 4.27 Analysis of mixed families of FA:69560 and FA:117688.

Analyzing relations of mixed SCOP families defined by the proposed method with 70% similarity. 2O57 and 2FK8 are associated with FA:69560 which is Mycolic acid cyclopropane synthase and all others are associated with FA:117688 which is CAC2371-like family.

Figure 4.27 shows a cluster consisting with two different families *Mycolic acid cyclopropane synthase* (69560) and *CAC2371-like* (117688). These two families are subgroup of super-family, *S-adenosyl-L-methionine-dependent methyltransferases* (53335). Indeed, *Mycolic acid cyclopropane synthase* corresponds to Enzyme Commission (EC) 2.1.1.79 which is a *cyclopropane-fatty-acyl-phospholipid synthase*, the family of transferases that catalyzes the transfer of a methyl group from the donor to Delta9-olefinic acyl chain in phosphatidylethanolamine, phosphatidylglycerol or phosphatidylinositol [155], and CAC2371 corresponds to EC 2.1.1.- which is Methyltransferase. Putative methyltransferase including *Hydroxymycolate synthase* (2fk8) which transfers a methyl group from the S-adenosylmethionine (SAM) cofactor and, subsequently or simultaneously, a water molecule onto the double bound of ethylene substrates, leading to the formation of the hydroxylated product at the distal position [156]. By considering the facts that SCOP classification is based on

structural similarity, and R_{scr} is derived from SCOP classification, the expected scores are supposed to highly correlated to structural similarity. However, the final integrated scores (i.e, both R_{scr} and G_{scr}) show that overall scores tend to give higher scores to the mixed families having similar roles or functions than structural similarity. For example, in Figure 4.22 and 4.24~6, their functional roles are very much the same as expected from their names, but they do not share any common classification level until it reaches the top level structure classification. This observation is very important to explain the results showing lower structural similarity in cluster consisting of mixed families than clusters consisting of same family. Indeed, this analysis shows that the proposed methods are neither dominant at structural similarity nor other specific similarities, but the method more importantly considers the similarity in roles and functions in GPs. In fact, this result clearly shows that the proposed bidirectional integration method well fit the goal of this study, identifying functional similarity.

It is possible to argue that the previous experiments are not fair to compare the performance between the proposed method and others since SCOP classification is already integrated in the proposed method as one of the features making R_{scr} . However, by considering the fact that the SCOP itself is considered as one of features to define final score, and R_{scr} itself cannot reconstruct SCOP since the SCOP classification is reinterpreted to get statistical significance of GO relations. Nevertheless, it is still interesting to evaluate and compare the proposed method in different ways. More detailed analysis about each cluster is attached to [S-10] at supplementary section.

4.3 Experiment III: identifying new disease related genes

4.3.1 Dataset

To identify disease related genes, OMIM dataset is derived from previous studies of Schlicker et al. [60]. OMIM provides information about genetic disorders and related human genes, and the dataset used in experiments contains total 99 disease and 413 genes. OMIM dataset used in the experiments are listed in supplementary material [S-11]. To identify the relations between genes and specific disease, all possible pairs derived from 413 genes are involved to get their similarity scores from BSM score and other conventional methods. Based on the score, OMIM disease network is constructed, and their relations are emphasized by using the threshold of functional similarity. In order to compare the performances, the threshold is changed until all methods involved in this experiment get reasonable results.

4.3.2 Results

Online Mendelian Inheritance in Man (OMIM) database [157] is used to collect disease related genes. OMIM contains information about human gene and genetic disorders. For the experiments total 99 disease and 413 genes are retrieved from OMIM. Functional similarities are calculated from all possible pairs of genes. The results from all methods are drawn in Figure 4.28. The Figure located in top left of Figure 4.28 is drawn with 70% similarity as a threshold. As previously discussed as human cognition issue, the score showing greater than 50% similarity should give some meaningful information if the similarity range from 0 to 1.0 is considered. However, the results show that none of them give any meaningful results. It may imply that the scoring scheme applied in conventional method is somewhat different from human cognition, or at least it requires extra efforts or processes to determine problem dependent threshold value.

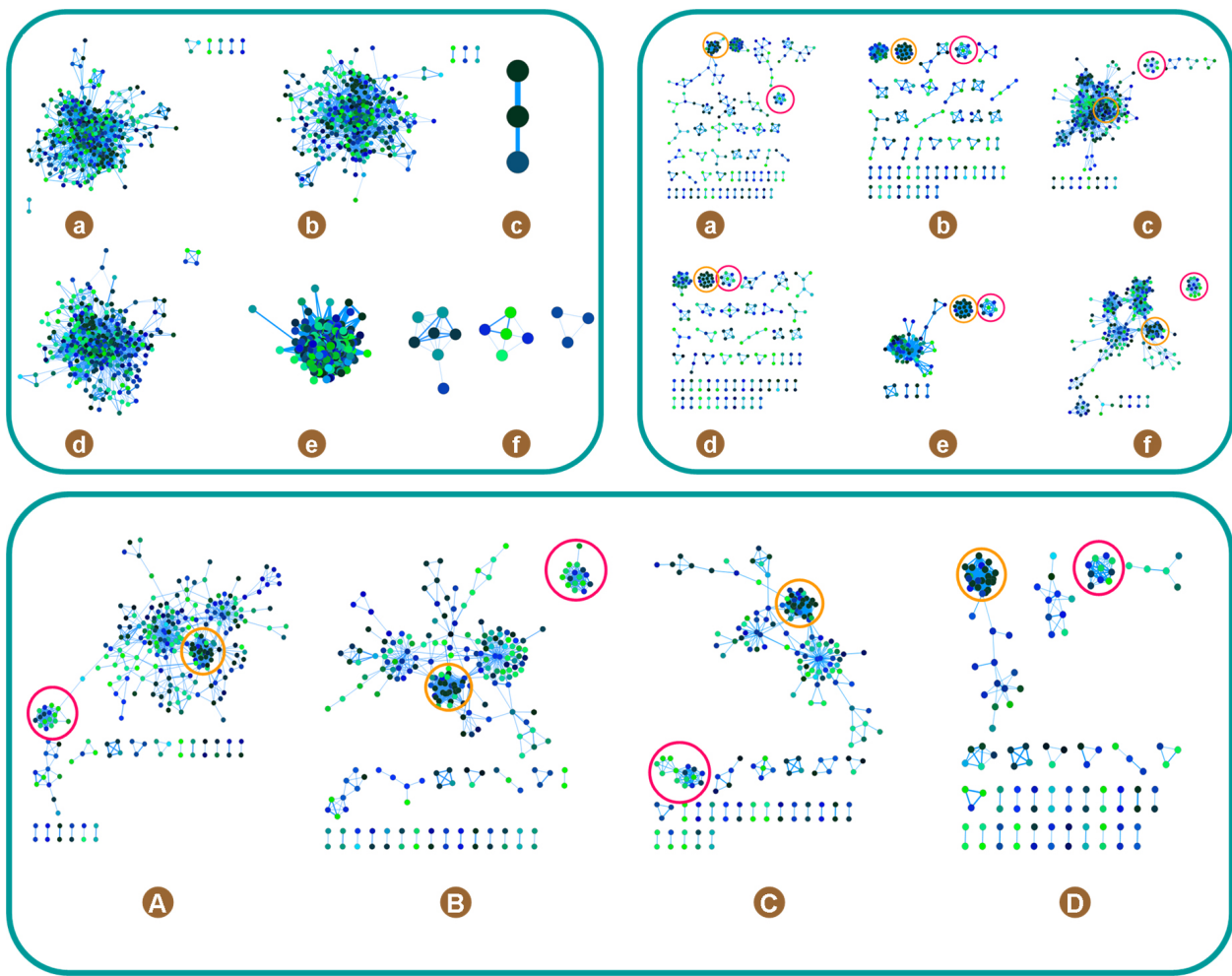


Figure 4.28 OMIM network generated by different methods.

OMIM network with threshold: 1) top-left: threshold with 70% GP similarity. 2) top-right: clusters identified with highest precision measured by SCOP definition. Two distinct clusters are identified by all methods which are emphasized by yellow and red circles. 3) Bottom – the variations of network upon changing threshold of new methods. Lower case a~f indicates Schlicker (1.0), Lin (1.0), Resnik (0.6), Gentleman (1.0), Jaing (1.0), and Ye's method (1.0) respectively in which the number in parenthesis indicates threshold value. Upper cases A~D in the bottom Figure indicate GP similarity greater than 0.6, 0.65, 0.7, and 0.75 respectively.

In fact, to find optimized values for following experiments, threshold values with finding maximum number of target genes are used such that Schlicker with 0.85, Lin with 0.9, Resnik with 0.3, Gentleman with 0.9, Jaing with 0.95, and Ye with 0.35 in which the order corresponds

to lower case of alphabet from ‘*a*’ to ‘*f*’ in both top-left and top-right of Figure 4.28. We note that the optimal threshold values used in following experiments and previous experiments are different as using the threshold corresponding to maximum number of clusters and the highest precision respectively. As shown above, the threshold value of certain methods is dramatically changed based on the given problem. For example, Ye and Resnik’s method were 0.35 and 0.3 in current experiment respectively, and 1.0 and 0.6 chosen by producing highest precision on SCOP clustering problem respectively. In contrast to these cases, the proposed method is very stable on choosing threshold. In fact this varied between 0.65 and 0.75. Again, this experiment also shows the importance of human cognition between the calculated score and functional similarity. To illustrate the changes of network based on similarity scores, Figure 4.28 is drawn as changing the threshold of the proposed method. As expected, the structure of network is more intuitive than other conventional methods as showing the different levels of information while changing the threshold value. Interestingly no matter what methods were applied, in Figure 4.28, all methods have two distinct disease groups: mitochondrial deficiency related disease which is enclosed by a red circle and diseases dominated by protocadherin beta which is enclosed by a yellow circle.

To further explore the differences of similarity analyzers, mitochondrial deficiency related disease are analyzed since at the current stage, resources in this group have more specific information than the other group. In fact, literatures show that some diseases are strongly associated with mitochondrial deficiency related disease which is the target cluster. *Leber optic atrophy* is a mitochondrially inherited degeneration of retinal ganglion cells and their axons that leads to an acute or subacute loss of central vision; this affects predominantly young adult males [158].

Table 4.1 Disease-related genes identified by BSM score.

UniProt ID	DISEASE	EC	GENE	Name of Protein	OMIM
P03891	LEBER OPTIC ATROPHY	1.6.5.3	MT-ND2	NADH-ubiquinone oxidoreductase chain 2	535000
P03901	LEBER OPTIC ATROPHY	1.6.5.3	MT-ND4L	NADH-ubiquinone oxidoreductase chain 4L	535000
P03915	LEBER OPTIC ATROPHY	1.6.5.3	MT-ND5	NADH-ubiquinone oxidoreductase chain 5	535000
O75251	LEIGH SYNDROME	1.6.5.3	NDUFS7	NADH dehydrogenase [ubiquinone] iron-sulfur protein 7, mitochondrial	256000
O00217	LEIGH SYNDROME	1.6.5.3	NDUFS8	NADH dehydrogenase [ubiquinone] iron-sulfur protein 8, mitochondrial	256000
P49821	LEIGH SYNDROME	1.6.5.3	NDUFV1	NADH dehydrogenase [ubiquinone] flavoprotein 1, mitochondrial	256000
P03897	LEIGH SYNDROME	1.6.5.3	MT-ND3	NADH-ubiquinone oxidoreductase chain 3	256000
P03923	MELAS SYNDROME	1.6.5.3	MT-ND6	NADH-ubiquinone oxidoreductase chain 6	540000
P03905	MELAS SYNDROME	1.6.5.3	MT-ND4	NADH-ubiquinone oxidoreductase chain 4	540000
P03886	MELAS SYNDROME	1.6.5.3	MT-ND1	NADH-ubiquinone oxidoreductase chain 1	540000
	MITOCHONDRIAL			NADH dehydrogenase [ubiquinone] 1 alpha subcomplex subunit 1	
O15239	COMPLEX I DEFICIENCY	N/A	NDUFA1	NADH-ubiquinone oxidoreductase 75 kDa	252010
	MITOCHONDRIAL			subunit, mitochondrial	
P28331	COMPLEX I DEFICIENCY	1.6.5.3	NDUFS1	NADH dehydrogenase [ubiquinone] iron-sulfur protein 1, mitochondrial	252010
	MITOCHONDRIAL				
O43181	COMPLEX I DEFICIENCY	N/A	NDUFS4	NADH dehydrogenase [ubiquinone] iron-sulfur protein 4, mitochondrial	252010
	MITOCHONDRIAL				
Q8N183	COMPLEX I DEFICIENCY	N/A	NDUFAF2	Mimitin, mitochondrial	252010
	MITOCHONDRIAL			NADH dehydrogenase [ubiquinone] iron-sulfur protein 2, mitochondrial	
O75306	COMPLEX I DEFICIENCY	1.6.5.3	NDUFS2	Succinate dehydrogenase [ubiquinone] iron-sulfur subunit, mitochondrial	252010
P21912	PHEOCHROMOCYTOMA	1.3.5.1	SDHB		171300

Leigh syndrome is a rare neurometabolic disorder caused by mutations in mitochondrial DNA and leads to loss of head control and motor skills by affecting the central nervous system [159].

Melas syndrome is one of the families of mitochondrial cytopathies caused by defects in the mitochondrial genome which is inherited purely from the female parent and leads to vision loss, problems with movement, and a loss of intellectual function [160]. *Pheochromocytoma* is a rare tumor of adrenal gland tissue caused by germline and a mitochondrial complex II gene mutation [161]. It results in the release of too much epinephrine and norepinephrine, hormones that control heart rate, metabolism, and blood pressure [162]. *Mitochondrial complex I deficiency* is the most common enzymatic defect of the oxidative phosphorylation disorders and causes a wide range of clinical disorders, ranging from lethal neonatal disease to adult-onset neurodegenerative

disorders [163]. As shown above, all diseases are connected through neurodegenerative disorders and their signs and symptoms. More precisely they are all caused by mitochondrial mutations or deficiency. Indeed 12 out of 16 genes have exact same EC number, EC 1.6.5.3 which is NADH:ubiquinone reductase (H(+)-translocating) presented in mitochondria and aerobic bacteria. More information about identified disease related genes are shown in table 4.1. Based on these evidences showing strong connecting between genes and diseases, the power of identifying related genes are analyzed by counting the number of genes in table 4.1.

Table 4.2 Disease-related genes identified by conventional methods.

Method	Threshold	Previous threshold	Identified genes
Schlicker	0.85	1.0	MT-ND2, MT-ND3, MT-ND4, MT-ND5, MT-ND6, NDUFA1, NDUFS4
Lin	0.90	1.0	MT-ND2, MT-ND3, MT-ND4, MT-ND5, MT-ND6, NDUFA1, NDUFS4
Resnik	0.30	0.6	MT-ND2, MT-ND3, MT-ND4, MT-ND5, MT-ND6, NDUFA1, NDUFS4, DLD
Gentleman	0.90	1.0	MT-ND2, MT-ND3, MT-ND4, MT-ND5, MT-ND6, NDUFA1, NDUFS4
Jiang	0.95	1.0	MT-ND2, MT-ND3, MT-ND4, MT-ND5, MT-ND6, NDUFA1, NDUFS4 MT-ND1, MT-ND4L, NDUFAF2, NDUFS1, NDUFS2, NDUFS7, NDUFS8,
Ye	0.35	1.0	NDUFS1

The results shown in table 4.2 show that Schlicker, Lin, Gentleman, and Jiang group exactly same genes. Resnik's method found a gene, DLD, which is related to *Maple syrup urine disease*. However, this disease is caused by homozygous or compound heterozygous mutation in specific genes, so they are different from mitochondrial mutations or deficiency. Ye's method detect 15 genes out of 16 genes, so this method is only compatible to the proposed method. However, by considering their threshold value, 0.35, as Ye's method point of view, this cluster may not be considered as sharing strong functional similarity when the range of minimum score 0 and maximum score 1 is considered. Indeed, the optimal threshold value used in this experiment was defined by sequentially increasing the threshold value until it creates a cluster with the maximum

number of related genes. Therefore, in real case, these genes may not be found by Ye's method due to the dramatic difference of threshold values defined upon precision and number of clusters. Overall results clearly show that the proposed methods outperform conventional methods upon both statistical analysis and biological relevancies. Therefore, the possible application derived from the proposed method is of interested to promise the success in real world problems.

To test the proposed method into more realistic problems, the proposed method is applied to finding new disease related genes such that the previous mitochondrial mutation and deficiency disease related genes are used as template genes to discover new disease related genes. To identify related genes, proteins in UniProt are used as a pool of potentially related genes. To get both benefits of improving the relationships and reducing searching space, the pool of potential genes are screened by keeping genes with at least one exact same cellular component GO term with the template genes since functionally related genes often share their cellular component. To make the balance reducing search space and increasing the detection rate of functionally related genes, threshold value 0.6 is used. In fact, this value is slightly lower than the recommended range of threshold value (0.65~0.75). The newly identified disease related genes are depicted in Figure 20. As expected, the survey of the newly discovered genes shows that some of them are highly related to mitochondrial mutation or deficiency. For example, FDX1L is a mitochondrial iron-sulfur (Fe/S) protein that transfers electrons from NADPH via FDXR and functions in Fe/S protein biosynthesis, and strongly connected to activities of mitochondrial complex I [164]. NDUFA2 gene encodes one of the accessory subunits of ubiquinone oxidoreductase, and a homozygous splice site mutation. More importantly NDUFA2 can cause Leigh syndrome [165].

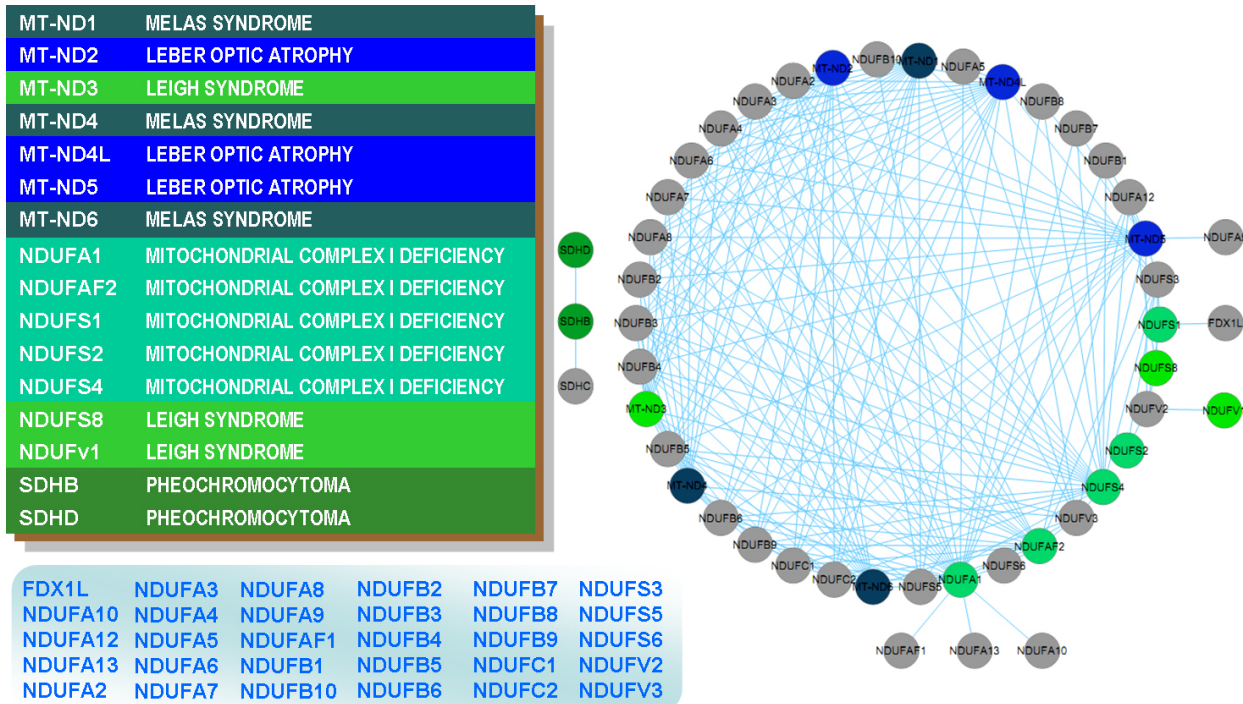


Figure 4.29 New disease related genes identified by BSM score.

Mitochondrial dysfunction related genes retrieved from OMIM and newly discovered genes: left-top shows the list of target genes used for searching UniProt database. The right shows the association between target genes and newly discovered genes. Bottom-left shows the 30 newly discovered genes with threshold value 0.6.

Loeffen et al. [166] found that NDUFV1, NDUFV2, and NDUFV3 are the subunits of NADH:ubiquinone oxidoreductase which is enzyme complex in the electron transport chain of mitochondria. The authors also thought that HP fraction proteins NDUFA7, NDUFA10, NDUFB2, NDUFB4, and NDUFB10 participated in the transfer of protons from the mitochondrial matrix to the intermembrane space and suggested that HP fraction contribute to communicate with mitochondrial matrix or intermembrane space. Bugianie et al. found that variants of NDUFA8 can cause mitochondrial complex I deficiency [167]. Osterquaaard et al. [168] found that NDUFA12 is required either at a late step in the assembly of complex I, or in the stability of complex I. Lu and Cao [169] show that NDUFA13 which is also known as

GRIM-19 is essential for electron transfer activity of mitochondrial complex I. Puissegur et al. [170] found that NDUFA4 is a target of miR-210 and strongly related to a loss of mitochondrial membrane potential and the apparition of an aberrant mitochondrial phenotype. Marui et al. [171] show that NDUFA5 is strongly related to mitochondria dysfunction by analyzing the relations between SNPs of NDUFA5 and Autism which is caused by central nervous system dysfunction commonly associated with mitochondrial disorders. Melick et al. [172] show that NDUFA6 is associated with mitochondrial complex I deficiency by showing SNPs of NDUFA6 can lead Parkinson's disease which is known to be affected by mitochondrial DNA mutation [173, 174]. Most recently van den Bosch et al. identified a homozygous mutation in the NDUFA9 gene from a patient with fatal neonatal Leigh syndrome due to mitochondrial complex I deficiency [175]. The NDUFAF1 gene encodes the human homolog of a *Neurospora crassa* Cia30 protein involved in the assembly of mitochondrial respiratory complex I [176]. Fassone et al. [177] identified compound heterozygosity for 2 mutations in the NDUFAF1 from the patient with fatal infantile hypertrophic cardiomyopathy which requires diagnosing mitochondrial cardiomyopathy caused by mitochondrial dysfunction. Calvo et al. identified a homozygous mutation in the NDUFB3 from a patient with severe mitochondrial complex I deficiency [178]. Most recently Haack et al. [179] found that mutations of NDUFB9 could cause mitochondrial complex I deficiency by screening the reduction of NDUFB9 and both amount and activity of complex I. Szklarczyk et al. identified that NDUFB7 protein lacks a mitochondrial targeting signal and transmembrane domains [180]. Loublier et al. [181] proved that NDUFB6 is essential for mitochondrial complex I activity by showing the shRNA expression resulted in extinction of additional genes. Ugalde et al. [182] shows that mutations of NDUFS3, NDUFS5, and NDUFA9 severally affect the assembly and/or stability of mitochondrial complex I. From two unrelated

families with mitochondrial complex I deficiency, Kirby et al. [183] identified homozygous mutations in the NDUFS6 gene, causing a splicing abnormality and a large deletion, respectively. Although some of newly discovered genes do not show direct evidences for relations with mitochondrial deficiency, their relations can be deduced from related studies. For example, Granata et al [184] found that based on microarray and pathway analysis, certain genes including NDUFB1, NDUFA6, and NDUFS5 could effectively discriminate chronic kidney disease (CKD) and hemodialysis patients, and many of them were involved in mitochondrial oxidative phosphorylation system. By considering the fact that mitochondria are involved in calcium and iron hemostasis, it is possible that mutations of NDUFB1, NDUFA6, and NDUFS5 can lead mitochondrial dysregulation. The study from Su et al. [185] showed that NDUFB5 gene was the one of the highest number of dysregulated genes appeared in the mitochondrial dysfunction and oxidative phosphorylation pathways. Tucker et al. [186] found that NDUFB8 reflected instability of mitochondrial complex I in the absence of mtDNA-encoded protein found in fibroblast patients. In summary, 24 genes out of 30 newly discovered genes had direct evidences of relations toward mitochondrial complex I deficiency. Studies also showed that three out of rest six genes including NDUFB1, NDUFB5, and NDUFB8 had relatively strong relations to complex I deficiency. Unfortunately no literature has been found that showed the relation between complex I deficiency and three newly discovered genes including NDUFA3, NDUFC1, and NDUFC2. As a result, based on the literature survey, the proposed method shows more than 80% overall accuracy. More importantly, most of literatures shown above have not been added to the most recent OMIM, so the reported literatures in this study should be valuable information to explore or expand current knowledge in mitochondrial complex I deficiency.

4.4 Experiment IV: drawing disease network

4.4.1 Dataset

Disease similarity network is drawn based on the average GP similarity measured by BSM score and OMIM database which contains 93 diseases out of 99 OMIM diseases used in this experiments. Disease and associated genes are attached in supplementary section. It is important to notice that this network is different from conventional disease networks by containing functional similarity information among them. To calculate similarity between two diseases, all GP similarity scores associated with a pair of diseases are averaged, and the averaged scores are projected proportionally into the thickness of edges and the intensity between green and red color that correspond to minimum and maximum disease similarity respectively. The degree of each node is depicted proportionally to the radius of nodes. Average similarity score 0.25 is used as a threshold value to avoid making complete connections among nodes in the network which is unfavorable conditions to analyze network with Cytoscape program [187] since this makes circular shaped fully connected network. Upon the proposed drawing strategy and threshold cutoff, existing similarity scores in Figure 4.30 are ranged between 0.25 and 0.85.

4.4.2 Results

As shown in Figure 4.30, majority diseases which are depicted in the middle of the network with relevantly higher degree (i.e. the big circles in the middle) are densely connected to each other, and this is not trivial task to analyze each individual edge even if BSM-based network provides similarity score instead of just showing their connections. Besides these high degree disease nodes, four interesting groups have been found that they are relatively loose but show clear and strong relations among them. Each group has been analyzed starting from top right to top left with clockwise direction.

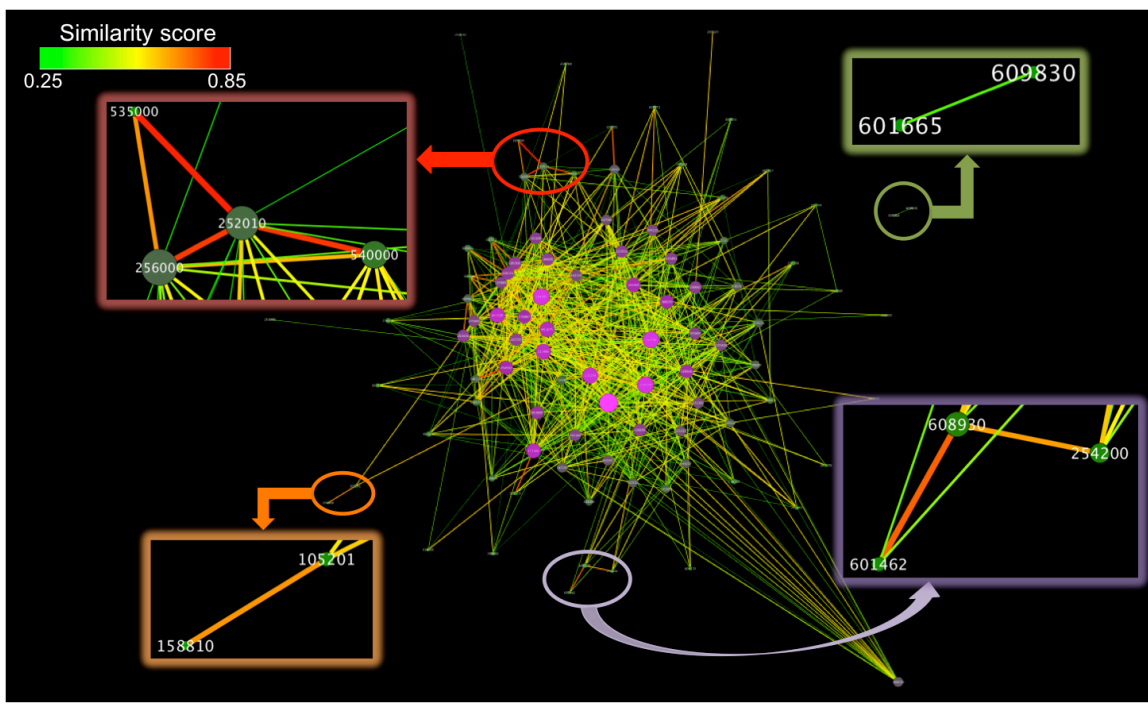


Figure 4.30 Disease Similarity Network created by BSM score.

The size of nodes corresponds to degree of edges. The thickness of edges is corresponds to the similarity. The colors of edges are ranged from green to red that are the minimum and maximum similarity respectively. Four interesting groups of disease are magnified, and the numbers belonging to each node correspond to OMIM ID. The group located in top right corner consists of 601665 and 609830 which are *obesity* and *abdominal body fat distribution* respectively. The group located in bottom right corner consists of 254200, 601462, and 608930 which are *myasthenia gravis* (MG), *slow-channel congenital myasthenic syndrome* (SCCMS), and *fast-channel congenital myasthenic syndrome* respectively. The group located in bottom left norner consists of 105201 which now is 105210 and 158810 which are *amyloidosis* and *bethlem myopathy* respectively. The group located in the top left corner consists of 252010, 256000, 535000, 540000 which are *mitochondrial complex I deficiency*, *leigh syndrome*, *leber optic atrophy*, and *melas syndrome* respectively.

The group consisting of 601665 and 609830 are *obesity* and *abdominal body fat distribution* respectively. These diseases are the only group that is completely isolated from other diseases. It is interesting that although obesity is well known disease related to many diseases, the proposed network does not show significant relations to others except this pair. Indeed their similarity is 2.8, so they are not significantly related to each other, although their names are somewhat

related. There are two reasons why this happens. First, well known obesity related diseases, for example, caused by heterozygous mutations in the melanocortin-4 receptor gene (MC4R) such as *leptin deficiency* [188], *leptin receptor deficiency* [189], *prohormone convertase-1 deficiency* [190], and *proopiomelanocortin deficiency* [191] do not appear in applied datasets. Indeed, although the direct causal relations between obesity and many diseases are suspected, they are still unclear [192-195]. Second, the similarity score between *obesity* and *abdominal body fat distribution* are low due to high numbers of the diverse functional terms. In fact, *obesity* consists of total 27 unique functional terms and *abdominal body fat distribution* consists of total 18 unique functional terms; therefore, these diverse functional terms could affect to decrease similarity between two diseases since BSM-score is based on average similarity score, so the higher number of lower similarity scores could be dominant to make final similarity. In fact, abdominal body fat distribution has been removed from OMIM database due to unclear distinction of phenotype from that in another entry and increasing number of related genes and their variants [196].

The second group consists of 254200, 601462, and 608930 which are *myasthenia gravis* (MG), *slow-channel congenital myasthenic syndrome* (SCCMS), and *fast-channel congenital myasthenic syndrome* (FCCMS) respectively. This groups shows relatively higher similarity among three diseases. The similarity score between MG and FCCMS is 0.52 and between SCCMS and FCCMS is 0.63. Interestingly, MG and SCCMS do not show direct, although these three diseases are linked to *generalized epilepsy with febrile seizures plus* which corresponds to OMIM 604233 which is a syndromic autosomal dominant disorder where afflicted individuals can exhibit numerous epilepsy phenotypes which are diverse set of chronic neurological disorders characterized by seizures [197, 198]. MG is a neuromuscular disorder caused by

producing antibodies to block the muscle cells receiving messages from the nerve cell [199]. Researches [200, 201] showed that CHRNA1 gene encodes the alpha subunit of the muscle acetylcholine receptor (AChR), which is the main target of pathogenic autoantibodies in autoimmune MG. FCCMS is a genetic disorder of the neuromuscular junction that can be classified by the site of the transmission defect. Studies [202-205] showed that FCCMS is caused by heterozygous mutations within the AChR subunit genes, for example, CHRNA1, CHRND, CHRNE genes that affect AChR kinetics and results in infrequent and brief ion channel activations. SCCMS is a genetic disorder of the neuromuscular junction and an autosomal dominant form of postsynaptic CMS, which can be caused by mutation in the subunits of the AChR that can be resulted in kinetic abnormalities of the AChR. Studies [206-209] show that SCCMS is strongly related to mutations of CHRNA1, CHRNB1, CHRND, or CHRNE gene. The relations shown in the network are meaningful such that SCCMS and FCCMS are strongly related to each other by sharing majority of causing genes, CHRNA1, CHRND, and CHRNE genes. The reason of absent links between MG and SCCMS can be explained that other unrelated genes are dominant to defining final similarities. It is important that the absent links in the BSM-based network do not necessary to be showing absence of actual relations since the proposed networks are drawn based on similarity cut-off. In other words, the relation between MG and SCCMS still exist since they share one gene, but by considering their similarity, their similarity is not strong enough because SCCMS consists of much more functions than MG, and the definition of similarity between a pair of GPs or diseases in proposed method is equilibrium on their functions with specific functional terms. Therefore, the lack of functional equilibrium between MG and SCCMS leads the less similarity in this case.

The third group consists of 105210 and 158810 which are *amyloidosis* and *bethlem myopathy* respectively. Hereditary *amyloidoses* are a clinically and genetically heterogeneous group of autosomal dominantly inherited diseases characterized by the deposit of unsoluble protein fibrils in the extracellular matrix due to the mutations in transthyretin (TTR) gene [210]. Studies show TTR aggregations are significantly related to clinical syndromes, for example, familial amyloid polyneuropathy (FAP) and cardiomyopathy are caused by mutant TTR protein aggregation in peripheral and autonomic nerves and heart, respectively. [211]. *Bethlem myopathy* is a skeletal muscular disease of which the muscle fibers do not function for any one of many reasons, resulting in muscular weakness. People with this condition experience progressive muscle weakness and develop joint stiffness (contractures) in their fingers, wrists, elbows, and ankles that can restrict movement. Many studies show significant relations between *amyloidosis* and *myopathy* including causal relations (i.e. amyloidosis causes myopathy) [212-217]. Indeed, myopathy is diagnosed with muscle biopsy by identifying *amyloidosis*. For example, *amyloid myopathy* (AM) is a manifestation of primary systemic amyloidosis and diagnosed by identifying *amyloidosis* in the gastric mucosal biopsy [218].

The group located in the top left corner consists of 252010, 256000, 535000, 540000 which are *mitochondrial complex I deficiency*, *leigh syndrome*, *leber optic atrophy*, and *melas syndrome* respectively. For this group, the details of similarities upon related genes are already discussed in the section ‘Identifying disease related genes’ (i.e. please refer the context associated with Figure 20). In short, this group shows strong relations among them such that all these diseases are caused by mutations in mitochondrial genomes and related to neurodegenerative disorders. Indeed, their signs and symptoms are very similar each other including lost of vision and motor skills. Results show that BSM score can be applied to

constructing disease similarity network which gives more information than simple diseases network by providing semantic confidences of disease similarity. Indeed, the successful identifications of similar diseases show that the proposed method can be applied to real world problems for screening similar and outlier diseases in high throughput manner.

5 Gene Ontology Analysis Layer (GOAL)

5.1 Introduction

One of the most fundamental and important tasks of computational biology or bioinformatics is providing solutions to help understanding inter-relationship between genes and GPs. Although significant progress in the conventional methods based on sequence and structure similarity has been made, their roles in defining functional similarity that has significant impact on revealing inter-cellular relationship are still limited [111, 219-221]. Due to their limitations and computational complexity many studies have been conducted by directly targeting measuring functional similarities among genes or GPs [59, 62, 90, 91, 95, 98, 101]. Identifying functionally similar or closely related genes and GPs has especially significant impacts on clinical studies and trials by supporting the prediction of metastasis or development of treatments for certain diseases since the identified similar genes and GPs can give critical information to understand molecular mechanisms or functions in cellular life of unknown or newly discovered diseases by referring the gene or GPs having similar functions [26, 54-57, 222, 223]. Therefore, it is not surprising that the interest of measuring the semantic similarity among genes and GPs have been significantly increased. Indeed, identifying functional similarities are particularly useful in validating drugs and targets by making possible to recycle the information obtained from target/drug validations and clinical trials [26]. The current vast amount of GPs with known functions stored in various databases, and systematically defined functional annotations like Gene Ontology (GO) [77] are of promising to develop biologically and statistically more relevant method toward measuring functional similarities among GPs. Although several methods have been introduced, their services are limited on their interests and do not provide stand-alone

outputs that can be used for further analysis of the results. More details of existing services and GOAL are compared and summarized in table 5.1. Four web-services are compared to GOAL: FuSSiMeG [73], FunSimMat [58], ProteInOn [61], and G-SESAME [73].

Table 5.1 Comparing GOAL and other existing services

Contents	FuSSiMeG	FunSimMat	ProteinOn	G-SESAME	GOAL
Source DB (1=GO, 2=UniProt)	1	1,2	1	1	1,2
# of method for GO similarity	3	1	6	1	7
# of method for GP similarity	3	N/A	1	N/A	5
# of all possible scores for GP	6	N/A	6	N/A	42
GO similarity between groups	No	No	No	No	Yes
Supporting direct input	Yes	Yes	Yes	Yes	Yes
Supporting file upload	No	No	No	No	Yes
Supporting batch process	No	Yes	Yes	No	Yes
Navigating 2 nodes	No	No	No	No	Yes
Navigating 1 node	No	No	No	No	Yes
Handling root-shared GO term	No	No	No	No	Yes
Handling GPs without annotation	No	No	No	No	Yes
Providing root shared term pairs	No	No	No	No	Yes
Providing GO statistics	No	No	No	No	Yes
Continuing Service	discontinue	continue	continue	continue	continue

In addition to limited accessibility, two significant drawbacks have been found in current existing methods: *i) the nil similarity resulted from GPs with no annotation* and *ii) the nil similarity from root-shared GO terms*. Most of conventional methods are based on two distinct features of GO graph: nearest common ancestor (NCA) and information contents-based score. NCA is the common ancestor of two GO terms located furthest from the root node of GO graph, and IC-based scores are calculated using the number of annotated GPs. Due to the incompleteness of GO annotation for existing GPs and unsynchronized update between GO terms and GP annotations in GO database, there exists GO terms having no annotated GPs. NCA-based scores implicitly allows zero similarity score of which NCA of two GO terms is the root node of GO graph. All possible combinations of GO term pairs among 9,013 GO terms have been calculated in current version of GOAL. The results shows that 20,986,023 pairs out of

40,621,591 pairs have root-shared relations which are about 52% of total possible GO terms pairs (i.e. GOAL provides the list of root-shared GO terms as a submenu). The scores are not only statistically significant toward the number of available GPs for measuring their similarities, but it also shows that this kind of scoring scheme under estimates biological relations. For example, the NCA of GO:0004525 and GO:0046872 which are *ribonuclease III activity* and *metal ion binding* respectively is the root node of GO graph (i.e. GO:0003674, molecular function), but annotated GPs have significant relations in their functional roles such that all corresponding GPs are associated with *dicer-like endoribonuclease* protein, match enzyme commission number (EC) EC3.1.26.- which is *ribonuclease*, and even share cofactors *magnesium* and *manganese* (please refer supplementary table S-1 and S-2 for details and more examples). GOAL is designed to minimize the risk of resulting nil similarity by integrating biological characteristics of GPs and statistical significance of GO term relations in GO databases and provides user interfaces to get maximum 42 different scores from embedded methods that can be used for determining the confidence of resulted scores.

5.2 Input

GOAL provides user-friendly graphic user interface (GUI) for both measuring GO term and GP similarity. For GO term similarity GOAL provides three different types of interfaces for measuring semantic similarity between two GO terms: i) direct input of two GO terms, ii) list of GO terms pairs through input text box, and iii) list of GO terms through file upload. GP similarity provides two types of GUI: i) direct inputs from input text boxes, and ii) file uploads. Compared to GO similarity GP similarity requires two inputs: GP contents and GP pairs. GP contents define unique GP name and corresponding GO annotations. GP pairs are the list of GP pairs appeared in GP contents. Besides common inputs, Jiang's method requires extra parameters, and they can be easily defined through input forms.

5.3 Output

The results of GOAL can be further used and analyzed by researchers, and the size of results can be very large since GO and GP similarities are often resulted in the permutations of seed lists; therefore, GOAL provides tab delimited text file outputs. BSM provides four different scores GLOBAL_MUL, GLOBAL_AVE, LOCAL_MUL, and LOCAL_AVE in which GLOBAL and LOCAL are defined by normalization factor E_{max} and d_{max} shown in equation (4). MUL and AVE denote whether BSM is defined by multiply of B_{scr} and S_{scr} or average of them. Besides BSM, GOAL also provides four different scores for six conventional methods: DIR_GO, ANC_GO, DIR_UniProt, and ANC_UniProt. At the name, GO and UniProt [224] are the two different sources to get annotated GPs. DIR and ANC denotes whether considering annotated GO term only or including ancestors of the GO terms toward calculating GO and GP similarity. The results of six different methods are also provided as downloadable text files.

5.4 Submenus

Besides calculating GO and GP similarity, GOAL provides comprehensive GO analysis platform including GO Navigator, GP annotation writer, and daily GO statistics. GO Navigator visualize either single GO term or GO term pairs based on user preference. Writing the input of calculating GP similarity is often cumbersome since it often requires retrieving annotated GO terms of target GPs. To improve user accessibility, GOAL provides automatic input writer to get annotated GPs from the list of UniProt IDs or gene names. The daily updated GO statistics is one of unique service in GOAL. Statistics menu provides statistics of GO terms and annotated GPs from 2005 to present. In fact, from August 2011 to present, GOAL provides daily updated GO statistics. To help the people developing new method for measuring GP similarity, GOAL also provides GUI for retrieving root-shared GO terms. At the current version GOAL contains total 20,986,023 root-shared GO term pairs. The results provided by GOAL are all downloadable, so that users can easily redistribute and analyze the results. Overall schematic diagram of GOAL is shown in Figure 5.1.

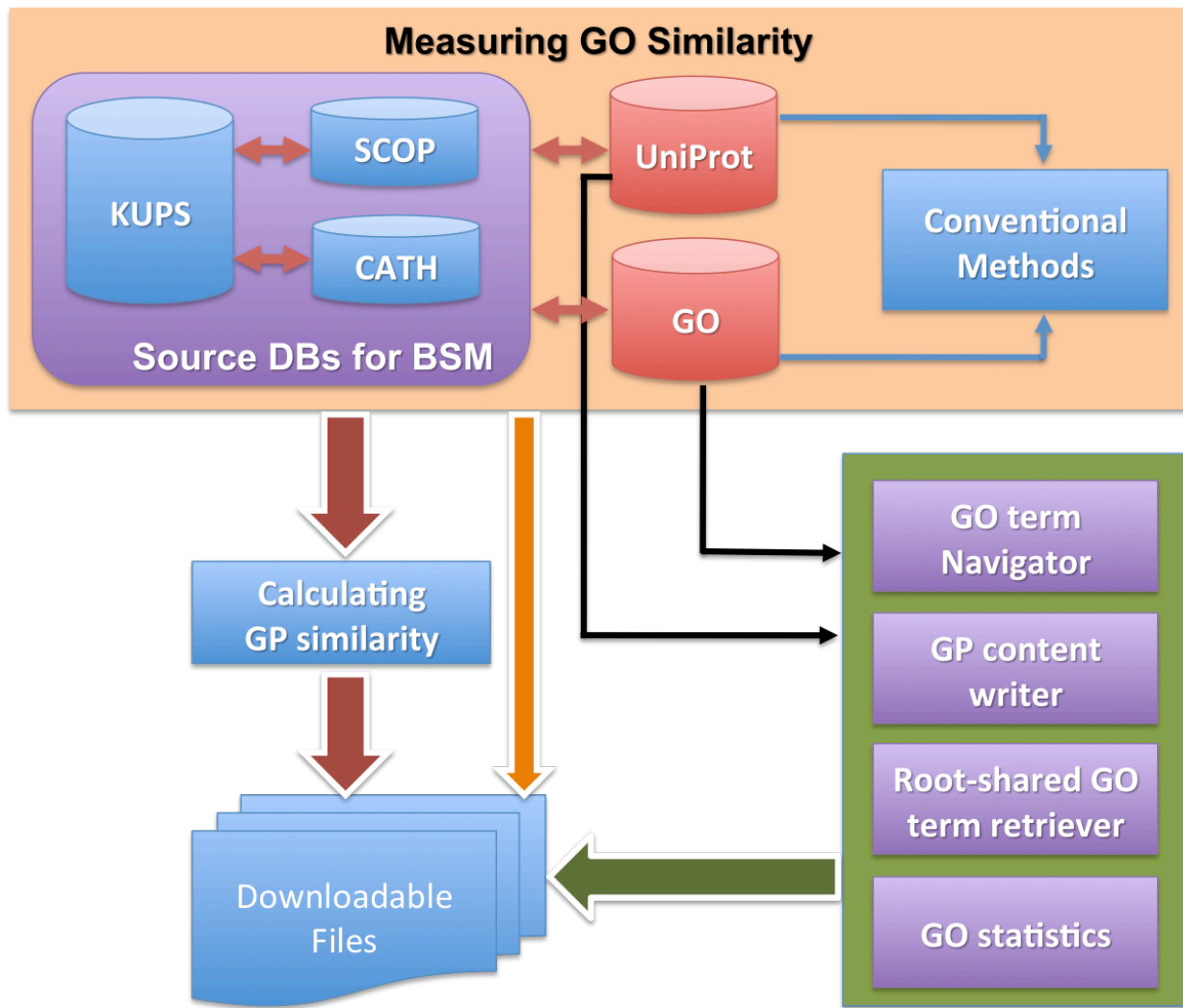


Figure 5.1 GOAL schematic diagram.

GOAL contains two major semantic similarity scores: BSM and six conventional methods. BSM is derived from five DBs: KUPS, SCOP, CATH, UniProt, and GO. Six conventional methods simultaneously calculate GO similarity scores based on known GP annotations from UniProt and GO which is one of unique features in GOAL. Upon user's request GOAL can calculate GP similarity from five different methods. Thus compared to other existing services, GOAL provides multiple scores resulted from two different DBs and five different GP scoring methods so that users can determine the confidence of resulted scores by comparing consistence of the scores. Besides measuring functional similarity of GO terms and GPs, GOAL also provides various tools to support researchers analyzing resulted scores and developing new methods to define semantic similarity between GPs. To help user's accessibility and post analysis, GOAL also provides all results through downloadable files and web-view including images and text files.

6 Conclusion and future works

The significance of the proposed method can be found in several aspects: 1) solving problems of the nil similarity and root-shared terms: the most critical defects in current methods are resulted in nil similarity or giving same similarity scores to any pairs of root-shared GO terms which are resulted from the absence of annotated GPs and root-shared GO terms respectively. Proposed method prevents the nil similarity by calculating functional similarity through the topology of GO graph instead of using the statistics of annotated GPs. To minimize the effects resulted from root-shared GO terms, reference score matrix derived from GO term distributions among known domains is introduced. 2) reflecting specificity and fidelity of GO terms into final score: methods relying on the rationale of nearest common ancestor (NCA) often ignore the specificity and fidelity of GO terms due to shadow problem in which the specificity of target GO term located below the NCA GO term is ignored by considering NCA only. To handle this problem, density and depth of GO terms are integrated in proposed score function such that the deeper and simpler path from root to NCA will reward higher similarity score. 3) combining top-down and bottom-up approaches: by solving the problems stated above, integration of top-down and bottom-up approaches are proposed. As an initial effort, the weight of each approaches are evenly distributed; therefore, the final score will have unbiased results from both graph search-based method and statistical results of GO term distribution upon known functional domains. 4) Narrowing down gaps between theoretical background and biological relevancies: conventional methods dealing with functional similarity are often derived form theoretical background of information theory, but there exist certain gaps between the background theory and real clinical trials as discussed in preliminary study. The proposal is designed for minimizing

the gaps between theoretical approaches and practical usages by comprehensively evaluating the proposed method in multiple steps. 5) Providing guidelines on evaluation process: conventional methods are often focused on evaluations on statistical point of view (e.g. evaluating the similarity score upon sequence and structure similarity). However, statistical evaluations are not enough to elucidate specific characteristics of the methods. The proposed method is evaluated through multiple steps including statistical evaluations with multiple comparisons on conventional methods, and biological analysis based on literature review. It is also emphasized that the human cognition on reported scores by showing unfavorable differences between reported score and user expectation or interpretation on that score should be considered. To show the potentials of the proposed method to be used in real problems, disease related genes are identified. The results show that the proposed methods are very promising to discover disease related genes as showing overall accuracy greater than 80%. This thesis shows new way to define functional similarity between GPs by using terms associated with molecular function in GO database. GO contains three different categories: molecular function, biological process, and cellular component. In future, I will complete similarity scores in other categories and combine them to define more rigorous relations among GPs. Finally I will apply them as a pipeline to connect diverse data sources, so that users can easily explore *Big data*.

Supplementary materials

[S-1] Statistics of root shared GO terms and GPs

300 randomly selected Gene Products (GPs) annotated at least a pair of root-shared terms

- # GPs: number of GPs annotated at least a pair of root-shared terms (i.e. GO term1 and GO term2)
- # PPIs: number of protein-protein interactions among # of GPs selected above step

GO term1	GO term2	# of GPs	# of PPIs	GO term1	GO term2	# of GPs	# of PPIs
GO:0004674	GO:0005524	2517	372	GO:0004748	GO:0046914	99	9
GO:0004715	GO:0005524	186	86	GO:0004702	GO:0005524	10	9
GO:0004842	GO:0008270	400	77	GO:0004872	GO:0005525	35	9
GO:0016563	GO:0043565	295	52	GO:0004842	GO:0043130	13	9
GO:0004674	GO:0042802	35	38	GO:0030374	GO:0046966	12	9
GO:0016563	GO:0046982	58	36	GO:0004672	GO:0042802	6	9
GO:0004674	GO:0046872	435	34	GO:0004716	GO:0046982	4	9
GO:0004709	GO:0005524	58	32	GO:0004674	GO:00046872	172	8
GO:0004714	GO:0005524	134	28	GO:0004697	GO:0046872	33	8
GO:0004707	GO:0005524	178	27	GO:0004715	GO:0046872	20	8
GO:0004842	GO:0005524	264	25	GO:0004708	GO:0005524	26	8
GO:0004713	GO:0005524	251	24	GO:0004579	GO:0042802	4	8
GO:0004749	GO:0005524	200	24	GO:0016563	GO:0019901	18	8
GO:0016563	GO:0042803	51	24	GO:0004639	GO:0005524	539	7
GO:0004693	GO:0005524	264	23	GO:0004523	GO:0008270	112	7
GO:0004871	GO:0046982	26	22	GO:0004523	GO:0005198	76	7
GO:0004872	GO:0005524	267	21	GO:0004748	GO:0005524	72	7
GO:0004672	GO:0005524	245	19	GO:0004533	GO:0008270	75	7
GO:0004716	GO:0005524	22	19	GO:0004533	GO:0005198	61	7
GO:0004872	GO:0042802	15	19	GO:0005083	GO:0005524	30	7
GO:0016769	GO:0030170	417	18	GO:0004872	GO:0046966	15	7
GO:0004550	GO:0005524	751	17	GO:0004872	GO:0030374	10	7
GO:0004697	GO:0005524	71	17	GO:0004872	GO:0042809	10	7
GO:0005024	GO:0005524	7	17	GO:0004526	GO:0042802	3	7
GO:0004889	GO:0015464	25	17	GO:0004871	GO:0016563	29	7
GO:0005024	GO:0046872	6	17	GO:0004523	GO:0046872	1203	6
GO:0004722	GO:0046872	186	16	GO:0004519	GO:0046872	553	6
GO:0004871	GO:0005524	87	16	GO:0004824	GO:0046872	452	6
GO:0004826	GO:0005524	1028	15	GO:0004849	GO:0005524	235	6
GO:0016847	GO:0030170	126	15	GO:0004674	GO:0005083	27	6
GO:0004842	GO:0042802	21	15	GO:0004702	GO:0046872	24	6
GO:0004749	GO:0042802	5	15	GO:0004871	GO:0008134	20	6
GO:0004871	GO:0005096	56	14	GO:0004674	GO:0004871	15	6
GO:0004872	GO:0046872	93	13	GO:0004871	GO:0046872	14	6
GO:0004691	GO:0005524	29	13	GO:0004674	GO:0042803	13	6
GO:0004871	GO:0019901	25	13	GO:0004871	GO:0043565	15	6
GO:0004519	GO:0005524	180	12	GO:0005009	GO:0043559	7	6
GO:0016566	GO:0043565	46	12	GO:0005009	GO:0043560	7	6
GO:0016702	GO:0031418	292	11	GO:0005009	GO:0046872	7	6
GO:0004683	GO:0005524	69	11	GO:0004704	GO:0005524	7	6
GO:0004871	GO:0042802	18	11	GO:0005009	GO:0005524	7	6
GO:0004824	GO:0005524	592	10	GO:0005024	GO:0046332	6	6
GO:0004871	GO:0005525	204	10	GO:0004888	GO:0042802	6	6

GO:0004871	GO:0008270	44	10	GO:0004815	GO:0005524	1026	5
GO:0004683	GO:0005516	66	10	GO:0004813	GO:0005524	728	5
GO:0005003	GO:0005524	44	10	GO:0004775	GO:0005524	564	5
GO:0004871	GO:0005109	21	10	GO:0004519	GO:0008270	81	5
GO:0004871	GO:0005110	14	10	GO:0004743	GO:0005524	102	5
GO:0004872	GO:0051740	5	10	GO:0004743	GO:0030955	103	5
GO:0004550	GO:0046872	733	9	GO:0004518	GO:0005524	81	5
GO:0004802	GO:0046872	73	5	GO:0004740	GO:0005524	19	4
GO:0004890	GO:0005254	68	5	GO:0005096	GO:0005524	12	4
GO:0004970	GO:0005234	67	5	GO:0004758	GO:0030170	18	4
GO:0016740	GO:0030976	54	5	GO:0004709	GO:0046872	16	4
GO:0004535	GO:0046872	50	5	GO:0004842	GO:0004871	14	4
GO:0004525	GO:0005524	42	5	GO:0004705	GO:0005524	12	4
GO:0004843	GO:0008270	38	5	GO:0004888	GO:0005529	12	4
GO:0005021	GO:0005524	31	5	GO:0004709	GO:0042803	10	4
GO:0004645	GO:0030170	29	5	GO:0004872	GO:0005047	9	4
GO:0004872	GO:0019864	20	5	GO:0004871	GO:0005125	10	4
GO:0004842	GO:0042803	18	5	GO:0004674	GO:0043621	4	4
GO:0004674	GO:0019901	13	5	GO:0004842	GO:0043621	4	4
GO:0004842	GO:0031625	16	5	GO:0004674	GO:0046982	7	4
GO:0005096	GO:0005525	9	5	GO:0005009	GO:0042169	6	4
GO:0004871	GO:0042803	15	5	GO:0005009	GO:0043548	6	4
GO:0016563	GO:0019904	23	5	GO:0005009	GO:0051425	6	4
GO:0016566	GO:0042803	20	5	GO:0005096	GO:0042802	4	4
GO:0004972	GO:0005234	11	5	GO:0004888	GO:0042803	3	4
GO:0004715	GO:0042169	8	5	GO:0005006	GO:0005524	4	4
GO:0004871	GO:0005070	6	5	GO:0004639	GO:0042802	4	4
GO:0004715	GO:0005131	5	5	GO:0004714	GO:0046982	4	4
GO:0016566	GO:0019901	9	5	GO:0004674	GO:0047485	3	4
GO:0004715	GO:0030145	9	5	GO:0000978	GO:0003704	34	4
GO:0004972	GO:0005262	3	5	GO:0004872	GO:0005161	2	4
GO:0017124	GO:0017128	3	5	GO:0016564	GO:0019901	2	4
GO:0004748	GO:0042802	3	5	GO:0004716	GO:0019903	2	4
GO:0016564	GO:0031625	6	5	GO:0005006	GO:0019903	2	4
GO:0016564	GO:0042803	26	5	GO:0030617	GO:0031625	2	4
GO:0004821	GO:0005524	934	4	GO:0030617	GO:0034713	2	4
GO:0004820	GO:0005524	859	4	GO:0004617	GO:0042802	2	4
GO:0004618	GO:0005524	719	4	GO:0004643	GO:0042802	2	4
GO:0004831	GO:0005524	544	4	GO:0004716	GO:0042802	2	4
GO:0004825	GO:0005524	496	4	GO:0004849	GO:0042802	2	4
GO:0004812	GO:0005524	358	4	GO:0004867	GO:0042802	2	4
GO:0004872	GO:0005529	108	4	GO:0005006	GO:0042802	2	4
GO:0004830	GO:0005524	166	4	GO:0004704	GO:0042803	2	4
GO:0004890	GO:0005230	63	4	GO:0004872	GO:0043184	2	4
GO:0004735	GO:0005488	56	4	GO:0004704	GO:0046982	2	4
GO:0004672	GO:0004872	42	4	GO:0005006	GO:0046982	2	4
GO:0004523	GO:0005524	45	4	GO:0004871	GO:0070411	4	4
GO:0004638	GO:0005524	45	4	GO:0030617	GO:0070411	2	4
GO:0004784	GO:0008270	18	4	GO:0004813	GO:0046872	705	4
GO:0004703	GO:0005524	30	4	GO:0004798	GO:0005524	609	3
GO:0004703	GO:0004871	30	4	GO:0004642	GO:0005524	522	3
GO:0005089	GO:0046872	23	4	GO:0004527	GO:0046872	133	3
GO:0004672	GO:0005525	29	4	GO:0004797	GO:0005524	245	3
GO:0004697	GO:0008270	29	4	GO:0004601	GO:0020037	187	3

GO:0005096	GO:0046872	31	4	GO:0004819	GO:0005524	153	3
GO:0000978	GO:0003700	21	4	GO:0004591	GO:0030976	109	3
GO:0004617	GO:0051287	27	4	GO:0004791	GO:0050660	84	3
GO:0016740	GO:0030170	87	3	GO:0019899	GO:0030374	4	3
GO:0004616	GO:0050661	57	3	GO:0015421	GO:0042605	3	3
GO:0004674	GO:0005516	53	3	GO:0005083	GO:0042802	4	3
GO:0004887	GO:0008270	35	3	GO:0004724	GO:0046872	4	3
GO:0016829	GO:0030170	55	3	GO:0004724	GO:0048037	4	3
GO:0017147	GO:0042813	11	3	GO:0005100	GO:0017048	4	3
GO:0030165	GO:0042813	3	3	GO:0004888	GO:0019901	3	3
GO:0016538	GO:0019901	6	3	GO:0004714	GO:0033612	3	3
GO:0004517	GO:0005516	31	3	GO:0004638	GO:0042802	3	3
GO:0004930	GO:0017147	19	3	GO:0005034	GO:0043424	3	3
GO:0004867	GO:0008201	26	3	GO:0004842	GO:0046625	3	3
GO:0004930	GO:0030165	6	3	GO:0004871	GO:0050681	2	3
GO:0004517	GO:0020037	25	3	GO:0005010	GO:0005158	2	3
GO:0004517	GO:0010181	23	3	GO:0004674	GO:0008307	3	3
GO:0004776	GO:0005525	28	3	GO:0004713	GO:0008307	3	3
GO:0004725	GO:0046872	15	3	GO:0016564	GO:0019904	4	3
GO:0004517	GO:0050661	21	3	GO:0015433	GO:0042605	2	3
GO:0004517	GO:0050660	20	3	GO:0004818	GO:0005524	886	2
GO:0004494	GO:0031419	20	3	GO:0004828	GO:0005524	844	2
GO:0004494	GO:0046872	20	3	GO:0004827	GO:0005524	833	2
GO:0005089	GO:0005524	19	3	GO:0004817	GO:0005524	813	2
GO:0005096	GO:0017124	20	3	GO:0004829	GO:0005524	698	2
GO:0016301	GO:0042803	17	3	GO:0004594	GO:0005524	640	2
GO:0005057	GO:0005524	16	3	GO:0004826	GO:0046872	635	2
GO:0000739	GO:0003700	16	3	GO:0004822	GO:0005524	579	2
GO:0004674	GO:0005089	14	3	GO:0004592	GO:0005524	563	2
GO:0004871	GO:0008083	13	3	GO:0004641	GO:0005524	486	2
GO:0005125	GO:0042056	13	3	GO:0004781	GO:0005524	450	2
GO:0004872	GO:0005178	14	3	GO:0004834	GO:0030170	455	2
GO:0016566	GO:0046982	16	3	GO:0004825	GO:0046872	431	2
GO:0005096	GO:0042803	6	3	GO:0004784	GO:0046872	378	2
GO:0004706	GO:0005524	8	3	GO:0004810	GO:0005524	365	2
GO:0004871	GO:0008013	9	3	GO:0004636	GO:0005524	346	2
GO:0005021	GO:0019838	12	3	GO:0004832	GO:0005524	339	2
GO:0004872	GO:0019901	8	3	GO:0004789	GO:0046872	334	2
GO:0004872	GO:0005518	8	3	GO:0004721	GO:0046872	229	2
GO:0004871	GO:0008009	8	3	GO:0016706	GO:0031418	9	2
GO:0004675	GO:0005524	4	3	GO:0004721	GO:0005524	149	2
GO:0005010	GO:0043548	6	3	GO:0016811	GO:0070403	139	2
GO:0004674	GO:0005262	5	3	GO:0004637	GO:0005524	114	2
GO:0005034	GO:0005524	5	3	GO:0004637	GO:0046872	110	2
GO:0004972	GO:0016594	5	3	GO:0004652	GO:0005524	71	2
GO:0004550	GO:0042802	3	3	GO:0004635	GO:0005524	65	2
GO:0004871	GO:0005201	5	3	GO:0004525	GO:0046872	53	2
GO:0004871	GO:0008022	5	3	GO:0004794	GO:0030170	52	2
GO:0004842	GO:0019899	2	3	GO:0004887	GO:0043565	30	2
GO:0005001	GO:0019901	4	3	GO:0004587	GO:0030170	50	2
GO:0004722	GO:0030165	4	3	GO:0004655	GO:0046872	45	2
GO:0004725	GO:0030165	4	3	GO:0004519	GO:0051539	43	2
GO:0016314	GO:0030165	4	3	GO:0004872	GO:0042803	32	2

[S-2] GPs containing root shared GO terms I

- GO:0004525: Ribonuclease III activity
- GO:0046872: Metal ion binding

Accession ID	A0MQH0 (DICER_CRIGR) Reviewed, UniProtKB/Swiss-Prot
Protein Names	<p>Recommended name: Endoribonuclease Dicer EC=3.1.26.-</p>
Gene Names	Name:DICER1 Synonyms:DICER
Organism	Cricetulus griseus (Chinese hamster) (Cricetulus barabensis griseus)
Taxonomic identifier	10029 [NCBI]
Function	Required for formation of the RNA induced silencing complex (RISC). Component of the RISC loading complex (RLC), also known as the micro-RNA (miRNA) loading complex (miRLC), which is composed of DICER1, EIF2C2/AGO2 and TARBP2. Within the RLC/miRLC, DICER1 and TARBP2 are required to process precursor miRNAs (pre-miRNAs) to mature miRNAs and then load them onto EIF2C2/AGO2. EIF2C2/AGO2 bound to the mature miRNA constitutes the minimal RISC and may subsequently dissociate from DICER1 and TARBP2. Also cleaves double-stranded RNA to produce short interfering RNAs (siRNAs) which target the selective destruction of complementary RNAs
Cofactor	Binds 2 magnesium or manganese ions per subunit
Subcellular location	Cytoplasm
Accession ID	A1C9M6 (DCL2_ASPLC) Reviewed, UniProtKB/Swiss-Prot
Protein Names	<p>Recommended name: Dicer-like protein 2 Including the following 2 domains: Endoribonuclease dcl2 EC=3.1.26.-</p>
Gene Names	<p>Name: dcl2 ORF Names: ACLA_055980</p>
Organism	Aspergillus clavatus (strain ATCC 1007 / CBS 513.65 / DSM 816 / NCTC 3887 / NRRL 1) [Complete proteome]
Taxonomic identifier	344612 [NCBI]
Function	Dicer-like endonuclease involved in cleaving double-stranded RNA in the RNA interference (RNAi) pathway. Produces 21 to 25 bp dsRNAs (siRNAs) which target the selective destruction of homologous RNAs leading to sequence-specific suppression of gene expression, called post-transcriptional gene silencing (PTGS). Part of a broad host defense response against viral infection and transposons
Cofactor	Magnesium or manganese
Subcellular location	N/A
Accession ID	A1CBC9 (DCL1_ASPLC) Reviewed, UniProtKB/Swiss-Prot
Protein Names	<p>Recommended name: Dicer-like protein 1 Including the following 2 domains: Endoribonuclease dcl1 EC=3.1.26.-</p>
Gene Names	<p>Name: dcl1 ORF Names: ACLA_014840</p>
Organism	Aspergillus clavatus (strain ATCC 1007 / CBS 513.65 / DSM 816 / NCTC 3887 / NRRL 1)

Taxonomic identifier	[Complete proteome] 344612 [NCBI]
Function	Dicer-like endonuclease involved in cleaving double-stranded RNA in the RNA interference (RNAi) pathway. Produces 21 to 25 bp dsRNAs (siRNAs) which target the selective destruction of homologous RNAs leading to sequence-specific suppression of gene expression, called post-transcriptional gene silencing (PTGS). Part of a broad host defense response against viral infection and transposons
Cofactor	Magnesium or manganese
Subcellular location	
Accession ID	A1D9Z6 (DCL2_NEIFI) Reviewed, UniProtKB/Swiss-Prot
Protein Names	Recommended name: Dicer-like protein 2 Including the following 2 domains: Endoribonuclease dcl2 EC=3.1.26.- ATP-dependent helicase dcl2 EC=3.6.4.-
Gene Names	Name: dcl2 ORF Names: NFIA_030600
Organism	Neosartorya fischeri (strain ATCC 1020 / DSM 3700 / FGSC A1164 / NRRL 181) (Aspergillus fischerianus) [Complete proteome]
Taxonomic identifier	331117 [NCBI]
Function	Dicer-like endonuclease involved in cleaving double-stranded RNA in the RNA interference (RNAi) pathway. Produces 21 to 25 bp dsRNAs (siRNAs) which target the selective destruction of homologous RNAs leading to sequence-specific suppression of gene expression, called post-transcriptional gene silencing (PTGS). Part of a broad host defense response against viral infection and transposons
Cofactor	Magnesium or manganese
Subcellular location	N/A
Accession ID	A1DE13 (DCL1_NEIFI) Reviewed, UniProtKB/Swiss-Prot
Protein Names	Recommended name: Dicer-like protein 1 Including the following 2 domains: Endoribonuclease dcl1 EC=3.1.26.- ATP-dependent helicase dcl1 EC=3.6.4.-
Gene Names	Name: dcl1 ORF Names: NFIA_075500
Organism	Neosartorya fischeri (strain ATCC 1020 / DSM 3700 / FGSC A1164 / NRRL 181) (Aspergillus fischerianus) [Complete proteome]
Taxonomic identifier	331117 [NCBI]
Function	Dicer-like endonuclease involved in cleaving double-stranded RNA in the RNA interference (RNAi) pathway. Produces 21 to 25 bp dsRNAs (siRNAs) which target the selective destruction of homologous RNAs leading to sequence-specific suppression of gene expression, called post-transcriptional gene silencing (PTGS). Part of a broad host defense response against viral infection and transposons
Cofactor	Magnesium or manganese
Subcellular location	N/A
Accession ID	A2R345 (DCL21_ASNC) Reviewed, UniProtKB/Swiss-Prot
Protein Names	Recommended name: Dicer-like protein 2-1 Including the following 2 domains: Endoribonuclease dcl2-1

Gene Names	EC=3.1.26.- ATP-dependent helicase dcl2-1 EC=3.6.4.- Name: dcl2-1 ORF Names: An14g03000
Organism	<i>Aspergillus niger</i> (strain CBS 513.88 / FGSC A1513) [Complete proteome]
Taxonomic identifier	425011 [NCBI]
Function	Dicer-like endonuclease involved in cleaving double-stranded RNA in the RNA interference (RNAi) pathway. Produces 21 to 25 bp dsRNAs (siRNAs) which target the selective destruction of homologous RNAs leading to sequence-specific suppression of gene expression, called post-transcriptional gene silencing (PTGS). Part of a broad host defense response against viral infection and transposons
Cofactor	Magnesium or manganese
Subcellular location	N/A
Accession ID	A2RAF3 (DCL1_ASPPNC) Reviewed, UniProtKB/Swiss-Prot
Protein Names	Recommended name: Dicer-like protein 1 Including the following 2 domains: Endoribonuclease dcl1 EC=3.1.26.- ATP-dependent helicase dcl1 EC=3.6.4.-
Gene Names	Name: dcl1 ORF Names: An18g02950
Organism	<i>Aspergillus niger</i> (strain CBS 513.88 / FGSC A1513) [Complete proteome]
Taxonomic identifier	425011 [NCBI]
Function	Dicer-like endonuclease involved in cleaving double-stranded RNA in the RNA interference (RNAi) pathway. Produces 21 to 25 bp dsRNAs (siRNAs) which target the selective destruction of homologous RNAs leading to sequence-specific suppression of gene expression, called post-transcriptional gene silencing (PTGS). Part of a broad host defense response against viral infection and transposons
Cofactor	Magnesium or manganese
Subcellular location	N/A
Accession ID	A4RHU9 (DCL2_MAGO7) Reviewed, UniProtKB/Swiss-Prot
Protein Names	Recommended name: Dicer-like protein 2 Including the following 2 domains: Endoribonuclease DCL2 EC=3.1.26.- ATP-dependent helicase DCL2 EC=3.6.4.-
Gene Names	Name: DCL2 Synonyms: MDL2 ORF Names: MGG_12357
Organism	<i>Magnaporthe oryzae</i> (strain 70-15 / ATCC MYA-4617 / FGSC 8958) (Rice blast fungus)
Taxonomic identifier	(<i>Pyricularia oryzae</i>) [Complete proteome]
Function	242507 [NCBI] Dicer-like endonuclease involved in cleaving double-stranded RNA in the RNA interference (RNAi) pathway. Produces 21 to 25 bp dsRNAs (siRNAs) which target the selective destruction of homologous RNAs leading to sequence-specific suppression of gene expression, called post-transcriptional gene silencing (PTGS). Part of a broad host defense response against viral infection and transposons.
Cofactor	Magnesium or manganese
Subcellular location	N/A

Accession ID	A4RKC3 (DCL1_MAGO7) Reviewed, UniProtKB/Swiss-Prot
Protein Names	<p>Recommended name: Dicer-like protein 1 Including the following 2 domains: Endoribonuclease DCL1 EC=3.1.26.- ATP-dependent helicase DCL1 EC=3.6.4.-</p>
Gene Names	<p>Name: DCL1 Synonyms: MDL1 ORF Names: MGG_01541</p>
Organism	Magnaporthe oryzae (strain 70-15 / ATCC MYA-4617 / FGSC 8958) (Rice blast fungus) (Pyricularia oryzae) [Complete proteome]
Taxonomic identifier	242507 [NCBI]
Function	Dicer-like endonuclease which seems not to be involved in cleaving double-stranded RNA in the RNA interference (RNAi) pathway, contrary to its DCL2 counterpart.
Cofactor	Magnesium or manganese
Subcellular location	N/A
Accession ID	A7LFZ6 (DCL4_ORYSJ) Reviewed, UniProtKB/Swiss-Prot
Protein Names	<p>Recommended name: Endoribonuclease Dicer homolog 4 EC=3.1.26.- Alternative name(s): Dicer-like protein 4 Short name=OsDCL4 Protein SHOOT ORGANIZATION 1</p>
Gene Names	<p>Name: DCL4 Synonyms: SHO1 Ordered Locus Names: Os04g0509300, LOC_Os04g43050 ORF Names: OSJNBB0065L13.5</p>
Organism	Oryza sativa subsp. japonica (Rice) [Complete proteome]
Taxonomic identifier	39947 [NCBI]
Function	Involved in the RNA silencing pathway. Cleaves double-stranded RNA to produce small interfering RNAs (siRNAs) which target the selective destruction of complementary RNAs. Required for the production of 21 nucleotide siRNAs. Regulates shoot apical meristem (SAM) initiation and maintenance, leaf polarization and lemma polarity through the trans-acting siRNAs (ta-siRNAs) pathway, which probably modulate the expression of the ARF2, ARF3, ARF4, ARF14 and ARF15 genes. Can process endogenous 21 nucleotide siRNAs derived from an imperfect inverted repeat. May not be involved in microRNAs (miRNAs) production.
Cofactor	Magnesium or manganese
Subunit structure	May interact with ARGONAUTE1 or PINHEAD through their common PAZ domains
Subcellular location	Nucleus
Accession ID	A8BQJ3 (DCL_GIAIC) Reviewed, UniProtKB/Swiss-Prot
Protein Names	<p>Recommended name: Endoribonuclease Dicer-like EC=3.1.26.-</p>
Gene Names	ORF Names: GL50803_103887
Organism	Giardia intestinalis (strain ATCC 50803 / WB clone C6) (Giardia lamblia)
Taxonomic identifier	184922 [NCBI]
Function	Involved in cleaving double-stranded RNA in the RNA interference (RNAi) pathway. It produces 21 to 23 bp dsRNAs (siRNAs) which target the selective destruction of homologous RNAs.
Cofactor	Binds 2 magnesium or manganese ions per subunit

Subunit structure	Subunit structure
Accession ID	B3DLA6 (DICER_XENTR) Reviewed, UniProtKB/Swiss-Prot
Protein Names	<p>Recommended name: Endoribonuclease Dicer EC=3.1.26.-</p>
Gene Names	Name: dicer1
Organism	Xenopus tropicalis (Western clawed frog) (<i>Silurana tropicalis</i>)
Taxonomic identifier	8364 [NCBI]
Function	Required for formation of the RNA induced silencing complex (RISC). Component of the RISC loading complex (RLC), also known as the micro-RNA (miRNA) loading complex (miRLC), which is composed of dicer1, eif2c2/ago2 and tarbp2. Within the RLC/miRLC, dicer1 and tarbp2 are required to process precursor miRNAs (pre-miRNAs) to mature miRNAs and then load them onto eif2c2/ago2. eif2c2/ago2 bound to the mature miRNA constitutes the minimal RISC and may subsequently dissociate from dicer1 and tarbp2. Also cleaves double-stranded RNA to produce short interfering RNAs (siRNAs) which target the selective destruction of complementary RNAs
Cofactor	Binds 2 magnesium or manganese ions per subunit
Subunit structure	Component of the RISC loading complex (RLC), or micro-RNA (miRNA) loading complex (miRLC), which is composed of dicer1, eif2c2/ago2 and tarbp2. Note that the trimeric RLC/miRLC is also referred to as RISC
Subcellular location	Cytoplasm
Accession ID	O01326 (RNC_CAEEL) Reviewed, UniProtKB/Swiss-Prot
Protein Names	<p>Recommended name: Ribonuclease 3 EC=3.1.26.3</p> <p>Alternative name(s): Protein drsh Ribonuclease III Short name=RNase III</p>
Gene Names	<p>Name: drsh-1 ORF Names: F26E4.10</p>
Organism	Caenorhabditis elegans
Taxonomic identifier	6239 [NCBI]
Function	Executes the initial step of microRNA (miRNA) processing in the nucleus, that is the cleavage of pri-miRNA to release pre-miRNA. Involved in pre-rRNA processing. Cleaves double-strand RNA and does not cleave single-strand RNA. Involved in fertility. Required for the function or synthesis of the let-7 miRNA.
Catalytic activity	Endonucleolytic cleavage to 5'-phosphomonoester.
Cofactor	Magnesium or manganese
Subcellular location	Nucleus
Accession ID	P0C5H7 (DCL2_EMENI) Reviewed, UniProtKB/Swiss-Prot
Protein Names	<p>Recommended name: Dicer-like protein 2</p> <p>Including the following 2 domains: Endoribonuclease dcl2 EC=3.1.26.- ATP-dependent helicase dcl2 EC=3.6.4.-</p>
Gene Names	<p>Name: dcl2 ORF Names: AN10380</p>
Organism	Emericella nidulans (strain FGSC A4 / ATCC 38163 / CBS 112.46 / NRRL 194 / M139) (<i>Aspergillus nidulans</i>)
Taxonomic identifier	227321 [NCBI]
Function	Dicer-like endonuclease involved in cleaving double-stranded RNA in the RNA interference

	(RNAi) pathway. Produces 21 to 25 bp dsRNAs (siRNAs) which target the selective destruction of homologous RNAs leading to sequence-specific suppression of gene expression, called post-transcriptional gene silencing (PTGS). Part of a broad host defense response against viral infection and transposons
Cofactor	Magnesium or manganese
Subcellular location	N/A
Accession ID	P22192 (PAC1_SCHPO) Reviewed, UniProtKB/Swiss-Prot
Protein Names	Recommended name: Double-strand-specific pac1 ribonuclease EC=3.1.26.3 Alternative name(s): Protein hcs
Gene Names	Name: pac1 Synonyms: hcs ORF Names: SPBC119.11c
Organism	Schizosaccharomyces pombe (strain 972 / ATCC 24843) (Fission yeast)
Taxonomic identifier	284812 [NCBI]
Function	Digests double-stranded RNA. Converts long double-stranded RNAs into short oligonucleotides, leaving 5'-phosphates on their cleavage products. Probably inhibits mating and meiosis by degrading a specific mRNA required for sexual development.
Catalytic activity	Endonucleolytic cleavage to 5'-phosphomonoester.
Cofactor	Magnesium
Subcellular location	N/A
Accession ID	P34529 (DCR1_CAEEL) Reviewed, UniProtKB/Swiss-Prot
Protein Names	Recommended name: Endoribonuclease dcr-1 EC=3.1.26.-
Gene Names	Name: dcr-1 ORF Names: K12H4.8
Organism	Caenorhabditis elegans
Taxonomic identifier	6239 [NCBI]
Function	Involved in cleaving double-stranded RNA in the RNA interference (RNAi) pathway. It produces 21 to 23 bp dsRNAs (siRNAs) which target the selective destruction of homologous RNAs. Seems to process the precursor of the small temporal RNA let-7 which is involved in developmental timing.
Cofactor	Magnesium or manganese
Subcellular location	N/A
Accession ID	P84634 (DCL4_ARATH) Reviewed, UniProtKB/Swiss-Prot
Protein Names	Recommended name: Dicer-like protein 4 EC=3.1.26.-
Gene Names	Name: DCL4 Ordered Locus Names: At5g20320 ORF Names: F5O24.210
Organism	Arabidopsis thaliana (Mouse-ear cress)
Taxonomic identifier	3702 [NCBI]
Function	Ribonuclease (RNase) III involved in RNA-mediated post-transcriptional gene silencing (PTGS). Functions in the biogenesis of trans-acting small interfering RNAs (ta-siRNAs, derived from the TAS1, TAS2 or TAS3 endogenous transcripts) by cleaving small dsRNAs into 21-24 nucleotide ta-siRNAs. Functions with the dsRNA-binding protein DRB4 in ta-siRNAs processing. Acts in the RDR6/SGS3/DCL4/AGO7 ta-siRNA pathway involved in leaf developmental timing. Plays a role in transitive silencing of transgenes by processing secondary siRNAs. This pathway, which requires DCL2 and RDR6, amplifies silencing by using the target RNA as substrate to generate secondary siRNAs, providing an efficient

Cofactor	Magnesium or manganese
Subunit structure	Interacts with DRB4.
Subcellular location	Nucleus
Accession ID	Q09884 (DCR1_SCHPO) Reviewed, UniProtKB/Swiss-Prot
Protein Names	<p>Recommended name: Protein Dicer</p> <p>Alternative name(s): Cell cycle control protein dcr1 RNA interference pathway protein dcr1</p> <p>Including the following 2 domains: Endoribonuclease dcr1 EC=3.1.26.- ATP-dependent helicase dcr1 EC=3.6.4.-</p>
Gene Names	<p>Name: dcr1</p> <p>ORF Names: SPCC188.13c, SPCC584.10c</p>
Organism	<i>Schizosaccharomyces pombe</i> (strain 972 / ATCC 24843) (Fission yeast)
Taxonomic identifier	284812 [NCBI]
Function	<p>Required for G1 arrest and mating in response to nitrogen starvation. Ago1 regulation of cytokinesis and cell cycle checkpoints occurs downstream of dcr1. Required, indirectly, for regulated hyperphosphorylation of cdc2.</p> <p>Has a role in the RNA interference (RNAi) pathway which is important for heterochromatin formation, accurate chromosome segregation, centromere cohesion and telomere function during mitosis and meiosis. Digests double-stranded RNA (dsRNA) producing 21 to 23 bp dsRNAs, so-called interfering RNAs (siRNA). Required for both post-transcriptional and transcriptional gene silencing. Required for silencing at the centromeres and for initiation of transcriptionally silent heterochromatin at the mating type locus. Promotes histone H3 'Lys-10' methylation necessary for centromere function. Required for recruitment of swi6 and cohesin to an ectopic dg repeat.</p>
Cofactor	Magnesium or manganese
Subcellular location	Cytoplasm. Nucleus
Accession ID	Q0CEI2 (DCL2_ASPTN) Reviewed, UniProtKB/Swiss-Prot
Protein Names	<p>Recommended name: Dicer-like protein 2</p> <p>Including the following 2 domains: Endoribonuclease dcl2 EC=3.1.26.- ATP-dependent helicase dcl2 EC=3.6.4.-</p>
Gene Names	<p>Name: dcl2</p> <p>ORF Names: ATEG_07902</p>
Organism	<i>Aspergillus terreus</i> (strain NIH 2624 / FGSC A1156) [Complete proteome]
Taxonomic identifier	341663 [NCBI]
Function	Dicer-like endonuclease involved in cleaving double-stranded RNA in the RNA interference (RNAi) pathway. Produces 21 to 25 bp dsRNAs (siRNAs) which target the selective

Cofactor	Magnesium or manganese
Subcellular location	N/A
Accession ID	Q0CW42 (DCL1_ASPTN) Reviewed, UniProtKB/Swiss-Prot
Protein Names	<p>Recommended name: Dicer-like protein 1</p> <p>Including the following 2 domains: Endoribonuclease dcl1 EC=3.1.26.- ATP-dependent helicase dcl1 EC=3.6.4.-</p>
Gene Names	<p>Name: dcl1</p> <p>ORF Names: ATEG_02092</p>
Organism	Aspergillus terreus (strain NIH 2624 / FGSC A1156) [Complete proteome]
Taxonomic identifier	341663 [NCBI]
Function	Dicer-like endonuclease involved in cleaving double-stranded RNA in the RNA interference (RNAi) pathway. Produces 21 to 25 bp dsRNAs (siRNAs) which target the selective destruction of homologous RNAs leading to sequence-specific suppression of gene expression, called post-transcriptional gene silencing (PTGS). Part of a broad host defense response against viral infection and transposons
Cofactor	Magnesium or manganese
Subcellular location	N/A
Accession ID	Q0UI93 (DCL1_PHANO) Reviewed, UniProtKB/Swiss-Prot
Protein Names	<p>Recommended name: Dicer-like protein 1</p> <p>Including the following 2 domains: Endoribonuclease DCL1 EC=3.1.26.- ATP-dependent helicase DCL1 EC=3.6.4.-</p>
Gene Names	<p>Name: DCL1</p> <p>ORF Names: SNOG_08521</p>
Organism	Phaeosphaeria nodorum (strain SN15 / ATCC MYA-4574 / FGSC 10173) (Glume blotch fungus) (Septoria nodorum)
Taxonomic identifier	321614 [NCBI]
Function	Dicer-like endonuclease involved in cleaving double-stranded RNA in the RNA interference (RNAi) pathway. Produces 21 to 25 bp dsRNAs (siRNAs) which target the selective destruction of homologous RNAs leading to sequence-specific suppression of gene expression, called post-transcriptional gene silencing (PTGS). Part of a broad host defense response against viral infection and transposons
Cofactor	Magnesium or manganese
Subcellular location	N/A
Accession ID	Q0UL22 (DCL2_PHANO) Reviewed, UniProtKB/Swiss-Prot
Protein Names	<p>Recommended name: Dicer-like protein 2</p> <p>Including the following 2 domains: Endoribonuclease DCL2 EC=3.1.26.- ATP-dependent helicase DCL2 EC=3.6.4.-</p>
Gene Names	<p>Name: DCL2</p> <p>ORF Names: SNOG_07542</p>

Organism	Phaeosphaeria nodorum (strain SN15 / ATCC MYA-4574 / FGSC 10173) (Glume blotch fungus) (<i>Septoria nodorum</i>)
Taxonomic identifier	321614 [NCBI]
Function	Dicer-like endonuclease involved in cleaving double-stranded RNA in the RNA interference (RNAi) pathway. Produces 21 to 25 bp dsRNAs (siRNAs) which target the selective destruction of homologous RNAs leading to sequence-specific suppression of gene expression, called post-transcriptional gene silencing (PTGS). Part of a broad host defense response against viral infection and transposons
Cofactor	Magnesium or manganese
Subcellular location	N/A
Accession ID	Q10HL3 (DCL2A_ORYSJ) Reviewed, UniProtKB/Swiss-Prot
Protein Names	<p>Recommended name: Endoribonuclease Dicer homolog 2a</p> <p>Alternative name(s): Dicer-like protein 2a Short name=OsDCL2a EC=3.1.26.-</p>
Gene Names	<p>Name: DCL2A Ordered Locus Names: Os03g0583900, LOC_Os03g38740 ORF Names: OJ1785_A05.30</p>
Organism	Oryza sativa subsp. japonica (Rice) [Complete proteome]
Taxonomic identifier	39947 [NCBI]
Function	Probably involved in the RNA silencing pathway. May cleave double-stranded RNA to produce short 21-24 nucleotides (nt) RNAs which target the selective destruction of complementary RNAs
Cofactor	Magnesium or manganese
Subunit structure	May interact with ARGONAUTE1 or PINHEAD through their common PAZ domains
Subcellular location	Nucleus
Accession ID	Q1DKI1 (DCL1_CO CIM) Reviewed, UniProtKB/Swiss-Prot
Protein Names	<p>Recommended name: Dicer-like protein 1 Including the following 2 domains: Endoribonuclease DCL1 EC=3.1.26.- ATP-dependent helicase DCL1 EC=3.6.4.-</p>
Gene Names	<p>Name: DCL1 ORF Names: CIMG_09182</p>
Organism	Coccidioides immitis (strain RS) (Valley fever fungus)
Taxonomic identifier	246410 [NCBI]
Function	Dicer-like endonuclease involved in cleaving double-stranded RNA in the RNA interference (RNAi) pathway. Produces 21 to 25 bp dsRNAs (siRNAs) which target the selective destruction of homologous RNAs leading to sequence-specific suppression of gene expression, called post-transcriptional gene silencing (PTGS). Part of a broad host defense response against viral infection and transposons
Cofactor	Magnesium or manganese
Subcellular location	N/A
Accession ID	Q1DW80 (DCL2_CO CIM) Reviewed, UniProtKB/Swiss-Prot
Protein Names	<p>Recommended name: Dicer-like protein 2 Including the following 2 domains: Endoribonuclease DCL2 EC=3.1.26.- ATP-dependent helicase DCL2</p>

Gene Names	EC=3.6.4.- Name: DCL2
Organism	ORF Names: CIMG_05433
Taxonomic identifier	Coccidioides immitis (strain RS) (Valley fever fungus)
Function	246410 [NCBI] Dicer-like endonuclease involved in cleaving double-stranded RNA in the RNA interference (RNAi) pathway. Produces 21 to 25 bp dsRNAs (siRNAs) which target the selective destruction of homologous RNAs leading to sequence-specific suppression of gene expression, called post-transcriptional gene silencing (PTGS). Part of a broad host defense response against viral infection and transposons
Cofactor	Magnesium or manganese
Subcellular location	N/A
Accession ID	Q25BN1 (DICER_CHICK) Reviewed, UniProtKB/Swiss-Prot
Protein Names	Recommended name: Endoribonuclease Dicer EC=3.1.26.-
Gene Names	Name: DICER1
Organism	Synonyms: DICER
Taxonomic identifier	Gallus gallus (Chicken)
Function	9031 [NCBI] Required for formation of the RNA induced silencing complex (RISC). Component of the RISC loading complex (RLC), also known as the micro-RNA (miRNA) loading complex (miRLC), which is composed of DICER1, EIF2C2/AGO2 and TARBP2. Within the RLC/miRLC, DICER1 and TARBP2 are required to process precursor miRNAs (pre-miRNAs) to mature miRNAs and then load them onto EIF2C2/AGO2. EIF2C2/AGO2 bound to the mature miRNA constitutes the minimal RISC and may subsequently dissociate from DICER1 and TARBP2. Also cleaves double-stranded RNA to produce short interfering RNAs (siRNAs) which target the selective destruction of complementary RNAs
Cofactor	Binds 2 magnesium or manganese ions per subunit
Subunit structure	Component of the RISC loading complex (RLC), or micro-RNA (miRNA) loading complex (miRLC), which is composed of DICER1, EIF2C2/AGO2 and TARBP2. Note that the trimeric RLC/miRLC is also referred to as RISC
Subcellular location	Cytoplasm
Accession ID	Q2H0G2 (DCL1_CHAGB) Reviewed, UniProtKB/Swiss-Prot
Protein Names	Recommended name: Dicer-like protein 1 Including the following 2 domains: Endoribonuclease DCL1 EC=3.1.26.- ATP-dependent helicase DCL1 EC=3.6.4.-
Gene Names	Name: DCL1
Organism	ORF Names: CHGG_04734
Taxonomic identifier	Chaetomium globosum (strain ATCC 6205 / CBS 148.51 / DSM 1962 / NBRC 6347 / NRRL 1970) (Soil fungus) [Complete proteome]
Function	306901 [NCBI] Dicer-like endonuclease involved in cleaving double-stranded RNA in the RNA interference (RNAi) pathway. Produces 21 to 25 bp dsRNAs (siRNAs) which target the selective destruction of homologous RNAs leading to sequence-specific suppression of gene expression, called post-transcriptional gene silencing (PTGS). Part of a broad host defense response against viral infection and transposons
Cofactor	Magnesium or manganese
Subcellular location	N/A
Accession ID	Q2U6C4 (DCL1_ASPOR) Reviewed, UniProtKB/Swiss-Prot

Protein Names	Recommended name: Dicer-like protein 1 Including the following 2 domains: Endoribonuclease dcl1 EC=3.1.26.- ATP-dependent helicase dcl1 EC=3.6.4.-
Gene Names	Name: dcl1 ORF Names: AO090120000297
Organism	Aspergillus oryzae (strain ATCC 42149 / RIB 40) (Yellow koji mold) [Complete proteome]
Taxonomic identifier	510516 [NCBI]
Function	Dicer-like endonuclease involved in cleaving double-stranded RNA in the RNA interference (RNAi) pathway. Produces 21 to 25 bp dsRNAs (siRNAs) which target the selective destruction of homologous RNAs leading to sequence-specific suppression of gene expression, called post-transcriptional gene silencing (PTGS). Part of a broad host defense response against viral infection and transposons
Cofactor	Magnesium or manganese
Subcellular location	N/A
Accession ID	Q2UNX5 (DCL2_ASPOR) Reviewed, UniProtKB/Swiss-Prot
Protein Names	Recommended name: Dicer-like protein 2 Including the following 2 domains: Endoribonuclease dcl2 EC=3.1.26.- ATP-dependent helicase dcl2 EC=3.6.4.-
Gene Names	Name: dcl2 ORF Names: AO090001000193
Organism	Aspergillus oryzae (strain ATCC 42149 / RIB 40) (Yellow koji mold) [Complete proteome]
Taxonomic identifier	510516 [NCBI]
Function	Dicer-like endonuclease involved in cleaving double-stranded RNA in the RNA interference (RNAi) pathway. Produces 21 to 25 bp dsRNAs (siRNAs) which target the selective destruction of homologous RNAs leading to sequence-specific suppression of gene expression, called post-transcriptional gene silencing (PTGS). Part of a broad host defense response against viral infection and transposons
Cofactor	Magnesium or manganese
Subcellular location	N/A
Accession ID	Q2VF18 (DCL2_CRYPA) Reviewed, UniProtKB/Swiss-Prot
Protein Names	Recommended name: Dicer-like protein 2 Including the following 2 domains: Endoribonuclease DCL-2 EC=3.1.26.- ATP-dependent helicase DCL-2 EC=3.6.4.-
Gene Names	Name: DCL-2
Organism	Cryphonectria parasitica (Chesnut blight fungus) (Endothia parasitica)
Taxonomic identifier	5116 [NCBI]
Function	Dicer-like endonuclease involved in cleaving double-stranded RNA in the RNA interference (RNAi) pathway. Produces 21 to 25 bp dsRNAs (siRNAs) which target the selective destruction of homologous RNAs leading to sequence-specific suppression of gene expression, called post-transcriptional gene silencing (PTGS). Part of a broad host defense, DCL-2 is involved in antiviral defense against mycoviruses like the hypovirus CHV1-EP713 and the reovirus MyRV1-Cp9B21.

Cofactor	Magnesium or manganese
Subcellular location	N/A
Accession ID	Q2VF19 (DCL1_CRYPA) Reviewed, UniProtKB/Swiss-Prot
Protein Names	<p>Recommended name: Dicer-like protein 1</p> <p>Including the following 2 domains: Endoribonuclease DCL-1 EC=3.1.26.- ATP-dependent helicase DCL-1 EC=3.6.4.-</p>
Gene Names	Name: DCL-1
Organism	<i>Cryphonectria parasitica</i> (Chesnut blight fungus) (<i>Endothia parasitica</i>)
Taxonomic identifier	5116 [NCBI]
Function	Dicer-like endonuclease involved in cleaving double-stranded RNA in the RNA interference (RNAi) pathway. Produces 21 to 25 bp dsRNAs (siRNAs) which target the selective destruction of homologous RNAs leading to sequence-specific suppression of gene expression, called post-transcriptional gene silencing (PTGS). Part of a broad host defense response against viral infection and transposons
Cofactor	Magnesium or manganese
Subcellular location	N/A
Accession ID	Q3EBC8 (DCL2_ARATH) Reviewed, UniProtKB/Swiss-Prot
Protein Names	<p>Recommended name: Endoribonuclease Dicer homolog 2 EC=3.1.26.-</p> <p>Alternative name(s): Dicer-like protein 2 Short name=AtDCL2</p>
Gene Names	<p>Ordered Locus Names: At3g03300</p> <p>ORF Names: T17B22.1</p>
Organism	<i>Arabidopsis thaliana</i> (Mouse-ear cress)
Taxonomic identifier	3702 [NCBI]
Function	Ribonuclease (RNase) III involved in RNA-mediated post-transcriptional gene silencing (PTGS). Involved in the processing of natural small interfering RNAs (nat-siRNAs, derived from cis-natural antisense transcripts) by cleaving small dsRNAs into 24 nucleotide nat-siRNAs. Plays an essential role in transitive silencing of transgenes by processing secondary siRNAs. This pathway, which requires DCL4 and RDR6, amplifies silencing by using the target RNA as substrate to generate secondary siRNAs, providing an efficient mechanism for long-distance silencing. May participate with DCL3 in the production of 24 nucleotide repeat-associated siRNAs (ra-siRNAs) which derive from heterochromatin and DNA repeats such as transposons. Plays a role in antiviral RNA silencing. Involved in the production of viral siRNAs derived from the turnip crinkle virus (TCV) and tobacco rattle virus (TRV). Targeted by the viral silencing suppressor (VSR) protein 2b of the cucumber mosaic virus (CMV) that inactivates DCL2 function in RNA silencing. Does not seem to be involved in microRNAs (miRNAs) processing.
Cofactor	Magnesium or manganese
Subcellular location	Nucleus. Cytoplasm
Accession ID	Q4WA22 (DCL2_ASPEFU) Reviewed, UniProtKB/Swiss-Prot
Protein Names	<p>Recommended name: Dicer-like protein 2</p> <p>Including the following 2 domains: Endoribonuclease dcl2 EC=3.1.26.- ATP-dependent helicase dcl2 EC=3.6.4.-</p>

Gene Names	Name: dcl2 ORF Names: AFUA_4G02930
Organism	Neosartorya fumigata (strain ATCC MYA-4609 / Af293 / CBS 101355 / FGSC A1100) (Aspergillus fumigatus)
Taxonomic identifier	330879 [NCBI]
Function	Dicer-like endonuclease involved in cleaving double-stranded RNA in the RNA interference (RNAi) pathway. Produces 21 to 25 bp dsRNAs (siRNAs) which target the selective destruction of homologous RNAs leading to sequence-specific suppression of gene expression, called post-transcriptional gene silencing (PTGS). Part of a broad host defense response against viral infection and transposons
Cofactor	Magnesium or manganese
Subcellular location	N/A
Accession ID	Q4WVE3 (DCL1_ASFP) Reviewed, UniProtKB/Swiss-Prot
Protein Names	Recommended name: Dicer-like protein 1 Including the following 2 domains: Endoribonuclease dcl1 EC=3.1.26.- ATP-dependent helicase dcl1 EC=3.6.4.-
Gene Names	Name: dcl1 ORF Names: AFUA_5G11790
Organism	Neosartorya fumigata (strain ATCC MYA-4609 / Af293 / CBS 101355 / FGSC A1100) (Aspergillus fumigatus)
Taxonomic identifier	330879 [NCBI]
Function	Dicer-like endonuclease involved in cleaving double-stranded RNA in the RNA interference (RNAi) pathway. Produces 21 to 25 bp dsRNAs (siRNAs) which target the selective destruction of homologous RNAs leading to sequence-specific suppression of gene expression, called post-transcriptional gene silencing (PTGS). Part of a broad host defense response against viral infection and transposons
Cofactor	Magnesium or manganese
Subcellular location	N/A
Accession ID	Q5HZJ0 (RNC_MOUSE) Reviewed, UniProtKB/Swiss-Prot
Protein Names	Recommended name: Ribonuclease 3 EC=3.1.26.3 Alternative name(s): Protein Drosha Ribonuclease III Short name=RNase III
Gene Names	Name: Drosha
Organism	Synonyms: Etohi2, Rn3, Rnasen
Taxonomic identifier	Mus musculus (Mouse)
Function	10090 [NCBI] Ribonuclease III double-stranded (ds) RNA-specific endoribonuclease that is involved in the initial step of microRNA (miRNA) biogenesis. Component of the microprocessor complex that is required to process primary miRNA transcripts (pri-miRNAs) to release precursor miRNA (pre-miRNA) in the nucleus. Within the microprocessor complex, DROSHA cleaves the 3' and 5' strands of a stem-loop in pri-miRNAs (processing center 11 bp from the dsRNA-ssRNA junction) to release hairpin-shaped pre-miRNAs that are subsequently cut by the cytoplasmic DICER to generate mature miRNAs. Involved also in pre-rRNA processing. Cleaves double-strand RNA and does not cleave single-strand RNA. Involved in the formation of GW bodies
Catalytic activity	Endonucleolytic cleavage to 5'-phosphomonoester.

Cofactor	Magnesium or manganese
Subunit structure	Component of the microprocessor complex, or pri-miRNA processing protein complex, which is composed of DROSHA and DGCR8. The microprocessor complex may contain multiple subunit of DGCR8 and DROSHA. Interacts with DGCR8, SP1 and SNIP1
Subcellular location	Interacts with SRRT/ARS2 Nucleus By similarity. Nucleus > nucleolus By similarity. Note: A fraction is translocated to the nucleolus during the S phase of the cell cycle. Localized in GW bodies (GWBS), also known as P-bodies
Accession ID	Q5JK90 (RTL1_ORYSJ) Reviewed, UniProtKB/Swiss-Prot
Protein Names	Recommended name: Ribonuclease 3-like protein 1 EC=3.1.26.- Alternative name(s): Ribonuclease III-like protein 1 Short name=RNase III-like protein 1
Gene Names	Ordered Locus Names: Os01g0551100, LOC_Os01g37050 ORF Names: OSJNBa0024F24.33, OSJNBa0066C06.2
Organism	Oryza sativa subsp. japonica (Rice) [Complete proteome]
Taxonomic identifier	39947 [NCBI]
Function	Cleaves double-stranded RNA (dsRNA)
Cofactor	Magnesium or manganese
Subcellular location	N/A
Accession ID	Q5N870 (DCL3A_ORYSJ) Reviewed, UniProtKB/Swiss-Prot
Protein Names	Recommended name: Endoribonuclease Dicer homolog 3a Alternative name(s): Dicer-like protein 3a Short name=OsDCL3a EC=3.1.26.-
Gene Names	Name: DCL3A Ordered Locus Names: Os01g0909200, LOC_Os01g68120 ORF Names: P0456E05.21
Organism	Oryza sativa subsp. japonica (Rice) [Complete proteome]
Taxonomic identifier	39947 [NCBI]
Function	Probably involved in the RNA silencing pathway. May cleave double-stranded RNA to produce short 21-24 nucleotides (nt) RNAs which target the selective destruction of complementary RNAs
Cofactor	Magnesium or manganese
Subunit structure	May interact with ARGONAUTE1 or PINHEAD through their common PAZ domains
Subcellular location	Nucleus
Accession ID	Q61XX9 (RNC_CAEBR) Reviewed, UniProtKB/Swiss-Prot
Protein Names	Recommended name: Ribonuclease 3 EC=3.1.26.3 Alternative name(s): Protein drosha Ribonuclease III Short name=RNase III
Gene Names	Name: drsh-1 ORF Names: CBG03798
Organism	Caenorhabditis briggsae
Taxonomic identifier	6238 [NCBI]
Function	Executes the initial step of microRNA (miRNA) processing in the nucleus, that is the

Catalytic activity	cleavage of pri-miRNA to release pre-miRNA. Involved in pre-rRNA processing. Cleaves double-strand RNA and does not cleave single-strand RNA. Involved in fertility. Required for the function or synthesis of the let-7 miRNA
Cofactor	Endonucleolytic cleavage to 5'-phosphomonoester.
Subcellular location	Magnesium or manganese Nucleus
Accession ID	Q69KJ0 (RTL3_ORYSJ) Reviewed, UniProtKB/Swiss-Prot
Protein Names	Recommended name: Ribonuclease 3-like protein 3 EC=3.1.26.- Alternative name(s): Ribonuclease III-like protein 3 Short name=RNase III-like protein 3
Gene Names	Ordered Locus Names: Os06g0358800, LOC_Os06g25250 ORF Names: OsJ_21299, OSJNBb0027A16.25
Organism	Oryza sativa subsp. japonica (Rice) [Complete proteome]
Taxonomic identifier	39947 [NCBI]
Function	Cleaves double-stranded RNA (dsRNA)
Cofactor	Magnesium or manganese
Subcellular location	N/A
Accession ID	Q69LX2 (DCL2B_ORYSJ) Reviewed, UniProtKB/Swiss-Prot
Protein Names	Recommended name: Endoribonuclease Dicer homolog 2b Alternative name(s): Dicer-like protein 2b Short name=OsDCL2b EC=3.1.26.-
Gene Names	Name: DCL2B Ordered Locus Names: Os09g0315100, LOC_Os09g14610 ORF Names: OSJNBa0057D11.8-1, OSJNBb0079G12.35-1
Organism	Oryza sativa subsp. japonica (Rice) [Complete proteome]
Taxonomic identifier	39947 [NCBI]
Function	Probably involved in the RNA silencing pathway. May cleave double-stranded RNA to produce short 21-24 nucleotides (nt) RNAs which target the selective destruction of complementary RNAs
Subunit structure	May interact with ARGONAUTE1 or PINHEAD through their common PAZ domains
Cofactor	Magnesium or manganese
Subcellular location	Nucleus
Accession ID	Q6ATG6 (RTL2_ORYSJ) Reviewed, UniProtKB/Swiss-Prot
Protein Names	Recommended name: Ribonuclease 3-like protein 2 EC=3.1.26.- Alternative name(s): Ribonuclease III-like protein 2 Short name=RNase III-like protein 2
Gene Names	Ordered Locus Names: Os05g0271300, LOC_Os05g18850 ORF Names: OJ1653_D06.9, OSJNBb0061M13.3
Organism	Oryza sativa subsp. japonica (Rice) [Complete proteome]
Taxonomic identifier	39947 [NCBI]
Function	Cleaves double-stranded RNA (dsRNA)
Cofactor	Magnesium or manganese
Subcellular location	N/A
Accession ID	Q6TUI4 (DICER_BOVIN) Reviewed, UniProtKB/Swiss-Prot
Protein Names	Recommended name:

Gene Names	Endoribonuclease Dicer EC=3.1.26.-
Organism	Name: DICER1
Taxonomic identifier	Synonyms: DICER
Function	Bos taurus (Bovine) 9913 [NCBI]
Cofactor	Required for formation of the RNA induced silencing complex (RISC). Component of the RISC loading complex (RLC), also known as the micro-RNA (miRNA) loading complex (miRLC), which is composed of DICER1, EIF2C2/AGO2 and TARBP2. Within the RLC/miRLC, DICER1 and TARBP2 are required to process precursor miRNAs (pre-miRNAs) to mature miRNAs and then load them onto EIF2C2/AGO2. EIF2C2/AGO2 bound to the mature miRNA constitutes the minimal RISC and may subsequently dissociate from DICER1 and TARBP2. Also cleaves double-stranded RNA to produce short interfering RNAs (siRNAs) which target the selective destruction of complementary RNAs
Subunit structure	Binds 2 magnesium or manganese ions per subunit
Subcellular location	Component of the RISC loading complex (RLC), or micro-RNA (miRNA) loading complex (miRLC), which is composed of DICER1, EIF2C2/AGO2 and TARBP2. Note that the trimeric RLC/miRLC is also referred to as RISC. Interacts with DHX9, EIF2C1, PIWIL1 and PRKRA. Associates with the 60S ribosome
Accession ID	Cytoplasm Q6TV19 (DICER_DANRE) Reviewed, UniProtKB/Swiss-Prot
Protein Names	Recommended name: Endoribonuclease Dicer
Gene Names	EC=3.1.26.-
Organism	Name: dicer1
Taxonomic identifier	Danio rerio (Zebrafish) (Brachydanio rerio)
Function	7955 [NCBI]
Cofactor	Required for formation of the RNA induced silencing complex (RISC). Component of the RISC loading complex (RLC), also known as the micro-RNA (miRNA) loading complex (miRLC), which is composed of dicer1, eif2c2/ago2 and tarbp2. Within the RLC/miRLC, dicer1 and tarbp2 are required to process precursor miRNAs (pre-miRNAs) to mature miRNAs and then load them onto eif2c2/ago2. eif2c2/ago2 bound to the mature miRNA constitutes the minimal RISC and may subsequently dissociate from dicer1 and tarbp2. Also cleaves double-stranded RNA to produce short interfering RNAs (siRNAs) which target the selective destruction of complementary RNAs
Subunit structure	Binds 2 magnesium or manganese ions per subunit
Subcellular location	Component of the RISC loading complex (RLC), or micro-RNA (miRNA) loading complex (miRLC), which is composed of dicer1, eif2c2/ago2 and tarbp2. Note that the trimeric RLC/miRLC is also referred to as RISC
Accession ID	Cytoplasm Q7S8J7 (DCL1_NEUCR) Reviewed, UniProtKB/Swiss-Prot
Protein Names	Recommended name: Dicer-like protein 1
Gene Names	Including the following 2 domains: Endoribonuclease dcl-1
Organism	EC=3.1.26.-
Taxonomic identifier	ATP-dependent helicase dcl-1
Function	EC=3.6.4.-
Gene Names	Name: dcl-1
Organism	ORF Names: NCU08270
Taxonomic identifier	Neurospora crassa (strain ATCC 24698 / 74-OR23-1A / CBS 708.71 / DSM 1257 / FGSC 987)
Function	367110 [NCBI]
	Dicer-like endonuclease involved in cleaving double-stranded RNA in the RNA interference

	(RNAi) pathway. Produces 21 to 25 bp dsRNAs (siRNAs) which target the selective destruction of homologous RNAs leading to sequence-specific suppression of gene expression, called post-transcriptional gene silencing (PTGS). Part of a broad host defense response against viral infection and transposons. Controls the expression of the non-LTR retrotransposon Tad in the African strain, Adiomopoume.
Cofactor Induction	Magnesium or manganese By double-stranded RNA (dsRNA)
Accession ID	Q7SCC1 (DCL2_NEUCR) Reviewed, UniProtKB/Swiss-Prot
Protein Names	Recommended name: Dicer-like protein 2 Including the following 2 domains: Endoribonuclease dcl-2 EC=3.1.26.- ATP-dependent helicase dcl-2 EC=3.6.4.-
Gene Names	Name: dcl-2 ORF Names: B14D6.490, NCU06766
Organism	Neurospora crassa (strain ATCC 24698 / 74-OR23-1A / CBS 708.71 / DSM 1257 / FGSC 987)
Taxonomic identifier	367110 [NCBI]
Function	Dicer-like endonuclease involved in cleaving double-stranded RNA in the RNA interference (RNAi) pathway. Produces 21 to 25 bp dsRNAs (siRNAs) which target the selective destruction of homologous RNAs leading to sequence-specific suppression of gene expression, called post-transcriptional gene silencing (PTGS). Part of a broad host defense response against viral infection and transposons. Controls the expression of the non-LTR retrotransposon Tad in the African strain, Adiomopoume
Cofactor Induction	Magnesium or manganese By double-stranded RNA (dsRNA).
Accession ID	Q7XD96 (DCL3B_ORYSJ) Reviewed, UniProtKB/Swiss-Prot
Protein Names	Recommended name: Endoribonuclease Dicer homolog 3b Alternative name(s): Dicer-like protein 3b Short name=OsDCL3b EC=3.1.26.-
Gene Names	Name: DCL3B Ordered Locus Names: Os10g0485600, LOC_Os10g34430 ORF Names: OSJNBa0029C15.23
Organism	Oryza sativa subsp. japonica (Rice) [Complete proteome]
Taxonomic identifier	39947 [NCBI]
Function	Probably involved in the RNA silencing pathway. May cleave double-stranded RNA to produce short 21-24 nucleotides (nt) RNAs which target the selective destruction of complementary RNAs
Cofactor	Magnesium or manganese
Subunit structure	May interact with ARGONAUTE1 or PINHEAD through their common PAZ domains
Subcellular location	Nucleus
Accession ID	Q8LMR2 (DCL1_ORYSJ) Reviewed, UniProtKB/Swiss-Prot
Protein Names	Recommended name: Endoribonuclease Dicer homolog 1 Alternative name(s): Dicer-like protein 1 Short name=OsDCL1 EC=3.1.26.-
Gene Names	Name: DCL1

Organism	Ordered Locus Names: Os03g0121800, LOC_Os03g02970 ORF Names: OJ1705B08.11, OsJ_09217 Oryza sativa subsp. japonica (Rice) [Complete proteome]
Taxonomic identifier	39947 [NCBI]
Function	Involved in the RNA silencing pathway. Cleaves double-stranded RNA to produce microRNAs (miRNAs) of 21-24 nucleotides which target the selective destruction of complementary RNAs. Regulates by this way the development of the plant. May not be involved in small interfering RNAs (siRNAs) production
Cofactor	Magnesium or manganese
Subunit structure	May interact with ARGONAUTE1 or PINHEAD through their common PAZ domains
Subcellular location	Nucleus
Accession ID	Q8R418 (DICER_MOUSE) Reviewed, UniProtKB/Swiss-Prot
Protein Names	<p>Recommended name: Endoribonuclease Dicer EC=3.1.26.-</p> <p>Alternative name(s): Double-strand-specific ribonuclease mDCR-1</p>
Gene Names	<p>Name: Dicer1 Synonyms: Dicer, Mdcr</p>
Organism	Mus musculus (Mouse)
Taxonomic identifier	10090 [NCBI]
Function	<p>Required for formation of the RNA induced silencing complex (RISC). Component of the RISC loading complex (RLC), also known as the micro-RNA (miRNA) loading complex (miRLC), which is composed of DICER1, EIF2C2/AGO2 and TARBP2. Within the RLC/miRLC, DICER1 and TARBP2 are required to process precursor miRNAs (pre-miRNAs) to mature miRNAs and then load them onto EIF2C2/AGO2. EIF2C2/AGO2 bound to the mature miRNA constitutes the minimal RISC and may subsequently dissociate from DICER1 and TARBP2. Also cleaves double-stranded RNA to produce short interfering RNAs (siRNAs) which target the selective destruction of complementary RNAs</p> <p>Involved in cleaving double-stranded RNA in the RNA interference (RNAi) pathway. It produces 21 to 23 bp dsRNAs (siRNAs) which target the selective destruction of homologous RNAs.</p>
Cofactor	Binds 2 magnesium or manganese ions per subunit
Subunit structure	Component of the RISC loading complex (RLC), or micro-RNA (miRNA) loading complex (miRLC), which is composed of DICER1, EIF2C2/AGO2 and TARBP2. Note that the trimeric RLC/miRLC is also referred to as RISC. Interacts with DHX9, EIF2C1, PIWIL1 and PRKRA. Associates with the 60S ribosome
Subcellular location	Cytoplasm
Accession ID	Q9LTQ0 (RTL2_ARATH) Reviewed, UniProtKB/Swiss-Prot
Protein Names	<p>Recommended name: Ribonuclease 3-like protein 2 EC=3.1.26.-</p> <p>Alternative name(s): Ribonuclease III-like protein 2 Short name=RNase III-like protein 2 Ribonuclease three-like protein 2</p>
Gene Names	<p>Name: RTL2 Ordered Locus Names: At3g20420 ORF Names: MQC12.21</p>
Organism	Arabidopsis thaliana (Mouse-ear cress)
Taxonomic identifier	3702 [NCBI]
Function	Ribonuclease that cleaves double-stranded RNA (dsRNA). Required for 3'-external transcribed spacer (ETS) cleavage of the pre-rRNA precursors. May promote the production of 21 nucleotide small interfering RNA (siRNA) during post-transcriptional gene silencing

Cofactor	(PTGS).
Subunit structure	Binds magnesium or manganese
Subcellular location	Homodimer; disulfide-linked Nucleus. Cytoplasm
Accession ID	Q9LXW7 (DCL3_ARATH) Reviewed, UniProtKB/Swiss-Prot
Protein Names	Recommended name: Endoribonuclease Dicer homolog 3 EC=3.1.26.- Alternative name(s): Dicer-like protein 3 Short name=AtDCL3
Gene Names	Name: DCL3 Ordered Locus Names: At3g43920 ORF Names: T15B3.60
Organism	Arabidopsis thaliana (Mouse-ear cress)
Taxonomic identifier	3702 [NCBI]
Function	Ribonuclease (RNase) III involved in RNA-mediated post-transcriptional gene silencing (PTGS). Involved in the processing of repeat-associated small interfering RNAs (ra-siRNAs, derived from heterochromatin and DNA repeats such as transposons) by cleaving small dsRNAs into 24 nucleotide ra-siRNAs. Plays a role in antiviral RNA silencing. Involved in the production of viral siRNAs derived from the cabbage leaf curl virus (CaLCuV) and tobacco rattle virus (TRV). Targeted by the viral silencing suppressor (VSR) protein 2b of the cucumber mosaic virus (CMV) that inactivates DCL3 function in RNA silencing. Acts redundantly with DICER-LIKE 1 (DCL1) to promote flowering via repression of FLOWERING LOCUS C (FLC). Does not seem to be involved in microRNAs (miRNAs) processing.
Cofactor	Magnesium or manganese
Subunit structure	Interacts with DRB2 and DRB5
Subcellular location	Nucleus > nucleolus
Accession ID	Q9NR4 (RNC_HUMAN) Reviewed, UniProtKB/Swiss-Prot
Protein Names	Recommended name: Ribonuclease 3 EC=3.1.26.3 Alternative name(s): Protein Drosha Ribonuclease III Short name=RNase III p241
Gene Names	Name: DROSHA
	Synonyms: RN3, RNASE3L, RNASEN
Organism	Homo sapiens (Human)
Taxonomic identifier	9606 [NCBI]
Function	Ribonuclease III double-stranded (ds) RNA-specific endoribonuclease that is involved in the initial step of microRNA (miRNA) biogenesis. Component of the microprocessor complex that is required to process primary miRNA transcripts (pri-miRNAs) to release precursor miRNA (pre-miRNA) in the nucleus. Within the microprocessor complex, DROSHA cleaves the 3' and 5' strands of a stem-loop in pri-miRNAs (processing center 11 bp from the dsRNA-ssRNA junction) to release hairpin-shaped pre-miRNAs that are subsequently cut by the cytoplasmic DICER to generate mature miRNAs. Involved also in pre-rRNA processing. Cleaves double-strand RNA and does not cleave single-strand RNA. Involved in the formation of GW bodies
Catalytic activity	Endonucleolytic cleavage to 5'-phosphomonoester.
Cofactor	Magnesium or manganese
Subunit structure	Component of the microprocessor complex, or pri-miRNA processing protein complex,

Subcellular location	which is composed of DROSHA and DGCR8. The microprocessor complex may contain multiple subunit of DGCR8 and DROSHA. Interacts with DGCR8, SP1 and SNIP1. Interacts with SRRT/ARS2.
Accession ID	Q9SP32 (DCL1_ARATH) Reviewed, UniProtKB/Swiss-Prot
Protein Names	<p>Recommended name: Endoribonuclease Dicer homolog 1 EC=3.1.26.-</p> <p>Alternative name(s): Dicer-like protein 1 Short name=AtDCL1 Protein ABNORMAL SUSPENSOR 1 Protein CARPEL FACTORY Protein SHORT INTEGUMENTS 1 Protein SUSPENSOR 1</p>
Gene Names	<p>Name: DCL1</p> <p>Synonyms: ASU1, CAF SIN1, SUS1</p> <p>Ordered Locus Names: At1g01040</p> <p>ORF Names: T25K16.4</p>
Organism	Arabidopsis thaliana (Mouse-ear cress)
Taxonomic identifier	3702 [NCBI]
Function	Ribonuclease (RNase) III involved in RNA-mediated post-transcriptional gene silencing (PTGS). Functions in the microRNAs (miRNAs) biogenesis pathway by cleaving primary miRNAs (pri-miRNAs) and precursor miRNAs (pre-miRNAs). Functions with DRB1/HYL1 and SERRATE proteins for accurate pri-miRNAs to miRNAs processing. Indirectly involved in the production of trans-acting small interfering RNAs (ta-siRNAs) derived from the TAS1, TAS2 or TAS3 endogenous transcripts by participating in the production of their initiating miRNAs. Involved in the processing of natural siRNAs (nat-siRNAs, derived from cis-natural antisense transcripts) by cleaving 24 nucleotide nat-siRNAs into 21 nucleotide nat-siRNAs. Can produce RDR6-dependent endogenous ta-siRNAs derived from TAS1 and TAS2. Required for the production of 30-40 nucleotide bacterial-induced long siRNAs (lsiRNA). Acts redundantly with DICER-LIKE 3 (DCL3) to promote flowering via repression of FLOWERING LOCUS C (FLC). Represses antiviral RNA silencing through negative regulation of the expression of DCL4 and DCL3.
Cofactor	Magnesium or manganese
Subunit structure	Interacts (via N-terminus) with DDL. Interacts (via DRBM domains) with DRB1, DRB2 and DRB5. May interact with AGO1 or AGO10 through their common PAZ domains
Subcellular location	Nucleus. Note: Localizes to nuclear dicing body (also named D body), a nuclear body distributed throughout the nucleoplasm and involved in miRNA processing.
Accession ID	Q9UPY3 (DICER_HUMAN) Reviewed, UniProtKB/Swiss-Prot
Protein Names	<p>Recommended name: Endoribonuclease Dicer EC=3.1.26.-</p> <p>Alternative name(s): Helicase with RNase motif Short name=Helicase MOI</p>
Gene Names	<p>Name: DICER1</p> <p>Synonyms: DICER, HERNA, KIAA0928</p>
Organism	Homo sapiens (Human)
Taxonomic identifier	9606 [NCBI]
Function	Required for formation of the RNA induced silencing complex (RISC). Component of the RISC loading complex (RLC), also known as the micro-RNA (miRNA) loading complex (miRLC), which is composed of DICER1, EIF2C2/AGO2 and TARBP2. Within the

Cofactor	RLC/miRLC, DICER1 and TARBP2 are required to process precursor miRNAs (pre-miRNAs) to mature miRNAs and then load them onto EIF2C2/AGO2. EIF2C2/AGO2 bound to the mature miRNA constitutes the minimal RISC and may subsequently dissociate from DICER1 and TARBP2. Also cleaves double-stranded RNA to produce short interfering RNAs (siRNAs) which target the selective destruction of complementary RNAs
Subunit structure	Binds 2 magnesium or manganese ions per subunit Component of the RISC loading complex (RLC), or micro-RNA (miRNA) loading complex (miRLC), which is composed of DICER1, EIF2C2/AGO2 and TARBP2. Note that the trimeric RLC/miRLC is also referred to as RISC. Interacts with DHX9, EIF2C1, PIWIL1 and PRKRA. Associates with the 60S ribosome.
Subcellular location	Cytoplasm

PPI pairs having root-shared GO terms (i.e. GO:0004525 & GO:0046872)

PPI1	PPI2	Source DB	Taxonomy1	Taxonomy2	type	method
Q3EBC8	Q9LXW7	IntAct	3702	3702	direct interaction	far western blotting
Q3EBC8	Q9SP32	IntAct	3702	3702	direct interaction	far western blotting

[S-3] GPs containing root shared GO terms II

- GO:0004749: Ribose phosphate diphosphokinase activity
- GO:0042802: Identical protein binding
- GO:0000287: Magnesium ion binding
- Root shared except GO:0042802 – GO:0000287 which are shared by GO:0005488 (binding – 2nd direct child of root term, GO:0003674)

Accession ID	P32895 (KPR1_YEAST) Reviewed, UniProtKB/Swiss-Prot
Protein Names	<p>Recommended name: Ribose-phosphate pyrophosphokinase 1 EC=2.7.6.1</p> <p>Alternative name(s): Phosphoribosyl pyrophosphate synthase 1</p>
Gene Names	<p>Name: PRS1</p> <p>Synonyms: PPS1, PRP1, PRPS, PRPS1</p> <p>Ordered Locus Names: YKL181W</p>
Organism	Saccharomyces cerevisiae (strain ATCC 204508 / S288c) (Baker's yeast)
Taxonomic identifier	559292 [NCBI]
Function	5-phosphoribose 1-diphosphate synthase involved in nucleotide, histidine, and tryptophan biosynthesis. Active in heteromultimeric complexes with other 5-phosphoribose 1-diphosphate synthases (PRS2, PRS3, PRS4 and PRS5).
Catalytic activity	ATP + D-ribose 5-phosphate = AMP + 5-phospho-alpha-D-ribose 1-diphosphate.
Pathway	Metabolic intermediate biosynthesis; 5-phospho-alpha-D-ribose 1-diphosphate biosynthesis; 5-phospho-alpha-D-ribose 1-diphosphate from D-ribose 5-phosphate (route I): step 1/1.
Subcellular location	Cytoplasm
Accession ID	P38620 (KPR2_YEAST) Reviewed, UniProtKB/Swiss-Prot
Protein Names	<p>Recommended name: Ribose-phosphate pyrophosphokinase 2 EC=2.7.6.1</p> <p>Alternative name(s): Phosphoribosyl pyrophosphate synthase 2</p>
Gene Names	<p>Name: PRS2</p> <p>Synonyms: PRPS2, PRS</p> <p>Ordered Locus Names: YER099C</p>
Organism	Saccharomyces cerevisiae (strain ATCC 204508 / S288c) (Baker's yeast)
Taxonomic identifier	559292 [NCBI]
Function	5-phosphoribose 1-diphosphate synthase involved in nucleotide, histidine, and tryptophan biosynthesis. Active in heteromultimeric complexes with other 5-phosphoribose 1-diphosphate synthases (PRS2, PRS3, PRS4 and PRS5).
Catalytic activity	ATP + D-ribose 5-phosphate = AMP + 5-phospho-alpha-D-ribose 1-diphosphate.
Pathway	Metabolic intermediate biosynthesis; 5-phospho-alpha-D-ribose 1-diphosphate biosynthesis; 5-phospho-alpha-D-ribose 1-diphosphate from D-ribose 5-phosphate (route I): step 1/1.
Subcellular location	Cytoplasm
Accession ID	P38689 (KPR3_YEAST) Reviewed, UniProtKB/Swiss-Prot
Protein Names	<p>Recommended name: Ribose-phosphate pyrophosphokinase 3 EC=2.7.6.1</p> <p>Alternative name(s): Phosphoribosyl pyrophosphate synthase 3</p>
Gene Names	<p>Name: PRS3</p> <p>Synonyms: PRPS3</p> <p>Ordered Locus Names: YHL011C</p>
Organism	Saccharomyces cerevisiae (strain ATCC 204508 / S288c) (Baker's yeast)

Taxonomic identifier	559292 [NCBI]
Function	5-phosphoribose 1-diphosphate synthase involved in nucleotide, histidine, and tryptophan biosynthesis. Active in heteromultimeric complexes with other 5-phosphoribose 1-diphosphate synthases (PRS2, PRS3, PRS4 and PRS5).
Catalytic activity	ATP + D-ribose 5-phosphate = AMP + 5-phospho-alpha-D-ribose 1-diphosphate.
Pathway	Metabolic intermediate biosynthesis; 5-phospho-alpha-D-ribose 1-diphosphate biosynthesis; 5-phospho-alpha-D-ribose 1-diphosphate from D-ribose 5-phosphate (route I): step 1/1.
Subcellular location	Cytoplasm
Accession ID	Q12265 (KPR5_YEAST) Reviewed, UniProtKB/Swiss-Prot
Protein Names	<p>Recommended name:</p> <p>Ribose-phosphate pyrophosphokinase 5</p> <p>EC=2.7.6.1</p> <p>Alternative name(s):</p> <p>Phosphoribosyl pyrophosphate synthase 5</p> <p>Name: PRS5</p> <p>Synonyms: PRPS5</p> <p>Ordered Locus Names: YOL061W</p> <p>ORF Names: O1213</p>
Gene Names	
Organism	Saccharomyces cerevisiae (strain ATCC 204508 / S288c) (Baker's yeast)
Taxonomic identifier	559292 [NCBI]
Function	5-phosphoribose 1-diphosphate synthase involved in nucleotide, histidine, and tryptophan biosynthesis. Active in heteromultimeric complexes with other 5-phosphoribose 1-diphosphate synthases (PRS2, PRS3, PRS4 and PRS5).
Catalytic activity	ATP + D-ribose 5-phosphate = AMP + 5-phospho-alpha-D-ribose 1-diphosphate.
Pathway	Metabolic intermediate biosynthesis; 5-phospho-alpha-D-ribose 1-diphosphate biosynthesis; 5-phospho-alpha-D-ribose 1-diphosphate from D-ribose 5-phosphate (route I): step 1/1.
Subcellular location	Cytoplasm
Accession ID	Q14558 (KPRA_HUMAN) Reviewed, UniProtKB/Swiss-Prot
Protein Names	<p>Recommended name:</p> <p>Phosphoribosyl pyrophosphate synthase-associated protein 1</p> <p>Short name=PRPP synthase-associated protein 1</p> <p>Alternative name(s):</p> <p>39 kDa phosphoribosylpyrophosphate synthase-associated protein</p> <p>Short name=PAP39</p>
Gene Names	Name: PRPSAP1
Organism	Homo sapiens (Human)
Taxonomic identifier	9606 [NCBI]
Function	Seems to play a negative regulatory role in 5-phosphoribose 1-diphosphate synthesis.
Subunit structure	Binds to PRPS1 and PRPS2.
Subcellular location	N/A

[S-4] PPI pairs having root-shared GOterms

PPI pairs having root-shared GO terms (i.e. GO:0004749 & GO:0042802)

PPI1	PPI2	Source DB	Taxonomy1	Taxonomy2	type	method
P32895	P32895	mint	4932	4932	physical association	dhfr reconstruction
P32895	P38620	mint	4932	4932	physical association	two hybrid pooling
P32895	P38689	mint	4932	4932	physical association	two hybrid pooling
P32895	Q12265	mint	4932	4932	physical association	dhfr reconstruction
P32895	P38620	mint	4932	4932	physical association	two hybrid pooling
P38620	P38620	mint	4932	4932	physical association	dhfr reconstruction
P38620	Q12265	mint	4932	4932	physical association	two hybrid pooling
P32895	P38689	mint	4932	4932	physical association	two hybrid pooling
P38689	P38689	mint	4932	4932	physical association	dhfr reconstruction
P38689	Q12265	mint	4932	4932	physical association	dhfr reconstruction
P32895	Q12265	mint	4932	4932	physical association	dhfr reconstruction
P38620	Q12265	mint	4932	4932	physical association	two hybrid pooling
P38689	Q12265	mint	4932	4932	physical association	dhfr reconstruction
Q12265	Q12265	mint	4932	4932	physical association	dhfr reconstruction
Q14558	Q14558	mint	9606	9606	physical association	two hybrid

[S-5] GPs containing root shared GO terms III

- GO:0004716: Receptor signaling protein tyrosine kinase activity
- GO:0046982: Protein heterodimerization activity
- GO:0005524: ATP binding
- Root shared except GO:0046982 – GO:0005524 which are shared by GO:0005488 (binding – 2nd direct child of root term, GO:0003674)

Accession ID	P00533 (EGFR_HUMAN) Reviewed, UniProtKB/Swiss-Prot
Protein Names	<p>Recommended name: Epidermal growth factor receptor EC=2.7.10.1</p> <p>Alternative name(s): Proto-oncogene c-ErbB-1 Receptor tyrosine-protein kinase erbB-1</p> <p>Name: EGFR</p>
Gene Names	Synonyms: ERBB, ERBB1, HER1
Organism	Homo sapiens (Human)
Taxonomic identifier	9606 [NCBI]
Function	<p>Receptor tyrosine kinase binding ligands of the EGF family and activating several signaling cascades to convert extracellular cues into appropriate cellular responses. Known ligands include EGF, TGFA/TGF-alpha, amphiregulin, epigen/EPGN, BTC/betacellulin, epiregulin/EREG and HBEGF/heparin-binding EGF. Ligand binding triggers receptor homo- and/or heterodimerization and autophosphorylation on key cytoplasmic residues. The phosphorylated receptor recruits adapter proteins like GRB2 which in turn activates complex downstream signaling cascades. Activates at least 4 major downstream signaling cascades including the RAS-RAF-MEK-ERK, PI3 kinase-AKT, PLCgamma-PKC and STATs modules. May also activate the NF-kappa-B signaling cascade. Also directly phosphorylates other proteins like RGS16, activating its GTPase activity and probably coupling the EGF receptor signaling to the G protein-coupled receptor signaling. Also phosphorylates MUC1 and increases its interaction with SRC and CTNNB1/beta-catenin.</p> <p>Isoform 2 may act as an antagonist of EGF action.</p>
Catalytic activity	ATP + a [protein]-L-tyrosine = ADP + a [protein]-L-tyrosine phosphate.
Enzyme regulation	Endocytosis and inhibition of the activated EGFR by phosphatases like PTPRJ and PTPRK constitute immediate regulatory mechanisms. Upon EGF-binding phosphorylates EPS15 that regulates EGFR endocytosis and activity. Moreover, inducible feedback inhibitors including LRIG1, SOCS4, SOCS5 and ERRFI1 constitute alternative regulatory mechanisms for the EGFR signaling.
Subunit structure	<p>Binding of the ligand triggers homo- and/or heterodimerization of the receptor triggering its autophosphorylation. Heterodimer with ERBB2. Interacts with ERRFI1; inhibits dimerization of the kinase domain and autophosphorylation. Part of a complex with ERBB2 and either PIK3C2A or PIK3C2B. Interacts with GRB2; an adapter protein coupling the receptor to downstream signaling pathways. Interacts with GAB2; involved in signaling downstream of EGFR. Interacts with STAT3; mediates EGFR downstream signaling in cell proliferation. Interacts with RIPK1; involved in NF-kappa-B activation. Interacts (autophosphorylated) with CBL; involved in EGFR ubiquitination and regulation. Interacts with SOCS5; regulates EGFR degradation through TCEB1- and TCEB2-mediated ubiquitination and proteasomal degradation. Interacts with PRMT5; methylates EGFR and enhances interaction with PTPN6. Interacts (phosphorylated) with PTPN6; inhibits EGFR-dependent activation of MAPK/ERK. Interacts with COPG1; essential for regulation of EGF-dependent nuclear transport of EGFR by retrograde trafficking from the Golgi to the ER. Interacts with TNK2; this interaction is dependent on EGF stimulation and kinase activity of EGFR. Interacts with PCNA; positively regulates PCNA. Interacts with PELP1. Interacts with MUC1. Interacts with AP2M1. Interacts with FER. May interact with EPS8; mediates EPS8 phosphorylation. Interacts (via SH2 domains) with GRB2, NCK1 and</p>

Subcellular location	NCK2. Interacts with ATX2. Cell membrane; Single-pass type I membrane protein. Endoplasmic reticulum membrane; Single-pass type I membrane protein. Golgi apparatus membrane; Single-pass type I membrane protein. Nucleus membrane; Single-pass type I membrane protein. Endosome. Endosome membrane. Note: In response to EGF, translocated from the cell membrane to the nucleus via Golgi and ER. Endocytosed upon activation by ligand. Isoform 2: Secreted
Accession ID	P04626 (ERBB2_HUMAN) Reviewed, UniProtKB/Swiss-Prot
Protein Names	Recommended name: Receptor tyrosine-protein kinase erbB-2 EC=2.7.10.1 Alternative name(s): Metastatic lymph node gene 19 protein Short name=MLN 19 Proto-oncogene Neu Proto-oncogene c-ErbB-2 Tyrosine kinase-type cell surface receptor HER2 p185erbB2 CD_antigen=CD340
Gene Names	Name: ERBB2
Organism	Synonyms: HER2, MLN19, NEU, NGL
Taxonomic identifier	Homo sapiens (Human)
Function	Protein tyrosine kinase that is part of several cell surface receptor complexes, but that apparently needs a coreceptor for ligand binding. Essential component of a neuregulin-receptor complex, although neuregulins do not interact with it alone. GP30 is a potential ligand for this receptor. Regulates outgrowth and stabilization of peripheral microtubules (MTs). Upon ERBB2 activation, the MEMO1-RHOA-DIAPH1 signaling pathway elicits the phosphorylation and thus the inhibition of GSK3B at cell membrane. This prevents the phosphorylation of APC and CLASP2, allowing its association with the cell membrane. In turn, membrane-bound APC allows the localization of MACF1 to the cell membrane, which is required for microtubule capture and stabilization. In the nucleus is involved in transcriptional regulation. Associates with the 5'-TCAAATTC-3' sequence in the PTGS2/COX-2 promoter and activates its transcription. Implicated in transcriptional activation of CDKN1A; the function involves STAT3 and SRC. Involved in the transcription of rRNA genes by RNA Pol I and enhances protein synthesis and cell growth.
Catalytic activity	ATP + a [protein]-L-tyrosine = ADP + a [protein]-L-tyrosine phosphate.
Enzyme regulation	Activated by dimerization. Not activated by EGF, TGF-alpha and amphiregulin. Interaction with PTK6 increases its intrinsic kinase activity.
Subunit structure	Homodimer. Heterodimer with EGFR, ERBB3 and ERBB4. Part of a complex with EGFR and either PIK3C2A or PIK3C2B. May interact with PIK3C2B when phosphorylated on Tyr-1196. Interacts with PRKCABP and PLXNB1. Interacts (when phosphorylated on Tyr-1248) with MEMO1. Interacts with MUC1; the interaction is enhanced by heregulin (HRG). Interacts (when phosphorylated on Tyr-1139) with GRB7 (via SH2 domain). Interacts (when phosphorylated on Tyr-1248) with ERBB2IP. Interacts with KPNB1, RANBP2, EEA1, CRM1, CLTC, PTK6, RPA94 and ACTB. Interacts with SRC
Involvement in disease	Defects in ERBB2 are a cause of hereditary diffuse gastric cancer (HDGC) [MIM:137215]. A cancer predisposition syndrome with increased susceptibility to diffuse gastric cancer. Diffuse gastric cancer is a malignant disease characterized by poorly differentiated infiltrating lesions resulting in thickening of the stomach. Malignant tumors start in the stomach, can spread to the esophagus or the small intestine, and can extend through the stomach wall to nearby lymph nodes and organs. It also can metastasize to other parts of the body.

Defects in ERBB2 are involved in the development of glioma (GLM) [MIM:137800]. Gliomas are central nervous system neoplasms derived from glial cells and comprise astrocytomas, glioblastoma multiforme, oligodendrogiomas, and ependymomas. Defects in ERBB2 are a cause of susceptibility to ovarian cancer (OC) [MIM:167000]. Ovarian cancer common malignancy originating from ovarian tissue. Although many histologic types of ovarian neoplasms have been described, epithelial ovarian carcinoma is the most common form. Ovarian cancers are often asymptomatic and the recognized signs and symptoms, even of late-stage disease, are vague. Consequently, most patients are diagnosed with advanced disease. Defects in ERBB2 may be a cause of lung cancer (LNCR) [MIM:211980]. LNCR is a common malignancy affecting tissues of the lung. The most common form of lung cancer is non-small cell lung cancer (NSCLC) that can be divided into 3 major histologic subtypes: squamous cell carcinoma, adenocarcinoma, and large cell lung cancer. NSCLC is often diagnosed at an advanced stage and has a poor prognosis. Defects in ERBB2 are a cause of gastric cancer (GASC) [MIM:613659]. A malignant disease which starts in the stomach, can spread to the esophagus or the small intestine, and can extend through the stomach wall to nearby lymph nodes and organs. It also can metastasize to other parts of the body. The term gastric cancer or gastric carcinoma refers to adenocarcinoma of the stomach that accounts for most of all gastric malignant tumors. Two main histologic types are recognized, diffuse type and intestinal type carcinomas. Diffuse tumors are poorly differentiated infiltrating lesions resulting in thickening of the stomach. In contrast, intestinal tumors are usually exophytic, often ulcerating, and associated with intestinal metaplasia of the stomach, most often observed in sporadic disease.

Note=Chromosomal aberrations involving ERBB2 may be a cause gastric cancer. Deletions within 17q12 region producing fusion transcripts with CDK12, leading to CDK12-ERBB2 fusion leading to truncated CDK12 protein not in-frame with ERBB2.

Subcellular location
 Isoform 1: Cell membrane; Single-pass type I membrane protein. Cytoplasm → perinuclear region. Nucleus. Note: Translocation to the nucleus requires endocytosis, probably endosomal sorting and is mediated by importin beta-1/KPNB1.
 Isoform 2: Cytoplasm. Nucleus
 Isoform 3: Cytoplasm. Nucleus

Accession ID	P06494 (ERBB2_RAT) Reviewed, UniProtKB/Swiss-Prot
Protein Names	<p>Recommended name: Receptor tyrosine-protein kinase erbB-2 EC=2.7.10.1</p> <p>Alternative name(s): Epidermal growth factor receptor-related protein Proto-oncogene Neu Proto-oncogene c-ErbB-2 p185erbB2 p185neu CD_antigen=CD340</p>
Gene Names	<p>Name: Erbb2</p> <p>Synonyms: Neu</p>
Organism	Rattus norvegicus (Rat)
Taxonomic identifier	10116 [NCBI]
Function	Protein tyrosine kinase that is part of several cell surface receptor complexes, but that apparently needs a coreceptor for ligand binding. Essential component of a neuregulin-receptor complex, although neuregulins do not interact with it alone. GP30 is a potential ligand for this receptor. Regulates outgrowth and stabilization of peripheral microtubules (MTs). Upon ERBB2 activation, the MEMO1-RHOA-DIAPH1 signaling pathway elicits the phosphorylation and thus the inhibition of GSK3B at cell membrane. This prevents the phosphorylation of APC and CLASP2, allowing its association with the cell membrane. In turn, membrane-bound APC allows the localization of MACF1 to the cell

	membrane, which is required for microtubule capture and stabilization In the nucleus is involved in transcriptional regulation. Associates with the 5'-TCAAATTC-3' sequence in the PTGS2/COX-2 promoter and activates its transcription. Implicated in transcriptional activation of CDKN1A; the function involves STAT3 and SRC. Involved in the transcription of rRNA genes by RNA Pol I and enhances protein synthesis and cell growth
Catalytic activity	ATP + a [protein]-L-tyrosine = ADP + a [protein]-L-tyrosine phosphate.
Subunit structure	Homodimer. Heterodimer with EGFR, ERBB3 and ERBB4. Part of a complex with EGFR and either PIK3C2A or PIK3C2B. May interact with PIK3C2B when phosphorylated on Tyr-1198. Interacts with PRKCABP and PLXNB1. Interacts (when phosphorylated on Tyr-1250) with MEMO1. Interacts with MUC1. Interacts (when phosphorylated on Tyr-1141) with GRB7 (via SH2 domain). Interacts (when phosphorylated on Tyr-1250) with ERBB2IP. Interacts with SRC, KPNB1, RANBP2, EEA1, CRM1, CLTC, PTK6, RPA94 and ACTB
Post-translational modification	Autophosphorylated. Ligand-binding increases phosphorylation on tyrosine residues. Autophosphorylation occurs in trans, i.e. one subunit of the dimeric receptor phosphorylates tyrosine residues on the other subunit. Signaling via SEMA4C promotes phosphorylation at Tyr-1250
Subcellular location	Cell membrane; Single-pass type I membrane protein Cytoplasm → perinuclear region Nucleus
Accession ID	P21860 (ERBB3_HUMAN) Reviewed, UniProtKB/Swiss-Prot
Protein Names	Recommended name: Receptor tyrosine-protein kinase erbB-3 EC=2.7.10.1 Alternative name(s): Proto-oncogene-like protein c-ErbB-3 Tyrosine kinase-type cell surface receptor HER3 Name: ERBB3
Gene Names	Synonyms: HER3 Homo sapiens (Human) 9606 [NCBI]
Organism	Binds and is activated by neuregulins and NTAK.
Taxonomic identifier	ATP + a [protein]-L-tyrosine = ADP + a [protein]-L-tyrosine phosphate.
Function	Monomer and homodimer. Heterodimer with each of the other ERBB receptors
Catalytic activity	Interacts with CSPG5, PA2G4, GRB7 and MUC1.
Subunit structure	Ligand-binding increases phosphorylation on tyrosine residues and promotes its association with the p85 subunit of phosphatidylinositol 3-kinase
Post-translational modification	Subject to autophosphorylation
Involvement in disease	Defects in ERBB3 are the cause of lethal congenital contracture syndrome type 2 (LCCS2) [MIM:607598]; also called Israeli Bedouin multiple contracture syndrome type A. LCCS2 is an autosomal recessive neurogenic form of a neonatally lethal arthrogryposis that is associated with atrophy of the anterior horn of the spinal cord. The LCCS2 syndrome is characterized by multiple joint contractures, anterior horn atrophy in the spinal cord, and a unique feature of a markedly distended urinary bladder. The phenotype suggests a spinal cord neuropathic etiology.
Subcellular location	Isoform 1: Cell membrane; Single-pass type I membrane protein. Isoform 2: Secreted.

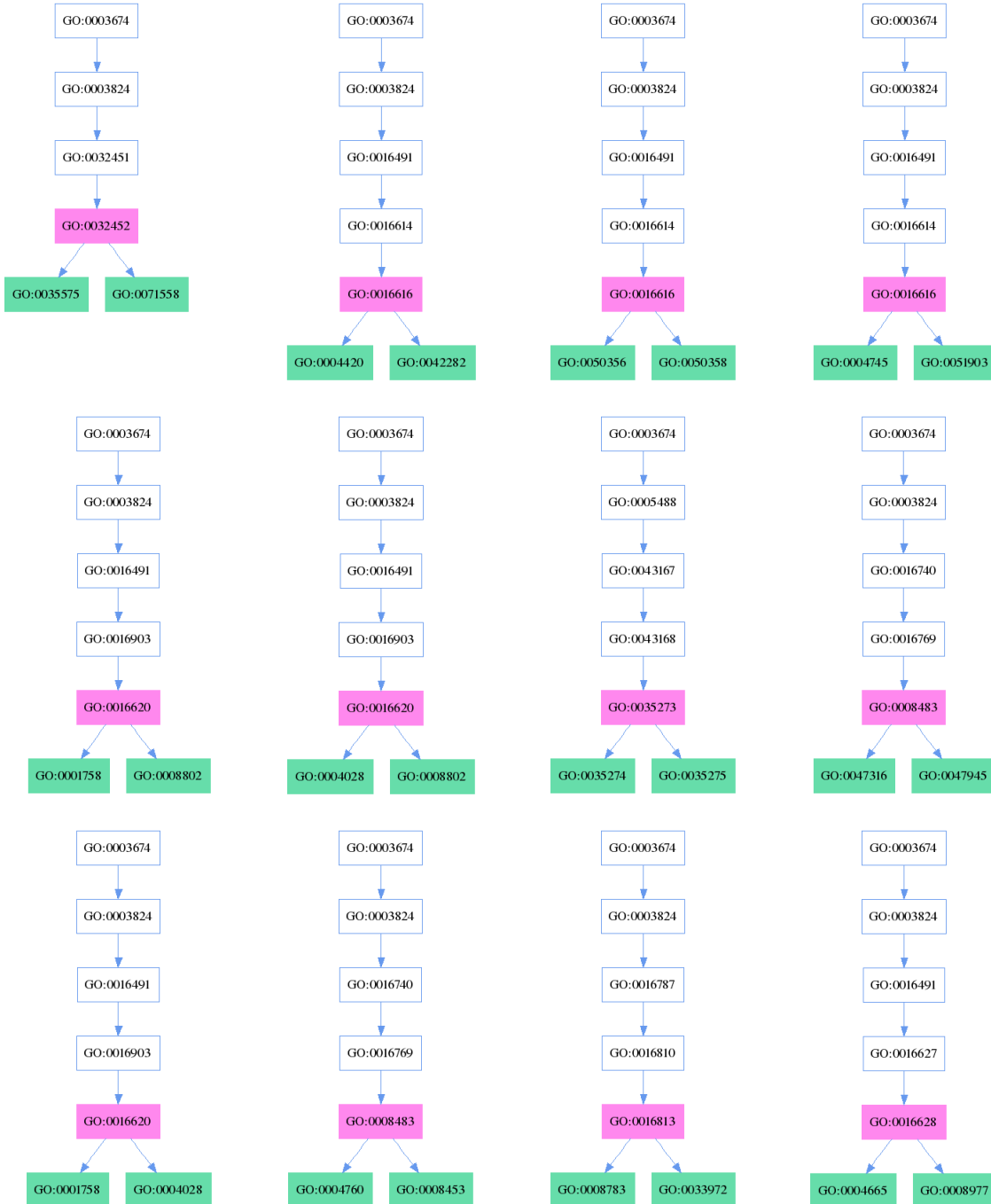
[S-6] PPI pairs having root-shared GO terms

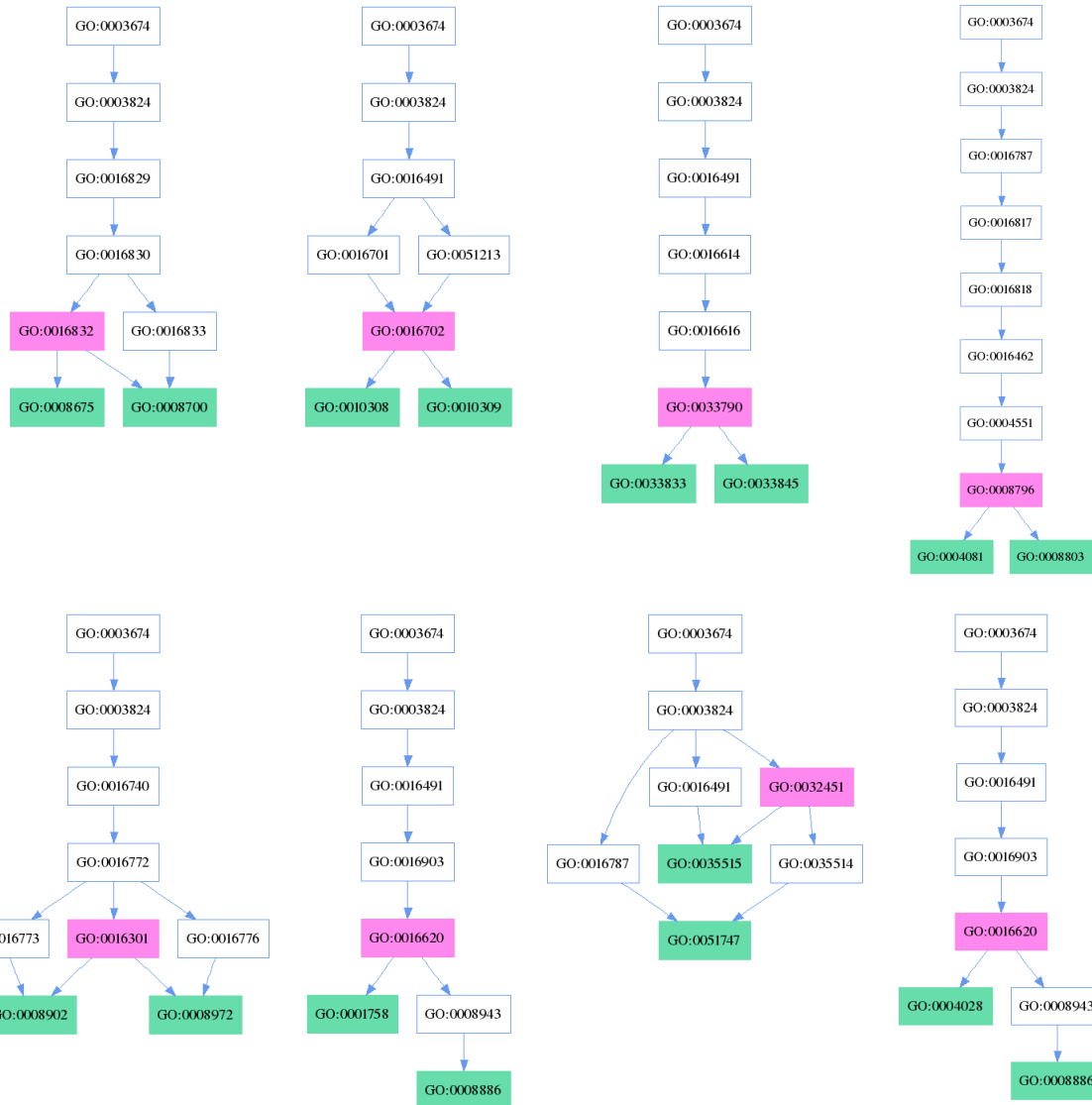
PPI pairs having root-shared GO terms (i.e. GO:0004716 & GO:0046982)

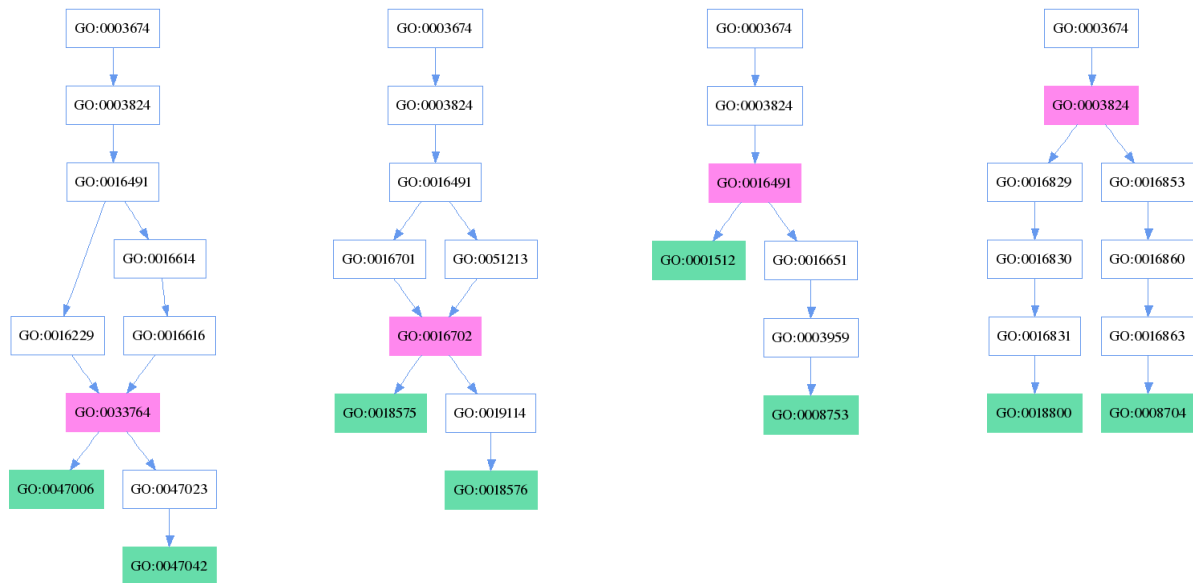
PPI1	PPI2	Source DB	Taxonomy1	Taxonomy2	type	method
P00533	P00533	mint	9606	9606	colocalization	fluorescence imaging
P00533	P04626	mint	9606	9606	physical association	anti bait coip
P00533	P21860	intact	9606	9606	physical association	anti bait coip
P00533	P04626	mint	9606	9606	physical association	anti bait coip
P04626	P04626	intact	9606	9606	physical association	protein kinase assay
P04626	P21860	intact	9606	9606	physical association	anti bait coip
P00533	P21860	intact	9606	9606	physical association	anti bait coip
P04626	P21860	intact	9606	9606	physical association	anti bait coip
P21860	P21860	intact	9606	9606	direct interaction	NMR

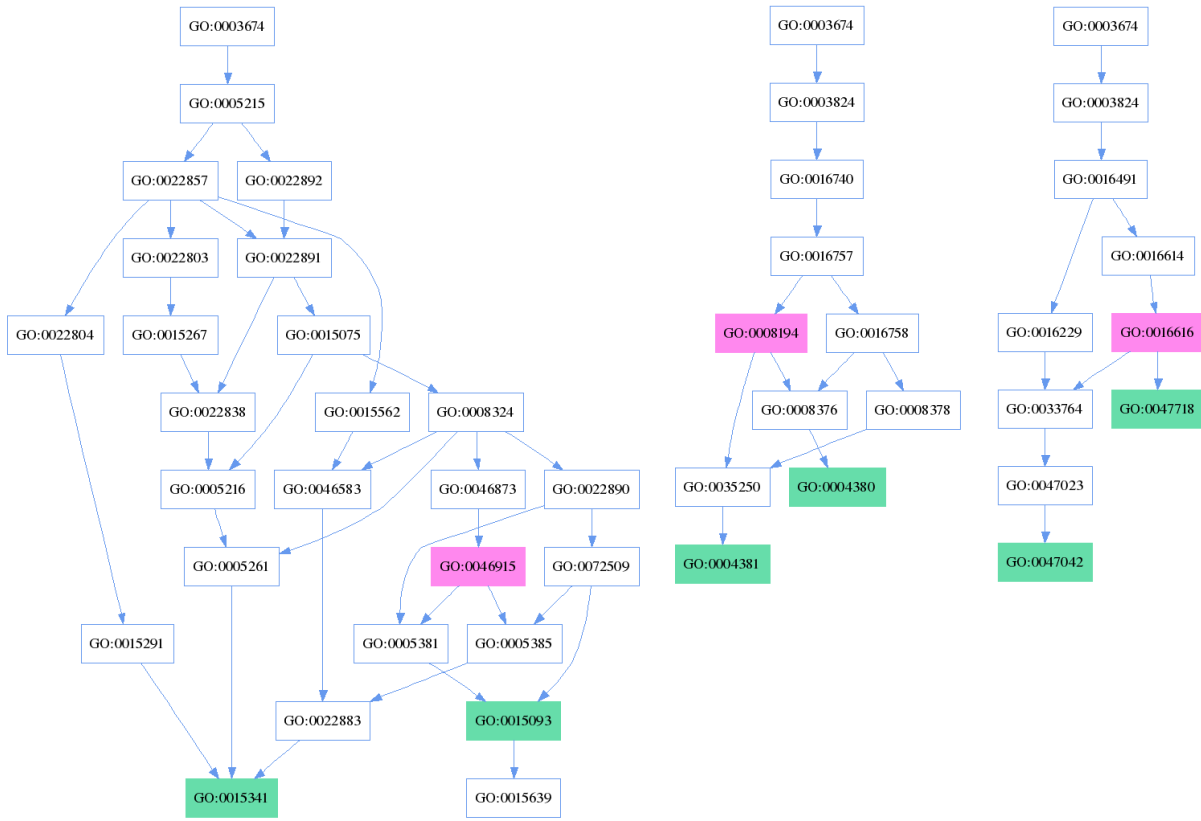
[S-7] Statistical significance of BSM score

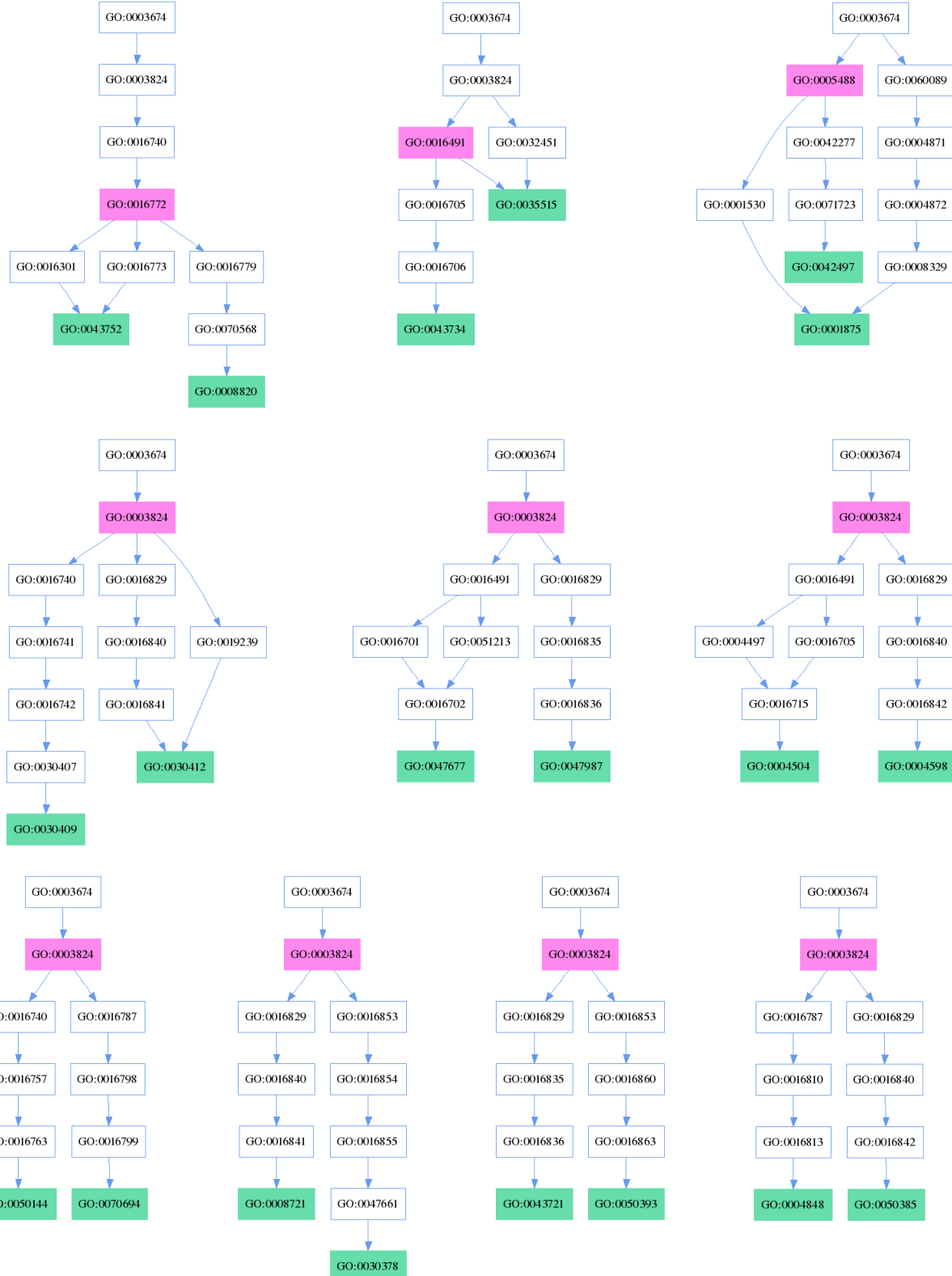
Visualization of randomly selected 50 GO term similarity scores: Green colors denote GO pairs and pink colors denote the nearest common ancestor of GO pairs.

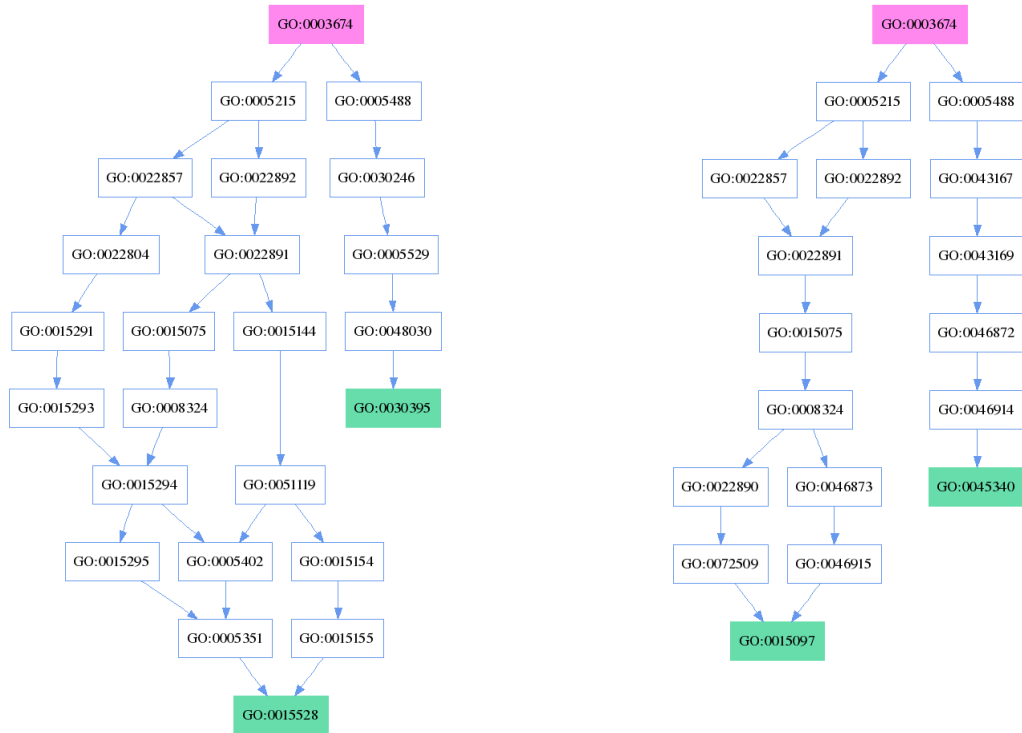
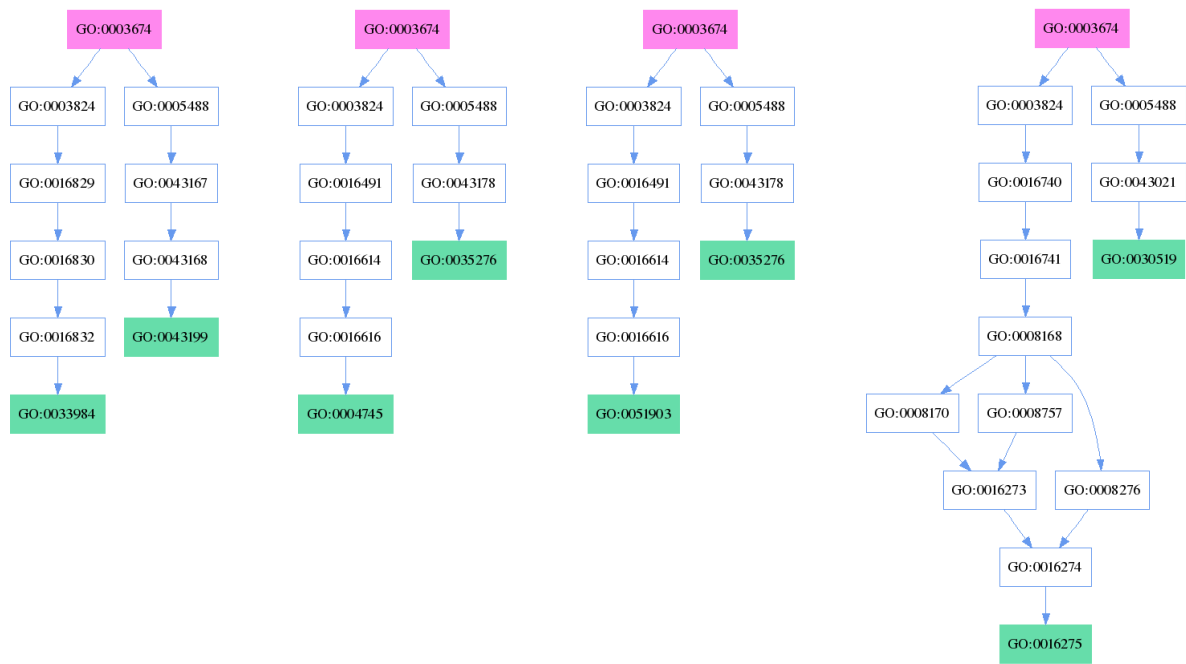


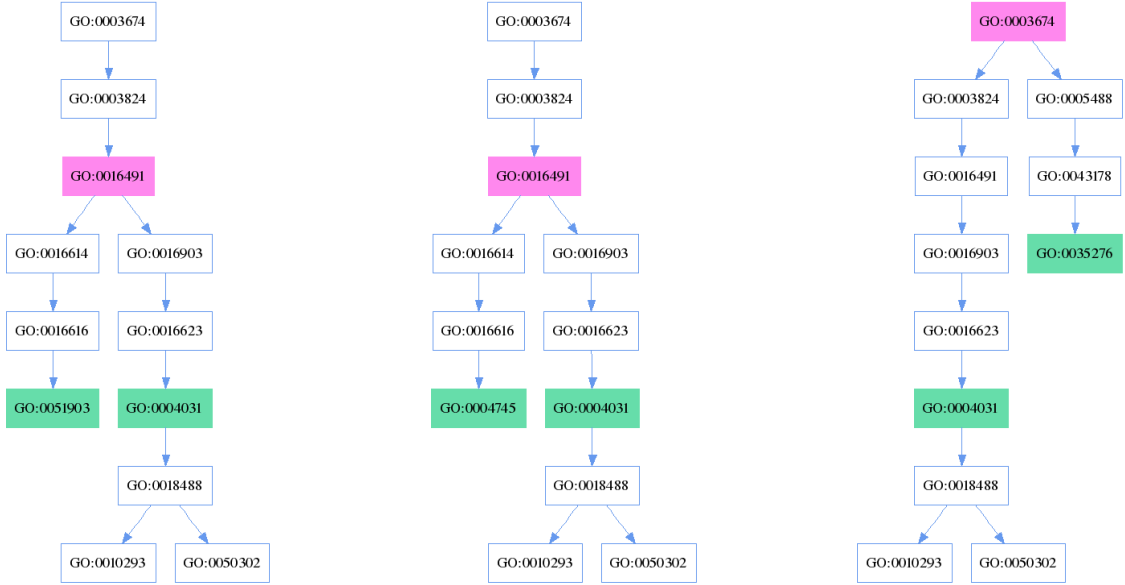












R_{scr} vs BSM

Scores derived from reference score (R_{scr}) only and proposed full scoring function for randomly selected 50 GO terms: GO1 and GO2 are the GO term pairs shown above. R_{scr} is the score derived from reference matrices. BSM is the final score calculated by proposed method which contains two parts reference score (R_{scr}) and graph based score (G_{scr}). #GPs_OR denotes the number of GPs annotated by either GO1 or GO2. #PPIs_OR denotes the number of existing PPIs in which each of GPs must be annotated by either GO1 or GO2. #GPs_AND denotes the number of GPs annotated by both GO1 and GO2. #PPIs_AND denotes the number of existing PPIs in which each of GPs must be annotated by both GO1 and GO2. Orange and green colors denote tight and loose relations between nearest common ancestor (NCA) and given GO pairs respectively.

GO1	GO2	R _{scr}	BSM	#GPs_OR	#PPIs_OR	#GPs_AND	#PPIs_AND
GO:0035575	GO:0071558	0.750	0.635	9	0	8	0
GO:0004420	GO:0042282	0.604	0.302	53	4	4	0
GO:0050356	GO:0050358	0.750	0.375	3	0	0	0
GO:0004745	GO:0051903	0.604	0.302	73	3	0	0
GO:0001758	GO:0008802	0.677	0.343	147	1	0	0
GO:0004028	GO:0008802	0.677	0.343	141	0	0	0
GO:0035274	GO:0035275	0.750	0.781	1	0	1	0
GO:0047316	GO:0047945	0.750	0.375	4	0	1	0
GO:0001758	GO:0004028	0.677	0.343	28	1	4	0
GO:0004760	GO:0008453	0.677	0.338	22	0	9	0
GO:0008783	GO:0033972	0.750	0.375	78	0	1	0
GO:0004665	GO:0008977	0.677	0.338	26	2	21	1
GO:0008675	GO:0008700	0.677	0.338	20	1	9	1
GO:0010308	GO:0010309	0.677	0.338	100	0	100	0
GO:0033833	GO:0033845	0.604	0.724	2	0	1	0
GO:0004081	GO:0008803	0.750	0.769	230	0	1	0
GO:0008902	GO:0008972	0.750	0.375	31	0	26	0

GO:0001758	GO:0008886	0.677	0.343	28	1	0	0
GO:0035515	GO:0051747	0.750	0.585	8	0	1	0
GO:0004028	GO:0008886	0.677	0.343	22	0	0	0
GO:0047312	GO:0047945	0.750	0.375	2	0	1	0
GO:0047312	GO:0047316	0.750	0.375	5	0	1	0
GO:0008802	GO:0008886	0.677	0.343	137	0	0	0
GO:0004557	GO:0008456	0.604	0.302	89	2	2	1
GO:0047006	GO:0047042	0.713	0.723	15	1	4	1
GO:0018575	GO:0018576	0.635	0.318	15	0	5	0
GO:0001512	GO:0008753	0.750	0.531	8	1	1	1
GO:0018800	GO:0008704	0.520	0.436	4	0	3	0
GO:0015093	GO:0015341	0.604	0.500	38	1	1	0
GO:0004380	GO:0004381	0.677	0.573	5	0	4	0
GO:0047042	GO:0047718	0.598	0.299	11	2	4	1
GO:0008820	GO:0043752	0.750	0.610	6	0	5	0
GO:0035515	GO:0043734	0.635	0.474	14	0	3	0
GO:0001875	GO:0042497	0.750	0.441	22	5	1	0
GO:0030409	GO:0030412	0.677	0.514	6	0	6	0
GO:0047677	GO:0047987	0.750	0.550	8	0	1	0
GO:0004504	GO:0004598	0.677	0.514	12	1	9	1
GO:0050144	GO:0070694	0.750	0.550	21	1	3	0
GO:0008721	GO:0030378	0.750	0.550	117	0	5	0
GO:0043721	GO:0050393	0.604	0.477	1	0	1	0
GO:0004848	GO:0050385	0.750	0.550	88	1	1	0
GO:0004031	GO:0051903	0.604	0.458	55	2	0	0
GO:0004031	GO:0004745	0.604	0.458	41	2	1	1
GO:0033984	GO:0043199	0.750	0.545	4	0	0	0
GO:0004745	GO:0035276	0.604	0.471	32	2	2	1
GO:0035276	GO:0051903	0.604	0.471	47	2	0	0
GO:0016275	GO:0030519	0.640	0.490	2	1	1	1
GO:0015528	GO:0030395	0.750	0.545	10	0	1	0
GO:0015097	GO:0045340	0.677	0.508	57	0	10	0
GO:0004031	GO:0035276	0.604	0.471	15	1	1	1

Average scores from 50 GO terms: Tight and loose denote the geometrically close or distant relations between nearest common ancestor (NCA) and given GO pairs. Tight relation requires parent-child relationship between NCA and both GO terms. Root relation requires both GO terms are shared by root node. In other words, NCA has to be root node (i.e. GO:0003674). Loose relations are defined as all GO term pairs except ‘Tight’ and ‘Root’ relations. Each color corresponds to the colors shown above table.

CATEGORY	R _{scr}	GO _{sim}	#GPs_OR	#PPIs_OR	#GPs_AND	#PPIs_AND
Tight	0.694	0.435	56.941	0.706	10.941	0.118
Loose	0.680	0.469	29.923	0.769	2.423	0.231
Root	0.661	0.500	23.857	0.857	2.143	0.429
Overall	0.682	0.462	38.260	0.760	5.280	0.220

[S-8] SCOP domains used in experiments

- SunID: unique SCOP ID
- Sunid_cl: SCOP level at class
- Sunid_cf: SCOP level at class family
- Sunid_sf: SCOP level at super family
- Sunid_fa: SCOP level at family
- Sunid_dm: SCOP level at domain
- Sunid_sp: SCOP level at species
- Pdbid: representing PDB ID corresponding to the sunID

SunID	sunid_cl	sunid_cf	sunid_sf	sunid_fa	sunid_dm	sunid_sp	pdbid
14984	46456	46457	46458	46463	46464	46465	3sdh
15010	46456	46457	46458	46463	46464	46466	1b0b
15018	46456	46457	46458	46463	46469	46470	1a6m
15149	46456	46457	46458	46463	46469	46471	1mba
15211	46456	46457	46458	46463	46479	46480	1ecd
15212	46456	46457	46458	46463	46481	46482	2gdm
15406	46456	46457	46458	46463	46486	46496	1cg5
15585	46456	46457	46458	46463	46500	46512	1cg5
15589	46456	46457	46458	46463	46500	46515	1gcv
15622	46456	46457	46458	46463	46520	46521	1ash
15623	46456	46457	46458	46463	46522	46523	1ith
15625	46456	46457	46458	46463	46524	46525	1hlb
15635	46456	46457	46458	46463	46528	46529	1cqx
15702	46456	46556	46579	46580	46581	46582	1fxk
15703	46456	46556	46579	46580	46583	46584	1fxk
15796	46456	46625	46626	46627	46628	46629	1c75
15798	46456	46625	46626	46627	46628	46630	1ctj
15801	46456	46625	46626	46627	46628	46631	1c53
15810	46456	46625	46626	46627	46636	46637	1c52
15822	46456	46625	46626	46627	46636	46639	1ql3
15834	46456	46625	46626	46627	46642	46643	1ycc
15899	46456	46625	46626	46627	46650	46657	1cot
15901	46456	46625	46626	46627	46658	46659	1cc5
15905	46456	46625	46626	46627	46660	46662	351c
15909	46456	46625	46626	46627	46660	46664	1gks
15911	46456	46625	46626	46627	46667	46668	1dw0
15989	46456	46688	46689	46690	46697	46698	1lfb
16003	46456	46688	46689	46690	46714	46715	1bw5
16014	46456	46688	46689	46690	46724	46725	1vnd
16017	46456	46688	46689	46690	46726	46727	1fjl
16144	46456	46688	46785	46832	46835	46836	1d5v
16417	46456	47094	47095	47096	47097	47098	1ckt
16425	46456	47094	47095	47096	47100	47101	1qrv
16433	46456	47094	47095	47096	47110	47111	2lef
16481	46456	47112	47113	47134	47135	47136	1taf
16482	46456	47112	47113	47134	47137	47138	1taf

16483	46456	47112	47113	47134	47139	47140	1bh9
16485	46456	47112	47113	47134	47141	47142	1bh9
16619	46456	47161	47216	47217	47218	47219	1avo
16740	46456	47239	47240	47253	88792	88793	1mty
16742	46456	47239	47240	47253	88789	88790	1mty
16805	46456	47239	47240	47253	47261	47262	1afr
16822	46456	47265	47266	47267	47268	47270	1bgc
16826	46456	47265	47266	47267	47272	47273	1alu
16829	46456	47265	47266	47267	47274	47275	1lki
16831	46456	47265	47266	47267	47276	47277	1huw
16839	46456	47265	47266	47267	47278	47279	1f6f
16840	46456	47265	47266	47267	47280	47281	1cnt
16844	46456	47265	47266	47267	47282	47283	1ax8
16845	46456	47265	47266	47267	47284	47285	1evs
16846	46456	47265	47266	47286	47287	47288	1eer
16849	46456	47265	47266	47286	47289	47290	2gmf
16865	46456	47265	47266	47286	47293	47294	1hul
16867	46456	47265	47266	47286	47295	47296	1hmc
16869	46456	47265	47266	47286	47297	47298	1ete
16873	46456	47265	47266	47286	47299	47300	1scf
16884	46456	47265	47266	47286	47303	47304	1jli
16885	46456	47265	47266	47305	47306	47307	2ilk
16889	46456	47265	47266	47305	47309	47310	1au1
16900	46456	47265	47266	47305	47316	47317	1b5l
16901	46456	47265	47266	47305	47318	47319	1d9c
17132	46456	47458	47459	47460	47464	47465	1mdy
17136	46456	47458	47459	47460	47466	47467	1an4
17138	46456	47458	47459	47460	47468	47469	1a0a
17140	46456	47458	47459	47460	47470	47471	1am9
17180	46456	47472	47473	47478	47479	47485	1psr
17185	46456	47472	47473	47478	47479	47486	1qls
17230	46456	47472	47473	47502	47503	47504	1ctd
17256	46456	47472	47473	47502	47509	47510	2scp
17258	46456	47472	47473	47502	47509	47511	2sas
17262	46456	47472	47473	47502	47514	47515	1c7v
17299	46456	47472	47473	47502	47516	47523	1exr
17302	46456	47472	47473	47502	47524	47525	1wdc
17308	46456	47472	47473	47502	47524	47526	2mys
17325	46456	47472	47473	47502	47530	47532	1au1
17330	46456	47472	47473	47502	47537	47538	1jba
17370	46456	47472	47473	63550	47552	47555	1alv
17387	46456	47472	47565	47566	47567	47568	1c3y
17388	46456	47472	47565	47566	47569	47570	1dqe
17394	46456	47575	47576	47577	47578	47579	1bkr
17396	46456	47575	47576	47577	47580	47581	1aoa
17397	46456	47575	47576	47577	47580	47581	1aoa
18146	46456	47873	47874	47875	47876	47877	1bo9
18392	46456	47972	47973	47974	47975	47977	1rss
18538	46456	48096	48097	48098	48099	48100	1agr
18542	46456	48096	48097	48098	48101	48102	1fq
18548	46456	48096	48097	48098	48105	48106	1dk8
18880	46456	48255	48256	48257	48258	48259	1csh

18968	46456	48263	48264	48265	48274	48275	1cpt
18971	46456	48263	48264	48265	48278	48279	1io7
19052	46456	48316	48317	48318	48319	48320	1d2t
19053	46456	48316	48317	48321	48322	48323	1qi9
19055	46456	48316	48317	48321	48322	48324	1qhb
19061	46456	48316	48317	48325	48326	48327	1vns
19119	46456	48370	48371	48372	48378	48379	1qgr
19127	46456	48370	48371	48372	48381	48382	1qbk
19155	53931	74651	48403	48404	48405	48406	1ycs
19156	53931	74651	48403	48404	48407	48408	1awc
19157	53931	74651	48403	48404	48409	48410	1bd8
19171	53931	74651	48403	48404	48417	48418	1ikn
19174	53931	74651	48403	48404	48419	48420	1myo
19176	53931	74651	48403	48404	48421	48422	1sw6
19178	53931	74651	48403	48404	48423	48424	1dcq
19191	46456	48370	48439	48440	48443	48444	1dce
19206	46456	48370	48452	48453	48454	48455	1a17
19207	46456	48370	48452	48453	48456	48457	1elw
19209	46456	48370	48452	48453	48456	48457	1elr
19210	46456	48370	48452	48453	48458	48459	1qqe
19212	46456	48370	48452	48453	48462	48463	1fch
19282	46456	48507	48508	48509	48515	48516	1fcy
19425	46456	48556	48557	48558	48568	48569	1c3c
19429	46456	48556	48557	48558	48568	48570	1dof
19436	46456	48575	48576	48577	48578	48579	1fps
19446	46456	48575	48576	48586	48587	48588	1di1
19450	46456	48575	48576	48586	48589	48590	1ps1
19630	46456	48661	48670	48671	48672	48673	1tbg
19636	46456	48661	48670	48671	48672	48673	1gg2
19704	48724	48725	48726	48727	48728	48729	1neu
19708	48724	48725	48726	48727	48732	48733	1qfo
19740	48724	48725	48726	48727	48737	48739	1cid
19741	48724	48725	48726	48727	48740	48741	1hnf
19758	48724	48725	48726	48727	48743	48744	1ccz
19762	48724	48725	48726	48727	48745	48746	1dr9
19763	48724	48725	48726	48727	48747	48748	1f97
20622	48724	48725	48726	48727	48933	48935	1bd2
20631	48724	48725	48726	48727	48933	48936	1fo0
20650	48724	48725	48726	48727	48933	48938	1tvd
20653	48724	48725	48726	48727	48939	48941	1dqf
21685	48724	48725	48726	49159	49160	49161	1vca
21689	48724	48725	48726	49159	49162	49163	1iam
21693	48724	48725	48726	49159	49164	49165	1zxq
21694	48724	48725	48726	49159	49166	49167	1epf
21695	48724	48725	48726	49159	49166	49167	1epf
21706	48724	48725	48726	49159	49170	49171	1fhg
21711	48724	48725	48726	49159	49172	49173	1tnn
21712	48724	48725	48726	49159	49174	49175	1ko
21713	48724	48725	48726	49159	49174	49175	1wiu
21715	48724	48725	48726	49159	49174	49176	1tiu
21717	48724	48725	48726	49159	49177	49178	1ira
21718	48724	48725	48726	49159	49177	49178	1ira

21719	48724	48725	48726	49159	49177	49178	1ira
21752	48724	48725	48726	49159	49182	49183	1bih
21753	48724	48725	48726	49159	49182	49183	1bih
21754	48724	48725	48726	49159	49182	49183	1bih
21755	48724	48725	48726	49159	49182	49183	1bih
21760	48724	48725	48726	49159	49184	49185	1cs6
21761	48724	48725	48726	49159	49184	49185	1cs6
21762	48724	48725	48726	49159	49184	49185	1cs6
21763	48724	48725	48726	49159	49184	49185	1cs6
21764	48724	48725	48726	49159	49186	49187	1f97
21765	48724	48725	48726	49159	49188	49189	1flt
21778	48724	48725	48726	49159	49194	49195	1wwc
21783	48724	48725	48726	49159	49196	49199	1fnl
21784	48724	48725	48726	49159	49196	49199	1fnl
21799	48724	48725	48726	49159	49202	49204	1nkr
21800	48724	48725	48726	49159	49202	49204	1nkr
22300	48724	48725	49329	49330	49341	49342	1ej8
22633	48724	49451	49482	49483	49484	49485	1dmh
23675	48724	49763	49764	49765	49766	49767	1shs
23928	48724	49898	49899	49900	49901	49902	1nls
24157	48724	49898	49899	49900	49920	49921	1dhk
24185	48724	49898	49899	49925	49930	49931	1dyp
24198	48724	49898	49899	49932	100926	49935	2gal
24216	48724	49898	49899	49932	49938	49939	1lcl
24344	48724	49898	49899	49978	49991	49992	2nlr
24656	48724	50128	50129	50130	50134	50135	1g31
24772	48724	50155	50156	50157	50160	50161	1kwa
24777	48724	50155	50156	50157	50164	50165	1qav
24779	48724	50155	50156	50157	50166	50167	1qau
24796	48724	50181	50182	50183	50184	50185	1b34
24797	48724	50181	50182	50183	50186	50187	1b34
24798	48724	50181	50182	50183	50188	50189	1d3b
24804	48724	50181	50182	50183	50190	50191	1d3b
25282	48724	50198	50249	50263	50264	50265	3ull
25284	48724	50198	50249	50263	50264	50266	1qvc
25300	48724	50198	50249	50263	50267	50268	1jmc
25301	48724	50198	50249	50263	50267	50268	1jmc
25325	48724	50198	50249	50282	50283	50286	1c9o
25327	48724	50198	50249	50282	50287	50288	1sro
25329	48724	50198	50249	50282	50290	50291	1hr0
25331	48724	50198	50249	50282	50292	50293	1d7q
25341	48724	50198	50249	50282	50296	50298	1bkb
25342	48724	50198	50249	50282	50299	50300	1rl2
25560	48724	50352	50353	50362	50368	50369	2ila
25591	48724	50352	50386	50387	50388	50389	1wba
25599	48724	50352	50386	50387	50394	50395	1avw
25747	48724	50474	50475	50476	50477	50478	1flm
25753	48724	50474	50475	50476	50479	50481	1dnl
26011	48724	50493	50494	50514	50515	50521	1gdn
26068	48724	50493	50494	50514	50522	50524	1eq9
26072	48724	50493	50494	50514	50527	50528	1azz
26074	48724	50493	50494	50514	50529	50530	2hlc

26284	48724	50493	50494	50514	50544	50545	1a7s
26314	48724	50493	50494	50514	50563	50564	1bio
26348	48724	50493	50494	50514	50579	50580	1aut
26378	48724	50493	50494	50514	50593	50594	1fiw
26819	48724	50629	50630	50646	50649	50651	2-Apr
26828	48724	50629	50630	50646	50649	50654	1dpj
26852	48724	50629	50630	50646	50658	50661	1htr
26856	48724	50629	50630	50646	50663	50664	1mpp
26878	48724	50629	50630	50646	50667	50670	1smr
26951	48724	50728	50729	50730	50731	50732	1mai
26952	48724	50728	50729	50730	50733	50734	1btn
26954	48724	50728	50729	50730	50733	50735	1dro
26957	48724	50728	50729	50730	50736	50737	2dyn
26959	48724	50728	50729	50730	50738	50739	1btk
26965	48724	50728	50729	50730	50740	50741	1pls
26967	48724	50728	50729	50730	50742	50744	1dbh
26969	48724	50728	50729	50730	50745	50746	1foe
26974	48724	50728	50729	50730	50749	50750	1fao
26976	48724	50728	50729	50730	50751	50752	1fgy
26982	48724	50728	50729	50730	50753	50754	1fho
27096	48724	50813	50814	50815	50821	50823	1dzk
27113	48724	50813	50814	50815	50824	50825	1bj7
27115	48724	50813	50814	50815	50827	50828	1beb
27126	48724	50813	50814	50815	50830	50831	1epb
27151	48724	50813	50814	50815	50839	50840	1qft
27173	48724	50813	50814	50847	50851	50852	1ifc
27198	48724	50813	50814	50847	50858	50859	1mdc
27214	48724	50813	50814	50847	50864	50865	1opa
27223	48724	50813	50814	50847	50866	50867	1lfo
27542	48724	50938	50939	50940	50941	50942	3sil
27591	48724	50938	50939	50940	50943	50945	1nsc
27611	48724	50938	50939	50940	50948	50949	2sli
27649	48724	50964	50978	50979	50980	50981	1tbg
27660	48724	50964	50978	50979	50983	50984	1erj
27955	48724	51068	51069	51070	51071	51076	1znc
27966	48724	51068	51069	51070	51071	51079	1kop
28022	48724	51125	51126	51127	51128	51131	1bn8
28024	48724	51125	51126	51127	51128	51132	1ee6
28028	48724	51125	51126	51133	51134	51136	1qcx
28029	48724	51125	51126	51137	51138	51139	1rmg
28030	48724	51125	51126	51137	51140	51141	1bhe
28090	48724	51181	51182	51187	51188	51190	1dgw
28091	48724	51181	51182	51187	51188	51190	1dgw
28124	48724	51181	51197	51198	51201	51202	1dcs
28349	48724	51268	51283	51284	51285	51286	1euw
28353	48724	51268	51283	51284	51285	51287	1f7d
28388	48724	51305	51306	51312	51313	51314	1b12
28392	48724	51315	51316	51317	51318	51319	1hxsr
28515	51349	51350	51351	51352	51353	51364	1aw1
28539	51349	51350	51366	51375	51376	51377	1dbt
28551	51349	51350	51366	51375	51376	51380	1dqw
28559	51349	51350	51366	51381	51382	51383	1pii

28560	51349	51350	51366	51381	51382	51384	1nsj
28563	51349	51350	51366	51381	51385	51386	1pii
28564	51349	51350	51366	51381	51385	51387	1a53
28570	51349	51350	51366	51381	51388	51389	1qop
28589	51349	51350	51366	51381	51388	51390	1geq
28597	51349	51350	51395	51396	51397	51399	1ep3
28600	51349	51350	51395	51396	51397	51400	1d3g
28604	51349	51350	51395	51396	51401	51402	1oya
28614	51349	51350	51395	51396	51406	51407	1dqj
28663	51349	51350	51419	51427	51428	51429	1ct5
28804	51349	51350	51445	51487	51488	51489	1xyz
28807	51349	51350	51445	51487	51491	51492	1edg
28808	51349	51350	51445	51487	51493	51494	1ceo
28813	51349	51350	51445	51487	51497	51498	1ece
28817	51349	51350	51445	51487	51499	51500	7a3h
28831	51349	51350	51445	51487	51502	51503	1bqc
28834	51349	51350	51445	51487	51502	51504	1qnr
28889	51349	51350	51445	51487	51512	51513	1bhg
28946	51349	51350	51445	51521	51526	51527	1pbg
28988	51349	51350	51445	51534	51537	51538	1nar
28989	51349	51350	51445	51534	51537	51539	1cnv
28990	51349	51350	51445	51534	51540	51541	2ebn
28991	51349	51350	51445	51534	51540	51542	1eok
28993	51349	51350	51445	51534	51540	51543	1edt
29002	51349	51350	51445	51534	51544	51545	1edq
29014	51349	51350	51556	51557	51558	51559	1a4m
29079	51349	51350	51569	51570	51571	51573	1f74
29169	51349	51350	51569	51570	51588	51589	1onr
29310	51349	51350	51621	51638	51639	51640	1dxe
29800	51349	51734	51735	51751	51752	51754	1ek6
29805	51349	51734	51735	51751	51757	51758	1e6u
29814	51349	51734	51735	51751	51761	51762	1eq2
29825	51349	51734	51735	51751	51765	51766	1cyd
29829	51349	51734	51735	51751	51767	51768	1oaa
29856	51349	51734	51735	51751	51774	51775	1fmc
29862	51349	51734	51735	51751	51776	51777	1hdc
29870	51349	51734	51735	51751	51778	51779	1fjh
29874	51349	51734	51735	51751	51780	51781	1bdb
29888	51349	51734	51735	51751	51786	51787	1 geg
29907	51349	51734	51735	51751	51791	51792	1d7o
29935	51349	51734	51735	51751	51791	51794	1qsg
29945	51349	51734	51735	51751	51795	51797	2ae2
30473	51349	51904	51905	51943	51944	51946	1ges
30474	51349	51904	51905	51943	51944	51946	1ges
30489	51349	51904	51905	51943	51947	51948	1fec
30490	51349	51904	51905	51943	51947	51948	1fec
30529	51349	51904	51905	51943	51950	51951	1trb
30530	51349	51904	51905	51943	51950	51951	1trb
30546	51349	51904	51905	51943	51950	51952	1vdc
30549	51349	51904	51905	51943	51955	51956	1nhp
30550	51349	51904	51905	51943	51955	51956	1nhp
30565	51349	51904	51905	51943	51957	51958	1d7y

30567	51349	51904	51905	51943	51959	51960	1lvl
30568	51349	51904	51905	51943	51959	51960	1lvl
30574	51349	51904	51905	51943	51959	51962	3lad
30578	51349	51904	51905	51943	51959	51963	1ebd
30581	51349	51904	51905	51943	51959	51964	1ojt
30582	51349	51904	51905	51943	51959	51964	1ojt
30593	51349	51904	51905	51943	51966	51967	1fcd
30594	51349	51904	51905	51943	51966	51967	1fcd
30903	51349	52095	52096	52103	52104	52105	1nzy
30918	51349	52095	52096	52103	52108	52109	1dci
30921	51349	52095	52096	52103	52110	52111	1ef8
30999	51349	52128	52129	52130	52135	52136	1qtn
31089	51349	52171	52172	52173	52178	52179	1a04
31095	51349	52171	52172	52173	52182	52183	1dbw
31104	51349	52171	52172	52173	52184	52185	1qkk
31105	51349	52171	52172	52173	52186	52187	1dz3
31120	51349	52171	52172	52173	52190	52191	1a2o
31395	51349	52171	52309	52310	52311	52312	1f8y
31438	51349	52171	52317	52325	52326	52327	1g2i
31578	51349	52373	52374	52375	52380	52381	1gtr
31591	51349	52373	52374	52375	52387	52388	1ile
31593	51349	52373	52374	52375	52387	52389	1ffy
31598	51349	52373	52374	52394	52395	52396	1coz
31753	51349	52498	52499	100948	52501	52502	1nba
31757	51349	52498	52499	100948	52504	52505	1yac
31839	51349	52539	52540	52541	52542	52543	1gky
31842	51349	52539	52540	52541	52546	52547	1dekk
31846	51349	52539	52540	52541	52548	52549	1cke
31848	51349	52539	52540	52541	52550	52551	1qf9
31854	51349	52539	52540	52541	52552	52553	1e2k
31886	51349	52539	52540	52541	52554	52556	1nks
31892	51349	52539	52540	52541	52554	52557	2ak3
31898	51349	52539	52540	52541	52554	52559	3aky
31915	51349	52539	52540	52541	52554	52562	1zin
31930	51349	52539	52540	52541	52563	52565	4tmk
31951	51349	52539	52540	52575	52582	52583	1inst
31952	51349	52539	52540	52584	52585	52586	1a7j
32002	51349	52539	52540	52592	52595	52596	1mh1
32018	51349	52539	52540	52592	52601	52602	3rab
32140	51349	52539	52540	52592	52631	52632	1f60
32147	51349	52539	52540	52592	52635	52636	1g7s
32152	51349	52539	52540	52592	52639	52640	1f5n
32199	51349	52539	52540	52652	52653	52654	1byi
32212	51349	52539	52540	52652	52655	52656	1qf5
32241	51349	52539	52540	52652	52659	52660	1eg7
32370	51349	52539	52540	52686	52687	52688	1b0u
32373	51349	52539	52540	52686	52691	52692	1f2t
32382	51349	52539	52540	52686	52695	52696	1qhl
32423	51349	52539	52540	81269	52711	52712	1a5t
32426	51349	52539	52540	81269	52715	52716	1fn
32428	51349	52539	52540	81269	52717	52718	1d2n
32450	51349	52539	52540	81269	52721	52723	1g41

32503	51349	52742	52743	52744	52745	52750	1gci
32606	51349	52767	52768	52773	52774	52775	1c3p
32642	51349	52787	52788	52789	52790	52793	1d1q
32651	51349	52798	52799	52800	52801	52802	1vhr
32654	51349	52798	52799	52800	52803	52804	1mkp
32697	51349	52798	52799	52800	52818	52819	1d5r
32732	51349	52832	52833	52834	52835	52837	1thx
32736	51349	52832	52833	52834	52835	52840	1f9m
32739	51349	52832	52833	52834	52835	52841	1fb6
32760	51349	52832	52833	52834	52843	52844	1aba
32767	51349	52832	52833	52834	52843	52845	1ego
32771	51349	52832	52833	52834	52843	52847	1kte
33066	51349	52832	52833	52901	52906	52908	1qmv
33076	51349	52832	52833	52901	52909	52910	1prx
33364	51349	53040	53056	53057	53058	53059	1ekj
33373	51349	53040	53056	53057	53058	53060	1ddz
33572	51349	53066	53098	53099	53103	53104	1eke
33681	51349	53066	53098	53118	53119	53120	1kfs
33695	51349	53066	53098	53118	53119	53121	1qtm
33721	51349	53066	53098	53118	53125	53128	1tgo
33763	51349	53162	53167	53168	53169	53171	3pnp
33790	51349	53162	53167	53168	53174	53175	1cb0
33994	51349	53253	53254	53258	53263	53265	1qfx
33996	51349	53253	53254	53258	53263	53266	1dkl
34011	51349	53270	53271	53272	53273	53274	1nul
34027	51349	53270	53271	53272	53275	53276	1hgx
34029	51349	53270	53271	53272	53275	53277	1fsg
34053	51349	53270	53271	53272	53278	53280	1ecf
34067	51349	53270	53271	53272	53281	53282	1dqf
34083	51349	53270	53271	53272	53286	53287	1tc1
34087	51349	53270	53271	53272	53288	53289	1qb7
34095	51349	53270	53271	53272	109612	53294	1a3c
34098	51349	53270	53271	53272	53293	53295	1bd3
34179	51349	53334	53335	53339	53340	53341	1ej0
34183	51349	53334	53335	53348	53349	53350	1xva
34244	51349	53334	53335	88786	53371	53372	1dct
34247	51349	53334	53335	88786	53375	53376	1g55
34276	51349	53382	53383	53384	53385	53388	1ajs
34385	51349	53382	53383	53384	53395	53396	1bw0
34395	51349	53382	53383	53402	53403	53404	1cl1
34399	51349	53382	53383	53402	53405	53406	1cs1
34403	51349	53382	53383	53402	53405	53407	1qgn
34411	51349	53382	53383	53402	53408	53409	1d2f
34413	51349	53382	53383	53402	53410	53411	1c7n
34429	51349	53382	53383	53402	53412	53413	1eg5
34434	51349	53382	53383	53402	53415	53416	1elu
34446	51349	53382	53383	53417	53420	53421	2gsa
34488	51349	53382	53383	53417	53434	53435	1b9h
34490	51349	53382	53383	53417	53436	53437	1bs0
34505	51349	53447	53448	53449	53450	53451	1qg8
34514	51349	53447	53448	68901	53456	53457	1eyr
34524	51349	53447	53448	53464	53465	53466	1fxo

34693	51349	53473	53474	53525	53528	53529	1ehy
34697	51349	53473	53474	53525	53528	53530	1qo7
34711	51349	53473	53474	53542	53543	53544	1tht
34713	51349	53473	53474	53542	53545	53546	1ei9
34795	51349	53473	53474	53577	53578	53584	1bu8
34810	51349	53589	53590	53591	53592	53593	2mas
34820	51349	53596	53597	53598	53599	53600	1ra9
34880	51349	53596	53597	53598	53599	53601	3dfr
34885	51349	53596	53597	53598	53599	53602	1df7
34889	51349	53596	53597	53598	53599	53603	1d1g
34893	51349	53596	53597	53598	53599	53604	1vdr
34923	51349	53596	53597	53598	53605	53609	1aoe
34928	51349	53612	53613	53614	53615	53616	1rkd
34935	51349	53612	53613	53614	53617	53618	1bx4
35030	51349	53648	53649	53653	53654	53655	1auk
35032	51349	53648	53649	53653	53656	53657	1fsu
35061	51349	53658	53659	53660	53661	53666	1cnz
35270	51349	53685	53686	53687	53688	53689	1qop
35297	51349	53685	53686	53687	53692	53693	1tdj
35335	51349	53719	53720	53721	53722	53723	1ad3
35369	51349	53719	53720	53721	53722	53729	1euh
35385	51349	53719	53720	53721	53722	53730	1ez0
35399	51349	53731	53732	53733	53734	53736	1aco
35575	51349	53783	53784	53785	53786	53787	1pfk
35587	51349	53789	53790	53791	53792	53793	1cbf
36020	51349	53926	53927	53928	53929	53930	1aln
36021	51349	53926	53927	53928	53929	53930	1aln
36597	53931	53954	53955	53960	53975	53977	1b9o
37032	53931	54000	54001	54002	54017	54018	3gcb
37035	53931	54000	54001	54002	54017	54019	2cb5
37065	53931	54000	54001	54002	54026	54027	1cs8
37085	53931	54000	54001	54002	54031	54032	1deu
37089	53931	54000	54001	54002	54033	54034	1cv8
37090	53931	54000	54001	54002	54035	54036	1dki
37121	53931	54000	54001	54047	54048	54049	1e2t
37163	53931	54075	54076	54077	54078	54079	1dy5
37278	53931	54075	54076	54077	54084	54083	1onc
37303	53931	54075	54076	54077	54094	54096	1agi
37410	53931	54116	54117	54118	54132	54133	1b3a
37420	53931	54116	54117	54118	54134	54135	1dok
37428	53931	54116	54117	54118	54138	54139	1el0
37432	53931	54116	54117	54118	54142	54143	1eig
37436	53931	54116	54117	54118	54146	54147	1f2l
37441	53931	54116	54117	54118	54148	54149	1tvx
37499	53931	54196	54197	54198	54201	54202	1fit
37507	53931	54196	54197	54198	54203	54204	1kpif
37642	53931	54235	54285	54286	54287	54288	1fm0
37676	53931	54235	54292	54293	54294	54302	1doi
37683	53931	54235	54292	54293	54294	54309	1b9r
37998	53931	54402	54403	54407	54408	54409	1eqk
38006	53931	54402	54403	54407	54414	54415	1stf
38142	53931	54446	54447	54448	54449	54450	1pcf

38431	53931	54533	54534	54535	54547	54548	1pin
38470	53931	54592	54593	54594	54595	54596	1qip
38484	53931	54592	54593	54594	54595	54597	1f9z
38629	53931	54664	54690	54691	54692	54693	1fm0
39167	53931	54861	54928	54929	54936	54937	2u2f
39168	53931	54861	54928	54929	54936	54937	1u2f
39183	53931	54861	54928	54929	54942	54943	1fxl
39184	53931	54861	54928	54929	54942	54943	1fxl
39189	53931	54861	54928	54929	54946	54947	2mst
39191	53931	54861	54928	54929	54948	54949	1cvj
39192	53931	54861	54928	54929	54948	54949	1cvj
39210	53931	54861	54928	54929	54952	54953	1fje
39212	53931	54861	54928	54929	54952	54953	1fjc
39299	53931	54861	54975	54976	54977	54979	1aps
39341	53931	54861	55008	55009	55012	55013	2aw0
39343	53931	54861	55008	55009	55014	55015	1cc8
39345	53931	54861	55008	55009	55014	55016	1fe0
39351	53931	54861	55008	55009	55017	55018	1cpz
39352	53931	54861	55008	55009	55019	55020	1qup
39408	53931	54861	55068	55069	55070	55071	1fvg
39862	53931	55330	55331	55339	55344	55345	1dpt
40151	53931	55417	55418	55419	55420	55422	1ap8
40310	53931	55485	55486	55516	55517	55518	1ast
40663	53931	55619	55620	55628	55629	55630	1dhn
40665	53931	55619	55620	55628	55631	55632	1b9l
40675	53931	55636	55637	55638	55639	55640	1puc
40708	53931	55680	55681	55682	55683	55684	1set
40714	53931	55680	55681	55682	55685	55686	1e1o
40745	53931	55680	55681	55682	55692	55693	1ati
40759	53931	55680	55681	55682	55694	55695	1qf6
40760	53931	55680	55681	55682	55696	55697	1eov
40765	53931	55680	55681	55682	55696	55698	1b8a
40783	53931	55680	55681	55682	55705	55706	12as
40798	53931	55728	55729	55730	55733	55734	1bo4
40808	53931	55728	55729	55730	55740	55741	1qsm
40816	53931	55728	55729	55730	55742	55743	1bob
40817	53931	55728	55729	55730	55744	55745	1fy7
40818	53931	55728	55729	55730	55746	55747	1cjw
40857	53931	55752	55753	55762	55763	55764	1f7s
40858	53931	55752	55753	55762	55763	55765	1cfy
40888	53931	55769	55770	55771	55772	55777	1ypr
40891	53931	55769	55770	55771	55772	55779	3nul
41029	53931	55830	55831	55832	55833	55836	1bkp
41056	53931	55830	55831	55832	55843	55844	1b5e
41062	53931	55845	55846	55847	55848	55849	1lba
41065	53931	55855	55856	55857	55858	55859	1cyo
41085	53931	55855	55856	55857	55862	55863	1cxxy
41104	53931	55873	55874	55879	55880	55881	1ei1
41107	53931	55873	55874	55879	55882	55883	1b63
41321	53931	55944	55961	55966	55967	55968	1em2
41450	53931	56023	56024	56025	56026	56027	1byr
41634	53931	56111	56112	88854	56120	56121	1a06

41635	53931	56111	56112	88854	56122	56123	1phk
41638	53931	56111	56112	88854	56124	56125	1tki
41640	53931	56111	56112	88854	56126	56127	1kob
41664	53931	56111	56112	88854	56139	56141	1csn
41685	53931	56111	56112	88854	56153	56154	1qpc
41766	53931	56203	56204	56205	56206	56207	1c4z
41779	53931	56218	56219	56220	56221	56222	1ako
41780	53931	56218	56219	56220	56223	56224	1hd7
41876	53931	56234	56235	56251	56252	56254	1ryp
41877	53931	56234	56235	56251	56252	56254	1ryp
41878	53931	56234	56235	56251	56252	56254	1ryp
41879	53931	56234	56235	56251	56252	56254	1ryp
41880	53931	56234	56235	56251	56252	56254	1ryp
41888	53931	56234	56235	56251	56252	56254	1ryp
41889	53931	56234	56235	56251	56252	56254	1ryp
41932	53931	56234	56235	56251	56255	56257	1ryp
41933	53931	56234	56235	56251	56255	56257	1ryp
41934	53931	56234	56235	56251	56255	56257	1ryp
41935	53931	56234	56235	56251	56255	56257	1ryp
41936	53931	56234	56235	56251	56255	56257	1ryp
41937	53931	56234	56235	56251	56255	56257	1ryp
41938	53931	56234	56235	56251	56255	56257	1ryp
41989	53931	56234	56235	56251	56258	56260	1g3k
42004	53931	56234	56235	56261	56262	56263	1apy
42012	53931	56234	56235	56261	56262	56264	2gac
42057	53931	56280	56281	56288	56289	56290	1qh5
42078	53931	56299	56300	56301	56304	56306	1ute
42088	53931	56321	56322	56323	56324	56325	1qdl
42177	53931	56370	56371	56372	56373	56374	1mrj
42197	53931	56370	56371	56372	56385	56386	1d6a
42222	53931	56370	56371	56372	56391	56392	1hwm
42324	53931	56435	56436	56437	56438	56439	1qdd
42327	53931	56435	56436	56437	56442	56443	1.00E+87
42333	53931	56435	56436	56437	56444	56445	1egg
42349	53931	56435	56436	56437	56450	56451	2afp
42350	53931	56435	56436	56437	56452	56453	1qo3
42352	53931	56435	56436	56437	56454	56455	1dv8
42419	53931	56435	56436	56437	56463	56464	1byf
42423	53931	56435	56436	56437	56465	56466	1tn3
42618	56572	56573	56574	56575	56576	56577	1hle
42623	56572	56573	56574	56575	56580	56581	1as4
42955	56572	56654	56655	56656	56663	56664	2hhm
42972	56572	56654	56655	56656	56667	56668	1inp
43270	56572	56751	56752	56753	56754	56755	1daa
43349	56572	56800	56801	56802	56803	56804	1lci
43351	56572	56800	56801	56802	56805	56806	1amu
43358	56572	56814	56815	56816	56817	56819	1epu
43398	56835	56836	56854	56855	56859	56860	2bid
43400	56835	56836	56854	56855	56862	56863	1f16
43627	56835	81443	81442	81441	81440	81439	1fft
43651	56835	81339	81338	56895	56898	56899	1fx8
43988	56992	56993	56994	56995	57000	57001	6rlx

43997	56992	56993	56994	56995	57004	57005	1bon
44102	56992	57015	57059	57072	57073	57074	1agg
44108	56992	57015	57059	57072	57075	57076	1eit
44109	56992	57015	57059	57072	57077	57078	1axh
44111	56992	57015	57059	57072	57077	57078	1vtx
44112	56992	57015	57059	57072	57079	57080	1dI0
44115	56992	57015	57059	57072	57085	57086	1i25
44116	56992	57015	57059	57072	57087	57088	1qk7
44119	56992	57015	57059	57072	57093	57094	1c6w
44120	56992	57015	57095	57096	57097	57098	2sn3
44127	56992	57015	57095	57096	57097	57102	1aho
44144	56992	57015	57095	57096	57114	57115	1bmrr
44154	56992	57015	57095	57116	57131	57132	1bah
44156	56992	57015	57095	57116	57135	57136	1agt
44161	56992	57015	57095	57116	57143	57144	1sis
44162	56992	57015	57095	57116	57145	57146	1pnh
44398	56992	57301	57302	57303	57306	57307	1tgx
44403	56992	57301	57302	57303	57308	57309	1fas
44420	56992	57301	57302	57303	57318	57319	2ctx
44435	56992	57301	57302	57303	57328	57329	1f94
44549	56992	57361	57362	57363	57372	57373	1bik
44551	56992	57361	57362	57363	57374	57375	1dtx
44552	56992	57361	57362	57363	57376	57377	1bun
44553	56992	57361	57362	57363	57378	57379	1shp
44706	56992	100894	100895	57468	57473	57475	1tgs
44715	56992	100894	100895	57468	57478	57479	1nub
44721	56992	100894	100895	57468	57482	57483	1pce
44722	56992	100894	100895	57468	57484	57485	1ldt
44809	56992	57500	57501	57528	63395	63397	1hcn
44810	56992	57500	57501	57528	63396	63398	1hcn
44998	56992	57666	57667	57668	57669	57670	1a1i
45025	56992	57666	57667	57668	57671	57672	1rmd
45026	56992	57666	57667	57668	57673	57674	2drp
45027	56992	57666	57667	57668	57673	57674	2drp
45036	56992	57666	57667	57668	57677	57678	1znf
45040	56992	57666	57667	57668	57681	57682	1ncs
45041	56992	57666	57667	57668	57683	57684	2gli
45042	56992	57666	57667	57668	57683	57684	2gli
45044	56992	57666	57667	57668	57683	57684	2gli
45046	56992	57666	57667	57668	57685	57686	1bbo
45052	56992	57666	57667	57668	57689	57690	1bhi
45053	56992	57666	57667	57668	57691	57692	1ubd
45057	56992	57666	57667	57668	57693	57694	1tf3
45059	56992	57666	57667	57668	57693	57694	1tf3
45072	56992	57666	57667	57668	57695	57696	1yuj
45212	56992	57769	57798	57799	57800	57801	1qf8
45321	56992	57849	57850	57851	57852	57853	1fbv
45322	56992	57849	57850	57851	57854	57855	1rmd
45323	56992	57849	57850	57851	57856	57857	1chc
45324	56992	57849	57850	57851	57858	57859	1bor
45325	56992	57849	57850	57851	57860	57861	1g25
45331	56992	57867	57868	57869	57870	57873	4mt2

45337	56992	57867	57868	57869	57870	57875	1dmc
45339	56992	57867	57868	57869	57870	57875	1dmf
45345	56992	57867	57868	57869	57870	57877	1qjk
45346	56992	57867	57868	57869	57870	57877	1qjl
59161	46456	46625	46626	46627	63459	63460	1.00E+29
59197	46456	46688	46689	46690	46699	46700	1e3o
59226	51349	51350	51445	51521	51522	51523	1e4m
59262	51349	53253	53254	53255	53256	64110	1.00E+58
59272	48724	50813	50814	50815	63805	63806	1e5p
59283	51349	53685	53686	53687	64172	64173	1e5x
59296	51349	52539	52540	52566	52567	52568	1e6c
59373	51349	51734	51735	51751	51769	63926	1e7w
59393	48724	50198	50324	50325	50326	50327	1e9g
59401	48724	48725	48726	48727	48730	48731	1eaj
59414	51349	52373	52374	52397	52400	63975	1ej2
59454	48724	50493	50494	50514	63789	63790	1elv
59486	53931	54533	54534	54535	64248	64249	1eq3
59507	46456	47239	47240	47241	63524	63525	1eum
59642	46456	47265	47266	47267	63530	63531	1f45
59662	51349	64004	64005	64006	64007	64008	1f75
59674	51349	52373	52374	52375	52392	52393	1f7u
59689	48724	49451	49472	49473	49474	49475	1f86
59694	48724	50938	50939	50940	50943	50944	1f8e
59760	51349	53382	53383	53417	64128	64129	1fc4
59771	53931	54533	54534	54535	64250	64251	1fd9
59803	46456	46688	46689	46739	63467	63468	1fex
59819	51349	53382	53383	53384	64121	64122	1fg7
59869	51349	51904	51905	51943	51953	63949	1fl2
59870	51349	51904	51905	51943	51953	63949	1fl2
59879	51349	52539	52540	52575	64015	64016	1fmj
59922	51349	52832	52833	52834	64054	64055	1fo5
59927	51349	53447	53448	64136	64137	64138	1fo8
59976	51349	52798	52799	52800	64049	64050	1fpz
60047	53931	56111	56112	88854	64406	64407	1fvr
60058	51349	53747	53748	53749	53750	53751	1fw8
60187	53931	55810	55811	55812	64365	64366	1g0s
60227	46456	48507	48508	48509	48534	63626	1g2n
60228	51349	53162	53167	53168	53169	64098	1g2o
60237	51349	52539	52540	52652	64019	64021	1g3q
60264	51349	53040	53056	53057	53058	64084	1g5c
60271	53931	55680	55681	55682	64349	64350	1g5h
60288	51349	52506	52507	52508	63996	63997	1g5q
60318	51349	52539	52540	52686	64025	64026	1g6h
60320	56992	57361	57362	57363	57364	57365	1g6x
60376	51349	52539	52540	81269	64040	64041	1g8p
60400	48724	50155	50156	50157	63754	63755	1g9o
60456	51349	53382	53383	53384	53392	64120	1gde
60625	53931	55680	55681	55682	55688	55691	1h4v
60643	51349	51734	51735	51751	63927	63928	1h5q
60693	51349	51904	51905	51943	63947	63948	1h6v
60694	51349	51904	51905	51943	63947	63948	1h6v
60711	53931	55908	55909	64380	64381	64382	1h70

60716	51349	52832	52833	52834	64052	64053	1h75
60717	51349	53447	53448	68901	64143	64144	1h7e
60726	51349	51350	51569	51594	51595	51596	1h7n
60737	48724	50493	50494	50514	50531	50532	1h8d
60793	53931	56435	56436	56437	64457	64458	1h8u
60812	46456	46457	46458	46463	63438	63439	1h97
60887	46456	47026	47027	47028	47029	63498	1hbk
60939	53931	55680	55681	55682	64347	64348	1hc7
60962	51349	52832	52833	52901	64066	64067	1hd2
60965	51349	51734	51735	51751	63931	63932	1hdo
60970	48724	48725	48726	49159	49190	49191	1he7
61006	53931	55330	55331	55339	55340	64323	1hfo
61042	46456	48370	48452	48453	48460	48461	1hh8
61127	53931	56435	56436	56437	64453	64454	1hq8
61154	51349	53658	53659	53660	53668	64171	1hqs
61160	46456	47472	47473	63550	63551	63552	1hvq
61254	46456	48096	48097	48098	63586	63587	1htj
61366	46456	48370	48452	48453	48462	63617	1hxi
61367	48724	48725	48726	48727	48933	63651	1hxm
61369	48724	48725	48726	48727	48933	48938	1hxm
61459	53931	55810	55811	64369	64370	64371	1hzt
61515	53931	55728	55729	55730	64351	64352	1i12
61548	46456	47265	47266	47267	47272	63528	1i1r
61568	51349	52539	52540	52592	52609	52611	1i2m
61585	51349	53066	53098	53099	53103	64093	1i39
61605	56992	57923	57924	57925	57928	57929	1i3o
61732	48724	50813	50814	50815	63807	63808	1i4u
61767	51349	53447	53448	68901	64140	64141	1i52
61848	51349	53040	53056	53057	53058	64085	1i6p
61889	53931	54494	54495	54496	54497	64243	1i7k
61901	53931	56321	56322	56323	56324	64443	1i7q
61979	46456	46625	46626	46627	46650	46655	1i8o
62099	51349	52798	52799	52800	64047	64048	1i9s
62119	46456	48096	48097	48098	63584	63585	1iap
62162	51349	53382	53383	53402	53403	64125	1ibj
62318	46456	48507	48508	48509	48528	48529	1ie9
62375	51349	53066	53098	53118	53125	53127	1ih7
62380	46456	48370	48452	48453	63618	63619	1ihg
62382	48724	50155	50156	50157	63756	63757	1ihj
62394	51349	52539	52540	52652	52668	52669	1ihu
62395	51349	52539	52540	52652	52668	52669	1ihu
62510	48724	50352	50353	50354	63779	63780	1ijt
62591	56572	56573	56574	56575	64471	64472	1imv
62598	51349	52539	52540	81269	52713	64037	1in4
62611	56572	64517	64518	64519	64520	64521	1io1
62650	51349	52539	52540	81269	64035	64036	1iqp
62661	46456	47972	47973	47974	47975	63577	1iqv
62669	48724	50629	50630	50646	50649	63795	1j71
62697	53931	56111	56112	64411	64412	64413	1j7l
62700	46456	47472	47473	47502	47514	47515	1j7q
62753	51349	56783	56784	64511	64512	64513	1j97
62817	51349	51734	51735	51751	63929	63930	1ja9

62819	53931	54494	54495	54496	54497	64241	1jat
62836	48724	50198	50249	50263	50273	50274	1jb7
62837	48724	50198	50249	50263	50273	50274	1jb7
62838	48724	50198	50249	50263	50273	50274	1jb7
62839	48724	50198	50249	50263	50275	50276	1jb7
62845	51349	52171	52172	52173	52174	52175	1jbe
62850	51349	53685	53686	53687	64174	64175	1jbq
62888	48724	51068	51069	51070	51071	63844	1jd0
62936	46456	47112	47113	47134	63507	63508	1jfi
62937	46456	47112	47113	47134	63509	63510	1jfi
62940	51349	52832	52833	52901	64068	64069	1jfu
63114	51349	52539	52540	52686	64029	64030	1jj7
63116	56992	57867	57868	57869	64581	64582	1jjd
63155	53931	56275	56276	56277	56278	56279	1jl0
63177	48724	48725	48726	48727	63637	63638	1jma
63223	56572	56654	56655	56656	64475	64476	1jp4
63234	51349	52539	52540	81269	64033	64034	1jq1
63279	48724	50198	50249	50282	63772	63773	1jt8
64709	48724	50198	50249	50282	68910	68911	1a62
64720	51349	53334	53335	53354	68927	68928	1dl5
64889	48724	50493	50494	50514	69284	69285	1eax
64986	51349	52539	52540	52592	69483	69484	1f6b
65078	48724	48725	48726	49159	49172	49173	1g1c
65104	53931	56435	56436	56437	56456	56457	1g1t
65117	51349	53270	53271	53272	53288	69541	1g2q
65171	56992	57015	57059	57072	69928	69929	1g9p
65288	48724	48725	48726	49159	69158	69159	1gl4
65305	48724	49763	49764	49765	49766	69208	1gme
65407	46456	47768	47819	69044	69045	69046	1go3
65414	51349	51350	51445	51534	51546	51547	1goi
65441	48724	51181	51197	51198	69346	69347	1gp6
65535	48724	48725	48726	49159	49168	49169	1gsm
65536	48724	48725	48726	49159	49168	49169	1gsm
65640	51349	52539	52540	52592	69485	69486	1h65
65643	46456	47575	47576	47577	69029	69030	1h67
65681	53931	64267	64268	64269	69718	69719	1h6h
65706	53931	55873	55874	55879	69800	69801	1h7s
65805	51349	53648	53649	53653	53656	69591	1hdh
65830	48724	51125	51126	51137	51140	69332	1hg8
65835	48724	50198	50249	50282	69265	69266	1hh2
65845	48724	50493	50494	50514	50515	50516	1hj9
65915	53931	55752	55753	55762	69793	69794	1hqz
65969	51349	52095	52096	52103	69440	69441	1hzd
65975	51349	52820	52821	52822	69507	69508	1hzm
66024	48724	50198	50324	50325	50326	50329	1i40
66041	51349	52373	52374	52375	52378	52379	1i6l
66153	53931	53954	53955	53960	53961	69627	1iiz
66205	51349	52832	52833	52834	69512	69513	1ilo
66211	51349	52498	52499	100948	69465	69466	1im5
66220	51349	53334	53335	69557	69558	69559	1inl
66258	51349	52373	52374	52375	52392	69454	1iq0
66365	46456	46457	46458	46463	68941	68942	1it2

66438	53931	54116	54117	54118	69632	69633	1j8i
66454	51349	51350	51726	51727	51728	69405	1j93
66482	48724	48725	48726	49159	69160	69161	1jbj
66544	56992	57923	57924	57925	69974	69975	1jd5
66549	46456	48370	48371	48372	48373	48375	1jdh
66581	51349	53162	53167	53168	53174	69536	1je0
66621	51349	52787	52788	52789	69504	69505	1jf8
66624	46456	48263	48264	48265	48270	48271	1jfb
66638	46456	47472	47473	47502	69021	69022	1jfj
66661	51349	53334	53335	53354	68927	69553	1jg1
66678	56992	57301	57302	57303	69949	69950	1jgk
66714	48724	49784	49785	69210	69211	69212	1jhj
66745	51349	52373	52374	52375	52376	69453	1jil
66758	53931	55680	55681	55682	55701	55702	1jjc
66763	53931	55680	55681	55682	55703	55704	1jjc
66770	56572	56573	56574	56575	69871	69872	1jjo
66795	53931	54402	54427	54431	69675	69676	1jkg
66796	53931	54402	54427	54431	69677	69678	1jkg
66808	53931	55810	55811	55812	64367	64368	1jkn
66821	51349	53066	53098	53099	53100	53101	1jl1
66880	56992	57849	57850	57851	69968	69969	1jm7
66881	56992	57849	57850	57851	69970	69971	1jm7
67111	51349	69617	69618	69619	69620	69621	1jr2
67215	51349	53382	53383	69565	69566	69567	1js3
67377	51349	69571	69572	69573	69574	69575	1jw9
67384	53931	56435	56436	56437	88867	88872	1jwi
67458	51349	53447	53448	68901	69569	69570	1jyk
67834	51349	51350	51445	51487	51510	51511	1jz8
67940	53931	56321	56322	56323	69838	69839	1k0g
67992	53931	74651	48403	48404	69091	69092	1k1a
68253	51349	53719	53720	69602	69603	69604	1k75
68308	48724	50964	50978	50979	69313	69314	1k8k
68333	46456	47472	47473	63550	47550	47551	1k94
68341	46456	47094	47095	47096	68982	68983	1k99
68356	56572	56573	56574	56575	64469	64470	1k9o
68369	56572	56654	56655	56656	56669	69878	1ka1
68582	51349	52539	52540	52541	69474	69475	1kgd
68597	51349	52171	52172	52173	52192	69445	1kgs
68644	51349	52539	52540	52541	69476	69477	1kjw
68790	56572	56795	56796	69892	69893	69895	1kq3
68810	56992	57015	57059	57072	69926	69927	1kqh
68863	56992	57361	57362	57363	57366	57367	1kth
70066	56992	57015	57059	57072	75666	75667	1cix
70113	48724	50728	50729	50730	74993	74994	1eaz
70150	53931	54116	54117	54118	75341	75342	1g2t
70168	51349	53382	53383	53402	64126	75271	1gc0
70180	48724	50493	50494	50514	50586	50587	1gj7
70214	48724	50813	50814	50815	63807	63808	1gka
70228	46456	48556	48557	48572	48573	48574	1gkm
70341	51349	52767	52768	52769	75227	75228	1gq6
70372	48724	49784	49785	69210	69211	74892	1gqp
70376	53931	54075	54076	54077	64205	64206	1gqv

70396	51349	52539	52540	52541	52563	69482	1gsi
70441	51349	51350	51395	51396	51410	51411	1gte
70597	51349	51350	51430	51431	75056	75057	1gve
70610	48724	50493	50494	50514	50536	50538	1gvk
70629	46456	48370	48371	74771	74772	74773	1gw5
70630	46456	48370	48371	74771	74774	74775	1gw5
70667	56572	56633	56634	56635	56636	56641	1gwe
70722	48724	50964	50978	50979	75009	75010	1gxr
70738	53931	54402	54427	54431	54432	75374	1gy7
70803	48724	49898	49899	49900	49904	74903	1gzc
70805	51349	51350	51569	51594	51595	51597	1gzg
70855	51349	51350	51445	51487	75066	75067	1h1n
70857	51349	53253	53254	53255	69539	69540	1h2e
70959	46456	47026	47027	47028	47029	47030	1hb6
71089	53931	54533	54534	54535	75388	75389	1hxv
71102	51349	53334	53335	53354	68927	69554	1i1n
71114	51349	51350	51366	51381	51385	75052	1i4n
71122	53931	54235	54292	54293	75366	75367	1l7h
71240	46456	47265	47266	47286	63532	63533	1ik0
71270	51349	51350	51713	51714	75096	75097	1iq8
71379	51349	52373	52374	52375	75159	75160	1irx
71425	51349	51350	51445	51534	75069	75070	1itx
71469	56992	100894	100895	57468	75678	75679	1iw4
71531	48724	51181	51182	51187	75033	75034	1j58
71589	53931	55680	55681	55682	75504	75505	1j5w
71618	51349	52539	52540	52575	52578	52579	1j99
71631	51349	52539	52540	81269	75211	75212	1jbk
71665	51349	52539	52540	52686	75207	75208	1ji0
71685	46456	47239	47240	47241	47250	74706	1jig
71696	48724	50198	50249	50282	74952	74954	1jjg
71710	53931	56111	56112	88854	75560	75561	1jks
71726	46456	46457	46458	46463	46467	46468	1jl7
71757	51349	51350	51445	51534	75071	75072	1jnd
71844	53931	55944	55961	55966	75545	75546	1jss
71907	53931	54533	54534	54535	64250	75387	1jvw
71978	48724	49784	49785	74896	74897	74898	1k12
72010	53931	55810	55811	55812	75527	75528	1k2e
72015	53931	54000	54001	54002	75330	75331	1k3b
72017	56835	56836	56854	56855	75637	75638	1k3k
72076	48724	51125	51126	51137	51140	75025	1k5c
72177	51349	53473	53474	53506	53507	75284	1k8q
72181	46456	47472	47473	47478	47479	74719	1k8u
72249	51349	52539	52540	52566	52567	75193	1kag
72254	51349	52373	52374	52397	52400	75164	1kam
72277	51349	51350	51395	51396	51408	51409	1kbi
72278	53931	55855	55856	55857	55864	55865	1kbi
72399	56835	81344	81343	81373	81370	81369	1kf6
72400	56835	81344	81343	81373	81372	81371	1kf6
72445	53931	56435	56436	56437	75583	75584	1kg0
72498	48724	50728	50729	50730	74991	74992	1ki1
72510	51349	53589	53590	53591	69587	69588	1kic
72636	51349	52539	52540	52592	75204	75205	1kk1

72663	51349	53382	53383	53417	53429	75272	1kl1
72678	51349	53685	53686	53687	64172	75313	1kl7
72722	56992	57666	57667	57668	57679	57680	1klr
72740	51349	51350	51366	51375	51376	51379	1km4
72744	53931	64267	64268	64269	75424	75425	1kmd
72757	51349	53596	53597	53598	53605	53607	1kmv
72777	51349	52832	52833	52901	75237	75238	1kng
72915	48724	48725	81296	81288	74846	74847	1ksh
72972	53931	55810	55811	55812	64367	75526	1ktg
73007	53931	55485	55486	55519	55520	75495	1kuf
73155	48724	50198	50249	50263	74948	74949	1kxl
73334	48724	50728	50729	50730	74989	74990	1kz7
73428	53931	55680	55681	55682	55696	55700	1l0w
73452	48724	51315	51316	75041	75042	75043	1l1d
73480	48724	50198	50249	50263	50267	50268	1l1o
73514	51349	52539	52540	52686	64027	64028	1l2t
73539	53931	54861	54928	54929	54930	54931	1l3k
73540	53931	54861	54928	54929	54930	54931	1l3k
73594	51349	53731	53732	53733	75319	75320	1l5j
73598	53931	54235	54292	54293	54294	75365	1l5p
73627	51349	51350	51569	51594	51595	51598	1l6s
73632	51349	51350	51569	51570	75085	75086	1l6w
73674	51349	52539	52540	52686	75209	75210	1l7v
73683	53931	55417	55418	55419	55420	55421	1l8b
73708	46456	47094	47095	47096	68982	68983	1l8y
73813	56572	56654	56655	56656	56665	75608	1lbv
73827	51349	53382	53383	53384	69563	69564	1lc5
73867	46456	46688	46689	46690	46693	46694	1le8
73878	48724	50813	50814	50815	74998	74999	1lf7
73896	51349	53270	53271	53272	53290	53291	1lh0
73913	51349	52373	52374	52375	75161	75162	1li5
73928	56572	56573	56574	56575	56587	56588	1lj5
73941	48724	50181	50182	50183	63758	74938	1lj0
74005	51349	53447	53448	75273	75274	75275	1ll2
74038	53931	55944	55961	55966	75547	75548	1ln1
74144	53931	54636	54637	54638	54639	54640	1lo7
74192	46456	47265	47266	47305	47306	74708	1lqs
74215	48724	51181	51182	51187	75030	75031	1lr5
74271	48724	50198	50249	50282	74952	74953	1luz
74295	51349	52373	52374	52397	75165	75166	1lw7
74296	51349	52539	52540	52541	75189	75190	1lw7
74334	51349	52539	52540	52541	75191	75192	1ly1
74442	46456	47265	47266	47286	47301	47302	1m47
74457	53931	55728	55729	55730	75506	75507	1m4i
74533	51349	51904	51905	51943	75126	75127	1m6i
74534	51349	51904	51905	51943	75126	75127	1m6i
74574	56572	56633	56634	56635	56636	75599	1m7s
74579	53931	54116	54117	54118	54128	75340	1m8a
74601	48724	50493	50494	50514	50536	74973	1m9u
74621	56992	57015	57059	57072	75658	75659	1mb6
75802	53931	81607	81606	81605	81604	81603	1a6q
76222	53931	55728	55729	55730	82747	82748	1ghe

76236	53931	54000	54001	54002	54022	54023	1gmy
76337	46456	47094	47095	47096	81718	81719	1gt0
76348	46456	46625	46626	46627	68950	68951	1gu2
76360	48724	50493	50494	50514	82122	82123	1gvz
76378	53931	54861	54975	54976	82675	82676	1gxu
76410	51349	51734	51735	51751	82294	82295	1gz6
76572	48724	51181	51197	82194	82195	82196	1h2k
76595	53931	54861	54928	54929	64274	64275	1h2v
76620	46456	46625	46626	46627	81675	81676	1h32
76631	51349	52373	52374	52375	52376	82354	1h3f
76643	51349	52373	52374	52375	82356	82357	1h3n
76644	46456	47112	47113	47134	81720	81721	1h3o
76645	46456	47112	47113	47134	81722	81723	1h3o
76725	51349	51734	51735	51751	82290	82291	1hxh
76732	51349	51350	51445	51487	51514	51518	1i1w
76755	53931	54636	54637	82636	82637	82638	1iq6
76773	48724	49898	49899	49932	82034	82035	1is3
76858	51349	52373	52374	52375	52390	52391	1ivs
76950	48724	50198	50249	50263	82099	82101	1iyj
76951	48724	50198	50249	50263	82099	82101	1iyj
76952	48724	50198	50249	50263	82099	82101	1iyj
77026	51349	52373	52374	52375	52382	52383	1j09
77051	46456	81777	81778	81779	81780	81781	1j0t
77075	53931	55845	55846	55847	82775	82776	1j3g
77078	46456	47472	47473	47478	47479	81755	1j55
77082	56992	57015	57095	57116	82883	82884	1j5j
77117	46456	47239	47240	47241	47250	81743	1ji4
77135	56572	56573	56574	56575	82833	82834	1jmj
77216	51349	53162	53167	53168	82448	82449	1jys
77237	46456	48255	48256	48257	48258	81862	1k3p
77258	51349	52373	52374	52397	52400	82358	1k4m
77270	46456	46688	46689	46690	46695	46696	1k61
77376	51349	51350	51445	51534	82249	82250	1kfw
77384	48724	48725	48726	48727	48933	48935	1kgc
77409	48724	50198	50249	50282	82105	82106	1khi
77442	48724	48725	81296	81288	49241	49242	1km
77528	46456	48370	48452	48453	81905	81907	1kt1
77628	51349	53719	53720	53721	82538	82539	1ky8
77653	51349	53270	53271	53272	53288	82455	1l1q
77655	48724	50352	50353	50362	50363	50364	1l2h
77768	51349	56783	56784	82388	82389	82390	1l6r
77770	48724	48725	48726	48727	81942	81943	1l6z
77771	48724	48725	48726	49159	81956	81957	1l6z
77810	51349	52539	52540	81269	82416	82417	1l8q
77873	46456	47239	47240	47241	47246	63526	1lb3
77926	46456	48263	48264	48265	81863	81864	1lfk
77960	51349	53612	53613	82515	82516	82517	1lh
78063	46456	47239	47240	47241	47242	47243	1lko
78171	51349	52539	52540	52652	52664	52665	1ls1
78184	51349	51350	82282	82283	82284	82285	1lt7
78232	51349	52539	52540	81269	82418	82419	1lv7
78265	51349	53658	53659	53660	82524	82525	1lwd

78401	48724	50036	50118	82075	82076	82077	1m1f
78508	51349	53382	53383	53402	82486	82487	1m32
78598	46456	47472	47473	47502	81756	81757	1m45
78602	53931	55752	55753	55762	82752	82753	1m4j
78666	53931	54533	54534	54535	82624	82625	1m5y
78676	48724	50155	50156	50157	82083	82084	1m5z
78701	51349	53382	53383	53384	64123	64124	1m6s
78724	51349	52539	52540	52572	52573	52574	1m7g
78761	51349	53382	53383	53417	53440	53441	1m7y
78865	53931	54235	54236	54237	82579	82580	1m94
78907	51349	52171	52172	52173	82342	82343	1mb3
79008	56572	56800	56801	56802	82843	82844	1mdb
79013	51349	53382	53383	53417	82488	82489	1mdo
79023	53931	54000	54001	54002	54020	54021	1me4
79129	53931	56275	56276	56277	56278	82801	1mhmm
79150	46456	46688	46689	46690	81681	81682	1mij
79183	51349	52095	52096	52103	52106	52107	1mj3
79189	53931	55855	55856	55857	55866	82777	1mj4
79198	51349	53334	53335	69557	82479	82480	1mjf
79250	51349	52539	52540	52592	82406	82407	1mkly
79251	51349	52539	52540	52592	82406	82407	1mkly
79341	51349	51904	51905	51943	82313	82314	1mo9
79342	51349	51904	51905	51943	82313	82314	1mo9
79414	56572	56814	56815	56816	82848	82849	1mq5
79469	51349	53066	53098	53099	53105	82443	1mu2
79617	53931	54861	55008	55009	82683	82684	1mwz
79758	51349	52539	52540	52592	82404	82405	1n0u
79778	53931	74651	48403	48404	82632	82633	1n11
79803	46456	47265	47266	47305	81744	81745	1n1f
79813	46456	47112	47113	47134	81724	81725	1n1j
79814	46456	47112	47113	47134	81726	81727	1n1j
79850	48724	48725	48726	49159	81958	81959	1n26
79857	51349	51734	51735	51751	75102	75103	1n2s
79966	51349	52373	52374	52375	52376	82355	1n3l
79977	46456	48263	48264	48265	81865	81866	1n40
80007	51349	51350	51351	51352	51353	51360	1n55
80250	51349	51734	51735	51751	51759	82289	1n7h
80304	51349	53382	53383	53402	82484	82485	1n8p
80335	46456	48263	48264	48265	81869	81870	1n97
80344	48724	50181	50182	50183	82087	82088	1n9r
80407	51349	53253	53254	53258	53259	53261	1nd6
80424	48724	50036	50118	82075	82078	82079	1ne8
80431	56835	81344	81343	81373	82870	82871	1nek
80432	56835	81344	81343	81373	82872	82873	1nek
80444	48724	50964	50978	50979	82169	82170	1nex
80531	51349	52539	52540	52592	82410	82411	1ni3
80541	56992	57015	57059	57072	82879	82880	1nix
80573	46456	47458	47459	47460	81750	81751	1nkp
80574	46456	47458	47459	47460	47461	47462	1nkp
80633	46456	47458	47459	47460	81752	81753	1nlw
80731	53931	54861	54928	54929	54932	54933	1nu4
80734	48724	50352	50353	50354	82107	82108	1nun

81092	53931	56111	56112	88854	82791	82792	1o6l
81106	53931	56111	56112	88854	82793	82794	1o6y
81178	48724	51125	51126	51127	51128	51129	1o88
83054	48724	50198	50249	50282	88670	88671	1go3
83251	56992	57301	57302	57303	90152	90153	1ff4
83255	51349	51350	51445	51487	89469	89470	1fob
83268	51349	52539	52540	52575	52576	75198	1g3m
83336	46456	46688	46689	46739	46740	46742	1gv2
83338	46456	46688	46689	46739	46740	46742	1gvd
83351	46456	48112	48113	48114	48125	48126	1gwu
83372	48724	48725	48726	49159	89185	89186	1gxe
83376	51349	51734	51735	51751	51752	89519	1gy8
83392	53931	56435	56436	56437	90059	90060	1gz2
83405	53931	56111	56112	88854	88855	88856	1gz8
83553	48724	48725	48726	48727	89178	89179	1hkf
83581	51349	51350	51569	51570	51571	51572	1hl2
83663	51349	51734	51735	51751	51763	51764	1i24
83698	46456	48255	48256	48257	48258	89115	1iom
83763	53931	54533	54534	54535	89879	89880	1ix5
83774	51349	51734	51735	51751	89523	89524	1iy8
83786	56572	56751	56752	56753	56757	56758	1iye
83806	56992	57849	57850	57851	90220	90221	1iyym
83838	51349	51350	51621	51638	89501	89502	1izc
83847	56572	90095	90096	90097	90098	90099	1izn
83848	56572	90095	90096	90100	90101	90102	1izn
83851	46456	48263	48264	48265	89116	89117	1izo
83871	51349	53685	53686	53687	53694	89777	1j0a
83980	51349	52373	52374	52375	52376	89611	1j1u
84048	53931	56435	56436	56437	88861	88862	1j34
84070	51349	53596	53597	53598	53610	88963	1j3k
84131	51349	53270	53271	53272	53286	89728	1j7j
84138	51349	52539	52540	52592	82410	89666	1jal
84185	53931	54533	54534	54535	89877	89878	1jns
84205	51349	52171	52266	89594	89595	89596	1jrl
84230	51349	51734	51735	51751	51772	51773	1jtv
84262	53931	56435	56436	56437	90061	90062	1jzn
84271	48724	50813	50814	50815	89364	89365	1jzu
84401	51349	52539	52540	52541	52554	89660	1kht
84467	48724	50813	50814	50815	50816	50817	1kt7
84475	48724	50813	50814	50815	50837	50838	1kxo
84625	53931	56370	56371	56372	90055	90056	1lln
84674	51349	51350	51430	51431	89461	89462	1lqa
84680	56992	100894	100895	57468	90166	90167	1lr7
84707	48724	50493	50494	50514	89341	89342	1lto
84743	56992	57867	57868	57869	57870	90225	1m0g
84744	56992	57867	57868	57869	57870	90225	1m0j
84761	53931	56370	56371	56372	56381	56382	1m2t
84808	48724	50181	50182	50183	89317	89318	1m5q
84979	53931	55728	55729	55730	90013	90014	1mk4
85092	56992	56993	56994	56995	56996	56998	1mso
85107	56572	56573	56574	56575	90080	90081	1mtp
85140	48724	49898	49899	49925	49926	89270	1mve

85146	51349	52506	52507	52508	52509	52510	1mvl
85197	46456	47239	47240	47253	47257	47258	1mxr
85241	46456	47873	47874	47875	89079	89080	1n00
85315	46456	48507	48508	48509	48530	48531	1n46
85328	51349	52171	52317	52325	89609	89610	1n57
85370	53931	55728	55729	55730	55731	55732	1n71
85374	51349	51350	51569	51570	69394	89493	1n7k
85401	51349	52832	52833	52901	69516	69517	1n8j
85553	48724	48725	48726	48727	63635	63636	1ncn
85592	48724	48725	48726	48727	48734	48736	1nez
85598	46456	47239	47240	47241	47244	89025	1nf4
85631	51349	52498	52499	100948	89643	89644	1nf9
85739	56572	56654	56655	90087	90088	90089	1ni9
85741	51349	52539	52540	52652	89671	89672	1nij
85781	51349	52539	52540	81269	52711	52712	1njf
85818	53931	54636	54637	54638	89900	89901	1njk
85866	51349	52832	52833	52834	89700	89701	1nm3
85867	51349	52832	52833	52901	89708	89709	1nm3
85874	51349	52128	52129	52130	52131	52132	1nme
85892	51349	52539	52540	52541	52563	64010	1nn5
85906	51349	56783	56784	64511	64512	89645	1nnl
85954	51349	52539	52540	52652	89673	89674	1np6
86077	53931	55810	55811	55812	90022	90023	1nqz
86078	48724	50964	50978	50979	89378	89379	1nr0
86079	48724	50964	50978	50979	89378	89379	1nr0
86125	51349	52539	52540	52592	89664	89665	1nrj
86128	51349	56783	56784	82388	89646	89647	1nrw
86137	53931	55728	55729	55730	90015	90016	1nsl
86209	51349	52373	52374	52397	89613	89614	1nuu
86211	56572	56654	56655	56656	56657	56658	1nuw
86224	51349	53334	53335	89743	89744	89745	1nv8
86250	51349	51350	51569	89494	89495	89496	1nvml
86268	53931	56111	56112	88854	64404	64405	1nvr
86276	46456	48365	48366	48367	48368	48369	1nvu
86294	51349	52128	52129	52130	69443	69444	1nw9
86295	53931	54861	55068	55069	55070	89956	1nwa
86296	48724	89359	89360	89361	89362	89363	1nwb
86508	51349	53719	53720	53721	53722	53726	1o04
86525	51349	56783	56784	75173	75174	75175	1o08
86535	53931	54861	54928	54929	54936	54937	1o0p
86555	51349	51350	51695	89508	89509	89510	1o1z
86556	51349	53719	53720	53721	89781	89782	1o20
86591	56572	56795	56796	69892	75612	75613	1o2d
86620	51349	53382	53383	53384	53385	89754	1o4s
86629	51349	88722	88723	89619	89620	89621	1o4w
86642	48724	50198	50249	50263	89324	89325	1o7i
86660	53931	54116	54117	54118	82573	82574	1o7z
86681	51349	52832	52833	52901	52904	52905	1o8x
86706	46456	47239	47240	47241	47250	89027	1o9r
86734	46456	48112	48113	48114	48123	89092	1oaf
86739	48724	48725	49329	49330	49331	49337	1oal
86832	48724	51181	51182	51187	51188	89412	1od5

86833	48724	51181	51182	51187	51188	89412	1od5
86836	51349	52373	52374	52397	52398	89612	1od6
86863	51349	53162	53167	53168	53169	89721	1odk
86875	48724	51181	51197	51198	51199	51200	1odm
86889	51349	51350	51445	51487	63908	63909	1odz
86924	48724	50629	50630	50646	50647	50648	1oew
86934	53931	54402	54427	54431	89849	89850	1of5
86936	51349	51350	51395	51396	69381	75055	1ofd
86990	48724	48725	48726	48727	48933	48935	1oga
86992	48724	48725	48726	48727	48933	48937	1oga
87001	53931	54235	54236	54237	54238	54239	1ogw
87013	51349	52798	52799	52800	89698	89699	1ohe
87014	51349	52798	52799	52800	89698	89699	1ohe
87036	53931	55845	55846	55847	90024	90025	1oht
87086	46456	48096	48097	48098	89090	89091	1omw
87087	48724	50728	50729	50730	50747	89354	1omw
87088	53931	56111	56112	88854	90034	90035	1omw
87142	51349	51904	51905	51943	51944	89548	1onf
87196	51349	51734	51735	51751	51769	89520	1ooe
87319	46456	47472	47473	47502	89053	89055	1oqp
87387	51349	52539	52540	52541	52552	89659	1osn
87494	53931	54861	54928	54929	89940	89941	1owx
87539	51349	52150	52151	89729	89730	89731	1oxw
87554	53931	74651	48403	48404	82634	82635	1oy3
87648	51349	51350	51395	51396	89454	89455	1p0k
87716	48724	50964	50978	50979	89376	89377	1p22
87721	51349	52171	52172	52173	89587	89588	1p2f
87752	51349	53382	53383	53402	89755	89756	1p3w
87775	53931	56111	56112	88854	69825	69826	1p4o
87815	51349	52539	52540	52541	89657	89658	1p5z
88034	46456	48507	48508	48509	89144	89145	1pdu
88067	56572	56800	56801	56802	90093	90094	1pg4
88069	48724	50964	50978	50979	89378	89380	1pgu
88070	48724	50964	50978	50979	89378	89380	1pgu
88139	46456	48507	48508	48509	89147	89148	1pk5
88147	48724	48725	48726	48727	89174	89175	1pko
88292	51349	52539	52540	52592	89667	89668	1pui
88294	51349	52539	52540	52592	89669	89670	1puj
88395	51349	51350	51569	51570	69394	89492	1ub3
88399	48724	50036	50118	82075	89303	89304	1ub4
88467	48724	48725	48726	49159	89188	89189	1uct
88485	53931	55728	55729	55730	90011	90012	1ufh
88490	51349	51350	51445	51521	51528	89476	1ug6
88491	56572	56573	56574	56575	56578	56579	1uhg
90443	51349	53648	53649	102651	102652	102653	1ei6
90509	51349	51734	51735	51751	51784	51785	1gee
90514	51349	51350	51569	51570	51586	51587	1gqn
90661	56572	56751	56752	56753	56759	56760	1i2k
90690	53931	55810	55811	55812	103207	103208	1iry
90699	51349	53382	53383	53402	102599	102600	1iug
90703	51349	69592	69593	69594	69595	69596	1iuq
90717	53931	54636	54637	89902	102916	102917	1ixl

90719	53931	74651	48403	48404	102881	102883	1ixv
90747	48724	50352	50353	50362	101782	101783	1j0s
90788	51349	52498	52499	100948	102298	102299	1j2r
90806	46456	47239	47240	47241	101130	101131	1j30
90833	53931	55769	103196	103197	103198	103199	1j3w
90882	53931	54494	54495	54496	54497	102840	1jas
90908	51349	51350	51395	51396	51397	51398	1jub
90912	51349	53596	53597	53598	53599	102635	1juv
90927	51349	51734	51735	51751	102148	102149	1k2w
90929	53931	56234	56235	56261	56262	103315	1k2x
90941	51349	52171	52172	52173	75152	102227	1k66
90943	51349	52171	52172	52173	75152	102226	1k68
90964	53931	54000	54001	54002	54005	54006	1khq
91020	53931	64267	64268	64269	64270	64271	1kq6
91024	51349	52171	52172	52173	52180	52181	1krw
91055	56992	57015	57059	57072	103531	103532	1la4
91080	56992	57015	57059	57072	103533	103534	1lmm
91086	48724	48725	48726	48727	48933	48934	1lp9
91124	51349	52832	52833	52901	102457	102458	1lu4
91127	48724	51068	51069	51070	51071	51073	1lug
91170	56992	57015	57095	57116	103542	103543	1m2s
91208	51349	52128	52129	52130	102526	102527	1m72
91235	56572	56573	56574	56575	56593	56594	1m93
91242	48724	50352	50353	50362	101780	101781	1md6
91302	48724	48725	48726	48727	88543	88552	1mju
91304	48724	48725	48726	48727	88519	88524	1mju
91384	53931	56111	56112	88854	103292	103293	1mp8
91394	53931	55810	55811	55812	64365	103200	1mqe
91453	51349	52373	52374	52397	102260	102261	1mrz
91469	51349	52539	52540	52686	102381	102382	1mv5
91500	51349	51350	51430	51431	51443	102053	1mzr
91636	46456	48207	48239	48246	48247	48248	1n4q
91691	48724	50155	50156	50157	101717	101718	1n7e
91705	56992	57015	57095	57116	103550	103551	1n8m
91767	53931	55619	55620	55628	55629	103143	1nbu
91815	53931	56111	56112	64411	103302	103303	1nd4
91817	53931	56203	56204	56205	103308	103309	1nd7
91849	51349	56783	56784	82388	102313	102314	1nf2
92005	53931	55680	55681	55682	103157	103158	1nnh
92006	46456	47239	47240	47241	47242	101129	1nnq
92018	53931	54861	54928	54929	102979	102980	1no8
92021	51349	51350	51445	51487	102073	102074	1nof
92047	46456	48507	48508	48509	74794	74795	1nq7
92077	53931	54116	54117	54118	102730	102731	1nr4
92091	46456	48507	48508	48509	63624	63625	1nrl
92102	51349	53253	53254	53258	102533	102534	1nt4
92215	51349	52832	52833	52834	52835	52839	1nw2
92316	48724	50198	50249	50282	101765	101766	1ny4
92317	51349	52171	52172	52173	102230	102231	1ny5
92318	51349	52539	52540	81269	102389	102390	1ny5
92335	46456	47472	47473	47502	101179	101180	1nya
92377	51349	52373	52374	52375	102257	102258	1nzj

92382	46456	48370	48452	48453	101417	101418	1nzn
92473	48724	49898	49899	49925	101636	101637	1o4y
92484	51349	53270	53271	53272	102539	102540	1o57
92499	51349	51734	51735	51751	51788	102150	1o5i
92504	51349	51350	51569	51570	51574	102090	1o5k
92509	51349	53270	53271	53272	53293	102538	1o5o
92560	51349	53382	53383	53417	102603	102604	1o69
92626	51349	53447	53448	64131	64132	64133	1o7q
92708	48724	48725	48726	48727	88534	101504	1oaq
92776	53931	64267	64268	64269	102952	102953	1ocs
92782	51349	52539	52540	52584	102356	102357	1odf
92783	46456	48263	48264	48265	101373	101374	1odo
92826	46456	46688	46689	46739	100996	100997	1ofc
92893	51349	102545	102546	102547	102548	102549	1ogd
93029	56835	56836	56854	56855	103424	103425	1ohu
93035	51349	53382	53383	53417	53424	53425	1ohw
93164	51349	51350	51569	51570	102088	102089	1ojx
93248	56835	103505	103506	103507	103508	103509	1okc
93313	48724	48725	48726	49159	101519	101520	1oll
93330	48724	49898	49899	49978	49991	101655	1olr
93341	48724	48725	48726	49159	101515	101516	1olz
93349	46456	47472	47473	47502	47533	47534	1omr
93383	46456	47472	47565	47566	101190	101191	1ooh
93447	46456	46457	46458	46463	100980	100981	1or4
93460	51349	51734	51735	51751	102138	102139	1orr
93496	46456	48507	48508	48509	101433	101434	1osh
93507	53931	74651	48403	48404	102879	102880	1ot8
93521	46456	47239	47240	47253	101136	101137	1otk
93628	46456	47472	47565	47566	101188	101189	1ow4
93716	51349	52539	52540	52686	89681	89682	1oxx
93775	46456	48370	48371	101410	101411	101412	1oyz
93845	48724	50155	50156	50157	50168	74930	1ozl
93866	53931	55728	55729	55730	103175	103176	1p0h
93897	48724	50155	50156	50157	82083	82084	1p1d
93899	53931	54861	54928	54929	102983	102984	1p1t
94071	51349	52506	52507	52508	102301	102302	1p3y
94089	51349	53648	53649	53653	102649	102650	1p49
94100	51349	51350	51395	51396	63898	63899	1p4c
94142	51349	52171	52317	52325	89603	89604	1p5f
94185	51349	53926	53927	89800	89801	89802	1p6o
94188	53931	54861	55008	55009	75441	75442	1p6t
94195	51349	52539	52540	52541	52552	102340	1p6x
94216	56992	57666	57667	57668	103597	103598	1p7a
94279	46456	46688	46689	46690	46691	46692	1p7i
94338	56572	56633	56634	56635	56642	56643	1p80
94595	48724	51125	51126	51127	51128	75024	1pe9
94661	51349	52373	52374	52375	52384	52386	1pfv
94758	51349	53473	53474	53542	102629	102630	1pj
94761	51349	52095	52096	52103	52108	63954	1pj
94767	51349	53789	53790	53791	102682	102683	1pj
94794	51349	53334	53335	102566	102567	102568	1pj
94832	48724	51268	51283	51284	89425	89426	1pk

94901	51349	53382	53383	69565	102596	102597	1pmm
94919	51349	52832	52833	52901	52911	52912	1pn0
94930	53931	54636	54637	82636	102907	102908	1pn2
94931	53931	54636	54637	82636	102907	102908	1pn2
94963	46456	48263	48264	48265	101375	101376	1po5
94986	56835	56836	56854	56855	56856	103423	1pq1
95004	46456	48507	48508	48509	89149	89150	1pq9
95076	51349	51350	51395	51396	102042	102043	1ps9
95131	46456	46688	46689	46690	100994	100995	1puf
95132	46456	46688	46689	46690	46711	46712	1puf
95133	53931	55810	55811	55812	55813	55814	1pun
95153	56835	103472	103473	103477	103478	103479	1pv7
95162	53931	55873	55874	55879	103226	103227	1pvg
95198	56835	103472	103473	103474	103475	103476	1pw4
95211	48724	50352	50353	50354	101778	101779	1pwa
95212	53931	56435	56436	56437	56461	56462	1pwb
95334	51349	51350	51430	51431	102054	102055	1pyf
95370	51349	52128	52129	52130	102528	102529	1pyo
95390	51349	51350	51430	51431	102056	102057	1pz1
95470	51349	53447	53448	53452	53453	53454	1pzt
95574	51349	53162	53167	53168	102500	102501	1q1g
95600	51349	51904	51905	51943	102185	102186	1q1r
95601	51349	51904	51905	51943	102185	102186	1q1r
95608	48724	50352	50353	50354	101776	101777	1q1u
95655	53931	55728	55729	55730	103169	103170	1q2y
95657	53931	55810	55811	55812	103205	103206	1q33
95700	48724	50155	50156	50157	101733	101734	1q3o
95771	53931	54402	54427	54431	89847	102808	1q40
95776	53931	54402	54427	54431	89849	102809	1q42
95779	51349	52539	52540	52575	102352	102353	1q44
95780	51349	51350	51395	51396	63896	102041	1q45
95828	53931	54636	54637	89902	102914	102915	1q4u
95846	51349	52095	52096	52103	102208	102209	1q52
95881	56835	56836	56854	56855	103426	103427	1q59
95891	46456	48263	48264	48265	101369	101370	1q5d
95901	46456	48556	48557	48558	101444	101445	1q5n
95904	53931	56234	56235	56251	56255	103314	1q5q
95911	53931	56234	56235	56251	56252	103313	1q5q
95975	53931	54533	54534	54535	102866	102867	1q6h
95986	51349	51350	51366	51375	75050	75051	1q6o
96000	53931	54636	54637	82636	102905	102906	1q6w
96203	51349	53589	53590	53591	102633	102634	1q8f
96208	51349	53066	53098	53118	53125	102482	1q8i
96214	53931	54861	55008	55009	55012	55013	1q8l
96234	53931	56111	56112	88854	56148	56149	1q8y
96258	46456	47112	47113	47134	101107	101108	1q9c
96346	46456	47472	47473	47502	47512	63541	1qv0
96446	51349	52171	52317	52325	102253	102254	1qvw
96467	51349	51350	51445	51487	102075	102076	1qw9
96471	48724	50813	50814	50815	101861	101862	1qwd
96478	51349	53447	53448	68901	53456	102608	1qwj
96581	51349	51734	51735	51751	102140	102141	1qyc

96611	48724	48725	48726	49159	49166	49167	1qz1
96621	51349	53382	53383	53402	102601	102602	1qz9
96643	48724	50198	50249	50263	101761	101762	1qzg
96651	51349	52539	52540	81269	102393	102394	1qzm
96734	53931	56111	56112	88854	103300	103301	1r0p
96736	56992	100894	100895	57468	57469	57470	1r0r
96754	51349	52539	52540	52686	102378	102379	1r0w
96816	56992	57015	57095	57116	103544	103545	1r1g
96847	51349	52832	52833	52834	52835	102430	1r26
96874	51349	52539	52540	52592	82399	82400	1r2q
96895	51349	51350	102114	102115	102116	102117	1r30
96963	51349	51350	51726	51727	51728	51729	1r3s
97080	53931	55728	55729	55730	103173	103174	1r57
97104	46456	47472	47565	47566	101192	101193	1r5r
97134	51349	51350	51713	51714	51715	51716	1r5y
97138	51349	52008	102198	102199	102200	102201	1r61
97148	51349	51734	51735	51751	51755	102133	1r6d
97151	48724	50155	50156	50157	89311	89312	1r6j
97161	51349	52373	52374	52375	52378	102256	1r6t
97205	51349	52539	52540	81269	64038	64039	1r7r
97247	51349	52539	52540	52592	52614	52615	1r8s
97281	56835	81339	81338	56895	103470	103471	1rc2
97314	53931	56111	56112	88854	56116	56119	1rdq
97455	48724	50155	50156	50157	101735	101736	1rgw
97465	56835	81407	103456	103457	103458	103459	1rh5
97469	48724	48725	48726	48727	101508	101509	1rhf
97470	48724	48725	48726	49159	101517	101518	1rhf
97517	53931	55680	55681	55682	103155	103156	1riq
97581	53931	54116	54117	54118	102732	102733	1rjt
97603	53931	54861	54928	54929	89938	89939	1rk8
97615	56835	81407	103464	103465	103466	103467	1rkl
97621	51349	56783	56784	82388	102315	102316	1rkq
97631	51349	51734	51735	51751	102136	102137	1rkx
97744	46456	48575	48576	48577	48578	101453	1rqj
97820	46456	48575	48576	48577	48578	101454	1rtr
98065	51349	53162	53167	53168	53176	53177	1rxy
98132	51349	52539	52540	52584	102358	102359	1rz3
98236	48724	50155	50156	50157	89315	101716	1rzx
98263	51349	53382	53383	53417	53438	53439	1s0a
98329	53931	55873	55874	55879	103228	103229	1s14
98344	48724	50933	101887	101888	101889	101890	1s1d
98377	51349	52171	52309	52310	102244	102245	1s2d
98573	53931	54636	54637	54638	102901	102902	1s5u
98594	46456	47472	47473	47502	101184	101185	1s6c
98634	56835	103480	103481	103482	103483	103484	1s7b
98777	46456	48661	101494	101495	101496	101497	1sa0
98790	53931	54861	55008	55009	55017	102998	1sb6
98814	56992	57923	57924	57925	69974	69975	1se0
98821	53931	54235	54236	54237	102782	102783	1se9
98892	48724	51268	51283	51284	51285	82213	1six
98900	53931	55810	55811	55812	103209	103210	1sjy
98958	51349	51734	51735	51751	102155	102156	1spx

98987	51349	52832	52833	52901	102455	102456	1st9
99028	51349	52832	52833	52834	52835	102431	1syr
99066	53931	54235	54236	54237	102786	102787	1t0y
99075	53931	55944	55961	64388	64389	64390	1t27
99125	46456	101477	101478	101479	101480	101481	1t5j
99161	53931	103364	103365	103366	103367	103368	1uc2
99229	51349	52539	52540	52592	82408	102368	1udx
99243	48724	50198	50249	50263	50264	101760	1ue1
99259	51349	64004	64005	64006	64007	64009	1ueh
99265	53931	54235	54236	54237	102777	102778	1uel
99270	48724	50155	50156	50157	101719	101720	1uep
99271	48724	50155	50156	50157	101719	101720	1ueq
99281	48724	50155	50156	50157	101719	101720	1uew
99288	48724	50155	50156	50157	101721	101722	1uf1
99326	51349	52539	52540	52541	75187	102344	1uf9
99358	53931	54861	54928	54929	102985	102986	1ufw
99359	48724	50155	50156	50157	101721	101722	1ufx
99403	51349	51350	51445	51487	102077	102078	1uhv
99429	51349	53334	53335	69557	69558	102586	1uir
99433	48724	50155	50156	50157	101725	101726	1uit
99448	51349	52095	52096	52103	52106	102207	1uiy
99452	51349	52539	52540	52584	102360	102361	1uj2
99454	48724	50155	50156	50157	101727	101728	1ujd
99462	51349	51350	51366	51381	51388	102038	1ujp
99470	48724	50155	50156	50157	101719	101720	1ujv
99549	48724	49898	49899	49932	101639	101640	1ule
99578	48724	50155	50156	50157	101729	101730	1um1
99580	51349	52539	52540	81269	102391	102392	1um8
99607	46456	47239	47240	47241	47250	101134	1umn
99639	48724	49898	49899	49925	101634	101635	1umz
99686	51349	53066	53098	102492	102493	102494	1uoc
99690	53931	74651	48403	48404	102881	102882	1uoh
99778	53931	56370	56371	56372	56389	56390	1uq5
99794	51349	53755	53756	82540	82541	82542	1uqt
99804	51349	51350	51445	51487	51488	102064	1ur1
99806	51349	51350	51430	51431	89459	89460	1ur3
99812	56992	57849	57850	57851	64579	64580	1ur6
99850	51349	51350	51430	51431	51436	51437	1us0
99881	48724	50938	50939	50940	63823	63824	1usr
99999	53931	56111	56112	88854	90036	90037	1uu3
100015	51349	51350	51445	51487	102068	102069	1uuq
100123	53931	56111	56112	88854	103290	103291	1uwh
100220	51349	53719	53720	53721	102675	102676	1uzb
100247	51349	53612	53613	53614	75295	102640	1v19
100275	53931	54235	54236	54237	102784	102785	1v2y
100287	48724	50938	50939	50940	101891	101892	1v3e
100296	46456	48575	48576	48577	101455	101456	1v4e
100321	56835	81443	81442	81441	81433	81432	1v54
100325	56835	81407	81406	81405	81404	81403	1v54
100383	48724	49898	49899	49900	49904	49912	1v6i
100424	51349	53747	53748	53749	53750	102677	1v6s
100446	51349	53685	53686	53687	64172	102667	1v7c

100458	46456	47265	47266	47286	101140	101141	1v7m
100495	53931	54235	54285	54286	102794	102795	1v8c
100519	51349	88722	88723	89619	102270	102271	1v8p
100557	51349	51350	51366	51381	51385	102037	1vc4
100561	46456	48556	48557	48558	48561	101443	1vdk
100569	56572	56654	56655	56656	56665	103398	1vdw
100637	51349	53447	53448	68901	64143	102607	1vh3
100640	48724	51125	101960	101961	101962	101963	1vh4
100642	53931	54636	54637	89902	102910	102911	1vh5
100661	51349	51350	51569	51570	102092	102093	1vhc
100693	51349	51350	51395	51396	102044	102045	1vhn
100696	51349	52171	52317	52325	89606	89607	1vhq
100698	53931	55728	55729	55730	103171	103172	1vhhs
100700	51349	52539	52540	52541	75187	82394	1vhvt
100706	51349	53162	53167	53168	53169	102499	1vhvw
100718	53931	55810	55811	55812	103203	103204	1vhz
100736	51349	52171	52313	52314	52315	102246	1vi6
100750	51349	53612	53613	82515	102638	102639	1vi9
100754	51349	52539	52540	52566	52567	102345	1via
100762	53931	100877	55120	75459	75460	103018	1vio
100771	53931	55810	55811	55812	103201	103202	1viu
100784	51349	51350	51395	51396	102046	102047	1viz
100801	46456	109603	109604	101340	101341	101342	1vj7
100827	51349	53382	53383	53402	89757	102598	1vjo
100832	51349	56783	56784	102317	102318	102319	1vjr
100835	53931	102885	102886	102887	102888	102889	1vju
100837	46456	47239	47240	47241	101132	101133	1vjjx
100838	51349	51350	51445	51487	102066	102067	1vjjz
100839	51349	53066	53098	53118	102483	102484	1vk0
100850	51349	53612	53613	53614	102641	102642	1vk4
103833	46456	47094	47095	47096	109762	109763	1j3d
103874	48724	50728	50729	50730	110264	110265	1nty
103971	56572	56795	56796	69892	111308	111309	1oj7
104019	48724	50493	50494	50514	50570	110238	1op0
104022	53931	54861	55008	55009	55010	110979	1osd
104060	51349	51350	51569	51570	69394	69395	1p1x
104062	46456	47575	47576	47577	101196	101197	1p2x
104067	51349	53685	53686	53687	102668	110721	1p5j
104074	51349	52171	52172	52173	52174	102225	1p6q
104084	51349	52787	52788	52789	52790	110595	1p8a
104121	48724	48725	48726	49159	89185	89186	1pd6
104137	51349	52171	52172	52173	52188	52189	1pey
104333	56992	57015	57095	57116	111396	111397	1pvz
104381	56992	57015	57095	57116	90137	90138	1px9
104393	46456	48507	48508	48509	109605	109987	1pzl
104397	48724	48725	49329	49330	49331	110065	1pzs
104475	53931	54533	54534	54535	82619	82620	1q1c
104476	46456	46457	46458	46463	100978	109625	1q1f
104525	51349	52539	52540	52541	52548	110525	1q3t
104526	48724	50493	50494	50514	110241	110242	1q3x
104537	53931	56111	56112	88854	69823	69824	1q5k
104555	53931	55752	55753	55762	55763	111104	1q8g

104620	51349	53253	53254	53258	53263	110657	1qwo
104812	51349	53926	53927	53928	75327	110764	1r5t
104820	51349	52539	52540	81269	82421	82422	1r6b
104839	51349	51350	51445	51487	51488	69386	1r85
104851	48724	50352	50386	50387	110213	110214	1r8n
104852	48724	50352	50386	50387	110215	110216	1r8o
105024	53931	54402	54403	54407	110819	110820	1roa
105027	46456	110018	110019	110020	110021	110022	1rp4
105058	51349	51350	51569	89494	110366	110367	1rqb
105064	51349	52373	52374	52375	52384	110490	1rqg
105081	56572	56795	56796	69892	111310	111311	1rrm
105095	46456	47575	47576	47577	47580	109828	1rt8
105140	51349	53755	53756	110734	110735	110736	1rzu
105250	53931	55728	55729	55730	111098	111099	1s3z
105310	46456	47472	47473	47502	109821	109822	1s6i
105317	53931	74651	48403	48404	110891	110892	1s70
105374	51349	52171	52172	52173	110464	110465	1s8n
105377	48724	89359	89360	89361	101849	101850	1s98
105379	48724	49451	49482	49483	110096	110097	1s9a
105410	51349	51734	51735	51751	110407	110408	1sb8
105412	51349	100949	100950	110520	110523	110524	1sbq
105416	51349	52128	52129	52130	52133	52134	1sc3
105448	48724	50198	50249	50263	50264	110194	1se8
105455	51349	53596	53597	53598	53610	102636	1sej
105465	51349	52832	52833	52834	110604	110605	1sen
105482	51349	53382	53383	53417	53424	110686	1sff
105535	51349	51350	51621	51638	110375	110376	1sgj
105541	51349	52539	52540	52686	110560	110561	1sgw
105543	46456	47575	47576	47577	89056	89057	1sh5
105549	53931	54636	54637	89902	110900	110901	1sh8
105764	48724	48725	48726	48727	101506	101507	1smo
105772	48724	50198	50249	50282	110198	110199	1smx
105778	56572	64483	64484	64485	64488	75609	1smy
105779	56572	64483	64484	64490	64493	75610	1smy
105833	51349	51734	51735	51751	110413	110414	1sny
105858	51349	100949	100950	110520	110521	110522	1sou
105881	48724	48725	48726	48727	110042	110043	1sq2
105882	51349	52539	52540	52584	52587	52588	1sq5
105889	48724	50964	50978	50979	110287	110288	1sq9
105961	51349	51350	51569	89494	110364	110365	1sr9
105966	56992	57666	57667	57668	111434	111435	1srk
106048	51349	52539	52540	52592	89667	110534	1svi
106051	51349	52539	52540	52592	52623	52625	1svs
106054	51349	53382	53383	53384	64123	110676	1svv
106082	51349	52539	52540	81269	110566	110567	1sxj
106090	51349	52539	52540	81269	110574	110575	1sxj
106101	53931	55845	55846	55847	111139	111140	1sxr
106126	46456	47239	47240	47253	47257	109786	1syy
106164	51349	52095	52096	52103	82331	82332	1szo
106208	51349	52539	52540	52541	110527	110528	1t0h
106238	53931	54533	54534	54535	75388	110869	1t11
106354	51349	53382	53383	53402	110684	110685	1t3i

106357	51349	52820	52821	52822	110598	110599	1t3k
106397	53931	56111	56112	88854	103296	103297	1t46
106420	53931	56111	56112	88854	111196	111197	1t4h
106459	51349	100949	100950	110513	110518	110519	1t5o
106543	51349	52767	52768	52773	110587	110588	1t64
106564	48724	50629	50630	50646	110247	110248	1t6e
106635	46456	48507	48508	48509	63621	109986	1t7r
106639	53931	54636	54637	89902	110898	110899	1t82
106679	51349	53162	53167	53168	110645	110646	1t8s
106685	51349	52539	52540	52575	110532	110533	1t8t
106729	51349	56783	56784	110509	110510	110511	1ta0
106731	51349	51350	51445	51534	89478	89479	1ta3
106785	53931	56435	56436	56437	111260	111261	1tdq
106792	51349	56783	56784	75173	110504	110505	1te2
106794	46456	48370	48371	101410	109963	109964	1te4
106818	51349	52539	52540	52575	110530	110531	1tex
106854	53931	54000	54001	110773	110774	110775	1tff
107010	53931	55728	55729	55730	111100	111101	1tiq
107014	46456	47472	47473	47502	109823	109824	1tiz
107054	46456	48556	48557	48558	48564	48566	1tjv
107161	51349	51350	51569	51570	110358	110359	1to3
107201	51349	52539	52540	52592	110546	110547	1tq4
107228	51349	51350	51366	51372	51373	110343	1tqj
107238	46456	48263	48264	48265	109958	109959	1tqn
107309	51349	52832	52833	52834	110606	110607	1ttz
107320	46456	46457	46458	46463	109628	109629	1tu9
107323	51349	52539	52540	81269	110576	110577	1tue
107423	48724	50728	50729	50730	110270	110271	1txd
107424	48724	51315	51316	63873	63874	110332	1txj
107476	51349	53447	53448	68901	110689	110690	1tzf
107530	46456	47112	47113	47114	47115	47116	1tzy
107531	46456	47112	47113	47114	47119	47120	1tzy
107532	46456	47112	47113	47114	47122	47123	1tzy
107543	51349	53382	53383	53384	110679	110680	1u08
107546	51349	52539	52540	81269	110564	110565	1u0j
107551	48724	50198	50249	50282	110200	110201	1u0l
107566	51349	52171	52172	52173	52174	52177	1u0s
107567	56572	111330	111331	111332	111333	111335	1u0t
107656	53931	56111	56112	88854	111200	111201	1u46
107714	53931	54533	54534	54535	110870	110871	1u79
107723	56835	111351	111352	111353	111354	111355	1u7g
107783	48724	50198	50249	50282	110196	110197	1ueb
107784	48724	50198	50249	50282	110196	110197	1ueb
107823	46456	46688	46689	46739	109649	109650	1ug2
107828	48724	48725	48726	49159	49206	49207	1ugn
107853	46456	46688	46689	46690	109647	109648	1uhs
107900	46456	47575	47576	47577	109830	109831	1ujo
107968	48724	50728	50729	50730	89355	89356	1unq
107998	53931	54861	54975	54976	110974	110975	1urr
108073	51349	51350	51445	51521	51531	51532	1uws
108275	56572	56800	56801	56802	111314	111315	1v25
108281	51349	53382	53383	53384	110677	110678	1v2d

108379	48724	50728	50729	50730	110256	110257	1v5m
108381	53931	54235	54236	54237	110796	110797	1v5o
108382	48724	50728	50729	50730	110258	110259	1v5p
108383	48724	50155	50156	50157	82083	110177	1v5q
108385	53931	54235	54236	54237	110798	110799	1v5t
108386	48724	50728	50729	50730	110260	110261	1v5u
108389	48724	50728	50729	50730	110262	110263	1v61
108390	48724	50155	50156	50157	110180	110181	1v62
108392	46456	47094	47095	47096	68982	109764	1v64
108394	48724	50155	50156	50157	110182	110183	1v6b
108407	53931	56435	56436	56437	88867	103347	1v7p
108415	51349	53447	53448	53467	110687	110688	1v82
108421	53931	54235	54236	54237	110800	110801	1v86
108422	56992	57849	57850	57851	111457	111458	1v87
108423	48724	50728	50729	50730	110266	110267	1v88
108424	48724	50728	50729	50730	110268	110269	1v89
108448	53931	100877	55120	75459	103019	103020	1v9f
108449	53931	100877	55120	75459	111010	111011	1v9k
108451	48724	50890	50891	50892	50901	50902	1v9t
108466	48724	50155	50156	50157	110184	110185	1vae
108474	48724	50155	50156	50157	110186	110187	1vb7
108475	51349	53334	53335	53354	68927	110668	1vbf
108509	51349	52539	52540	52652	110551	110553	1vco
108554	53931	55769	103196	103197	111123	111124	1vet
108631	53931	54235	54285	54286	54287	110806	1vjk
108633	53931	56111	56112	88854	56144	56145	1vjy
108643	53931	110856	110857	110858	110859	110860	1vkb
108669	53931	55752	55753	55762	111110	111111	1vkk
108704	51349	51734	51735	51751	110409	110410	1vl0
108720	51349	53334	53335	110671	110672	110673	1vl5
108732	48724	50474	50475	50476	110234	110235	1vl7
108733	51349	51734	51735	51751	110411	110412	1vl8
108816	46456	47239	47240	47241	63524	109783	1vlg
108832	56572	56795	56796	69892	111312	111313	1vlj
108836	51349	53334	53335	110671	110674	110675	1vlm
108864	51349	53719	53720	53721	89781	110731	1vlu
108884	51349	53612	53613	53614	53615	110706	1vm7
108897	53931	56218	56219	56220	111211	111212	1vyb
108902	48724	50813	50814	50847	110276	110277	1vyf
108906	51349	51350	51395	51396	63900	63901	1vyr
109027	51349	51350	51351	51352	51353	110342	1w0m
109040	48724	50938	50939	50940	50950	50951	1w0p
109125	53931	56103	56104	111188	111189	111190	1w2f
109130	51349	100949	100950	110513	110516	110517	1w2w
109149	46456	48370	48452	48453	109973	109974	1w3b
109152	51349	51350	51569	51570	110360	110361	1w3i
109171	51349	51904	51905	51943	110440	110441	1w4x
109172	51349	51904	51905	51943	110440	110441	1w4x
109216	46456	47239	47240	47253	47257	47260	1w68
109232	56992	57849	57850	57851	111459	111460	1wd2
109253	51349	52095	52096	52103	110450	110451	1wdk
109286	53931	56218	56219	56220	111215	111216	1wdx

109330	48724	50128	50129	50130	50131	110172	1we3
109393	51349	53926	53927	89800	110765	110766	1wkq
109395	48724	50629	50630	50646	50649	110246	1wkr
109406	56992	57015	57095	57116	111398	111399	1wm7
109409	51349	52742	52743	52744	110578	110579	1wmd
109414	51349	52539	52540	52592	110537	110539	1wms
109422	53931	56435	56436	56437	111262	111263	1wmz
109446	51349	52767	52768	52769	110585	110586	1woh
109494	48724	50198	50249	50282	50296	110195	1x6o
109527	51349	52498	52499	100948	110502	110503	1x9g
111575	48724	50198	50249	50282	74950	74951	1kl9
111639	51349	53473	53474	117714	117715	117716	1pv1
111643	48724	51125	51126	51127	117306	117307	1pxz
111694	53931	55485	55486	55519	118046	118047	1r55
111710	51349	52742	52743	52744	117569	117570	1r6v
111772	51349	51350	51366	51381	51388	117361	1rd5
111789	46456	48263	48264	48265	48266	48267	1re9
111796	48724	50474	50475	50476	117232	117233	1rfe
111801	48724	50352	50353	50354	50357	50359	1rg8
111835	56992	57867	57868	57869	57870	57876	1rju
111854	51349	52539	52540	52541	52554	117527	1rkb
111859	53931	56370	56371	56372	103335	103336	1rl0
111860	51349	56783	56784	82388	117503	117504	1rlm
111924	48724	50493	50494	50514	50561	50562	1rrk
111959	51349	52798	52799	52800	102418	117578	1rxd
112008	46456	48263	48264	48265	116991	116992	1s1f
112040	51349	53066	53098	53118	53125	117647	1s5j
112044	46456	46688	46689	46690	116780	116781	1s7e
112049	53931	56111	56112	88854	118137	118138	1s9j
112068	51349	52506	52507	52508	117500	117501	1sbz
112077	51349	51350	51569	51570	51586	117378	1sfl
112091	48724	50493	50494	50514	110239	110240	1si5
112106	48724	50938	50939	50940	117274	117275	1so7
112126	51349	52539	52540	81269	89688	89689	1svm
112213	56992	57015	57095	57096	57097	118240	1t0z
112259	46456	48556	48557	48572	117028	117029	1t6j
112358	48724	50198	50249	50282	110200	117197	1t9h
112359	51349	52539	52540	52592	110542	117534	1t9h
112364	48724	50474	50475	50476	50479	117226	1t9m
112429	51349	52832	52833	52834	52835	117590	1ti3
112440	46456	48370	48452	48453	117007	117008	1tjc
112461	46456	47239	47240	47241	47250	101135	1tjo
112614	51349	51350	51366	51372	51373	117359	1tqx
112683	48724	49784	49785	69210	117104	117105	1tvg
112690	48724	50813	50814	50847	89368	89369	1tw4
112725	56572	64483	64484	64490	64486	64487	1twf
112726	56572	64483	64484	64485	64491	64492	1twf
112731	46456	63561	63562	55294	55295	64318	1twf
112736	53931	55247	55257	64311	64312	64313	1twf
112779	53931	102885	102886	102887	110896	110897	1txn
112781	53931	81607	81606	81605	118149	118150	1txo
112850	51349	53612	53613	53614	117720	117721	1tyy

112852	51349	53685	53686	53687	53694	110722	1tyz
112953	56835	81322	81321	81320	56876	56877	1u19
113037	51349	51350	51621	51638	110375	117388	1u5h
113050	53931	56111	56112	88854	118127	118128	1u5r
113069	53931	55728	55729	55730	118070	118071	1u6m
113093	56572	118202	118203	118204	118205	118206	1u7l
113233	46456	47071	47072	117033	117034	117035	1u97
113234	51349	52171	52317	52325	117481	117482	1u9c
113283	53931	54861	54975	54976	54977	117977	1ulr
113392	48724	50728	50729	50730	117244	117245	1upq
113394	48724	49898	49899	49925	117134	117135	1ups
113402	51349	51350	51445	51487	89469	117367	1ur4
113414	46456	46457	46458	46463	109626	109627	1urv
113422	53931	55680	55681	55682	118058	118059	1usy
113490	48724	50198	50249	50263	117191	117192	1v1q
113496	53931	110856	110857	110858	117851	117852	1v30
113497	51349	53253	53254	53255	117669	117670	1v37
113544	51349	52742	52743	52744	117571	117572	1v6c
113547	53931	54235	54236	54237	102786	117798	1v6e
113548	56992	57301	57302	57303	57341	57342	1v6p
113561	56992	57015	57059	57072	118233	118234	1v7f
113581	53931	55810	55811	55812	64365	118083	1v8y
113604	51349	100949	100950	110513	117517	117518	1vb5
113637	53931	54861	54913	54914	54915	102972	1vfj
113663	53931	55728	55729	55730	118072	118073	1vkc
113676	46456	101385	101386	116993	116994	116995	1vmg
113935	51349	53382	53383	53384	117691	117692	1vp4
113948	51349	53447	53448	68901	64140	117699	1vpa
113966	51349	52539	52540	52686	117548	117549	1vpl
113967	53931	54636	54637	54638	117883	117884	1vpm
114004	51349	53926	53927	89800	117756	117757	1vq2
114060	51349	53658	53659	53660	53661	117725	1w0d
114064	51349	53066	53098	53118	117648	117649	1w0h
114076	48724	50728	50729	50730	117246	117247	1w1h
114080	51349	52539	52540	52686	52693	117544	1w1w
114088	51349	53382	53383	53417	53426	117697	1w23
114090	51349	52171	52172	52173	117472	117473	1w25
114091	51349	52171	52172	52173	117472	117473	1w25
114096	46456	48556	48557	48572	117028	117030	1w27
114120	51349	51350	51445	51487	51514	51517	1w32
114197	51349	53447	53448	68901	117700	117701	1w55
114252	51349	52539	52540	81269	117556	117557	1w5s
114275	48724	49898	49899	49932	100925	101638	1w6n
114288	51349	51734	51735	51751	117421	117422	1w6u
114317	46456	47873	47874	47875	116947	116948	1w7b
114368	51349	88722	88723	89619	117492	117493	1w8i
114376	48724	50938	50939	50940	50946	50947	1w8o
114408	48724	50474	50475	50476	117230	117231	1w9a
114412	51349	51350	51445	51534	51548	117368	1w9p
114432	46456	48370	48371	48372	48383	48384	1wa5
114433	46456	48370	48371	48372	116998	116999	1wa5
114439	51349	52539	52540	52592	117537	117538	1wb1

114524	51349	53270	53271	53272	117673	117674	1wd5
114526	51349	69617	69618	69619	117738	117739	1wd7
114534	51349	53789	53790	53791	102684	117735	1wde
114541	53931	74651	48403	48404	117879	117880	1wdy
114546	53931	54235	54236	54237	117799	117801	1we6
114561	56992	57849	57850	57851	118294	118295	1weo
114568	53931	54861	54928	54929	117951	117952	1wex
114569	53931	54861	54928	54929	117953	117954	1wey
114571	53931	54861	54928	54929	117957	117958	1wf0
114573	53931	54861	54928	54929	117961	117962	1wf2
114574	51349	52539	52540	52592	52637	117533	1wf3
114589	48724	50198	50249	50282	117198	117199	1wfq
114599	53931	54861	54928	54929	117963	117964	1wg1
114602	53931	54861	54928	54929	117955	117956	1wg5
114603	48724	50155	50156	50157	117178	117179	1wg6
114604	48724	50728	50729	50730	117248	117249	1wg7
114610	53931	54235	54236	54237	117802	117803	1wgd
114611	46456	47094	47095	47096	68982	109764	1wgf
114613	53931	54235	54236	54237	117806	117807	1wgh
114620	48724	50728	50729	50730	117250	117251	1wgq
114626	46456	46688	46689	46739	116782	116783	1wgx
114629	48724	50155	50156	50157	101723	101724	1wh1
114631	53931	54235	54236	54237	117808	117809	1wh3
114635	46456	46688	46689	46690	116774	116775	1wh7
114638	48724	50155	50156	50157	101731	101732	1wha
114652	53931	54861	54928	54929	117967	117968	1whv
114653	53931	54861	54928	54929	117969	117970	1whw
114654	53931	54861	54928	54929	117969	117970	1whx
114655	53931	54861	54928	54929	117971	117972	1why
114658	48724	50728	50729	50730	117252	117253	1wi1
114661	48724	50198	50249	50282	117200	117201	1wi5
114662	53931	54861	54928	54929	117973	117974	1wi8
114664	53931	54235	54236	54237	117810	117811	1wia
114669	48724	50155	50156	50157	117184	117185	1wif
114675	51349	52832	52833	52834	117591	117592	1wik
114677	56992	57849	57850	57851	118296	118297	1wim
114699	48724	50198	50249	50263	117193	117194	1wjj
114700	51349	52832	52833	52834	117593	117594	1wjk
114703	53931	54235	54236	54237	117812	117813	1wjn
114704	46456	47575	47576	47577	47580	47581	1wjo
114705	56992	57666	57667	57668	118267	118268	1wjp
114706	56992	57666	57667	57668	118267	118268	1wjp
114707	56992	57666	57667	57668	118267	118268	1wjp
114712	53931	54235	54236	54237	117814	117815	1wju
114719	53931	56435	56436	56437	118166	118167	1wk1
114724	51349	100949	100950	110520	117519	117520	1wkc
114734	51349	53066	53098	53118	117652	117653	1wlj
114736	53931	54235	54236	54237	117816	117817	1wm3
114751	51349	53719	53720	53721	117733	117734	1wnd
114830	51349	53658	53659	53660	53661	117724	1wpw
114836	51349	56783	56784	82388	82389	117502	1wr8
114838	53931	54235	54292	54293	54294	54301	1wri

114915	51349	56783	56784	102317	117507	117508	1wvi
114966	48724	50813	50814	50815	50845	50846	1x8q
114983	46456	46457	46458	46463	116752	116753	1x9f
114984	46456	46457	46458	46463	116754	116755	1x9f
114985	46456	46457	46458	46463	116756	116757	1x9f
114999	51349	53066	53098	53118	53123	53124	1x9m
115041	48724	48725	48726	49159	117041	117042	1xau
115077	53931	56111	56112	88854	118131	118132	1xbb
115145	53931	54000	54001	54050	54051	54052	1xd3
115160	51349	51904	51905	51943	51959	117441	1xdi
115219	53931	55728	55729	55730	118066	118067	1xeb
115229	48724	48725	48726	48727	117038	117039	1xed
115235	51349	52539	52540	52686	52693	117545	1xew
115264	51349	52767	52768	52769	117573	117574	1xfk
115277	51349	51734	51735	51751	117411	117412	1xg5
115286	51349	51734	51735	51751	69407	69408	1xgk
115291	51349	53447	53448	117702	117703	117704	1xhb
115292	51349	51904	51905	51943	117442	117443	1xhc
115293	51349	51904	51905	51943	117442	117443	1xhc
115304	53931	110856	110857	110858	117853	117854	1xhs
115355	51349	53382	53383	53384	117693	117694	1xi9
115367	48724	48725	48726	49159	69162	110051	1xiw
115368	48724	48725	48726	49159	117043	117044	1xiw
115387	51349	52539	52540	52652	89673	117539	1xjc
115396	48724	50198	50249	50263	101761	117190	1xjv
115397	48724	50198	50249	50263	101761	117190	1xjv
115408	48724	50813	50814	50815	117265	117266	1xki
115409	53931	56111	56112	88854	82795	82796	1xkk
115561	53931	55728	55729	55730	118064	118065	1xmt
115580	46456	48370	48452	48453	117009	117010	1xnf
115680	46456	47472	47473	47502	47541	47542	1xo5
115768	53931	55247	55257	64311	118020	118021	1xpp
115879	51349	52798	52799	52800	117579	117580	1xri
115892	48724	51268	51283	51284	117335	117336	1xs1
116017	53931	64267	64268	64269	117932	117933	1xte
116031	51349	53334	53335	117685	117686	117687	1xtp
116052	51349	51734	51735	51751	117423	117424	1xu9
116088	51349	56783	56784	82388	117505	117506	1xvi
116091	46456	48507	48508	48509	117014	117016	1xvp
116094	51349	52832	52833	52901	102452	117600	1xvq
116133	53931	56111	56112	88854	118133	118134	1xws
116143	46456	109603	109604	101340	116971	116972	1xx7
116203	51349	53334	53335	110671	117683	117684	1xxl
116322	46456	47768	47819	69044	69045	116939	1y14
116323	48724	50198	50249	50282	88670	117195	1y14
116341	51349	52787	52788	52789	69504	117577	1y1l
116374	46456	47472	47473	63550	116903	116904	1y1x
116394	53931	54196	54197	54198	117789	117790	1y23
116400	56992	57015	57059	57072	118235	118236	1y29
116494	51349	52539	52540	52541	117528	117529	1y63
116563	51349	53334	53335	117688	117689	117690	1y8c
116599	51349	51734	51735	51751	117426	117427	1yb1

116609	51349	53162	53167	53168	110645	117658	1ybf
116646	53931	55153	55154	118007	118008	118009	1yem
118730	46456	47472	47473	140538	140539	140540	1pul
118773	51349	51350	51445	51487	51502	141774	1rh9
118846	51349	56783	56784	82388	142163	142164	1s2o
118878	53931	55728	55729	55730	143678	143679	1s7k
118890	53931	54636	54637	82636	102907	143168	1s9c
118930	51349	51734	51735	51751	51782	51783	1sby
118957	51349	52095	52096	52103	52108	141999	1sg4
119053	51349	53334	53335	53336	142573	142574	1sus
119136	48724	50493	50494	50514	50548	50549	1t32
119141	53931	55752	55753	55762	111105	111107	1t3y
119171	53931	56435	56436	56437	143957	143958	1t8d
119205	51349	51350	51395	51396	141761	141762	1tb3
119264	48724	50181	50182	50183	63758	141290	1th7
119305	48724	50155	50156	50157	50162	50163	1tp5
119340	53931	54235	54236	54237	142954	142955	1ttn
119347	51349	51350	51395	51396	51397	141759	1tv5
119360	51349	51350	51445	51487	51499	141773	1tvn
119463	53931	55810	55811	55812	143764	143765	1u20
119536	48724	50728	50729	50730	141403	141404	1u5d
119540	48724	50728	50729	50730	141417	141418	1u5e
119572	53931	54861	54928	54929	143322	143323	1u6f
119811	51349	51734	51735	51751	51788	141875	1uzm
119838	51349	51904	51905	51943	51959	63950	1v59
119839	51349	51904	51905	51943	51959	63950	1v59
119859	51349	53685	53686	53687	142749	142750	1v71
119860	51349	53382	53383	53384	142659	142660	1v72
119877	51349	88722	88723	89619	142112	142113	1v96
119903	48724	50155	50156	50157	141275	141276	1va8
119942	51349	53685	53686	53687	64172	142748	1vb3
119970	53931	55810	55811	55812	143758	143759	1vcf
119974	51349	51350	51395	51396	89454	141760	1vcf
119980	51349	53270	53271	53272	142558	142559	1vch
119988	51349	51350	51569	51570	69394	141830	1vcv
119991	51349	51350	51695	89508	141864	141865	1vd6
119994	51349	53270	53271	53272	142560	142561	1vdm
120007	51349	53685	53686	53687	53690	142743	1ve1
120008	51349	53789	53790	53791	117736	142780	1ve2
120010	51349	53334	53335	117688	142599	142600	1ve3
120013	51349	53685	53686	53687	53692	142747	1ve5
120018	51349	53382	53383	53417	142674	142675	1vef
120029	51349	51350	51445	51534	63910	63911	1vf8
120033	51349	51350	51445	51521	51528	141785	1vff
120362	48724	50198	50249	50282	50299	50301	1vqo
120373	51349	52079	52080	52081	52082	52083	1vqo
120375	51349	53066	53137	53138	53139	53140	1vqo
120376	51349	52079	52080	52081	52084	52085	1vqo
120378	48724	50036	50104	50105	50108	50109	1vqo
120381	48724	50036	50104	50105	50106	50107	1vqo
120385	53931	54574	54575	54576	54577	54578	1vqo
120417	51349	51350	51366	51375	51376	141746	1vqt

120427	53931	55680	55681	143642	143645	143646	1vqz
120431	48724	51181	51182	82191	82192	141601	1vr3
120548	48724	51268	51283	51284	51285	141654	1vyq
120639	53931	54000	54001	54047	54048	142855	1w4t
120643	53931	54000	54001	54047	54048	75335	1w5r
120652	53931	55680	55681	143642	143643	143644	1w66
120679	51349	53447	53448	68901	64140	142690	1w77
120779	48724	50155	50156	50157	89311	89312	1w9e
120801	48724	51181	51197	51198	141621	141622	1w9y
120802	51349	51350	51569	51570	51584	110357	1wa3
120809	46456	47239	140453	140454	140455	140456	1wa8
120810	46456	47239	140453	140454	140457	140458	1wa8
120834	51349	52539	52540	52686	52697	52699	1wb9
120845	51349	51350	51569	51570	51584	51585	1wbh
120888	51349	51350	51445	51521	141786	141787	1wcg
120965	53931	54861	54928	54929	143349	143350	1wel
120967	48724	50155	50156	50157	141277	141278	1wf8
120968	53931	54235	54236	54237	142934	142935	1wf9
120973	48724	50155	50156	50157	141271	141272	1wi4
120989	51349	53685	53686	53687	53690	142742	1wkv
121008	46456	47472	47473	140538	140541	140542	1wlm
121015	53931	54636	54637	89902	89903	102909	1wlw
121042	51349	51734	51735	51751	63935	141878	1wma
121132	51349	52832	52833	52901	102459	142371	1wp0
121276	53931	55680	55681	55682	55688	143637	1wu7
121335	46456	46625	46626	46627	46669	46670	1wve
121358	53931	54861	54928	54929	143330	143331	1wwh
121366	51349	53926	53927	89800	142840	142843	1wwr
121380	53931	55728	55729	55730	143648	143649	1wwz
121382	51349	51350	51569	51570	75085	141836	1wx0
121393	53931	54235	54236	54237	142950	142951	1wx8
121394	53931	54235	54236	54237	142952	142953	1wx9
121406	51349	52539	52540	52592	142251	142252	1wxq
121409	53931	54235	54236	54237	142932	142933	1wxv
121471	51349	53789	53790	53791	142783	142784	1wyd
121483	51349	52095	52096	52103	142000	142001	1wz8
121491	51349	56783	56784	82388	117505	142156	1wzc
121525	51349	53334	53335	117688	142601	142602	1wzn
121529	53931	54494	54495	54496	54497	143052	1wzv
121579	48724	50728	50729	50730	141405	141406	1x1f
121592	53931	54235	54236	54237	142942	142943	1x1m
121595	51349	52539	52540	52592	142283	142284	1x1r
121597	51349	51734	51735	51751	141886	141887	1x1t
121645	46456	46688	46689	46690	140147	140148	1x2m
121646	46456	46688	46689	46690	140153	140154	1x2n
121660	56992	57666	57667	57668	144133	144134	1x3c
121676	46456	46688	46689	46690	140145	140146	1x41
121678	48724	48725	48726	49159	141013	141014	1x44
121679	48724	50155	50156	50157	141282	141283	1x45
121683	53931	54861	54928	54929	143346	143347	1x4a
121686	53931	54861	54928	54929	143306	143307	1x4d
121687	53931	54861	54928	54929	143320	143321	1x4e

121688	53931	54861	54928	54929	143306	143307	1x4f
121689	53931	54861	54928	54929	143298	143299	1x4g
121690	53931	54861	54928	54929	143358	143359	1x4h
121705	46456	46688	46689	46690	140157	140158	1x58
121714	48724	50155	50156	50157	110182	141263	1x5n
121715	53931	54861	54928	54929	143356	143357	1x5o
121721	53931	54861	54928	54929	143318	143319	1x5u
121722	56992	57666	57667	57668	144149	144150	1x5w
121723	56992	57666	57667	57668	144149	144150	1x5w
121742	56992	57666	57667	57668	144137	144138	1x6f
121743	56992	57666	57667	57668	144153	144154	1x6h
121768	48724	50813	50814	50815	50835	50836	1x71
121840	53931	55297	55315	55316	55319	111033	1xbi
121850	46456	46688	46689	46739	140171	140172	1xc5
122007	48724	50474	50475	50476	141356	141357	1xhn
122022	51349	52832	52833	52901	52909	142367	1xiy
122055	46456	47472	47473	47478	47479	47487	1xk4
122057	46456	47472	47473	47478	47479	69020	1xk4
122081	53931	54000	54001	54002	142848	142849	1xkg
122094	51349	51350	51569	51570	51574	141832	1xky
122119	53931	54235	54292	54293	54294	54307	1xlq
122143	56835	81443	81442	81441	81438	81437	1xme
122211	53931	56435	56436	56437	69857	69858	1xph
122297	51349	52539	52540	52592	142275	142276	1xtq
122300	51349	53270	53271	53272	53293	142555	1xtt
122387	51349	52832	52833	52901	142381	142382	1xvw
122433	51349	51350	51569	51570	51574	141831	1xxx
122474	51349	52832	52833	52901	102459	102460	1xz0
122476	51349	53270	53271	53272	142556	142557	1y0b
122550	51349	51734	51735	51751	117413	117414	1y1p
122608	53931	56280	56281	143916	143917	143918	1y44
122674	51349	53648	53649	53650	53651	53652	1y6v
122700	48724	50155	50156	50157	141282	141283	1y7n
122716	53931	55728	55729	55730	143674	143675	1y7r
122769	53931	54494	54495	54496	54497	143058	1y8x
122779	53931	55728	55729	55730	143696	143697	1y9k
122783	53931	55728	55729	55730	143650	143651	1y9w
122785	46456	48370	48452	48453	140843	140844	1ya0
122837	53931	56234	56235	56251	56255	56256	1yar
122844	53931	56234	56235	56251	56252	56253	1yar
122865	53931	55845	55846	55847	143780	143781	1yb0
122980	51349	51734	51735	51751	141907	141908	1yde
123006	51349	51350	51695	89508	110382	110383	1ydy
123054	53931	54494	54495	54496	54497	143049	1yf9
123214	53931	56111	56112	88854	56146	56147	1yhw
123381	51349	52539	52540	52541	142213	142214	1yj5
123493	53931	55728	55729	55730	143668	143669	1yk3
123519	46456	140717	140718	140719	140720	140721	1ykh
123651	53931	54636	54637	54638	102903	102904	1yli
123699	51349	52820	52821	52822	52825	52826	1ymk
123718	46456	109603	109604	101340	140763	140764	1ynb
123769	51349	51734	51735	51751	141913	141914	1yo6

123778	53931	54636	54637	89902	143182	143183	1yoc
123785	51349	69571	69572	89763	89766	89767	1yov
123786	51349	69571	69572	89763	89764	89765	1yov
123799	51349	53447	53448	53464	142688	142689	1yp2
123833	53931	56435	56436	56437	143955	143956	1ypq
123876	53931	54235	54236	54237	142946	142947	1yqb
123915	51349	52539	52540	52652	142297	142298	1yrb
123919	53931	55728	55729	55730	143686	143687	1yre
123941	53931	54494	54495	54496	54497	143053	1yrv
123994	51349	53066	53098	53118	142495	142496	1yt3
124066	46456	47472	47473	47478	47479	140535	1yut
124077	46456	47239	47240	47241	140440	140441	1yuz
124099	46456	47161	47226	47230	140413	140414	1yvi
124106	53931	55728	55729	55730	143694	143695	1yvo
124131	51349	53162	53187	142526	142527	142531	1yw4
124132	51349	53162	53187	142526	142527	142530	1yw6
124168	53931	55728	55729	55730	143654	143655	1yx0
124192	51349	51734	51735	51751	141884	141885	1yxm
124264	48724	51315	51316	63873	63874	117337	1yz1
124275	51349	52171	52266	89594	142056	142057	1yzf
124277	51349	53334	53335	142647	142648	142649	1yzh
124301	51349	52539	52540	52592	142279	142280	1z06
124328	56572	111330	111331	111332	111333	111334	1z0s
124369	48724	50813	50814	50815	141462	141463	1z24
124374	51349	52539	52540	52592	142231	142232	1z2a
124387	53931	54235	54236	54237	142936	142937	1z2m
124388	53931	54235	54236	54237	142936	142937	1z2m
124389	53931	54494	54495	54496	54497	143060	1z2u
124421	51349	51350	51395	51396	141763	141764	1z41
124431	53931	55728	55729	55730	143658	143659	1z4e
124444	53931	55728	55729	55730	55737	143647	1z4r
124450	53931	54636	54637	54638	143152	143153	1z54
124498	51349	52832	52833	52901	75237	142370	1z5y
124530	51349	52832	52833	52834	142353	142354	1z6n
124531	46456	47239	47240	47241	47246	140436	1z6o
124543	46456	47239	47240	47241	47246	140437	1z6o
124624	51349	53270	53271	53272	53283	53284	1z7g
124631	56992	100894	100895	57468	57469	57470	1z7k
124632	53931	55680	55681	55682	118058	143639	1z7m
124722	46456	48263	48264	48265	48272	48273	1z8o
124774	46456	47239	47240	47253	140442	140443	1za0
124850	51349	53066	53098	53099	142490	142491	1zbf
124881	48724	50728	50729	50730	141399	141400	1zc3
124903	51349	51350	51695	89508	141866	141867	1zcc
124931	51349	53473	53474	53525	53526	102626	1zd3
124938	51349	52539	52540	52592	52614	142219	1zd9
124943	53931	54494	54495	54496	54497	143048	1zdn
124980	51349	53648	53649	53650	53651	64165	1zed
124981	46456	140958	140959	140963	140964	140965	1zee
124984	51349	51734	51735	51751	141882	141883	1zem
124994	51349	52171	52172	52173	52192	52193	1zes
125065	51349	52171	52172	52173	142033	142034	1zgz

125074	53931	54861	54928	54929	89940	89941	1zh5
125112	53931	143999	144000	144001	144002	144003	1zbx
125176	51349	51734	51735	51751	89521	89522	1zk4
125182	48724	50890	50891	50892	141505	141506	1zkc
125198	53931	54235	54236	54237	117799	142931	1zkh
125199	53931	54636	54637	89902	143175	143176	1zki
125354	51349	52832	52833	52834	142355	142356	1zma
125363	51349	51734	51735	51751	102153	102154	1zmt
125380	48724	50813	50814	50815	50832	50833	1znd
125416	53931	55728	55729	143714	143715	143716	1zo0
125437	51349	53382	53383	53417	53418	53419	1zod
125555	48724	51181	51182	82191	82192	82193	1zrr
125573	46456	47239	47240	47241	47250	140433	1zs3
125600	51349	56783	56784	142186	142189	142190	1zs9
125662	46456	48370	48452	48453	140839	140840	1zu2
125679	51349	52539	52540	52592	142269	142270	1zun
125680	53931	54494	54495	54496	143068	143069	1zuo
125757	51349	53334	53335	69550	69551	142580	1zx0
125812	56835	56836	56854	56855	90103	90104	1zy3
125938	46456	46688	46785	46832	140265	140266	2a07
125944	48724	50813	50814	50847	141467	141468	2a0a
125960	51349	52767	52768	52769	52770	142347	2a0m
125997	56572	56751	56752	56753	56757	64508	2a1h
126033	48724	50474	50475	50476	50479	141347	2a2j
126072	51349	51734	51735	51751	141911	141912	2a35
126091	51349	51350	51556	51557	141800	141801	2a3l
126139	53931	56218	56219	56220	56225	56226	2a40
126150	51349	51350	51569	51570	51576	141833	2a4a
126163	51349	52832	52833	52901	142387	142388	2a4v
126293	53931	143119	143120	143121	143122	143123	2a6q
126341	51349	52095	52096	52103	142004	142005	2a7k
126389	51349	52373	52374	63976	63977	89615	2a84
126408	51349	53926	53927	89800	142835	142836	2a8n
126528	51349	53612	53613	53614	142712	142713	2abq
126534	51349	53612	53613	53614	53617	53619	2abs
126545	53931	55153	55154	118007	143487	143488	2aca
126581	53931	54861	54928	54929	54950	54951	2adb
126582	53931	54861	54928	54929	54950	54951	2adc
126583	53931	54861	54928	54929	54950	54951	2adc
126599	48724	50728	50729	50730	141411	141412	2adz
126600	53931	55728	55729	55730	143664	143665	2ae6
126617	51349	52767	52768	52769	52770	142346	2aeb
126620	51349	53270	53271	53272	53290	142553	2aee
126674	51349	53612	53613	53614	75295	75296	2afb
126683	51349	52539	52540	52652	52661	52662	2afh
126707	51349	53162	53187	142532	142533	142534	2afw
126719	51349	51734	51735	51751	141894	141895	2ag5
126740	48724	50938	50939	50940	82164	89371	2ah2
126742	51349	56783	56784	75173	142145	142146	2ah5
126771	48724	50198	50249	50282	74950	141310	2aho
126841	53931	55728	55729	55730	143690	143691	2aj6
126892	51349	53612	53613	53614	82518	82519	2ajr

126914	51349	52539	52540	52592	69488	142228	2aka
126976	53931	54636	54637	54638	143162	143163	2ali
127024	51349	51350	51556	51557	51558	141799	2amx
127135	56992	57769	144210	144211	144214	144216	2apo
127168	56992	57769	144210	144211	144212	144213	2aqa
127225	48724	50474	50475	50476	141350	141351	2arz
127244	48724	50198	50249	50282	69265	69267	2asb
127253	48724	50474	50475	50476	141362	141363	2asf
127274	51349	52046	52047	52055	52056	52057	2ast
127305	53931	55728	55729	55730	143680	143681	2atr
127377	51349	53334	53335	53336	142571	142572	2avd
127380	51349	53334	53335	110671	142595	142596	2avn
127432	53931	54494	54495	54496	54497	143056	2awf
127497	51349	52539	52540	52541	142211	142212	2axp
127571	53931	143112	143113	143114	143115	143116	2ayu
127574	51349	52171	52172	52173	142023	142024	2ayx
127615	53931	55810	55811	55812	143756	143757	2azw
127624	53931	55810	55811	55812	143762	143763	2b06
127632	51349	52008	102198	102199	141972	141973	2b0a
127650	53931	55810	55811	55812	143760	143761	2b0v
127759	51349	56783	56784	82388	142165	142166	2b30
127786	48724	50198	50249	50263	50267	50268	2b3g
127792	53931	54636	54637	82636	143171	143172	2b3n
127796	51349	53334	53335	89743	89744	110666	2b3t
127804	51349	53731	53732	53733	142758	142759	2b3y
127817	51349	52171	52172	52173	142029	142030	2b4a
127892	53931	55728	55729	55730	143652	143653	2b5g
127905	56572	56573	56574	56575	56584	56586	2b5t
127914	51349	52832	52833	52901	142373	142374	2b5x
127974	51349	51734	51735	51751	141880	141881	2b69
128042	51349	52832	52833	52901	102459	142372	2b7k
128093	51349	82543	82544	82545	82546	82547	2b8n
128103	53931	54861	54919	54920	54921	143286	2b8q
128117	46456	47265	47266	47286	47291	47292	2b8u
128257	51349	53789	53790	53791	142785	142786	2bb3
128302	51349	53162	53187	142526	142527	142529	2bco
128321	51349	51734	51735	51751	141892	141893	2bd0
128456	51349	53755	53756	110734	110735	142768	2bfw
128480	51349	51734	51735	51751	141898	141899	2bgk
128505	53931	55845	55846	55847	143782	143783	2bgx
128565	53931	54636	54637	82636	143169	143170	2bi0
128566	53931	54636	54637	82636	143169	143170	2bi0
128633	48724	50629	50630	50646	50673	50674	2bju
128666	51349	51734	51735	51751	141904	141905	2bka
128714	51349	53382	53383	53402	89757	142664	2bkw
128733	51349	51734	51735	51751	117419	117420	2bll
128797	51349	52539	52540	52592	142249	142250	2bmj
128817	51349	52832	52833	52901	69516	142368	2bmx
128869	51349	53447	53448	142691	142692	142693	2bo4
128951	46456	48370	48371	48372	48378	140814	2bpt
129090	56992	144121	144122	144123	144124	144125	2bsk
129091	56992	144121	144122	144123	144126	144127	2bsk

129129	48724	51268	51283	51284	141655	141656	2bsy
129130	48724	51268	51283	51284	141655	141656	2bsy
129152	53931	54235	54292	54293	54310	54311	2bt6
129227	48724	49451	49482	49483	49486	49488	2bur
129228	48724	49451	49482	49483	49489	49491	2bur
129238	51349	52539	52540	52592	52633	52634	2bv3
129324	48724	49898	49899	49978	49991	89275	2bw8
129363	53931	54235	54236	54237	142940	142941	2bwf
129368	51349	53382	53383	53417	142676	142677	2bwn
129486	46456	47112	47113	47134	140400	140401	2byk
129487	46456	47112	47113	47134	140398	140399	2byk
129490	51349	53382	53383	53417	53422	53423	2byl
129533	53931	54861	54928	54929	143302	143303	2bz2
129552	48724	50493	50494	50514	50550	50551	2bz6
129559	51349	53334	53335	102566	102567	142579	2bzg
129577	51349	51734	51735	51751	51788	141877	2c07
129594	51349	51350	51445	51487	141781	141782	2c0h
129644	53931	142876	142877	142878	142879	142880	2c1w
129670	53931	54636	54637	82636	143173	143174	2c2i
129672	46456	48370	48452	48453	140837	140838	2c2l
129711	46456	47768	47819	69044	69045	140642	2c35
129837	51349	56783	56784	102317	142169	142170	2c4n
129894	51349	51734	51735	51751	141890	141891	2c5a
130039	51349	52539	52540	52592	52626	52629	2c78
130080	51349	53334	53335	88786	53367	53368	2c7p
130123	46456	46625	46626	46627	109645	109646	2c8s
130129	48724	48725	48726	49159	141015	141016	2c9a
130143	48724	48725	49329	49330	49331	49333	2c9v
130145	53931	54235	54236	54237	54246	54247	2c9w
130540	46456	46688	46689	46739	140167	140168	2cjj
130570	51349	53334	53335	53336	53337	53338	2cl5
130672	48724	50728	50729	50730	141419	141420	2coa
130674	48724	50728	50729	50730	141415	141416	2coc
130675	48724	50728	50729	50730	141395	141396	2cod
130676	48724	50728	50729	50730	141407	141408	2cof
130697	53931	54861	54928	54929	143326	143327	2cpd
130698	53931	54861	54928	54929	143340	143341	2cpe
130699	53931	54861	54928	54929	117969	117970	2cpf
130700	53931	54861	54928	54929	117969	117970	2cph
130701	53931	54861	54928	54929	143294	143295	2cipi
130702	53931	54861	54928	54929	143354	143355	2cpj
130708	53931	54861	54928	54929	143296	143297	2cpx
130709	53931	54861	54928	54929	143349	143350	2cpy
130710	53931	54861	54928	54929	143336	143337	2cpz
130711	53931	54861	54928	54929	143304	143305	2cq0
130712	53931	54861	54928	54929	143332	143333	2cq1
130713	53931	54861	54928	54929	143334	143335	2cq2
130714	53931	54861	54928	54929	143314	143315	2cq3
130715	53931	54861	54928	54929	143352	143353	2cq4
130717	53931	54861	54928	54929	143310	143311	2cq5
130718	53931	54861	54928	54929	143312	143313	2cq6
130719	53931	54861	54928	54929	143360	143361	2cq7

130722	53931	54861	54928	54929	117957	117958	2cqg
130723	53931	54861	54928	54929	143344	143345	2cqh
130724	53931	54861	54928	54929	143298	143299	2cqj
130727	53931	54861	54928	54929	143349	143351	2cqp
130728	46456	46688	46689	46739	140169	140170	2cqg
130729	46456	46688	46689	46739	140169	140170	2cqr
130730	48724	48725	48726	49159	49170	141012	2cqv
130739	46456	46688	46689	46739	140163	140164	2crg
130747	48724	50155	50156	50157	141286	141287	2cs5
130769	56992	57666	57667	57668	144145	144146	2csh
130770	56992	57666	57667	57668	144145	144146	2csh
130771	48724	50155	50156	50157	141265	141266	2csj
130780	48724	50155	50156	50157	141279	141281	2css
130788	56992	57666	57667	57668	144153	144154	2ct1
130789	56992	57666	57667	57668	144153	144154	2ct1
130792	56992	57666	57667	57668	144135	144136	2ctd
130793	56992	57666	57667	57668	144135	144136	2ctd
130800	51349	53382	53383	53402	142665	142666	2ctz
130805	46456	46688	46689	46739	140173	140174	2cu7
130809	46456	46688	46689	46690	140159	140160	2cuf
130859	51349	52832	52833	52901	142389	142390	2cvb
130973	51349	52832	52833	52901	142377	142378	2cx4
131013	51349	52539	52540	52592	142257	142258	2cxx
131016	53931	55728	55729	55730	118068	118069	2cy2
131021	53931	54636	54637	54638	143150	143151	2cye
131025	51349	51350	51445	51487	51507	141777	2cyg
131035	53931	54861	54913	54914	143281	143282	2cz4
131093	46456	140958	140959	140963	140966	140967	2d0t
131151	51349	51734	51735	51751	141896	141897	2d1y
131269	51349	52373	52374	52375	52384	52385	2d5b
131357	48724	48725	48726	49159	141013	141014	2dav
131374	51349	53612	53613	53614	142714	142715	2dcn
131430	51349	53789	53790	53791	102684	142779	2dek
131470	48724	49898	49899	49978	49979	49985	2dfb
131515	53931	54861	54928	54929	143324	143325	2dgx
131532	53931	54861	54928	54929	143328	143329	2dis
131533	53931	54861	54928	54929	143290	143291	2dit
131558	56992	57666	57667	57668	144139	144140	2dlk
131559	56992	57666	57667	57668	144139	144140	2dlk
131563	56992	57666	57667	57668	144147	144148	2dlq
131565	56992	57666	57667	57668	144147	144148	2dlq
131573	56992	57666	57667	57668	144149	144150	2dmd
131793	51349	51350	51556	141819	141822	141823	2dvt
131980	48724	50198	50242	50243	50246	50248	2e2d
132022	46456	48112	48113	48114	88935	48118	2.00E+39
132104	46456	46688	46689	46690	116778	116779	2ecc
132304	51349	52539	52540	52592	142267	142268	2erx
132351	48724	51181	51182	51187	63853	63854	2et1
132360	51349	53066	53098	53099	53103	142489	2etj
132387	53931	55728	55729	55730	143692	143693	2eui
132407	46456	48112	48113	48114	48119	48120	2eut
132447	51349	51734	51735	51751	141902	141903	2ew8

132516	51349	53334	53335	117685	142597	142598	2ex4
132649	51349	53612	53613	53614	142710	142711	2f02
132661	48724	50155	50156	50157	89313	89314	2f0a
132673	53931	54636	54637	89902	143179	143181	2f0x
132782	53931	56218	56219	56220	111213	143901	2f1n
132843	53931	55845	55846	55847	143784	143785	2f2l
132844	53931	55845	55846	55847	143784	143785	2f2l
132904	53931	54636	54637	89902	143184	143185	2f41
132915	51349	53783	53784	53785	75321	75322	2f48
132958	53931	54494	54495	54496	54497	143050	2f4w
133015	48724	50155	50156	50157	117180	141264	2f5y
133021	51349	52171	52309	52310	52311	142064	2f62
133047	51349	51350	51556	141819	141828	141829	2f6k
133055	51349	52095	52096	52103	142006	142007	2f6q
133061	51349	51350	51395	51396	141765	141766	2f6u
133119	51349	52832	52833	52901	52902	142365	2f8a
133128	51349	53382	53383	53384	64121	102594	2f8j
133153	51349	53066	53098	53118	142497	142498	2f96
133159	53931	54861	54928	54929	143316	143317	2f9d
133161	51349	53755	53756	110734	142769	142770	2f9f
133223	53931	54235	54236	54237	142948	142949	2faz
133249	53931	55153	55154	118007	143489	143490	2fb1
133254	46456	48370	48452	48453	140841	140842	2fbn
133272	53931	55728	55729	55730	143684	143685	2fck
133299	48724	48725	48726	49159	49179	49180	2fdb
133311	48724	51181	51197	141628	141629	141630	2fdi
133319	51349	56783	56784	75173	142141	142142	2fdr
133320	51349	51350	51366	51375	141749	141752	2fds
133322	51349	88722	88723	89619	142114	142115	2fe1
133323	48724	50155	50156	50157	101713	101714	2fe5
133325	53931	55728	55729	55730	143676	143677	2fe7
133354	51349	52171	52317	52325	142072	142073	2fex
133385	51349	51350	51556	141819	141820	141821	2ffi
133426	48724	50474	50475	50476	141364	141365	2fg9
133478	51349	52539	52540	52592	89664	142224	2fh5
133497	48724	50474	50475	50476	141358	141359	2fhq
133504	53931	54116	54117	54118	54128	54131	2fht
133514	53931	55728	55729	55730	143662	143663	2fia
133539	53931	55728	55729	55730	143708	143709	2fiw
133559	46456	47239	47240	47241	47250	140435	2fjc
133611	48724	50728	50729	50730	141413	141414	2fjl
133648	51349	53334	53335	69560	142591	142592	2fk8
133650	53931	55810	55811	64369	143770	143771	2fkb
133688	46456	47239	47240	47241	47244	140431	2fkz
133706	53931	55728	55729	55730	143682	143683	2fl4
133799	53931	56321	56322	56323	143943	143944	2fn0
133810	51349	52539	52540	81269	142326	142327	2fna
133831	51349	53382	53383	53417	142672	142673	2fnu
133868	53931	54494	54495	54496	143070	143071	2fo3
133961	51349	51734	51735	51751	141909	141910	2fr1
133962	51349	51734	51735	51751	141909	141910	2fr1
133965	51349	53926	53927	53928	75327	142830	2fr5

134003	53931	54636	54637	89902	89903	89904	2fs2
134005	48724	50813	50814	50847	50861	50862	2fs6
134036	53931	55728	55729	55730	143704	143705	2fsr
134119	51349	56783	56784	82388	142161	142162	2fue
134124	51349	52832	52833	142405	142406	142407	2fug
134129	56572	56761	56762	144028	144029	144030	2fug
134130	53931	143242	143243	143244	143245	143246	2fug
134131	56572	56769	56770	144031	144032	144033	2fug
134175	53931	54636	54637	54638	143146	143147	2fuj
134185	48724	50474	50475	50476	141366	141367	2fur
134197	51349	53612	53613	53614	53615	142709	2fv7
134226	53931	55810	55811	55812	143766	143767	2fvv
134231	51349	52095	52096	52103	142002	142003	2fw2
134242	51349	52832	52833	52834	102435	102436	2fwh
134245	48724	50181	50182	50183	141291	141292	2fwk
134344	51349	52832	52833	52901	142385	142386	2fy6
134391	51349	53334	53335	53351	142581	142582	2fyt
134437	46456	47239	47240	47241	140438	140439	2fzf
134448	51349	53596	53597	53598	53605	53608	2fzi
134499	51349	52539	52540	52652	142299	142300	2g0t
134557	53931	55728	55729	55730	143656	143657	2g3a
134654	53931	56321	56322	56323	143945	143946	2g5f
134674	48724	48725	48726	48727	89176	89177	2g5r
134741	51349	56783	56784	142186	142187	142188	2g80
134766	51349	53926	53927	89800	142833	142834	2g84
134779	53931	55830	55831	55832	55833	55834	2g8o
134889	53931	55728	55729	55730	143666	143667	2gan
134903	51349	53382	53383	53384	142661	142662	2gb3
135015	53931	55330	55331	55339	55340	55343	2gdg
135043	51349	51734	51735	51751	141888	141889	2gdz
135044	53931	55728	55729	55730	143660	143661	2ge3
135077	53931	54636	54637	54638	143156	143157	2gf6
135096	51349	56783	56784	75173	142137	142138	2ghf
135109	53931	56111	56112	88854	56129	56130	2gfs
135155	53931	54861	55008	55009	64279	64280	2ggp
135175	56992	57666	57667	57668	144141	144142	2ghf
135176	56992	57666	57667	57668	144141	144142	2ghf
135184	53931	54861	54928	54929	143338	143339	2ghp
135185	53931	54861	54928	54929	143338	143339	2ghp
135186	53931	54861	54928	54929	143338	143339	2ghp
135254	48724	48725	48726	48727	141008	141009	2giy
135270	51349	52539	52540	52592	102366	102367	2gj8
135287	51349	52539	52540	52592	142295	142296	2gjs
135415	51349	52539	52540	81269	64031	142324	2gno
135434	51349	56783	56784	75173	142139	142140	2go7
135630	46456	101385	101386	116993	140790	140791	2gta
135737	51349	53066	53098	53118	82444	82445	2gui
135759	51349	51904	51905	51943	117444	117445	2gv8
135760	51349	51904	51905	51943	117444	117445	2gv8
135776	53931	54636	54637	54638	143148	143149	2gvh
135777	53931	54636	54637	54638	143148	143149	2gvh
135805	51349	51350	51556	141819	141826	141827	2gwg

135850	51349	52079	52080	52081	52082	141994	2gyc
135853	48724	50036	50104	50105	50106	141241	2gyc
135944	51349	88722	88723	89619	142110	142111	2h1c
136046	48724	50155	50156	50157	82085	82086	2h3l
136185	46456	48370	48439	48440	48441	69093	2h6f
136186	46456	48207	48239	48246	48247	69090	2h6f
136219	51349	51734	51735	51751	51791	51793	2h7m
136231	56992	57301	57302	57303	144103	144104	2h7z
136246	56992	57301	57302	57303	111404	111405	2h8u
136314	51349	53066	53098	53118	142493	142494	2hbk
136319	53931	54636	54637	89902	143177	143178	2hbo
136320	51349	51350	51556	141819	141824	141825	2hbv
136333	51349	56783	56784	75173	142147	142148	2hcf
136345	51349	56783	56784	75173	142135	142136	2hdo
136354	46456	109603	109604	101340	140765	140766	2hek
136514	51349	53066	53098	53118	53119	53122	2hhv
136555	53931	55873	55874	55879	82778	82779	2hkj
136570	53931	54636	54637	54638	143144	143145	2hlj
136633	48724	50813	50814	50847	50856	110275	2hnx
136644	51349	53382	53383	53384	82482	82483	2hox
136657	48724	50474	50475	50476	141360	141361	2hq7
136659	48724	50474	50475	50476	141354	141355	2hq9
136726	51349	56783	56784	75173	142143	142144	2hsz
136744	48724	50474	50475	50476	141348	141349	2hti
136776	46456	47112	47113	47114	47125	47127	2hue
136837	53931	54636	54637	54638	143160	143161	2hx5
136860	51349	53926	53927	89800	142837	142839	2hxv
136936	48724	50474	50475	50476	141352	141353	2i02
137095	53931	55728	55729	55730	143700	143701	2i6c
137195	46456	109603	109604	140769	140770	140771	2ibn
137266	51349	52742	52743	52744	89692	89693	2id4
137335	48724	48725	48726	49159	49190	49191	2ifg
137343	51349	52832	52833	52834	52835	52842	2ifq
137449	46456	48263	48264	48265	48268	48269	2ij2
137521	53931	54494	54495	143072	143073	143074	2in1
137524	46456	47239	47240	47253	109788	109789	2inc
137525	46456	47239	47240	47253	109790	109791	2inc
137709	48724	51181	51197	141628	141631	141632	2iuw
137738	51349	53755	53756	110734	142771	142772	2iw1
137739	46456	46688	46689	46739	140165	140166	2iw5
137812	51349	52539	52540	52566	52567	75194	2iyv
137920	48724	50198	50242	50243	50244	50245	2j0t
138009	53931	56111	56112	88854	90038	90039	2j4z
138130	46456	48507	48508	48509	48521	48523	2j7y
138131	53931	54116	54117	54118	54150	54151	2j7z
138240	46456	48370	48371	140819	140820	140821	2jak
138243	53931	56111	56112	88854	143893	143894	2jav
138356	56835	56836	56854	56855	118212	118213	2jm6
138392	48724	49898	49899	49932	49940	49941	2nn8
138562	51349	51350	51445	51487	89473	89474	2nt0
138608	53931	54636	54637	54638	143154	143155	2nuj
138714	46456	140958	140959	140960	140961	140962	2nw8

138721	56835	118214	118215	118216	118217	118218	2nww
138745	48724	48725	48726	48727	48737	48738	2nxy
138862	51349	53334	53335	69557	69558	142590	2o07
138884	51349	51734	51735	51751	63933	102152	2o23
138920	46456	109603	109604	101340	140767	140768	2o6i
139030	53931	143119	143120	143121	143124	143125	2odk
139092	46456	101385	101386	116993	140792	140793	2oie
139443	53931	56111	56112	88854	82789	82790	2oza
139497	46456	48507	48508	48509	69109	69110	2p54
139643	46456	109603	109604	101340	116969	116970	2paq
139645	51349	51350	51445	51487	51495	51496	2pb1
139762	51349	52742	52743	52744	52762	52763	2pwa
139825	51349	51734	51735	51751	117417	117418	2q46
139941	53931	54861	54999	55000	55001	55002	2uub
139942	51349	53066	53137	53138	53141	53142	2uub
139943	48724	50198	50249	50282	50302	50303	2uub
144534	48724	50964	50978	50979	159257	159258	1vyh
144580	56992	57500	57501	57528	64562	64563	1xwd
144607	51349	69571	69572	89763	89764	89765	1y8x
144615	46456	47161	47216	47217	158392	158393	1yar
144649	48724	48725	48726	48727	158865	158866	1yjd
144710	48724	48725	48726	48727	48933	63651	1ypz
144788	51349	52539	52540	81269	159577	159578	2a5y
144808	48724	48725	48726	48727	48933	48935	2ak4
144837	48724	48725	48726	48727	48734	158864	2atp
144996	48724	48725	48726	48727	48933	48935	2bnq
145078	48724	50728	50729	50730	159209	159210	2dfk
145109	48724	48725	48726	49159	158879	158880	2dyp
145162	48724	50352	50353	50354	159145	159146	2fdb
145176	53931	74651	48403	48404	160152	160153	2fo1
145232	51349	52171	52313	52314	52315	159491	2gy9
145237	48724	50198	50249	50282	50304	159088	2gy9
145271	51349	53066	53137	53138	53139	159642	2gyc
145525	48724	48725	48726	48727	48933	48937	2ij0
145572	51349	52079	52080	52081	52082	159454	2j01
145656	48724	50728	50729	50730	159213	159214	2j59
145694	53931	54861	54913	54914	54917	160309	2ns1
145736	48724	50964	50978	50979	159259	159260	2ovr
145768	53931	54494	54495	54496	54497	54503	2uyz
145841	53931	55680	55681	143642	160607	160608	1x2g
145891	53931	110848	110849	160095	160096	160097	1xw3
145918	56835	81339	81338	56895	103468	118226	1ymg
146035	53931	56111	56112	64411	160818	160819	1zyt
146036	51349	100949	100950	110513	159543	159544	2a0u
146040	56835	161069	161070	161071	161072	161073	2a65
146047	51349	53755	53756	159785	159788	159789	2acv
146061	53931	55297	55315	55316	160504	160505	2ale
146085	53931	54861	54928	54929	54932	160313	2b0g
146096	48724	50198	50249	50282	159100	159103	2ba0
146161	53931	55297	55315	55316	55317	89986	2bo1
146163	56572	111330	111331	160984	160985	160987	2bon
146219	51349	53447	53448	159726	159731	159732	2bvl

146225	51349	53755	53756	159785	159786	159787	2c1x
146379	53931	55680	55681	143642	160604	160606	2c8m
146398	46456	48263	48264	48265	48276	48277	2cib
146411	46456	46688	46689	46739	158244	158245	2ckx
146423	48724	48725	48726	48727	158867	158868	2cry
146459	53931	55728	55729	55730	160640	160641	2d4p
146466	51349	53066	53098	102492	159633	159634	2d5r
146608	51349	52539	52540	52592	52633	142226	2dy1
146654	46456	48507	48508	48509	81916	81917	2e2r
146687	53931	143112	143113	143114	160140	160141	2.00E+50
146706	53931	56280	56281	143916	143917	143920	2e7y
146789	46456	46688	46689	46690	158242	158243	2ecb
146896	48724	50728	50729	50730	159211	159212	2elb
146971	56992	57666	57667	57668	161152	161153	2epp
146973	56992	57666	57667	57668	161152	161153	2epr
146974	56992	57666	57667	57668	161152	161153	2eps
146989	56992	100894	100895	57468	57476	161138	2erw
147177	51349	53162	53187	142526	159649	159650	2gu2
147196	46456	109603	109604	101340	158725	158726	2gz4
147239	56835	161083	161084	161085	161088	161089	2h8a
147437	53931	56299	56300	160875	160876	160877	2hy1
147460	53931	55769	103196	103197	118074	118075	2hz5
147512	48724	50728	50729	50730	50740	50741	2i5f
147657	51349	53066	53098	53118	89719	142492	2igi
147818	48724	50198	50249	50282	159089	159090	2ix0
147819	48724	50198	50249	50282	159089	159090	2ix0
147820	48724	50198	50249	50282	159089	159090	2ix0
147903	56992	57666	57667	57668	57693	57694	2j7j
147905	56992	57666	57667	57668	57693	57694	2j7j
147950	48724	50198	50249	50282	159091	159092	2ja9
147962	51349	53473	53474	159762	159763	159764	2jbw
147977	53931	55728	55729	55730	143670	143671	2jdc
147995	48724	50198	50249	50282	159100	159102	2je6
148002	51349	51350	51445	51487	159385	159386	2je8
148032	53931	56111	56112	88854	160812	160813	2jfl
148140	53931	55153	55154	118007	160428	160429	2jmu
148163	48724	50036	50104	159031	159032	159033	2joy
148164	48724	50813	50814	50815	159228	159229	2joz
148310	48724	50198	50249	50282	159096	159097	2nn6
148313	48724	50198	50249	50282	159098	159099	2nn6
148392	48724	48725	48726	48727	48933	48937	2nts
148532	51349	53755	53756	159794	159795	159796	2nzw
148541	46456	48370	48445	48446	48449	48450	2o02
148591	51349	53334	53335	69560	159680	159681	2o57
148596	53931	55810	55811	64369	103217	160692	2o5f
148616	53931	54636	54637	54638	143158	143159	2o5u
148679	46456	48370	48445	48446	158768	158769	2o8p
148695	53931	54636	54637	54638	160180	160181	2oaf
148714	51349	102545	102546	102547	159677	159678	2ob5
148780	53931	54196	54197	54198	159880	159881	2oik
148794	53931	54636	54637	54638	160182	160183	2oiw
148903	51349	52539	52540	52686	159569	159570	2onk

148997	46456	47265	47266	47286	158425	158426	2oqp
149025	53931	54000	54001	54002	142846	142847	2oul
149034	53931	54636	54637	89902	160184	160185	2ov9
149100	48724	48725	48726	49159	49162	49163	2oz4
149101	48724	48725	48726	49159	49162	49163	2oz4
149135	53931	55680	55681	143642	160604	160605	2p0l
149171	48724	89359	89360	89361	159226	159227	2p2e
149189	48724	50493	50494	50514	50574	50575	2p3u
149207	48724	48725	48726	48727	88563	88564	2p49
149248	53931	55680	55681	143642	160609	160610	2p5i
149285	51349	53334	53335	110671	159682	159683	2p7i
149354	53931	55769	55770	55771	55772	55774	2pbpd
149493	48724	50198	50249	50263	50269	50270	2pi2
149497	48724	50198	50249	50263	50271	50272	2pi2
149569	46456	109603	109604	101340	158729	158730	2pjq
149669	51349	52539	52540	52686	89683	89684	2pmk
149781	53931	54533	54534	54535	54536	54537	2ppn
149782	53931	56111	56112	64411	160816	160817	2ppq
149785	51349	53755	53756	159785	159790	159791	2pq6
149786	46456	109603	109604	101340	158719	158720	2pq7
149793	46456	48370	48452	48453	101417	140836	2pqr
149824	53931	55944	55961	55966	160730	160731	2ps0
149865	53931	56111	56112	64411	160814	160815	2pul
149878	53931	54533	54534	54535	82624	82625	2pv2
149928	51349	53066	53098	53118	117650	117651	2py5
150034	53931	56370	56371	56372	160917	160918	2q3n
150097	56835	161083	161084	161085	161086	161087	2q7r
150105	51349	53382	53383	53384	53385	53390	2q7w
150112	46456	48575	48576	48577	158813	158814	2q80
150320	51349	51350	51569	51570	51576	51582	2qap
150676	53931	56280	56281	56288	56289	160851	2qed
150733	56992	57923	57924	57925	57930	57931	2qfa
150738	46456	46457	46458	46463	46530	46531	2qfk
150751	53931	56299	56300	56301	56302	56303	2qfr
150782	46456	109603	109604	101340	158723	158724	2qgs
150808	53931	54861	55008	55009	55017	69736	2qif
150815	53931	54402	54427	54431	159959	159960	2qiyl
150835	46456	47575	47576	47577	101194	101195	2qjz
150874	51349	52539	52540	52652	159564	159565	2qm8
151197	48724	50629	50630	50646	50671	50672	2qp8
151215	53931	55944	55961	160742	160745	160746	2qpv
151386	56572	111330	111331	160984	160988	160989	2qv7
151441	51349	52171	52218	52235	52240	52241	2qwx
151455	51349	53066	53098	53118	53132	159630	2qxfl
151470	51349	52539	52540	52652	52666	52667	2qy9
151529	46456	47161	47226	47230	47231	47232	2r25
151530	51349	52171	52172	52173	102228	102229	2r25
151572	46456	48507	48508	48509	101436	101437	2r40
151588	51349	53382	53383	53384	110681	142654	2r5e
151610	56835	161097	161098	161099	161106	161107	2r6g
151611	56835	161097	161098	161099	161104	161105	2r6g
151629	48724	50198	50249	50282	159094	159095	2r7d

151850	51349	56783	56784	82388	142157	142158	2rbk
152048	51349	51734	51735	51751	51788	117408	2rhc
152184	56835	161083	161084	161085	161090	161091	2uu
152457	51349	51350	51445	51487	141783	141784	2v3g
152460	51349	75216	75217	159513	159516	159517	2v3k
152871	53931	53954	53955	53960	53961	53962	2vb1
152917	51349	53755	53756	159785	159792	159793	2vch
153217	51349	53447	53448	159726	159729	159730	2vk9
153344	48724	50198	50249	50282	159104	159105	2vnu
153345	48724	50198	50249	50282	159104	159105	2vnu
153346	48724	50198	50249	50282	159104	159105	2vnu
153399	51349	52539	52540	52541	69478	69479	2vp4
153421	48724	50474	50475	50476	117228	117229	2vpa
153731	51349	51350	51445	51487	159383	159384	2vzs
153794	46456	47239	47240	47241	47250	109784	2yw6
153994	51349	53926	53927	53928	142831	142832	2z3g
154002	46456	47265	47266	47286	158422	158423	2z3q
154184	48724	50890	50891	50892	141511	141512	2z6w
154234	51349	52171	52218	52235	110470	110471	2z98
154343	51349	52832	52833	52901	117601	117602	2zct
154405	53931	54235	54236	54237	89831	89833	2zeq
154406	46456	47472	47473	47502	101182	101183	2zfd
154589	48724	50728	50729	50730	159207	159208	2zkm
154835	46456	109603	109604	101340	158721	158722	3b57
154838	48724	48725	48726	49159	158877	158878	3b5h
154839	48724	48725	48726	49159	158877	158878	3b5h
154901	51349	53066	53098	53118	159631	159632	3b6o
155055	53931	54861	54919	54920	54921	54922	3bbb
155061	51349	75216	75217	159513	159514	159515	3bbd
155161	53931	56435	56436	56437	56440	56441	3bdw
155185	53931	54861	54928	54929	143346	143347	3beg
155376	56835	56836	56854	56855	144081	144082	3bl2
155393	53931	56111	56112	88854	160810	160811	3blh
155446	51349	51350	82282	82283	102108	102109	3bof
155462	48724	48725	48726	48727	101510	101511	3bp5
155490	46456	46688	46785	46832	46833	46834	3bpy
155497	53931	56111	56112	88854	56142	160809	3bqc
155704	48724	50352	50386	50387	50396	50397	3bx1
155780	48724	50198	50249	50282	159106	159107	3bzk
155784	53931	56321	56322	56323	143941	143942	3bzn
155847	51349	52767	52768	52773	159582	159583	3c10
156848	53931	55944	55961	160742	160743	160744	3cnw
156903	53931	55769	103196	103197	111120	111121	3cpt
156985	53931	56370	56371	56372	160915	160916	3ctk
157035	56572	56800	56801	56802	111316	160961	3cw9
157149	46456	48263	48264	48265	158749	158750	3czh
157161	53931	56299	56300	160875	160878	160879	3d03
157208	46456	46457	46458	46463	46486	46497	3d1k
157209	46456	46457	46458	46463	46500	46513	3d1k
157265	56835	161097	161098	161099	161100	161101	3d31
157439	48724	48725	48726	49159	63665	63666	3d85
157463	56992	57923	57924	57925	57926	57927	3d9t

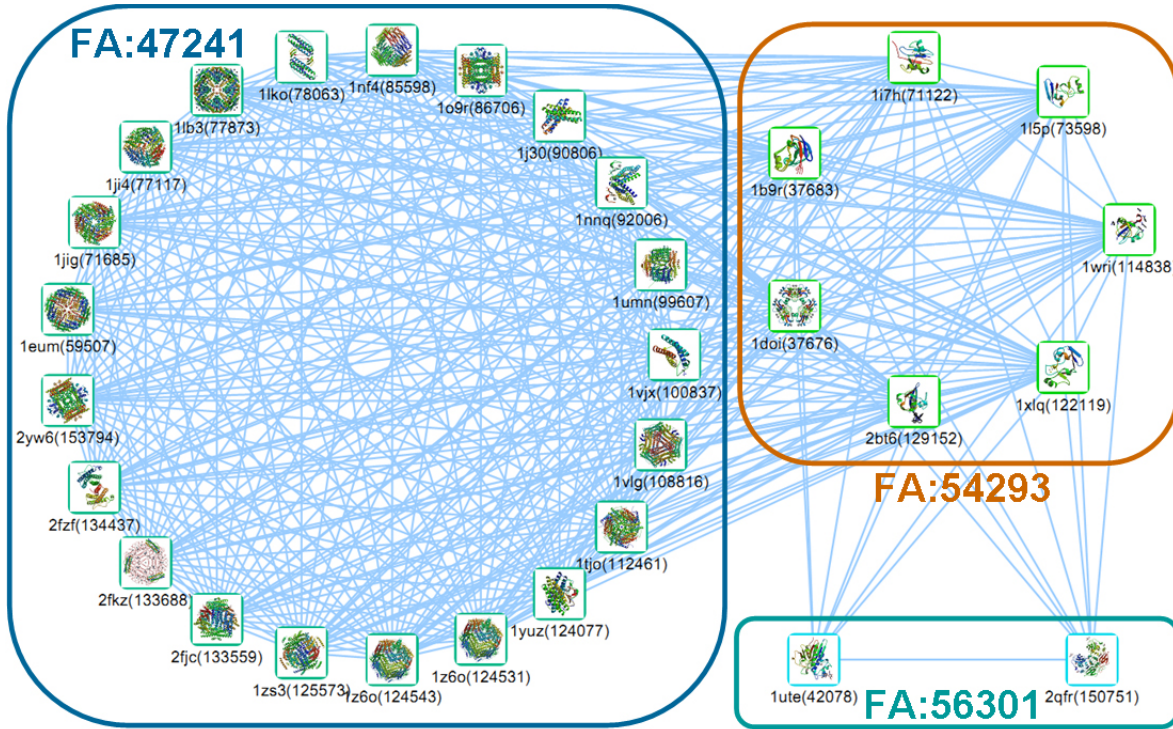
157466	48724	48725	48726	49159	49179	49181	3dar
157727	56835	161097	161098	161099	161108	161109	3dhw
157729	51349	52539	52540	52686	159571	159572	3dhw
157741	46456	47239	47240	47253	47257	69006	3dhz
157802	46456	47265	47266	47305	89036	89037	3dlq
157824	56992	57849	57850	57851	75693	75694	3dpl
157841	46456	48207	48239	48246	48249	48250	3dss
158080	51349	51350	51430	51431	51434	51435	3eau
158144	46456	48370	48445	48446	158770	158771	3efz
158154	48724	51268	51283	51284	51285	102010	3ehw

[S-9] 25 species used for creating phylogenetic profiles

Taxonomy	Scientific Name
9606	<i>Homo sapiens</i>
10090	<i>Mus musculus</i>
10116	<i>Rattus norvegicus</i>
3702	<i>Arabidopsis thaliana</i>
9913	<i>Bos taurus</i>
83333	<i>Escherichia coli</i> (strain K12)
559292	<i>Saccharomyces cerevisiae</i> (strain ATCC 204508 / S288c)
7227	<i>Drosophila melanogaster</i>
9031	<i>Gallus gallus</i>
1423	<i>Bacillus subtilis</i>
39947	<i>Oryza sativa</i> subsp. <i>japonica</i>
9823	<i>Sus scrofa</i>
7955	<i>Danio rerio</i>
6239	<i>Caenorhabditis elegans</i>
284812	<i>Schizosaccharomyces pombe</i> (strain ATCC 38366 / 972)
44689	<i>Dictyostelium discoideum</i>
83334	<i>Escherichia coli</i> O157:H7
1773	<i>Mycobacterium tuberculosis</i>
90371	<i>Salmonella typhimurium</i>
71421	<i>Haemophilus influenzae</i> (strain ATCC 51907 / DSM 11121 / KW20 / Rd)
287	<i>Pseudomonas aeruginosa</i>
9615	<i>Canis familiaris</i>
70601	<i>Pyrococcus horikoshii</i> (strain ATCC 700860 / DSM 12428 / JCM 9974 / NBRC 100139 / OT-3)
90370	<i>Salmonella typhi</i>
243232	<i>Methanocaldococcus jannaschii</i> (strain ATCC 43067 / DSM 2661 / JAL-1 / JCM 10045 / NBRC 100440)

[S-10] Analysis on domain clusters

From BSM score with 70% threshold, 1UTE and 2QFR are associated with FA:56301 which is Purple acid phosphatase-like. 1B9R, 1I7H, 1L5P, 1WRI, 1XLQ, 2BT6, and 1DOI are associated with FA:54293 which is 2Fe-2S ferredoxin-related. All others are associated with FA:47241 which is Ferritin



PDB1	PDB2	Sunid1	Sunid2	GPsim	dmTM	dmDali	dmSEQ	dmPHY	gpTM	gpDali	gpSEQ
1B9R	1EUM	37683	59507	0.72	0.215	0	0.286	0	0.215	0	0.286
1B9R	1JIG	37683	71685	0.72	0.223	0	0	0	0.223	0	0
1B9R	1JI4	37683	77117	0.72	0.214	0	0	0	0.214	0	0
1B9R	1LB3	37683	77873	0.72	0.203	0	0.235	0	0.203	0	0.235
1B9R	1LKO	37683	78063	0.72	0.247	0	0.75	0	0.182	0	0.4
1B9R	1NF4	37683	85598	0.72	0.189	0	0.276	0	0.189	0	0.276
1B9R	1O9R	37683	86706	0.72	0.236	0	0	0	0.236	0	0
1B9R	1J30	37683	90806	0.72	0.216	0	0.364	0	0.216	0	0.222
1B9R	1NNQ	37683	92006	0.72	0.202	0	0.461	0	0.201	0	0.461
1B9R	1UMN	37683	99607	0.72	0.197	0	0	0	0.197	0	0
1B9R	1VJX	37683	100837	0.72	0.217	0	0	0	0.217	0	0
1B9R	1VLG	37683	108816	0.72	0.218	0	0	0	0.218	0	0
1B9R	1TJO	37683	112461	0.72	0.181	0	0	0	0.181	0	0
1B9R	1YUZ	37683	124077	0.72	0.224	0	0	0	0.229	0	0
1B9R	1Z6O	37683	124531	0.72	0.183	0	0	0	0.175	0	0.353
1B9R	1Z6O	37683	124543	0.72	0.196	0	0.353	0	0.175	0	0.353
1B9R	1ZS3	37683	125573	0.72	0.195	0	0.333	0	0.195	0	0.333
1B9R	2FJC	37683	133559	0.72	0.243	0	0	0	0.243	0	0.227

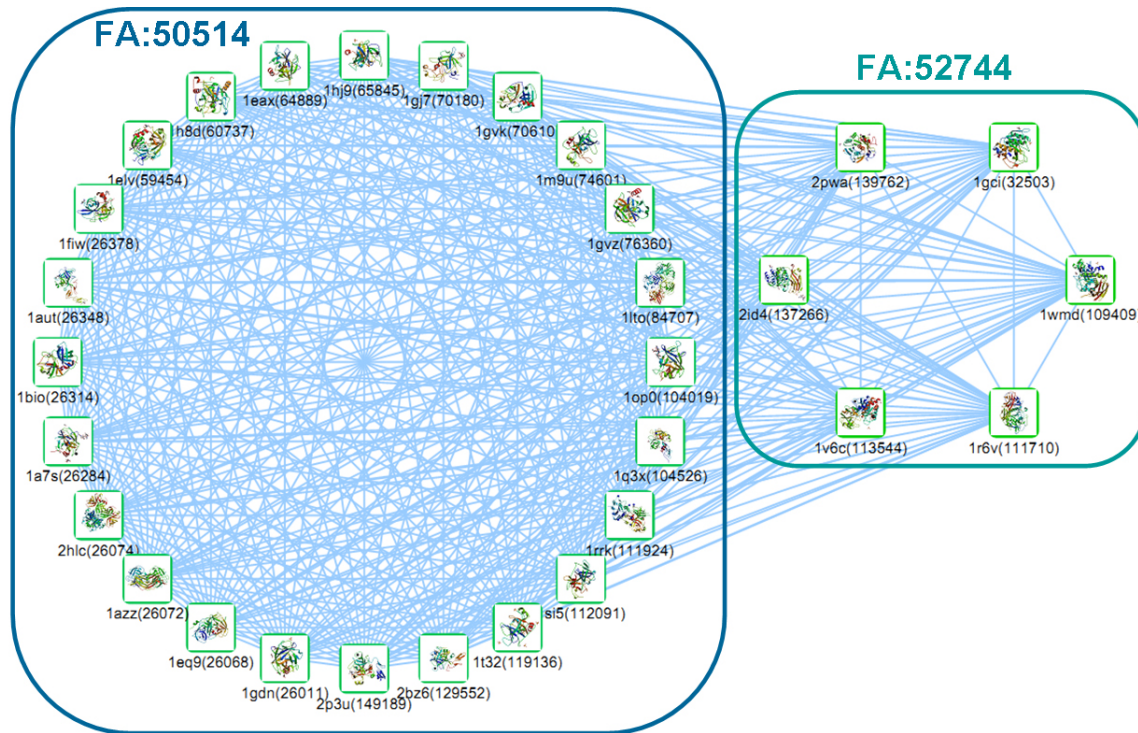
1B9R	2FKZ	37683	133688	0.72	0.217	0	0	0	0.213	0	0.179
1B9R	2FZF	37683	134437	0.72	0.264	0	0	0	0.264	0	0
1B9R	2YW6	37683	153794	0.72	0.204	0	0	0	0.211	0	0
1DOI	1EUM	37676	59507	0.72	0.19	0	0	0	0.19	0	0
1DOI	1JIG	37676	71685	0.72	0.234	0	0	0	0.234	0	0
1DOI	1JI4	37676	77117	0.72	0.224	0	0.267	0	0.224	0	0.267
1DOI	1LB3	37676	77873	0.72	0.211	0	0.444	0	0.211	0	0.444
1DOI	1LKO	37676	78063	0.72	0.239	0	0	0	0.196	0	0
1DOI	1NF4	37676	85598	0.72	0.223	0	0.615	0	0.223	0	0.615
1DOI	1O9R	37676	86706	0.72	0.221	0	0.3	0	0.221	0	0.3
1DOI	1J30	37676	90806	0.72	0.24	0	0	0	0.24	0	0
1DOI	1NNQ	37676	92006	0.72	0.262	0	0	0	0.239	0	0
1DOI	1UMN	37676	99607	0.72	0.225	0	0.233	0	0.225	0	0.233
1DOI	1VJX	37676	100837	0.72	0.232	0	0	0	0.232	0	0
1DOI	1VLG	37676	108816	0.72	0.217	0	0.667	0	0.217	0	0.667
1DOI	1TJO	37676	112461	0.72	0.206	0	0.5	0	0.206	0	0.5
1DOI	1YUZ	37676	124077	0.72	0.246	0	0.467	0	0.235	0	0.467
1DOI	1Z60	37676	124531	0.72	0.199	0	0.25	0	0.185	0	0.25
1DOI	1Z60	37676	124543	0.72	0.19	0	0.24	0	0.185	0	0.25
1DOI	1ZS3	37676	125573	0.72	0.209	0	0.385	0	0.209	0	0.455
1DOI	2FJC	37676	133559	0.72	0.233	0	0	0	0.233	0	0
1DOI	2FKZ	37676	133688	0.72	0.205	0	0	0	0.204	0	0
1DOI	2FZF	37676	134437	0.72	0.237	0	0.235	0	0.237	0	0.5
1DOI	2YW6	37676	153794	0.72	0.247	0	0.667	0	0.234	0	0.571
1I7H	1EUM	71122	59507	0.72	0.286	0	0.5	0.14	0.286	0	0.5
1I7H	1JIG	71122	71685	0.72	0.221	0	0	0.037	0.221	0	0
1I7H	1JI4	71122	77117	0.72	0.213	0	0	0.037	0.213	0	0
1I7H	1LB3	71122	77873	0.72	0.209	0	0	0.143	0.209	0	0
1I7H	1LKO	71122	78063	0.72	0.219	0	0	0	0.163	0	0.245
1I7H	1NF4	71122	85598	0.72	0.174	0	0	0.017	0.174	0	0
1I7H	1O9R	71122	86706	0.72	0.215	0	0.229	0.037	0.215	0	0.229
1I7H	1J30	71122	90806	0.72	0.203	0	0	0	0.203	0	0
1I7H	1NNQ	71122	92006	0.72	0.193	0	0	0	0.187	0	0
1I7H	1UMN	71122	99607	0.72	0.185	0	0.714	0.017	0.185	0	0.714
1I7H	1VJX	71122	100837	0.72	0.215	0	0	0	0.215	0	0
1I7H	1VLG	71122	108816	0.72	0.21	0	0.429	0.017	0.21	0	0.429
1I7H	1TJO	71122	112461	0.72	0.189	0	0.461	0	0.189	0	0.461
1I7H	1YUZ	71122	124077	0.72	0.252	0	1	0	0.175	0	0
1I7H	1Z60	71122	124531	0.72	0.193	0	0	0	0.172	0	0
1I7H	1Z60	71122	124543	0.72	0.195	0	0	0.094	0.172	0	0
1I7H	1ZS3	71122	125573	0.72	0.183	0	0.833	0	0.183	0	0.833
1I7H	2FJC	71122	133559	0.72	0.193	0	0	0.017	0.193	0	0
1I7H	2FKZ	71122	133688	0.72	0.226	0	0	0.053	0.228	0	0
1I7H	2FZF	71122	134437	0.72	0.214	0	0	0	0.214	0	0.225
1I7H	2YW6	71122	153794	0.72	0.235	0	0.333	0.037	0.212	0	0.333
1L5P	1EUM	73598	59507	0.72	0.302	0	0.364	0	0.302	0	0.364

1L5P	1JIG	73598	71685	0.72	0.248	0	0	0	0.248	0	0
1L5P	1JI4	73598	77117	0.72	0.228	0	0	0	0.228	0	0
1L5P	1LB3	73598	77873	0.72	0.199	0	0	0	0.199	0	0
1L5P	1LKO	73598	78063	0.72	0.211	0	0	0	0.192	0	0
1L5P	1NF4	73598	85598	0.72	0.191	0	0	0	0.191	0	0
1L5P	1O9R	73598	86706	0.72	0.174	0	0.32	0	0.174	0	0.32
1L5P	1J30	73598	90806	0.72	0.209	0	0	0	0.209	0	0
1L5P	1NNQ	73598	92006	0.72	0.195	0	0.368	0	0.146	0	0.429
1L5P	1UMN	73598	99607	0.72	0.242	0	0	0	0.242	0	0
1L5P	1VJX	73598	100837	0.72	0.215	0	0	0	0.215	0	0
1L5P	1VLG	73598	108816	0.72	0.209	0	0	0	0.209	0	0
1L5P	1TJO	73598	112461	0.72	0.189	0	0.296	0	0.189	0	0.296
1L5P	1YUZ	73598	124077	0.72	0.228	0	0	0	0.166	0	0
1L5P	1Z60	73598	124531	0.72	0.166	0	0.391	0	0.159	0	0.391
1L5P	1Z60	73598	124543	0.72	0.178	0	0.25	0	0.159	0	0.391
1L5P	1ZS3	73598	125573	0.72	0.201	0	0.5	0	0.201	0	0.5
1L5P	2FJC	73598	133559	0.72	0.225	0	0.625	0	0.225	0	0.625
1L5P	2FKZ	73598	133688	0.72	0.201	0	0.222	0	0.212	0	0.222
1L5P	2FZF	73598	134437	0.72	0.208	0	0	0	0.208	0	0
1L5P	2YW6	73598	153794	0.72	0.191	0	0	0	0.221	0	0.6
1UTE	1DOI	42078	37676	0.717	0.194	0	0	0	0.194	0	0
1UTE	1B9R	42078	37683	0.717	0.183	0	0	0	0.183	0	0
1UTE	1I7H	42078	71122	0.717	0.34	0	0	0.094	0.34	0	0.217
1UTE	1L5P	42078	73598	0.717	0.338	0	0.444	0	0.338	0	0.444
1UTE	1WRI	42078	114838	0.717	0.336	0	0.389	0.024	0.336	0	0.389
1UTE	1XLQ	42078	122119	0.717	0.435	0	0	0.027	0.435	0	0
1UTE	2BT6	42078	129152	0.717	0.398	0	0.444	0.091	0.398	0	0.444
1WRI	1EUM	114838	59507	0.72	0.268	0	0.357	0.025	0.268	0	0.357
1WRI	1JIG	114838	71685	0.72	0.261	0	0	0.016	0.261	0	0
1WRI	1JI4	114838	77117	0.72	0.248	0	0.266	0.016	0.248	0	0.266
1WRI	1LB3	114838	77873	0.72	0.296	0	0.353	0.008	0.296	0	0.353
1WRI	1LKO	114838	78063	0.72	0.27	0	0.25	0	0.269	0	0.455
1WRI	1NF4	114838	85598	0.72	0.269	0	0.667	0.008	0.269	0	0.667
1WRI	1O9R	114838	86706	0.72	0.255	0	0	0.016	0.255	0	0
1WRI	1J30	114838	90806	0.72	0.233	0	0	0	0.233	0	0
1WRI	1NNQ	114838	92006	0.72	0.196	0	0.258	0	0.232	0	0.256
1WRI	1UMN	114838	99607	0.72	0.246	0	0.286	0.008	0.246	0	0.286
1WRI	1VJX	114838	100837	0.72	0.242	0	0	0	0.242	0	0
1WRI	1VLG	114838	108816	0.72	0.27	0	0	0.066	0.27	0	0
1WRI	1TJO	114838	112461	0.72	0.274	0	0	0	0.274	0	0
1WRI	1YUZ	114838	124077	0.72	0.22	0	0.265	0	0.193	0	0.265
1WRI	1Z60	114838	124531	0.72	0.162	0	0	0	0.145	0	0.417
1WRI	1Z60	114838	124543	0.72	0.176	0	0.417	0.044	0.145	0	0.417
1WRI	1ZS3	114838	125573	0.72	0.18	0	0	0	0.18	0	0
1WRI	2FJC	114838	133559	0.72	0.192	0	0	0.008	0.192	0	0
1WRI	2FKZ	114838	133688	0.72	0.198	0	0	0.025	0.2	0	0

1WRI	2FZF	114838	134437	0.72	0.212	0	0	0	0.212	0	0
1WRI	2YW6	114838	153794	0.72	0.214	0	0.556	0.016	0.199	0	0.556
1XLQ	1EUM	122119	59507	0.72	0.267	0	0.3	0.068	0.267	0	0.3
1XLQ	1JIG	122119	71685	0.72	0.27	0	0	0.044	0.27	0	0
1XLQ	1JI4	122119	77117	0.72	0.256	0	0	0.044	0.256	0	0
1XLQ	1LB3	122119	77873	0.72	0.276	0	0	0.064	0.276	0	0
1XLQ	1LKO	122119	78063	0.72	0.265	0	0	0	0.285	0	0.75
1XLQ	1NF4	122119	85598	0.72	0.271	0	0	0.021	0.271	0	0
1XLQ	1O9R	122119	86706	0.72	0.247	0	0	0.044	0.247	0	0
1XLQ	1J30	122119	90806	0.72	0.273	0	0	0	0.273	0	0
1XLQ	1NNQ	122119	92006	0.72	0.191	0	0	0	0.285	0	0
1XLQ	1UMN	122119	99607	0.72	0.281	0	0	0.021	0.281	0	0
1XLQ	1VJX	122119	100837	0.72	0.291	0	0	0	0.291	0	0
1XLQ	1VLG	122119	108816	0.72	0.315	0	0	0.064	0.315	0	0
1XLQ	1TJO	122119	112461	0.72	0.266	0	0	0	0.266	0	0
1XLQ	1YUZ	122119	124077	0.72	0.255	0	0.385	0	0.192	0	0.225
1XLQ	1Z60	122119	124531	0.72	0.171	0	0	0	0.163	0	0
1XLQ	1Z60	122119	124543	0.72	0.211	0	0	0.144	0.163	0	0
1XLQ	1ZS3	122119	125573	0.72	0.214	0	0	0	0.214	0	0
1XLQ	2FJC	122119	133559	0.72	0.226	0	0.333	0.021	0.226	0	0.333
1XLQ	2FKZ	122119	133688	0.72	0.224	0	0	0.068	0.235	0	0
1XLQ	2FZF	122119	134437	0.72	0.241	0	0	0	0.241	0	0
1XLQ	2YW6	122119	153794	0.72	0.237	0	0	0.044	0.224	0	0
2BT6	1EUM	129152	59507	0.72	0.278	0	0.75	0.169	0.278	0	0.75
2BT6	1JIG	129152	71685	0.72	0.257	0	0.5	0.108	0.257	0	0.5
2BT6	1JI4	129152	77117	0.72	0.31	0	0	0.108	0.31	0	0.625
2BT6	1LB3	129152	77873	0.72	0.274	0	0.191	0.214	0.274	0	0.191
2BT6	1LKO	129152	78063	0.72	0.279	0	0	0	0.31	0	0
2BT6	1NF4	129152	85598	0.72	0.293	0	0	0.052	0.293	0	0
2BT6	1O9R	129152	86706	0.72	0.297	0	0.5	0.108	0.297	0	0.5
2BT6	1J30	129152	90806	0.72	0.22	0	0	0	0.22	0	0
2BT6	1NNQ	129152	92006	0.72	0.256	0	0	0	0.286	0	0.353
2BT6	1UMN	129152	99607	0.72	0.289	0	0.262	0.052	0.289	0	0.262
2BT6	1VJX	129152	100837	0.72	0.304	0	0	0	0.304	0	0
2BT6	1VLG	129152	108816	0.72	0.337	0	0.246	0.073	0.337	0	0.246
2BT6	1TJO	129152	112461	0.72	0.25	0	0.375	0	0.25	0	0.461
2BT6	1YUZ	129152	124077	0.72	0.263	0	0	0	0.321	0	0.286
2BT6	1Z60	129152	124531	0.72	0.304	0	0.5	0	0.299	0	0.5
2BT6	1Z60	129152	124543	0.72	0.306	0	0.357	0.311	0.299	0	0.5
2BT6	1ZS3	129152	125573	0.72	0.251	0	0	0	0.251	0	0
2BT6	2FJC	129152	133559	0.72	0.23	0	0	0.052	0.23	0	0
2BT6	2FKZ	129152	133688	0.72	0.186	0	0	0.169	0.195	0	0
2BT6	2FZF	129152	134437	0.72	0.232	0	0.235	0	0.232	0	0.235
2BT6	2YW6	129152	153794	0.72	0.244	0	0.4	0.108	0.196	0	0.244
2QFR	1DOI	150751	37676	0.717	0.208	0	0.625	0	0.149	0	0.625
2QFR	1B9R	150751	37683	0.717	0.18	0	0	0	0.127	0	0

2QFR	1I7H	150751	71122	0.717	0.176	0	0	0.017	0.139	0	0
2QFR	1L5P	150751	73598	0.717	0.165	0	0	0	0.137	0	0
2QFR	1WRI	150751	114838	0.717	0.147	0	0	0.186	0.117	0	0.444
2QFR	1XLQ	150751	122119	0.717	0.186	0	0.312	0.021	0.143	0	0.4
2QFR	2BT6	150751	129152	0.717	0.179	0	0	0.052	0.146	0	0

From BSM score with 70% threshold, 2PWA, 1GCI, 1WMD, 1R6V, 1V6C, and 2ID4 are associated with FA:52744 which is Subtilases family and all others are associated with FA:50514 which is Eukaryotic proteases family

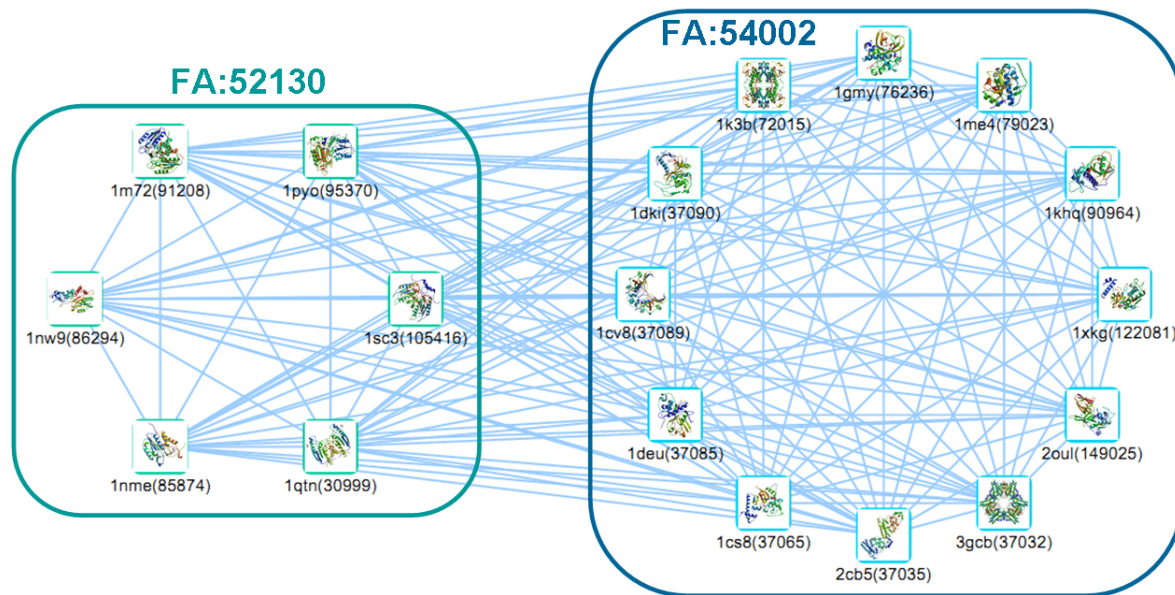


PDB1	PDB2	DM1	DM2	GPsim	domainTM	domainDali	domainSEQ	domainPHY	gpTM	gpDali	gpSEQ
1A7S	1WMD	26284	109409	0.72	0.248	0	0.232	0.055	0.189	0	0.333
1A7S	1R6V	26284	111710	0.72	0.141	0.015	0.294	0.026	0.141	0.015	0.294
1A7S	1V6C	26284	113544	0.72	0.178	0	0.375	0	0.178	0	0.375
1A7S	2ID4	26284	137266	0.72	0.228	0	0.29	0.091	0.166	0	0.29
1A7S	2PWA	26284	139762	0.72	0.265	0	0.857	0.055	0.265	0	0.857
1A7S	1GCI	26284	32503	0.72	0.261	0	0.3	0.026	0.261	0	0.3
1AUT	1WMD	26348	109409	0.72	0.266	0	0	0.044	0.202	0	0.256
1AUT	1R6V	26348	111710	0.72	0.147	0	0.308	0.021	0.147	0	0.308
1AUT	1V6C	26348	113544	0.72	0.199	0	0.857	0	0.199	0	0.857
1AUT	2ID4	26348	137266	0.72	0.249	0	0.571	0.163	0.192	0	0.278
1AUT	2PWA	26348	139762	0.72	0.276	0	0.625	0.044	0.276	0	0.625
1AUT	1GCI	26348	32503	0.72	0.279	0	0.296	0.021	0.279	0	0.296
1AZZ	1WMD	26072	109409	0.72	0.249	0	0.344	0.066	0.201	0	0.344
1AZZ	1R6V	26072	111710	0.72	0.147	0.021	0.4	0.032	0.147	0.021	0.4
1AZZ	2PWA	26072	139762	0.72	0.275	0	0	0.066	0.275	0	0
1AZZ	1V6C	26072	113544	0.72	0.188	0	0.255	0	0.188	0	0.255
1AZZ	1GCI	26072	32503	0.72	0.259	0	0.6	0.032	0.259	0	0.6
1AZZ	2ID4	26072	137266	0.72	0.208	0	0.4	0.162	0.182	0	0.417
1BIO	1WMD	26314	109409	0.72	0.255	0	0.312	0.044	0.196	0	0.312
1BIO	1R6V	26314	111710	0.72	0.136	0	0.222	0.021	0.136	0	0.222
1BIO	1V6C	26314	113544	0.72	0.195	0	0	0	0.195	0	0
1BIO	2ID4	26314	137266	0.72	0.239	0	0	0.163	0.173	0	0
1BIO	2PWA	26314	139762	0.72	0.272	0	0.222	0.044	0.272	0	0.222
1BIO	1GCI	26314	32503	0.72	0.281	0	0	0.021	0.281	0	0
1EAX	1WMD	64889	109409	0.72	0.27	0	0	0.034	0.222	0	0
1EAX	1R6V	64889	111710	0.72	0.143	0.013	0	0.017	0.143	0.013	0
1EAX	1V6C	64889	113544	0.72	0.229	0	0.5	0	0.229	0	0.375

1EAX	2ID4	64889	137266	0.72	0.249	0	0	0.322	0.193	0	0.461
1EAX	2PWA	64889	139762	0.72	0.269	0	0.308	0.034	0.269	0	0.308
1ELV	1WMD	59454	109409	0.72	0.239	0	0.387	0.055	0.204	0	0.387
1ELV	1R6V	59454	111710	0.72	0.15	0.001	0.286	0.026	0.18	0.015	0.5
1ELV	1V6C	59454	113544	0.72	0.194	0	0	0	0.226	0	0.194
1ELV	2ID4	59454	137266	0.72	0.23	0	1	0.091	0.2	0	0.184
1ELV	2PWA	59454	139762	0.72	0.282	0	0.4	0.055	0.28	0	0.5
1EQ9	1WMD	26068	109409	0.72	0.236	0	0.312	0	0.202	0	0.333
1EQ9	1R6V	26068	111710	0.72	0.143	0.004	0.385	0	0.143	0.004	0.385
1EQ9	1V6C	26068	113544	0.72	0.197	0	0.286	0	0.197	0	0.286
1EQ9	2ID4	26068	137266	0.72	0.228	0	0.389	0	0.168	0	0.389
1EQ9	2PWA	26068	139762	0.72	0.276	0	0.45	0	0.276	0	0.45
1EQ9	1GCI	26068	32503	0.72	0.265	0	0.429	0	0.265	0	0.429
1FIW	1WMD	26378	109409	0.72	0.262	0	0.333	0.044	0.21	0	0.231
1FIW	1R6V	26378	111710	0.72	0.137	0.02	0.438	0.021	0.148	0.02	0.438
1FIW	1V6C	26378	113544	0.72	0.223	0	0.385	0	0.208	0	0.385
1FIW	2ID4	26378	137266	0.72	0.249	0	0.32	0.163	0.188	0	0.32
1FIW	2PWA	26378	139762	0.72	0.289	0	0.269	0.044	0.283	0	0.269
1FIW	1GCI	26378	32503	0.72	0.288	0	0	0.021	0.283	0	0
1GCI	1OP0	32503	104019	0.72	0.285	0	0.529	0.026	0.285	0	0.529
1GCI	1Q3X	32503	104526	0.72	0.306	0	0.4	0.021	0.25	0	0.375
1GCI	1RRK	32503	111924	0.72	0.271	0	0.3	0.017	0.23	0.049	0.455
1GCI	1SI5	32503	112091	0.72	0.307	0	0.353	0.021	0.307	0	0.353
1GCI	1T32	32503	119136	0.72	0.29	0	0	0.008	0.29	0	0
1GCI	2BZ6	32503	129552	0.72	0.296	0	0	0.026	0.296	0	0
1GCI	2P3U	32503	149189	0.72	0.274	0	0	0.026	0.268	0	0
1GCI	1GVK	32503	70610	0.72	0.301	0	0.4	0.026	1	0	0.4
1GCI	1GVZ	32503	76360	0.72	0.293	0	0	0.017	0.293	0	0
1GCI	1LTO	32503	84707	0.72	0.3	0	0.429	0.008	0.3	0	0.429
1GCI	1H8D	32503	60737	0.72	0.279	0	0	0.026	0.298	0	0
1GCI	1EAX	32503	64889	0.72	0.305	0	0.312	0.017	0.305	0	0.312
1GCI	1ELV	32503	59454	0.72	0.275	0	0.625	0.026	0.251	0	0.318
1GCI	1M9U	32503	74601	0.72	0.291	0	0.333	0.021	0.291	0	0.333
1GCI	1GJ7	32503	70180	0.72	0.292	0	0.286	0.026	0.351	0	0.286
1GCI	1HJ9	32503	65845	0.72	0.284	0	0.522	0.026	0.284	0	0.522
1GDN	1WMD	26011	109409	0.72	0.233	0	0.35	0	0.199	0	0.35
1GDN	1R6V	26011	111710	0.72	0.143	0.006	0.333	0	0.143	0.006	0.333
1GDN	1V6C	26011	113544	0.72	0.199	0	0.36	0	0.199	0	0.36
1GDN	2ID4	26011	137266	0.72	0.23	0	0	0	0.179	0	0.385
1GDN	2PWA	26011	139762	0.72	0.274	0	0.4	0	0.274	0	0.4
1GDN	1GCI	26011	32503	0.72	0.268	0	0.345	0	0.268	0	0.345
1GJ7	1WMD	70180	109409	0.72	0.253	0	0.205	0.055	0.019	0	0.205
1GJ7	1R6V	70180	111710	0.72	0.144	0	0.257	0.026	0.013	0	0.375
1GJ7	1V6C	70180	113544	0.72	0.215	0	0.556	0	0.011	0	0.556
1GJ7	2ID4	70180	137266	0.72	0.246	0	0.8	0.091	0.019	0	0.556
1GJ7	2PWA	70180	139762	0.72	0.283	0	0.294	0.055	0.028	0	0.294
1GVK	1WMD	70610	109409	0.72	0.269	0	0.188	0.055	0.007	0	0.333
1GVK	1R6V	70610	111710	0.72	0.147	0.018	0.371	0.026	0.004	0.018	0.371
1GVK	1V6C	70610	113544	0.72	0.2	0	0.4	0	0.007	0	0.4
1GVK	2ID4	70610	137266	0.72	0.244	0	0.286	0.091	0.006	0	0.333
1GVK	2PWA	70610	139762	0.72	0.28	0	0.273	0.055	0.011	0	0.273
1GVZ	1WMD	76360	109409	0.72	0.237	0	0	0.034	0.203	0	0.571
1GVZ	1R6V	76360	111710	0.72	0.149	0.008	0.571	0.017	0.149	0.008	0.571
1GVZ	1V6C	76360	113544	0.72	0.195	0	0.4	0	0.195	0	0.4
1GVZ	2ID4	76360	137266	0.72	0.237	0	0.667	0.092	0.176	0	0.461
1GVZ	2PWA	76360	139762	0.72	0.258	0	0.296	0.034	0.258	0	0.296
1H8D	1WMD	60737	109409	0.72	0.259	0	0.412	0.055	0.223	0	0.444
1H8D	1R6V	60737	111710	0.72	0.151	0.013	0.243	0.026	0.148	0.013	0.243
1H8D	1V6C	60737	113544	0.72	0.209	0	0.257	0	0.205	0	0.257
1H8D	2ID4	60737	137266	0.72	0.274	0	0.273	0.091	0.192	0	0

1H8D	2PWA	60737	139762	0.72	0.282	0	0.455	0.055	0.286	0	0.375
1HJ9	1WMD	65845	109409	0.72	0.245	0	0.467	0.055	0.181	0	0.258
1HJ9	1R6V	65845	111710	0.72	0.134	0.019	0.35	0.026	0.134	0.019	0.35
1HJ9	1V6C	65845	113544	0.72	0.187	0	0.295	0	0.187	0	0.295
1HJ9	2ID4	65845	137266	0.72	0.228	0	0.344	0.091	0.176	0	0.344
1HJ9	2PWA	65845	139762	0.72	0.269	0	0.333	0.055	0.269	0	0.333
1LTO	1WMD	84707	109409	0.72	0.24	0	0.444	0.016	0.194	0	0.245
1LTO	1R6V	84707	111710	0.72	0.149	0.014	0.352	0.008	0.149	0.014	0.352
1LTO	1V6C	84707	113544	0.72	0.212	0	0.545	0	0.212	0	0.545
1LTO	2ID4	84707	137266	0.72	0.242	0	0.333	0.144	0.184	0	0.333
1LTO	2PWA	84707	139762	0.72	0.281	0	0.4	0.016	0.281	0	0.4
1M9U	1WMD	74601	109409	0.72	0.251	0	1	0.044	0.193	0	0.333
1M9U	1R6V	74601	111710	0.72	0.143	0	0.282	0.021	0.143	0	0.282
1M9U	1V6C	74601	113544	0.72	0.226	0	0.262	0	0.226	0	0.262
1M9U	2ID4	74601	137266	0.72	0.241	0	0.302	0.163	0.186	0	0.302
1M9U	2PWA	74601	139762	0.72	0.283	0	0.8	0.044	0.283	0	0.8
1OP0	1WMD	104019	109409	0.72	0.274	0	0.333	0.055	0.215	0	0.333
1OP0	1V6C	104019	113544	0.72	0.188	0	0.556	0	0.188	0	0.556
1OP0	2ID4	104019	137266	0.72	0.209	0	0.316	0.091	0.176	0	0.316
1OP0	1R6V	104019	111710	0.72	0.145	0	0.5	0.026	0.145	0	0.5
1OP0	2PWA	104019	139762	0.72	0.277	0	0.444	0.055	0.277	0	0.444
1Q3X	2ID4	104526	137266	0.72	0.239	0	0.289	0.04	0.236	0	0.289
1Q3X	1WMD	104526	109409	0.72	0.254	0	0.333	0.044	0.208	0	0.333
1Q3X	1V6C	104526	113544	0.72	0.224	0	0.241	0	0.225	0	0.241
1Q3X	1R6V	104526	111710	0.72	0.147	0.005	0.5	0.021	0.151	0.003	0.5
1Q3X	2PWA	104526	139762	0.72	0.277	0	0.222	0.044	0.279	0	0.625
1R6V	2BZ6	111710	129552	0.72	0.289	0.003	0.545	0.026	0.289	0.003	0.545
1R6V	1T32	111710	119136	0.72	0.314	0.008	0.4	0.008	0.314	0.008	0.4
1R6V	2P3U	111710	149189	0.72	0.306	0	0.267	0.026	0.267	0	0.267
1R6V	1RRK	111710	111924	0.72	0.31	0	0.444	0.017	0.294	0.045	0.538
1R6V	1S15	111710	112091	0.72	0.308	0.009	0.278	0.021	0.308	0.009	0.278
1RRK	2PWA	111924	139762	0.72	0.266	0	0	0.034	0.382	0.05	0
1RRK	1V6C	111924	113544	0.72	0.23	0	0.4	0	0.279	0.05	0.4
1RRK	2ID4	111924	137266	0.72	0.239	0	0.8	0.092	0.251	0.043	0.667
1S15	2PWA	112091	139762	0.72	0.274	0	0	0.044	0.274	0	0
1S15	2ID4	112091	137266	0.72	0.231	0	0.242	0.163	0.152	0	0.242
1S15	1V6C	112091	113544	0.72	0.189	0	0.318	0	0.189	0	0.318
1T32	2PWA	119136	139762	0.72	0.273	0	0.389	0.016	0.273	0	0.389
1T32	2ID4	119136	137266	0.72	0.227	0	0.833	0.144	0.166	0	0.389
1V6C	2BZ6	113544	129552	0.72	0.31	0	0	0	0.31	0	0.178
1V6C	2P3U	113544	149189	0.72	0.306	0	0.556	0	0.318	0	0.312
1V6C	1T32	113544	119136	0.72	0.322	0	0.333	0	0.322	0	0.333
1WMD	1S15	109409	112091	0.72	0.3	0	0	0.044	0.316	0	0
1WMD	2BZ6	109409	129552	0.72	0.271	0	0	0.055	0.298	0	0.389
1WMD	2P3U	109409	149189	0.72	0.305	0	0.533	0.055	0.309	0	0.5
1WMD	1RRK	109409	111924	0.72	0.286	0	0	0.034	0.237	0.033	0
1WMD	1T32	109409	119136	0.72	0.287	0	0.26	0.016	0.303	0	0.26
2BZ6	2PWA	129552	139762	0.72	0.283	0	0.353	0.055	0.283	0	0.353
2BZ6	2ID4	129552	137266	0.72	0.231	0	0.227	0.091	0.186	0	0.227
2HLC	1GCI	26074	32503	0.72	0.274	0	0.538	0.004	0.274	0	0.538
2HLC	2ID4	26074	137266	0.72	0.237	0	0.438	0.069	0.182	0.004	0.438
2HLC	2PWA	26074	139762	0.72	0.275	0	0	0.008	0.275	0	0
2HLC	1WMD	26074	109409	0.72	0.241	0	0.282	0.008	0.192	0	0.282
2HLC	1R6V	26074	111710	0.72	0.145	0.019	0.288	0.004	0.145	0.019	0.288
2HLC	1V6C	26074	113544	0.72	0.209	0	0	0	0.209	0	0
2ID4	2P3U	137266	149189	0.72	0.316	0	0.333	0.091	0.369	0	0.667
2PWA	2P3U	139762	149189	0.72	0.308	0	0	0.055	0.299	0	0

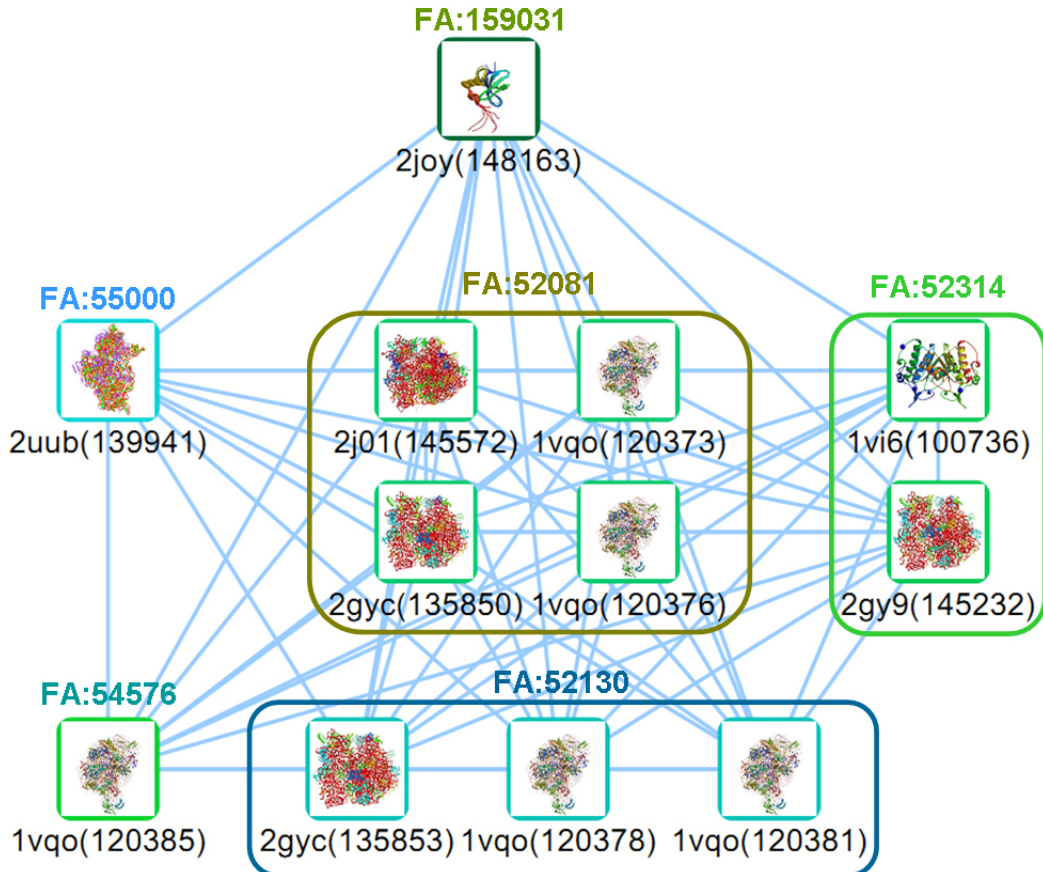
From BSM score with 70% threshold, 1M72, 1PYO, 1SC3, 1QTN, 1NME, and 1NW9 are associated with FA:52130 which is Caspase catalytic domain family and all others are associated with FA:54002 which is Papain-like family



PDB1	PDB2	DM1	DM2	GPsim	domainTM	domainDali	domainSEQ	domainPHY	gpTM	gpDali	gpSEQ
1CS8	1NME	37065	85874	0.731	0.261	0	0.375	0.296	0.311	0	0.375
1CS8	1SC3	37065	105416	0.731	0.299	0	0.28	0.052	0.296	0	0.28
1CS8	1NW9	37065	86294	0.731	0.31	0	0.294	0.396	0.307	0	0.294
1CS8	1M72	37065	91208	0.731	0.266	0	0.25	0.296	0.266	0	0.25
1CS8	1PYO	37065	95370	0.731	0.295	0	0.296	0.214	0.263	0	0.296
1CV8	1NME	37089	85874	0.731	0.277	0	0.625	0	0.274	0	0.5
1CV8	1SC3	37089	105416	0.731	0.264	0.001	0.438	0	0.273	0.001	0.438
1CV8	1PYO	37089	95370	0.731	0.279	0	0.243	0	0.291	0	0.243
1CV8	1M72	37089	91208	0.731	0.266	0.001	0.375	0	0.266	0.001	0.375
1CV8	1NW9	37089	86294	0.731	0.273	0.001	0.333	0	0.351	0.001	0.333
1DEU	1NME	37085	85874	0.731	0.273	0	0.133	0.322	0.308	0	0.231
1DEU	1SC3	37085	105416	0.731	0.291	0	0.278	0.124	0.273	0	0.267
1DEU	1M72	37085	91208	0.731	0.275	0	0.444	0.322	0.275	0	0.444
1DEU	1NW9	37085	86294	0.731	0.315	0	0	0.446	0.372	0	0
1DEU	1PYO	37085	95370	0.731	0.28	0	0.179	0.377	0.275	0	0.179
1DKI	1NME	37090	85874	0.731	0.294	0	0.22	0	0.285	0	0.22
1DKI	1SC3	37090	105416	0.731	0.293	0	0.345	0	0.302	0	0.429
1DKI	1PYO	37090	95370	0.731	0.267	0	0	0	0.298	0	0
1DKI	1M72	37090	91208	0.731	0.276	0	0.259	0	0.276	0	0.259
1DKI	1NW9	37090	86294	0.731	0.299	0	0	0	0.402	0	0.545
1GMY	1NME	76236	85874	0.731	0.257	0	0.8	0.505	0.285	0	0.8
1GMY	1SC3	76236	105416	0.731	0.29	0	0.286	0.069	0.277	0	0.389
1GMY	1NW9	76236	86294	0.731	0.317	0	0.294	0.557	0.35	0	0.75
1GMY	1M72	76236	91208	0.731	0.249	0	0	0.505	0.249	0	0
1GMY	1PYO	76236	95370	0.731	0.283	0	0.375	0.717	0.255	0	0.4
1K3B	1NME	72015	85874	0.731	0.245	0	0	0.557	0.242	0	0.364
1K3B	1SC3	72015	105416	0.731	0.281	0	0.271	0.091	0.2	0	0.265
1K3B	1M72	72015	91208	0.731	0.264	0	0.4	0.557	0.185	0	0.333
1K3B	1NW9	72015	86294	0.731	0.272	0	0.571	0.426	0.316	0	0.333
1K3B	1PYO	72015	95370	0.731	0.272	0	0.282	0.674	0.218	0	0.222
1KHQ	1SC3	90964	105416	0.731	0.243	0	0.389	0.06	0.251	0	0.389
1KHQ	1PYO	90964	95370	0.731	0.28	0	0	0.112	0.285	0	0.24

1KHQ	1M72	90964	91208	0.731	0.253	0	0.5	0.181	0.253	0	0.5
1M72	1XKG	91208	122081	0.731	0.259	0	0	0	0.209	0	0
1M72	2OUL	91208	149025	0.731	0.299	0	0.267	0	0.299	0	0.267
1ME4	1NME	79023	85874	0.731	0.278	0	0.5	0.037	0.275	0	0.5
1ME4	1SC3	79023	105416	0.731	0.249	0	0	0.149	0.25	0	0
1ME4	1PYO	79023	95370	0.731	0.273	0	0.5	0	0.274	0	0.5
1ME4	1NW9	79023	86294	0.731	0.289	0	0.429	0.001	0.379	0	0.256
1ME4	1M72	79023	91208	0.731	0.27	0	0	0.037	0.27	0	0
1NME	1KHQ	85874	90964	0.731	0.292	0	0.571	0.181	0.212	0	0.571
1NME	1XKG	85874	122081	0.731	0.227	0.001	0.385	0	0.152	0.001	0.385
1NME	2OUL	85874	149025	0.731	0.267	0	0.263	0	0.203	0	0.263
1NW9	1XKG	86294	122081	0.731	0.254	0	0.195	0	0.145	0	0.31
1NW9	2OUL	86294	149025	0.731	0.306	0.006	0.206	0.012	0.167	0	0.226
1NW9	1KHQ	86294	90964	0.731	0.277	0.01	0	0.194	0.199	0	0.438
1PYO	1XKG	95370	122081	0.731	0.266	0.003	0.417	0	0.177	0.003	0.385
1PYO	2OUL	95370	149025	0.731	0.289	0	0	0.025	0.201	0	0.267
1QTN	3GCB	30999	37032	0.731	0.21	0	0.625	0.163	0.137	0	0.625
1QTN	1XKG	30999	122081	0.731	0.24	0.001	0.281	0	0.193	0.001	0.455
1QTN	2OUL	30999	149025	0.731	0.287	0	0.316	0	0.213	0	0.333
1QTN	1DEU	30999	37085	0.731	0.276	0	0.5	0.322	0.202	0	0.391
1QTN	1CS8	30999	37065	0.731	0.224	0	0.196	0.296	0.16	0	0.196
1QTN	1CV8	30999	37089	0.731	0.326	0	0.348	0	0.276	0	0.273
1QTN	1DKI	30999	37090	0.731	0.228	0	0.267	0	0.18	0	0.267
1QTN	1GMY	30999	76236	0.731	0.245	0	0.417	0.505	0.185	0	0.417
1QTN	1K3B	30999	72015	0.731	0.257	0	0	0.557	0.303	0	0.25
1QTN	1ME4	30999	79023	0.731	0.304	0	0.273	0.037	0.213	0	0.194
1QTN	1KHQ	30999	90964	0.731	0.259	0	0	0.181	0.218	0	0
1QTN	2CB5	30999	37035	0.731	0.194	0	0.461	0.163	0.139	0	0.444
1SC3	1XKG	105416	122081	0.731	0.251	0.003	0.333	0	0.179	0.001	0.333
1SC3	2OUL	105416	149025	0.731	0.287	0.003	0	0.021	0.224	0.003	0.216
2CB5	1NME	37035	85874	0.731	0.284	0	0.28	0.163	0.323	0	0.28
2CB5	1SC3	37035	105416	0.731	0.319	0	0.467	0.106	0.355	0	0.263
2CB5	1PYO	37035	95370	0.731	0.286	0	0.28	0.212	0.346	0	0.28
2CB5	1M72	37035	91208	0.731	0.285	0	0.417	0.163	0.285	0	0.417
2CB5	1NW9	37035	86294	0.731	0.311	0	0.5	0.276	0.422	0	0.246
3GCB	1NME	37032	85874	0.731	0.267	0	0.167	0.163	0.329	0	0.167
3GCB	1M72	37032	91208	0.731	0.279	0	0.5	0.163	0.279	0	0.5
3GCB	1PYO	37032	95370	0.731	0.275	0	0.268	0.212	0.336	0	0.37
3GCB	1NW9	37032	86294	0.731	0.323	0	0.4	0.276	0.338	0	0.278
3GCB	1SC3	37032	105416	0.731	0.319	0	0	0.106	0.336	0	0

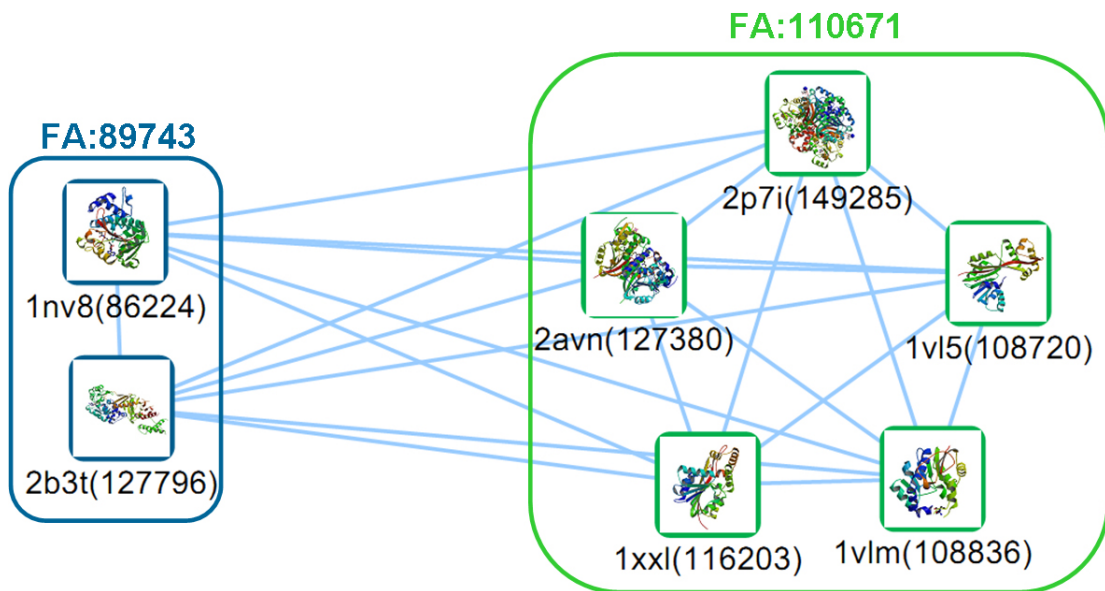
From BSM score with 70% threshold, 2JOY is associated with FA:159031 which is Ribosomal protein L14e. 2UUB is associated with FA:55000 which is Ribosomal protein S10. 1VQO (suid:120385) is associated with FA:54576 which is Ribosomal protein L31e. 1VI6 and 2GY9 are associated with FA52314 which is Ribosomal protein S2. 2GYC and two 1VQOs consisting of sunid 120378 and 120381 are associated with FA:50105 which is Ribosomal proteins L24p and L21e. 2J01, 1VQO (sunid: 120373, 120376), and 2GYC are associated with FA:52081 which is Ribosomal proteins L15p and L18e.



PDB1	PDB2	DM1	DM2	GPsim	domainTM	domainDali	domainSEQ	domainPHY	gpTM	gpDali	gpSEQ
1VI6	2JOY	100736	148163	0.703	0.356	0	0	0	0.356	0	0
1VI6	1VQO	100736	120381	0.703	0.275	0	0	0.026	0.205	0.028	0.75
1VI6	1VQO	100736	120373	0.703	0.272	0	0.312	0	0.205	0.028	0.75
1VI6	1VQO	100736	120378	0.703	0.283	0	0	0	0.205	0.028	0.75
1VI6	1VQO	100736	120376	0.703	0.37	0.005	0	0	0.205	0.028	0.75
1VI6	2J01	100736	145572	0.703	0.256	0	0	0.001	0.296	0.011	0.4
1VI6	2GYC	100736	135853	0.703	0.266	0	0	0.162	0.308	0.03	0.467
1VI6	2UUB	100736	139941	0.703	0.273	0	0	0.097	0.707	0.286	0.25
1VI6	1VQO	100736	120385	0.703	0.35	0	0.381	0	0.205	0.028	0.75
1VI6	2GYC	100736	135850	0.703	0.193	0	0	0.162	0.308	0.03	0.467
1VQO	2JOY	120381	148163	0.703	0.385	0.024	0.5	0	0.405	0	0.417
1VQO	2JOY	120376	148163	0.703	0.277	0	0	0	0.405	0	0.417
1VQO	2JOY	120385	148163	0.703	0.301	0	0.227	0	0.405	0	0.417
1VQO	2J01	120381	145572	0.703	0.157	0	0.455	0.149	0.286	0	0.444
1VQO	1VQO	120381	120385	0.703	0.316	0	0.409	0	1	0.125	1
1VQO	1VQO	120376	120381	0.703	0.266	0	0	0	1	0.125	1

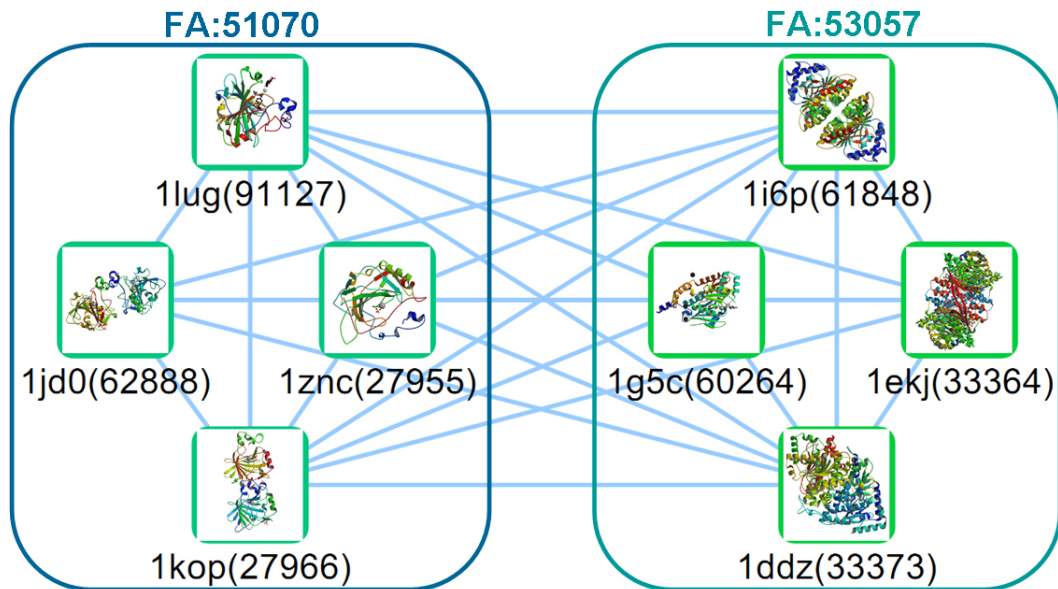
1VQO	2GY9	120381	145232	0.703	0.191	0	0	0.012	0.248	0	0.333
1VQO	2JOY	120378	148163	0.703	0.392	0.033	0.242	0	0.405	0	0.417
1VQO	2UUB	120381	139941	0.703	0.237	0	0.667	0.106	0.248	0	0.353
1VQO	2JOY	120373	148163	0.703	0.269	0	0.226	0	0.405	0	0.417
1VQO	1VQO	120373	120381	0.703	0.215	0	0.303	0	1	0.125	1
1VQO	2GYC	120381	135850	0.703	0.19	0	0	0.017	0.255	0	0.385
1VQO	1VQO	120373	120378	0.703	0.216	0	0.283	0	1	0.125	1
1VQO	2UUB	120373	139941	0.703	0.227	0	0	0	0.248	0	0.353
1VQO	2GY9	120373	145232	0.703	0.185	0	0	0	0.248	0	0.333
1VQO	2GYC	120373	135853	0.703	0.198	0	0	0	0.255	0	0.385
1VQO	1VQO	120373	120385	0.703	0.34	0	0	0	1	0.125	1
1VQO	2UUB	120376	139941	0.703	0.288	0	0	0	0.248	0	0.353
1VQO	1VQO	120376	120378	0.703	0.314	0	0.263	0	1	0.125	1
1VQO	2GYC	120376	135853	0.703	0.227	0	0	0	0.255	0	0.385
1VQO	1VQO	120376	120385	0.703	0.354	0	0	0	1	0.125	1
1VQO	2GY9	120376	145232	0.703	0.216	0.006	0	0	0.248	0	0.333
1VQO	2UUB	120378	139941	0.703	0.222	0	0	0	0.248	0	0.353
1VQO	2J01	120378	145572	0.703	0.16	0	0.309	0	0.286	0	0.444
1VQO	1VQO	120378	120385	0.703	0.275	0	0.25	0	1	0.125	1
1VQO	2GYC	120378	135850	0.703	0.187	0	0	0	0.255	0	0.385
1VQO	2GY9	120378	145232	0.703	0.16	0	0	0	0.248	0	0.333
1VQO	2GYC	120385	135850	0.703	0.185	0	0	0	0.255	0	0.385
1VQO	2GYC	120385	135853	0.703	0.237	0	0	0	0.255	0	0.385
1VQO	2GY9	120385	145232	0.703	0.14	0	0	0	0.248	0	0.333
1VQO	2UUB	120385	139941	0.703	0.296	0	0.75	0	0.248	0	0.353
1VQO	2J01	120385	145572	0.703	0.185	0	0	0	0.286	0	0.444
2GY9	2JOY	145232	148163	0.703	0.346	0	0.263	0	0.323	0	0.4
2GY9	2J01	145232	145572	0.703	0.229	0	0	0.028	0.297	0	0.35
2GYC	2JOY	135850	148163	0.703	0.245	0	0	0	0.295	0	0.545
2GYC	2JOY	135853	148163	0.703	0.383	0.024	0.444	0	0.295	0	0.545
2GYC	2GYC	135850	135853	0.703	0.21	0	0.444	0.722	1	0.147	1
2GYC	2GY9	135850	145232	0.703	0.152	0	0	0.448	0.296	0	0.364
2GYC	2UUB	135850	139941	0.703	0.211	0	0.375	0.214	0.318	0	0.467
2GYC	2J01	135853	145572	0.703	0.156	0	0	0.013	0.276	0.054	0.25
2GYC	2GY9	135853	145232	0.703	0.167	0	0.323	0.448	0.296	0	0.364
2GYC	2UUB	135853	139941	0.703	0.204	0	0.667	0.214	0.318	0	0.467
2J01	2JOY	145572	148163	0.703	0.256	0	0	0	0.225	0	0.5
2UUB	2JOY	139941	148163	0.703	0.257	0	0	0	0.351	0	0.3
2UUB	2GY9	139941	145232	0.703	0.148	0	0	0.367	0.916	0.382	0.444
2UUB	2J01	139941	145572	0.703	0.165	0	0.219	0.367	0.283	0.014	0.346

From BSM score with 70% threshold, 1NV8 and 2B3T are associated with FA:89743 which is N5-glutamine methyltransferase, HemK family and all others are associated with FA:110671 which is UbiE/COQ5 methyltransferase family



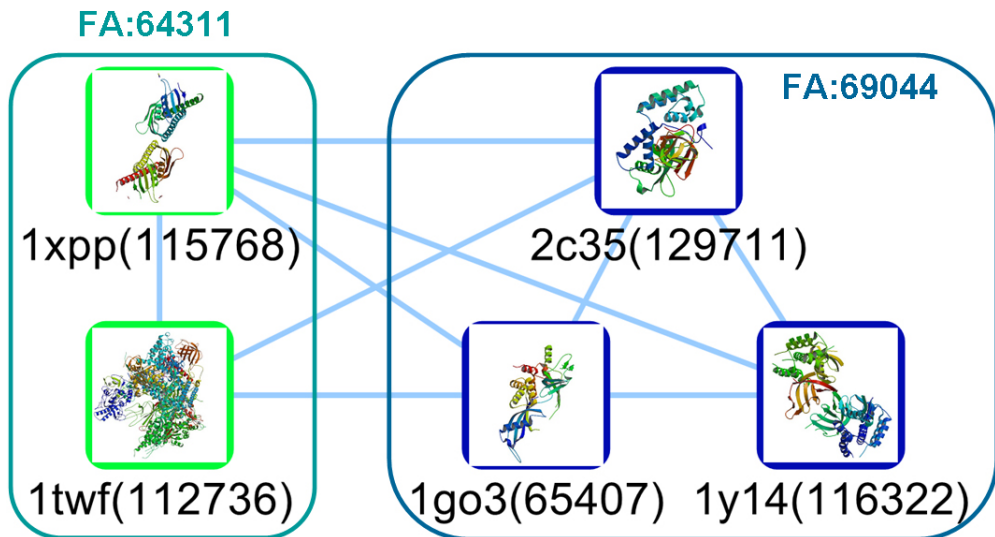
PDB1	PDB2	Sunid1	Sunid2	GPsim	dmTM	dmDali	dmSEQ	dmPHY	gpTM	gpDali	gpSEQ
1NV8	2AVN	86224	127380	0.723	0.529	0.132	0.267	0	0.527	0.132	0.267
1NV8	1VLM	86224	108836	0.723	0.481	0.126	0.316	0.008	0.481	0.126	0.316
1NV8	1VL5	86224	108720	0.723	0.547	0.171	0.269	0.09	0.547	0.171	0.269
1NV8	1XXL	86224	116203	0.723	0.543	0.177	0.302	0.09	0.543	0.177	0.302
1NV8	2P7I	86224	149285	0.723	0.565	0.133	0.37	0	0.565	0.132	0.37
2B3T	1VL5	127796	108720	0.723	0.489	0.204	0.229	0.057	0.489	0.206	0.23
2B3T	1VLM	127796	108836	0.723	0.469	0.157	0.209	0.012	0.469	0.158	0.209
2B3T	1XXL	127796	116203	0.723	0.489	0.208	0.25	0.057	0.489	0.208	0.25
2B3T	2AVN	127796	127380	0.723	0.489	0.15	0.344	0	0.489	0.15	0.312
2B3T	2P7I	127796	149285	0.723	0.601	0.166	0.4	0	0.604	0.166	0.4

From BSM score with 70% threshold, 1JD0, 1KOP, 1LUG, and 1ZNC are associated with FA:51070 which is Carbonic anhydrase family and all others are associated with FA:53057 which is beta-carbonic anhydrase, cab family



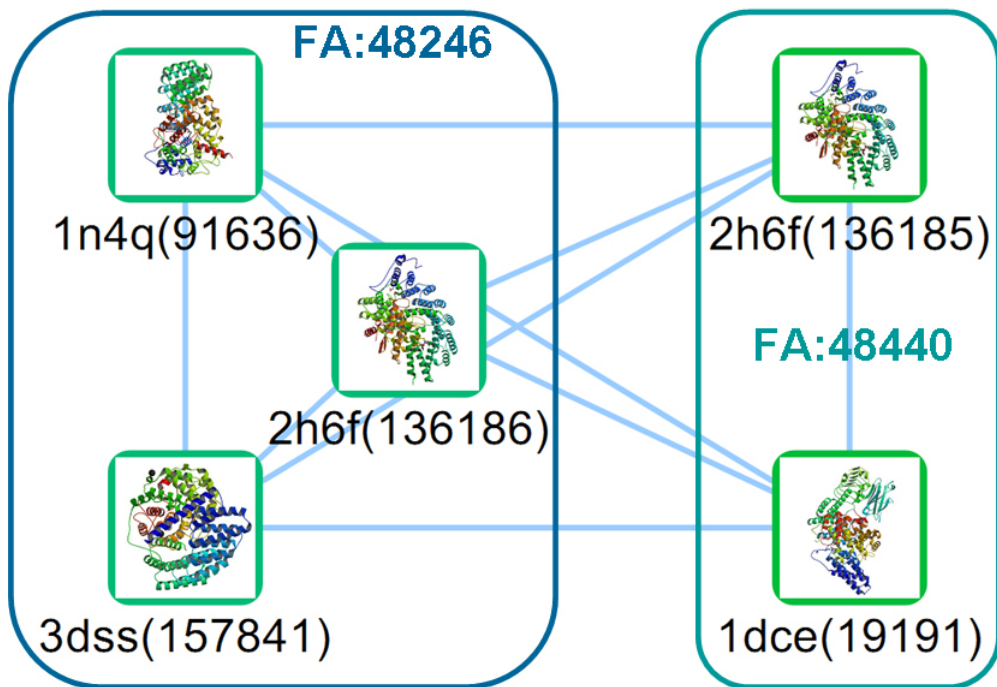
PDB1	PDB2	Sunid1	Sunid2	GPsim	dmTM	dmDali	dmSEQ	dmPHY	gpTM	gpDali	gpSEQ
1JD0	1EKJ	62888	33364	0.739	0.211	0	0.231	0.123	0.211	0	0.231
1JD0	1DDZ	62888	33373	0.739	0.221	0	0.4	0.223	0.327	0	0.667
1JD0	1G5C	62888	60264	0.739	0.203	0	0	0.079	0.203	0	0
1JD0	1I6P	62888	61848	0.739	0.244	0	0.333	0.223	0.244	0	0.333
1KOP	1G5C	27966	60264	0.739	0.254	0	0.357	0.066	0.254	0	0.357
1KOP	1EKJ	27966	33364	0.739	0.238	0	0	0.103	0.238	0	0
1KOP	1I6P	27966	61848	0.739	0.216	0	0.571	0.186	0.216	0	0.571
1KOP	1DDZ	27966	33373	0.739	0.199	0	0	0.186	0.167	0	0
1LUG	1EKJ	91127	33364	0.739	0.236	0	0.833	0.123	0.236	0	0.833
1LUG	1DDZ	91127	33373	0.739	0.201	0	0.6	0.223	0.323	0	0.364
1LUG	1G5C	91127	60264	0.739	0.221	0	0.667	0.079	0.221	0	0.667
1LUG	1I6P	91127	61848	0.739	0.247	0	0.296	0.223	0.247	0	0.296
1ZNC	1G5C	27955	60264	0.739	0.284	0	0	0.034	0.284	0	0
1ZNC	1DDZ	27955	33373	0.739	0.239	0	0.385	0.094	0.196	0	0
1ZNC	1I6P	27955	61848	0.739	0.279	0	0.538	0.094	0.279	0	0.538
1ZNC	1EKJ	27955	33364	0.739	0.277	0	0.417	0.053	0.277	0	0.417

From BSM score with 70% threshold, 1XPP and 1TWF are associated with FA:64311 which is RBP11/RpoL and all others are associated with FA:69044 which is RNA polymerase II subunit RBP4 (RpoF)



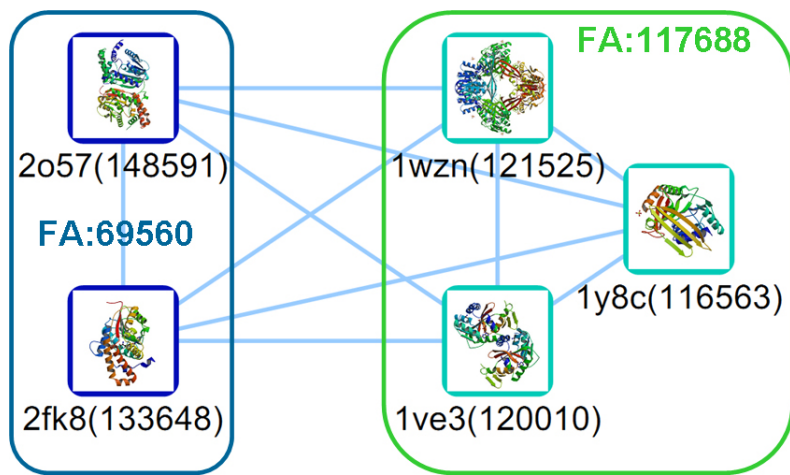
PDB1	PDB2	DM1	DM2	GPsim	domainTM	domainDali	domainSEQ	domainPHY	gpTM	gpDali	gpSEQ
1TWF	1GO3	112736	65407	0.719	0.269	0	0	0	0.071	0.028	0.333
1TWF	2C35	112736	129711	0.719	0.263	0	0	0.429	0.365	0.024	0.357
1TWF	1Y14	112736	116322	0.719	0.263	0	0	0.069	0.374	0.029	0.221
1XPP	1GO3	115768	65407	0.719	0.293	0	0	0	0.28	0.033	0.364
1XPP	2C35	115768	129711	0.719	0.26	0	0	0	0.26	0.018	0
1XPP	1Y14	115768	116322	0.719	0.25	0	0.5	0	0.25	0.023	0.5

From BSM score with 70% threshold, 2H6F and 1DCE are associated with FA:48440 which is Protein prenyltransferase and all others are associated with FA:48246 which is Protein prenyltransferases



PDB1	PDB2	DM1	DM2	GPsim	domainTM	domainDali	domainSEQ	domainPHY	gpTM	gpDali	gpSEQ
1DCE	3DSS	19191	157841	0.729	0.347	0.021	0.375	0.541	0.94	0.345	1
1DCE	1N4Q	19191	91636	0.729	0.344	0.023	0.308	0.541	0.743	0.219	0.269
1DCE	2H6F	19191	136186	0.729	0.301	0.038	0.412	0.541	0.741	0.221	0.269
1N4Q	2H6F	91636	136185	0.729	0.346	0.029	0.379	0.322	0.979	0.458	0.928
2H6F	3DSS	136185	157841	0.729	0.311	0.021	0.237	0.322	0.767	0.279	0.269
2H6F	2H6F	136185	136186	0.729	0.295	0.04	0.556	0.322	1	0.507	1

From BSM score with 70% threshold, 2O57 and 2FK8 are associated with FA:69560 which is Mycolic acid cyclopropane synthase and all others are associated with FA:117688 which is CAC2371-like family and also known to be similar overall fold to the Glycine N-methyltransferase (scop_fa 53348) and mRNA cap (Guanine N-7) methyltransferase (scop_fa 102560) families.



PDB1	PDB2	DM1	DM2	GPsim	domainTM	domainDali	domainSEQ	domainPHY	gpTM	gpDali	gpSEQ
2FK8	1VE3	133648	120010	0.703	0.573	0.205	0.198	0	0.572	0.204	0.198
2FK8	1WZN	133648	121525	0.703	0.592	0.206	0.393	0.008	0.59	0.205	0.393
2FK8	1Y8C	133648	116563	0.703	0.594	0.192	0.268	0.008	0.592	0.191	0.308
2O57	1VE3	148591	120010	0.703	0.586	0.239	0.294	0	0.586	0.245	0.294
2O57	1WZN	148591	121525	0.703	0.589	0.223	0.333	0	0.589	0.224	0.333
2O57	1Y8C	148591	116563	0.703	0.585	0.216	0.379	0	0.585	0.224	0.379

[S-11] OMIM dataset

Disease and gene product information used in OMIM-based experiments

OMIM	DISEASE	UniProt ID	Name of Protein
104300	ALZHEIMER DISEASE	P78380	Oxidized low-density lipoprotein receptor 1
104300	ALZHEIMER DISEASE	P49810	Presenilin-2
104300	ALZHEIMER DISEASE	P05067	Amyloid beta A4 protein
105200	AMYLOIDOSIS	P02647	Apolipoprotein A-I
105201	AMYLOIDOSIS	P02671	Fibrinogen alpha chain
105202	AMYLOIDOSIS	P61626	Lysozyme C
105830	ANGELMAN SYNDROME	P51608	Methyl-CpG-binding protein 2
105830	ANGELMAN SYNDROME	Q05086	Ubiquitin-protein ligase E3A
105830	ANGELMAN SYNDROME	O60312	Probable phospholipid-transporting ATPase VA
109100	AUTOIMMUNE DISEASE	P16410	Cytotoxic T-lymphocyte protein 4
109100	AUTOIMMUNE DISEASE	Q15116	Programmed cell death protein 1
109100	AUTOIMMUNE DISEASE	O60602	Toll-like receptor 5
109100	AUTOIMMUNE DISEASE	O43918	Autoimmune regulator
109800	BLADDER CANCER	P22607	Fibroblast growth factor receptor 3
109800	BLADDER CANCER	P06400	Retinoblastoma-associated protein
109800	BLADDER CANCER	P01112	GTPase HRas
114480	BREAST CANCER	P38398	Breast cancer type 1 susceptibility protein
114480	BREAST CANCER	P51587	Breast cancer type 2 susceptibility protein
114480	BREAST CANCER	Q9BX63	Fanconi anemia group J protein
114480	BREAST CANCER	Q96BI1	Solute carrier family 22 member 18 Phosphatidylinositol-4,5-bisphosphate 3-kinase catalytic subunit alpha isoform
114480	BREAST CANCER	P42336	
114480	BREAST CANCER	Q06609	DNA repair protein RAD51 homolog 1
114480	BREAST CANCER	O60934	Nibrin
114550	HEPATOCELLULAR CARCINOMA	Q16667	Cyclin-dependent kinase inhibitor 3
114550	HEPATOCELLULAR CARCINOMA	P08581	Hepatocyte growth factor receptor
114550	HEPATOCELLULAR CARCINOMA	Q9ULD2	Mitochondrial tumor suppressor 1
114550	HEPATOCELLULAR CARCINOMA	O15169	Axin-1
115150	CFC SYNDROME	P15056	B-Raf proto-oncogene serine/threonine-protein kinase
115150	CFC SYNDROME	Q02750	Dual specificity mitogen-activated protein kinase kinase 1
115150	CFC SYNDROME	P01116	GTPase KRas
115150	CFC SYNDROME	P36507	Dual specificity mitogen-activated protein kinase kinase 2
115200	DILATED CARDIOMYOPATHY 1A	O75112	LIM domain-binding protein 3
115200	DILATED CARDIOMYOPATHY 1A	P02545	Lamin-A/C
115200	DILATED CARDIOMYOPATHY 1A	P12883	Myosin-7
115200	DILATED CARDIOMYOPATHY 1A NONINSULIN-DEPENDENT	P68032	Actin, alpha cardiac muscle 1
125853	DIABETES MELLITUS NONINSULIN-DEPENDENT	Q9HC96	Calpain-10
125853	DIABETES MELLITUS NONINSULIN-DEPENDENT	P14672	Solute carrier family 2, facilitated glucose transporter member 4
125853	DIABETES MELLITUS	P35680	Hepatocyte nuclear factor 1-beta

	NONINSULIN-DEPENDENT		
125853	DIABETES MELLITUS NONINSULIN-DEPENDENT	P06213	Insulin receptor
125853	DIABETES MELLITUS NONINSULIN-DEPENDENT	P35568	Insulin receptor substrate 1
125853	DIABETES MELLITUS NONINSULIN-DEPENDENT	Q9UQF2	C-jun-amino-terminal kinase-interacting protein 1
125853	DIABETES MELLITUS NONINSULIN-DEPENDENT	Q13562	Neurogenic differentiation factor 1
125853	DIABETES MELLITUS NONINSULIN-DEPENDENT	P52945	Pancreas/duodenum homeobox protein 1
125853	DIABETES MELLITUS NONINSULIN-DEPENDENT	Q16821	Protein phosphatase 1 regulatory subunit 3A
125853	DIABETES MELLITUS NONINSULIN-DEPENDENT	O15357	Phosphatidylinositol-3,4,5-trisphosphate 5-phosphatase 2
125853	DIABETES MELLITUS NONINSULIN-DEPENDENT	Q8IWU4	Zinc transporter 8
125853	DIABETES MELLITUS	P22413	Ectonucleotide pyrophosphatase/phosphodiesterase family member 1
130600	ELLIPTOCYTOSIS 2	P02730	Band 3 anion transport protein
130600	ELLIPTOCYTOSIS 2	P11277	Spectrin beta chain, erythrocyte
130600	ELLIPTOCYTOSIS 2	P02549	Spectrin alpha chain, erythrocyte
133239	ESCC	Q9Y238	Deleted in lung and esophageal cancer protein 1
133239	ESCC	P37173	TGF-beta receptor type-2
133239	ESCC	Q9NZC7	WW domain-containing oxidoreductase
133239	ESCC	P04637	Cellular tumor antigen p53
142623	HIRSCHSPRUNG DISEASE	P42892	Endothelin-converting enzyme 1
142623	HIRSCHSPRUNG DISEASE	P14138	Endothelin-3
142623	HIRSCHSPRUNG DISEASE	P24530	Endothelin B receptor
142623	HIRSCHSPRUNG DISEASE	P32004	Neural cell adhesion molecule L1
142623	HIRSCHSPRUNG DISEASE	Q99748	Neurturin
142623	HIRSCHSPRUNG DISEASE	P07949	Proto-oncogene tyrosine-protein kinase receptor ret
142623	HIRSCHSPRUNG DISEASE	P39905	Glial cell line-derived neurotrophic factor
144700	RENAL CELL CARCINOMA 1	Q96SL1	Disrupted in renal carcinoma protein 2
144700	RENAL CELL CARCINOMA 1	P49789	Bis(5'-adenosyl)-triphosphatase
144700	RENAL CELL CARCINOMA 1	Q96EW2	HSPB1-associated protein 1
144700	RENAL CELL CARCINOMA 1	O15527	N-glycosylase/DNA lyase
144700	RENAL CELL CARCINOMA 1	P40337	Von Hippel-Lindau disease tumor suppressor
144700	RENAL CELL CARCINOMA 1	Q8WU17	RING finger protein 139
145900	DEJERINE-SOTTAS SYNDROME	P08034	Gap junction beta-1 protein
145900	DEJERINE-SOTTAS SYNDROME	P11161	Early growth response protein 2
145900	DEJERINE-SOTTAS SYNDROME	Q01453	Peripheral myelin protein 22
145900	DEJERINE-SOTTAS SYNDROME	Q9BXMO	Periaxin
145900	DEJERINE-SOTTAS SYNDROME HYPOGONADOTROPIC	P25189	Myelin P0 protein
146110	HYPOGONADISM HYPOGONADOTROPIC	P11362	Basic fibroblast growth factor receptor 1
146110	HYPOGONADISM HYPOGONADOTROPIC	P30968	Gonadotropin-releasing hormone receptor
146110	HYPOGONADISM HYPOGONADOTROPIC	Q6X4W1	Nasal embryonic luteinizing hormone-releasing hormone factor
146110	HYPOGONADISM LACRIMOAURICULODENTODIGITAL SYNDROME	Q969F8	KiSS-1 receptor
149730	SYNDROME	P21802	Fibroblast growth factor receptor 2

	LACRIMO AURICULO DENTO DIGITAL		
149730	SYNDROME LACRIMO AURICULO DENTO DIGITAL	P22607	Fibroblast growth factor receptor 3
149730	SYNDROME	O15520	Fibroblast growth factor 10
155255	MEDULLOBLASTOMA	P25054	Adenomatous polyposis coli protein
155255	MEDULLOBLASTOMA	Q9Y6C5	Protein patched homolog 2
155255	MEDULLOBLASTOMA	Q9UMX1	Suppressor of fused homolog
155255	MEDULLOBLASTOMA	P35222	Catenin beta-1
158000	MONILETHRIX	Q14533	Keratin, type II cuticular Hb1
158000	MONILETHRIX	P78385	Keratin, type II cuticular Hb3
158000	MONILETHRIX	O43790	Keratin, type II cuticular Hb6
158810	BETHLEM MYOPATHY	P12109	Collagen alpha-1(VI) chain
158810	BETHLEM MYOPATHY	P12111	Collagen alpha-3(VI) chain
158810	BETHLEM MYOPATHY	P12110	Collagen alpha-2(VI) chain
168600	PARKINSON DISEASE	P04062	Glucosylceramidase
168600	PARKINSON DISEASE	O43464	Serine protease HTRA2, mitochondrial
168600	PARKINSON DISEASE	Q5S007	Leucine-rich repeat serine/threonine-protein kinase 2
168600	PARKINSON DISEASE	Q99497	Protein DJ-1
168600	PARKINSON DISEASE	Q9BXM7	Serine/threonine-protein kinase PINK1, mitochondrial
168600	PARKINSON DISEASE	O60260	E3 ubiquitin-protein ligase parkin
168600	PARKINSON DISEASE	Q9Y6H5	Synphilin-1
168600	PARKINSON DISEASE HYPOKALEMIC PERIODIC	P37840	Alpha-synuclein
170400	PARALYSIS HYPOKALEMIC PERIODIC	Q9Y6H6	Potassium voltage-gated channel subfamily E member 3
170400	PARALYSIS HYPOKALEMIC PERIODIC	P35499	Sodium channel protein type 4 subunit alpha
170400	PARALYSIS	Q13698	Voltage-dependent L-type calcium channel subunit alpha-1S Succinate dehydrogenase [ubiquinone] iron-sulfur subunit, mitochondrial
171300	PHEOCHROMOCYTOMA	P21912	Succinate dehydrogenase [ubiquinone] cytochrome b small subunit, mitochondrial
171300	PHEOCHROMOCYTOMA	O14521	Proto-oncogene tyrosine-protein kinase receptor ret
171300	PHEOCHROMOCYTOMA	P07949	Von Hippel-Lindau disease tumor suppressor
176807	PROSTATE CANCER	O96017	Serine/threonine-protein kinase Chk2
176807	PROSTATE CANCER	P29323	Ephrin type-B receptor 2 Phosphatidylinositol-3,4,5-trisphosphate 3-phosphatase and dual-specificity protein phosphatase PTEN
176807	PROSTATE CANCER	P60484	2-5A-dependent ribonuclease
176807	PROSTATE CANCER	Q05823	Zinc phosphodiesterase ELAC protein 2
176807	PROSTATE CANCER	P50539	MAX-interacting protein 1
180300	RHEUMATOID ARTHRITIS	Q9UBC1	NF-kappa-B inhibitor-like protein 1
180300	RHEUMATOID ARTHRITIS	Q9UM07	Protein-arginine deiminase type-4
180300	RHEUMATOID ARTHRITIS	Q8TDQ0	Hepatitis A virus cellular receptor 2
180300	RHEUMATOID ARTHRITIS	P11021	78 kDa glucose-regulated protein
187500	TETRALOGY OF FALLOT	Q8WW38	Zinc finger protein ZFPM2
187500	TETRALOGY OF FALLOT	P78504	Protein jagged-1
187500	TETRALOGY OF FALLOT THROMBOPHILIA VENOUS	P52952	Homeobox protein Nkx-2.5
188050	THROMBOEMBOLISM	P01008	Antithrombin-III

	THROMBOPHILIA VENOUS		
188050	THROMBOEMBOLISM	P05546	Heparin cofactor 2
	THROMBOPHILIA VENOUS		
188050	THROMBOEMBOLISM	P05121	Plasminogen activator inhibitor 1
	THROMBOPHILIA VENOUS		
188050	THROMBOEMBOLISM	P00747	Plasminogen
	THROMBOPHILIA VENOUS		
188050	THROMBOEMBOLISM	P04070	Vitamin K-dependent protein C
	PAPILLARY CARCINOMA OF		
188550	THYROID	Q16204	Coiled-coil domain-containing protein 6
	PAPILLARY CARCINOMA OF		
188550	THYROID	Q8TBA6	Golgin subfamily A member 5
	PAPILLARY CARCINOMA OF		
188550	THYROID	Q13772	Nuclear receptor coactivator 4
	PAPILLARY CARCINOMA OF		
188550	THYROID	P04629	High affinity nerve growth factor receptor
	PAPILLARY CARCINOMA OF		
188550	THYROID	Q15154	Pericentriolar material 1 protein
	PAPILLARY CARCINOMA OF		
188550	THYROID	Q8IUD2	ELKS/RAB6-interacting/CAST family member 1
	PAPILLARY CARCINOMA OF		
188550	THYROID	P07949	Proto-oncogene tyrosine-protein kinase receptor ret
	PAPILLARY CARCINOMA OF		
188550	THYROID	Q92734	Protein TFG
	PAPILLARY CARCINOMA OF		
188550	THYROID	O15164	Transcription intermediary factor 1-alpha
	PAPILLARY CARCINOMA OF		
188550	THYROID	P06753	Tropomyosin alpha-3 chain
	PAPILLARY CARCINOMA OF		
188550	THYROID	P12270	Nucleoprotein TPR
	PAPILLARY CARCINOMA OF		
188550	THYROID	Q9UPN9	E3 ubiquitin-protein ligase TRIM33
	PAPILLARY CARCINOMA OF		
188550	THYROID	P14373	Zinc finger protein RFP
	FAMILIAL HYPERTROPHIC		
192600	CARDIOMYOPATHY	P56539	Caveolin-3
	FAMILIAL HYPERTROPHIC		
192600	CARDIOMYOPATHY	P10916	Myosin regulatory light chain 2, ventricular/cardiac muscle isoform
	FAMILIAL HYPERTROPHIC		
192600	CARDIOMYOPATHY	P13533	Myosin-6
	FAMILIAL HYPERTROPHIC		
192600	CARDIOMYOPATHY	P12883	Myosin-7
	FAMILIAL HYPERTROPHIC		
192600	CARDIOMYOPATHY	P08590	Myosin light chain 3
	FAMILIAL HYPERTROPHIC		
192600	CARDIOMYOPATHY	Q9H1R3	Myosin light chain kinase 2, skeletal/cardiac muscle
	FAMILIAL HYPERTROPHIC		
192600	CARDIOMYOPATHY	Q9UM54	Myosin-VI
	FAMILIAL HYPERTROPHIC		
192600	CARDIOMYOPATHY	Q14896	Myosin-binding protein C, cardiac-type
	FAMILIAL HYPERTROPHIC		
192600	CARDIOMYOPATHY	O15273	Telethonin
	FAMILIAL HYPERTROPHIC		
192600	CARDIOMYOPATHY	P19429	Troponin I, cardiac muscle
	FAMILIAL HYPERTROPHIC		
192600	CARDIOMYOPATHY	P45379	Troponin T, cardiac muscle
	FAMILIAL HYPERTROPHIC		
192600	CARDIOMYOPATHY	P09493	Tropomyosin alpha-1 chain
	FAMILIAL HYPERTROPHIC		
192600	CARDIOMYOPATHY	P68032	Actin, alpha cardiac muscle 1
194050	WILLIAMS-BEUREN SYNDROME	Q9UIGO	Bromodomain adjacent to zinc finger domain protein 1B
194050	WILLIAMS-BEUREN SYNDROME	Q9BQE9	B-cell CLL/lymphoma 7 protein family member B
194050	WILLIAMS-BEUREN SYNDROME	Q9UDT6	CAP-Gly domain-containing linker protein 2

194050	WILLIAMS-BEUREN SYNDROME	P15502	Elastin
194050	WILLIAMS-BEUREN SYNDROME	O75344	FK506-binding protein 6
194050	WILLIAMS-BEUREN SYNDROME	Q9UHL9	General transcription factor II-I repeat domain-containing protein 1
194050	WILLIAMS-BEUREN SYNDROME	P78347	General transcription factor II-I
194050	WILLIAMS-BEUREN SYNDROME	Q15056	Eukaryotic translation initiation factor 4H
194050	WILLIAMS-BEUREN SYNDROME	P53667	LIM domain kinase 1
194050	WILLIAMS-BEUREN SYNDROME	P35250	Replication factor C subunit 2
194050	WILLIAMS-BEUREN SYNDROME	Q9Y4P3	Transducin beta-like protein 2
194050	WILLIAMS-BEUREN SYNDROME	Q9NP71	Williams-Beuren syndrome chromosomal region 14 protein
194050	WILLIAMS-BEUREN SYNDROME	Q96I51	Williams-Beuren syndrome chromosomal region 16 protein
194050	WILLIAMS-BEUREN SYNDROME	O43709	Uncharacterized methyltransferase WBSCR22
194050	WILLIAMS-BEUREN SYNDROME	Q9H6D5	Williams-Beuren syndrome chromosomal region 23 protein
194050	WILLIAMS-BEUREN SYNDROME	Q8N6F8	Williams-Beuren syndrome chromosomal region 27 protein
194050	WILLIAMS-BEUREN SYNDROME NEONATAL	Q9GZY6	Linker for activation of T-cells family member 2
202370	ADRENOLEUKODYSTROPHY NEONATAL	Q92968	Peroxisomal membrane protein PEX13
202370	ADRENOLEUKODYSTROPHY NEONATAL	O43933	Peroxisome biogenesis factor 1
202370	ADRENOLEUKODYSTROPHY NEONATAL	Q7Z412	Peroxisome assembly protein 26
202370	ADRENOLEUKODYSTROPHY NEONATAL	P50542	Peroxisomal targeting signal 1 receptor
202370	ADRENOLEUKODYSTROPHY	O60683	Peroxisome assembly protein 10
203300	HERMANSKY-PUDLAK SYNDROME	O00203	AP-3 complex subunit beta-1
203300	HERMANSKY-PUDLAK SYNDROME	Q6QNY0	Biogenesis of lysosome-related organelles complex 1 subunit 3
203300	HERMANSKY-PUDLAK SYNDROME	Q96EV8	Dysbindin
203300	HERMANSKY-PUDLAK SYNDROME	Q969F9	Hermansky-Pudlak syndrome 3 protein
203300	HERMANSKY-PUDLAK SYNDROME	Q9NQG7	Hermansky-Pudlak syndrome 4 protein
203300	HERMANSKY-PUDLAK SYNDROME	Q9UPZ3	Hermansky-Pudlak syndrome 5 protein
203300	HERMANSKY-PUDLAK SYNDROME	Q86YV9	Hermansky-Pudlak syndrome 6 protein
203300	HERMANSKY-PUDLAK SYNDROME	Q92902	Hermansky-Pudlak syndrome 1 protein
203450	ALEXANDER DISEASE	P14136	Glial fibrillary acidic protein
203450	ALEXANDER DISEASE	P49821	NADH dehydrogenase [ubiquinone] flavoprotein 1, mitochondrial
203450	ALEXANDER DISEASE	P02511	Alpha-crystallin B chain
209880	CONGENITAL ONDINE CURSE	P23560	Brain-derived neurotrophic factor
209880	CONGENITAL ONDINE CURSE	P14138	Endothelin-3
209880	CONGENITAL ONDINE CURSE	Q99453	Paired mesoderm homeobox protein 2B
209880	CONGENITAL ONDINE CURSE	P07949	Proto-oncogene tyrosine-protein kinase receptor ret
209880	CONGENITAL ONDINE CURSE	P39905	Glial cell line-derived neurotrophic factor
209900	BARDET-BIEDL SYNDROME	Q9H0F7	ADP-ribosylation factor-like protein 6
209900	BARDET-BIEDL SYNDROME	Q8TAM1	Bardet-Biedl syndrome 10 protein
209900	BARDET-BIEDL SYNDROME	Q6ZW61	Bardet-Biedl syndrome 12 protein
209900	BARDET-BIEDL SYNDROME	Q8NFJ9	Bardet-Biedl syndrome 1 protein
209900	BARDET-BIEDL SYNDROME	Q9BXC9	Bardet-Biedl syndrome 2 protein
209900	BARDET-BIEDL SYNDROME	Q8N3I7	Bardet-Biedl syndrome 5 protein
209900	BARDET-BIEDL SYNDROME	Q8IWZ6	Bardet-Biedl syndrome 7 protein
209900	BARDET-BIEDL SYNDROME	Q9NPJ1	McKusick-Kaufman/Bardet-Biedl syndromes putative chaperonin

209900	BARDET-BIEDL SYNDROME	Q3SYG4	Protein PTHB1
209900	BARDET-BIEDL SYNDROME	Q8TAM2	Tetratricopeptide repeat protein 8
209900	BARDET-BIEDL SYNDROME FAMILIAL ATYPICAL	Q96RK4	Bardet-Biedl syndrome 4 protein
209950	MYCOBACTERIOSIS FAMILIAL ATYPICAL	P42701	Interleukin-12 receptor beta-1 chain
209950	MYCOBACTERIOSIS FAMILIAL ATYPICAL	P29460	Interleukin-12 subunit beta
209950	MYCOBACTERIOSIS FAMILIAL ATYPICAL	P15260	Interferon-gamma receptor alpha chain
209950	MYCOBACTERIOSIS FAMILIAL ATYPICAL	P38484	Interferon-gamma receptor beta chain
209950	MYCOBACTERIOSIS	P42224	Signal transducer and activator of transcription 1-alpha/beta
211980	ADENOCARCINOMA OF LUNG	P15056	B-Raf proto-oncogene serine/threonine-protein kinase
211980	ADENOCARCINOMA OF LUNG	Q9Y238	Deleted in lung and esophageal cancer protein 1
211980	ADENOCARCINOMA OF LUNG	P00533	Epidermal growth factor receptor
211980	ADENOCARCINOMA OF LUNG	Q96BI1	Solute carrier family 22 member 18
211980	ADENOCARCINOMA OF LUNG	P04637	Cellular tumor antigen p53
214100	ZELLWEGER SYNDROME	O60683	Peroxisome assembly protein 10
214100	ZELLWEGER SYNDROME	O75381	Peroxisomal membrane protein PEX14
214100	ZELLWEGER SYNDROME	Q9Y5Y5	Peroxisomal membrane protein PEX16
214100	ZELLWEGER SYNDROME	P40855	Peroxisomal biogenesis factor 19
214100	ZELLWEGER SYNDROME	Q7Z412	Peroxisome assembly protein 26
214100	ZELLWEGER SYNDROME	P28328	Peroxisome assembly factor 1
214100	ZELLWEGER SYNDROME	P56589	Peroxisomal biogenesis factor 3
214100	ZELLWEGER SYNDROME	P50542	Peroxisomal targeting signal 1 receptor
214100	ZELLWEGER SYNDROME	Q13608	Peroxisome assembly factor 2
214100	ZELLWEGER SYNDROME ACTH-INDEPENDENT MACRONODULAR ADRENAL	O00623	Peroxisome assembly protein 12
219080	HYPERPLASIA ACTH-INDEPENDENT MACRONODULAR ADRENAL	P84996	Protein ALEX
219080	HYPERPLASIA ACTH-INDEPENDENT MACRONODULAR ADRENAL	Q5JWF2	Guanine nucleotide-binding protein G(s) subunit alpha isoforms XLas
219080	HYPERPLASIA ACTH-INDEPENDENT MACRONODULAR ADRENAL	O95467	Neuroendocrine secretory protein 55
219080	HYPERPLASIA AUTOSOMAL RECESSIVE CUTIS	P63092	Guanine nucleotide-binding protein G(s) subunit alpha isoforms short
219100	LAXA AUTOSOMAL RECESSIVE CUTIS	O95967	EGF-containing fibulin-like extracellular matrix protein 2
219100	LAXA AUTOSOMAL RECESSIVE CUTIS	P28300	Protein-lysine 6-oxidase
219100	LAXA MITOCHONDRIAL COMPLEX IV	Q9UBX5	Fibulin-5
220110	DEFICIENCY MITOCHONDRIAL COMPLEX IV	Q12887	Protoheme IX farnesyltransferase, mitochondrial
220110	DEFICIENCY MITOCHONDRIAL COMPLEX IV	Q7KZN9	Cytochrome c oxidase assembly protein COX15 homolog
220110	DEFICIENCY MITOCHONDRIAL COMPLEX IV	P00395	Cytochrome c oxidase subunit 1
220110	DEFICIENCY MITOCHONDRIAL COMPLEX IV	P00414	Cytochrome c oxidase subunit 3
220110	DEFICIENCY	O75880	Protein SCO1 homolog, mitochondrial

	MITOCHONDRIAL COMPLEX IV		
220110	DEFICIENCY	O43819	Protein SCO2 homolog, mitochondrial
	MITOCHONDRIAL COMPLEX IV		
220110	DEFICIENCY	Q15526	Surfeit locus protein 1
	MITOCHONDRIAL COMPLEX IV		
220110	DEFICIENCY	P00403	Cytochrome c oxidase subunit 2
	PROGRESSIVE EPIDERMOLYSIS		
226650	BULLOSA JUNCTIONALIS	Q9UMD9	Collagen alpha-1(XVII) chain
	PROGRESSIVE EPIDERMOLYSIS		
226650	BULLOSA JUNCTIONALIS	Q13751	Laminin subunit beta-3
	PROGRESSIVE EPIDERMOLYSIS		
226650	BULLOSA JUNCTIONALIS	P16144	Integrin beta-4
	EPIDERMOLYSIS BULLOSA LETALIS	Q13751	Laminin subunit beta-3
226700	EPIDERMOLYSIS BULLOSA LETALIS	Q13753	Laminin subunit gamma-2
226700	EPIDERMOLYSIS BULLOSA LETALIS	Q16787	Laminin subunit alpha-3
227650	FANCONI ANEMIA	P51587	Breast cancer type 2 susceptibility protein
227650	FANCONI ANEMIA	Q9BXW9	Fanconi anemia group D2 protein
227650	FANCONI ANEMIA	O15360	Fanconi anemia group A protein
227650	FANCONI ANEMIA	Q8NB91	Fanconi anemia group B protein
227650	FANCONI ANEMIA	Q9HB96	Fanconi anemia group E protein
227650	FANCONI ANEMIA	Q9NPI8	Fanconi anemia group F protein
227650	FANCONI ANEMIA	O15287	Fanconi anemia group G protein
227650	FANCONI ANEMIA	Q9NVI1	Fanconi anemia group I protein
227650	FANCONI ANEMIA	Q9BX63	Fanconi anemia group J protein
227650	FANCONI ANEMIA	Q9NW38	E3 ubiquitin-protein ligase FANCL
227650	FANCONI ANEMIA	Q8IYD8	Fanconi anemia group M protein
227650	FANCONI ANEMIA	Q86YC2	Partner and localizer of BRCA2
227650	FANCONI ANEMIA	Q00597	Fanconi anemia group C protein
231200	GIANT PLATELET SYNDROME	P07359	Platelet glycoprotein Ib alpha chain
231200	GIANT PLATELET SYNDROME	P14770	Platelet glycoprotein IX
231200	GIANT PLATELET SYNDROME	P13224	Platelet glycoprotein Ib beta chain
235400	SYNDROME	P08603	Complement factor H
235400	ATYPICAL HEMOLYTIC UREMIC		
235400	SYNDROME	P05156	Complement factor I
235400	ATYPICAL HEMOLYTIC UREMIC		
235400	SYNDROME	P15529	Membrane cofactor protein
235400	ATYPICAL HEMOLYTIC UREMIC		
235400	SYNDROME	Q76LX8	A disintegrin and metalloproteinase with thrombospondin motifs 13
236670	WALKER-WARBURG SYNDROME	O75072	Fukutin
236670	WALKER-WARBURG SYNDROME	Q9H9S5	Fukutin-related protein
236670	WALKER-WARBURG SYNDROME	Q8WZA1	Protein O-linked-mannose beta-1,2-N-acetylglucosaminyltransferase 1
236670	WALKER-WARBURG SYNDROME	Q9UKY4	Protein O-mannosyl-transferase 2
236670	WALKER-WARBURG SYNDROME	Q9Y6A1	Protein O-mannosyl-transferase 1
236750	IDIOPATHIC HYDROPS FETALIS	P08236	Beta-glucuronidase
236750	IDIOPATHIC HYDROPS FETALIS	P04062	Glucosylceramidase
236750	IDIOPATHIC HYDROPS FETALIS	Q04446	1,4-alpha-glucan-branched enzyme
236750	IDIOPATHIC HYDROPS FETALIS	P10746	Uroporphyrinogen-III synthase
236750	IDIOPATHIC HYDROPS FETALIS	Q9NRA2	Sialin
236750	IDIOPATHIC HYDROPS FETALIS	P69905	Hemoglobin subunit alpha
242100	CONGENITAL NONBULLOUS	Q9BYJ1	Epidermis-type lipoxygenase 3

	ICHTHYOSIFORM ERYthroderma		
	CONGENITAL NONBULLOUS		
242100	ICHTHYOSIFORM ERYTHRODERMA	O75342	Arachidonate 12-lipoxygenase, 12R type
	CONGENITAL NONBULLOUS		
242100	ICHTHYOSIFORM ERYTHRODERMA	P22735	Protein-glutamine gamma-glutamyltransferase K
248600	MAPLE SYRUP URINE DISEASE	P09622	Dihydrolipoyl dehydrogenase, mitochondrial
248600	MAPLE SYRUP URINE DISEASE	P11182	Lipoamide acyltransferase component of branched-chain alpha-keto acid dehydrogenase complex, mitochondrial
248600	MAPLE SYRUP URINE DISEASE	P12694	2-oxoisovalerate dehydrogenase subunit alpha, mitochondrial
248600	MAPLE SYRUP URINE DISEASE	P21953	2-oxoisovalerate dehydrogenase subunit beta, mitochondrial
252010	DEFICIENCY	Q8N183	Mimitin, mitochondrial
	MITOCHONDRIAL COMPLEX I		
252010	DEFICIENCY	O15239	NADH dehydrogenase [ubiquinone] 1 alpha subcomplex subunit 1
	MITOCHONDRIAL COMPLEX I		
252010	DEFICIENCY	P28331	NADH-ubiquinone oxidoreductase 75 kDa subunit, mitochondrial
	MITOCHONDRIAL COMPLEX I		
252010	DEFICIENCY	O43181	NADH dehydrogenase [ubiquinone] iron-sulfur protein 4, mitochondrial
	MITOCHONDRIAL COMPLEX I		
252010	DEFICIENCY	O75251	NADH dehydrogenase [ubiquinone] iron-sulfur protein 7, mitochondrial
	MITOCHONDRIAL COMPLEX I		
252010	DEFICIENCY	P49821	NADH dehydrogenase [ubiquinone] flavoprotein 1, mitochondrial
	MITOCHONDRIAL COMPLEX I		
252010	DEFICIENCY	P03897	NADH-ubiquinone oxidoreductase chain 3
	MITOCHONDRIAL COMPLEX I		
252010	DEFICIENCY	O75306	NADH dehydrogenase [ubiquinone] iron-sulfur protein 2, mitochondrial
	MOLYBDENUM COFACTOR		
252150	DEFICIENCY	Q9NQX3	Gephyrin
	MOLYBDENUM COFACTOR		
252150	DEFICIENCY	Q9NZB8	Molybdenum cofactor biosynthesis protein 1 B
	MOLYBDENUM COFACTOR		
252150	DEFICIENCY	O96007	Molybdenum cofactor synthesis protein 2 large subunit
	MOLYBDENUM COFACTOR		
252150	DEFICIENCY	O96033	Molybdenum cofactor synthesis protein 2 small subunit
	MOLYBDENUM COFACTOR		
252150	DEFICIENCY	O14940	Molybdenum cofactor biosynthesis protein 1 A
254200	MYASTHENIA GRAVIS	P02708	Acetylcholine receptor subunit alpha
254200	MYASTHENIA GRAVIS	P11230	Acetylcholine receptor subunit beta
254200	MYASTHENIA GRAVIS	Q04844	Acetylcholine receptor subunit epsilon
254200	MYASTHENIA GRAVIS	P28329	Choline O-acetyltransferase
254200	MYASTHENIA GRAVIS	Q07001	Acetylcholine receptor subunit delta
254500	AMYLOIDOSIS	P24385	G1/S-specific cyclin-D1
	PRIMARY MYELOMA, MULTIPLE		
254500	AMYLOIDOSIS	P01857	Ig gamma-1 chain C region
	PRIMARY MYELOMA, MULTIPLE		
254500	AMYLOIDOSIS	Q15306	Interferon regulatory factor 4
	PRIMARY MYELOMA, MULTIPLE		
254500	AMYLOIDOSIS	P22607	Fibroblast growth factor receptor 3
256000	LEIGH SYNDROME	P00846	ATP synthase subunit a
256000	LEIGH SYNDROME	Q12887	Protoheme IX farnesyltransferase, mitochondrial
256000	LEIGH SYNDROME	Q7KZN9	Cytochrome c oxidase assembly protein COX15 homolog
			Succinate dehydrogenase [ubiquinone] flavoprotein subunit, mitochondrial
256000	LEIGH SYNDROME	P31040	
256000	LEIGH SYNDROME	O00217	NADH dehydrogenase [ubiquinone] iron-sulfur protein 8, mitochondrial
256000	LEIGH SYNDROME	P49821	NADH dehydrogenase [ubiquinone] flavoprotein 1, mitochondrial
256000	LEIGH SYNDROME	P03897	NADH-ubiquinone oxidoreductase chain 3

256000	LEIGH SYNDROME	Q15526	Surfeit locus protein 1
256000	LEIGH SYNDROME OSTEOPETROSIS, AUTOSOMAL	O75251	NADH dehydrogenase [ubiquinone] iron-sulfur protein 7, mitochondrial
259700	RECESSIVE 1 OSTEOPETROSIS, AUTOSOMAL	P51798	Chloride channel protein 7
259700	RECESSIVE 1 OSTEOPETROSIS, AUTOSOMAL	Q86WC4	Osteopetrosis-associated transmembrane protein 1
259700	RECESSIVE 1	Q13488	V-type proton ATPase 116 kDa subunit a isoform 3
262600	PITUITARY DWARFISM III	Q9UBX0	Homeobox expressed in ES cells 1
262600	PITUITARY DWARFISM III	O75360	Homeobox protein prophet of Pit-1
262600	PITUITARY DWARFISM III SURFACTANT METABOLISM	Q9UBR4	LIM/homeobox protein Lhx3
265120	DYSFUNCTION, PULMONARY, 1 SURFACTANT METABOLISM	P07988	Pulmonary surfactant-associated protein B
265120	DYSFUNCTION, PULMONARY, 1 SURFACTANT METABOLISM	P11686	Pulmonary surfactant-associated protein C
265120	DYSFUNCTION, PULMONARY, 1	P32927	Cytokine receptor common subunit beta
266600	INFLAMMATORY BOWEL DISEASE 1	P22301	Interleukin-10
266600	INFLAMMATORY BOWEL DISEASE 1	Q5VWK5	Interleukin-23 receptor
266600	INFLAMMATORY BOWEL DISEASE 1	Q9H015	Solute carrier family 22 member 4
266600	INFLAMMATORY BOWEL DISEASE 1	O76082	Solute carrier family 22 member 5
266600	INFLAMMATORY BOWEL DISEASE 1	Q9HC29	Nucleotide-binding oligomerization domain-containing protein 2
267430	RENAL TUBULAR DYSGENESIS	P12821	Angiotensin-converting enzyme
267430	RENAL TUBULAR DYSGENESIS	P00797	Renin
267430	RENAL TUBULAR DYSGENESIS	P30556	Type-1 angiotensin II receptor
268000	RETINITIS PIGMENTOSA	P29973	cGMP-gated cation channel alpha-1
268000	RETINITIS PIGMENTOSA	P82279	Crumbs homolog 1
268000	RETINITIS PIGMENTOSA	Q5IJ48	Crumbs homolog 2
268000	RETINITIS PIGMENTOSA	O43186	Cone-rod homeobox protein
268000	RETINITIS PIGMENTOSA	Q12866	Proto-oncogene tyrosine-protein kinase MER
268000	RETINITIS PIGMENTOSA	P08100	Rhodopsin
268000	RETINITIS PIGMENTOSA	P16499	Rod cGMP-specific 3',5'-cyclic phosphodiesterase subunit alpha
268000	RETINITIS PIGMENTOSA	P35913	Rod cGMP-specific 3',5'-cyclic phosphodiesterase subunit beta
268000	RETINITIS PIGMENTOSA	P23942	Peripherin-2
268000	RETINITIS PIGMENTOSA	P47804	RPE-retinal G protein-coupled receptor
268000	RETINITIS PIGMENTOSA	P12271	Retinaldehyde-binding protein 1
268000	RETINITIS PIGMENTOSA	Q03395	Rod outer segment membrane protein 1
268000	RETINITIS PIGMENTOSA	Q8TA86	Retinitis pigmentosa 9 protein
268000	RETINITIS PIGMENTOSA	O75445	Usherin
268220	RHABDOMYOSARCOMA 2	P23760	Paired box protein Pax-3
268220	RHABDOMYOSARCOMA 2	P23759	Paired box protein Pax-7
268220	RHABDOMYOSARCOMA 2	Q12778	Forkhead box protein O1
272200	MULTIPLE SULFATASE DEFICIENCY	P15289	Arylsulfatase A
272200	MULTIPLE SULFATASE DEFICIENCY	Q8NBK3	Sulfatase-modifying factor 1
272200	MULTIPLE SULFATASE DEFICIENCY	P15848	Arylsulfatase B
275355	SQUAMOUS CELL CARCINOMA	Q9UK53	Inhibitor of growth protein 1
275355	SQUAMOUS CELL CARCINOMA	Q9NXR8	Inhibitor of growth protein 3
275355	SQUAMOUS CELL CARCINOMA	P04637	Cellular tumor antigen p53

275355	SQUAMOUS CELL CARCINOMA	O14763	Tumor necrosis factor receptor superfamily member 10B Phosphatidylinositol-3,4,5-trisphosphate 3-phosphatase and dual-specificity protein phosphatase PTEN
275355	SQUAMOUS CELL CARCINOMA	P60484	
276300	TURCOT SYNDROME	P25054	Adenomatous polyposis coli protein
276300	TURCOT SYNDROME	P54278	Mismatch repair endonuclease PMS2
276300	TURCOT SYNDROME	P40692	DNA mismatch repair protein MLH1
276900	USHER SYNDROME, TYPE I	Q9H251	Cadherin-23
276900	USHER SYNDROME, TYPE I	Q13402	Myosin-VIIa
276900	USHER SYNDROME, TYPE I	Q96QU1	Protocadherin-15
276900	USHER SYNDROME, TYPE I	Q495M9	Usher syndrome type-1G protein
276900	USHER SYNDROME, TYPE I	Q9Y6N9	Harmonin
277580	WAARDENBURG-SHAH SYNDROME	P24530	Endothelin B receptor
277580	WAARDENBURG-SHAH SYNDROME	P56693	Transcription factor SOX-10
277580	WAARDENBURG-SHAH SYNDROME	P14138	Endothelin-3
535000	LEBER OPTIC ATROPHY	P00846	ATP synthase subunit a
535000	LEBER OPTIC ATROPHY	P00395	Cytochrome c oxidase subunit 1
535000	LEBER OPTIC ATROPHY	P00414	Cytochrome c oxidase subunit 3
535000	LEBER OPTIC ATROPHY	P00156	Cytochrome b
535000	LEBER OPTIC ATROPHY	P03886	NADH-ubiquinone oxidoreductase chain 1
535000	LEBER OPTIC ATROPHY	P03901	NADH-ubiquinone oxidoreductase chain 4L
535000	LEBER OPTIC ATROPHY	P03905	NADH-ubiquinone oxidoreductase chain 4
535000	LEBER OPTIC ATROPHY	P03915	NADH-ubiquinone oxidoreductase chain 5
535000	LEBER OPTIC ATROPHY	P03923	NADH-ubiquinone oxidoreductase chain 6
535000	LEBER OPTIC ATROPHY	P03891	NADH-ubiquinone oxidoreductase chain 2
540000	MELAS SYNDROME	P03905	NADH-ubiquinone oxidoreductase chain 4
540000	MELAS SYNDROME	P03923	NADH-ubiquinone oxidoreductase chain 6
540000	MELAS SYNDROME	P03886	NADH-ubiquinone oxidoreductase chain 1
580000	STREPTOMYCIN OTOTOXICITY	Q969Y2	tRNA modification GTPase GTPBP3, mitochondrial
580000	STREPTOMYCIN OTOTOXICITY	Q8WVM0	Dimethyladenosine transferase 1, mitochondrial
580000	STREPTOMYCIN OTOTOXICITY	O75648	Mitochondrial tRNA-specific 2-thiouridylase 1
601367	ISCHEMIC STROKE	P12821	Angiotensin-converting enzyme
601367	ISCHEMIC STROKE	P20292	Arachidonate 5-lipoxygenase-activating protein
601367	ISCHEMIC STROKE	P12259	Coagulation factor V
601367	ISCHEMIC STROKE	P05112	Interleukin-4
601367	ISCHEMIC STROKE	P24723	Protein kinase C eta type
601367	ISCHEMIC STROKE	P42898	Methylenetetrahydrofolate reductase
601367	ISCHEMIC STROKE	P00734	Prothrombin
601367	ISCHEMIC STROKE	P16109	P-selectin
601462	MYASTHENIC SYNDROME, CONGENITAL, SLOW-CHANNEL	P11230	Acetylcholine receptor subunit beta
601462	MYASTHENIC SYNDROME, CONGENITAL, SLOW-CHANNEL	Q07001	Acetylcholine receptor subunit delta
601462	MYASTHENIC SYNDROME, CONGENITAL, SLOW-CHANNEL	Q04844	Acetylcholine receptor subunit epsilon
601462	MYASTHENIC SYNDROME, CONGENITAL, SLOW-CHANNEL	P02708	Acetylcholine receptor subunit alpha
601495	AGAMMAGLOBULINEMIA, NON-BRUTON TYPE, AUTOSOMAL	P15814	Immunoglobulin lambda-like polypeptide 1

	RECESSIVE		
601495	AGAMMAGLOBULINEMIA, NON-BRUTON TYPE, AUTOSOMAL RECESSIVE	Q8IWT6	Leucine-rich repeat-containing protein 8A
601495	AGAMMAGLOBULINEMIA, NON-BRUTON TYPE, AUTOSOMAL RECESSIVE	P11912	B-cell antigen receptor complex-associated protein alpha-chain
601539	DISORDERS PEROXISOME BIOGENESIS	O60683	Peroxisome assembly protein 10
601539	DISORDERS PEROXISOME BIOGENESIS	O00623	Peroxisome assembly protein 12
601539	DISORDERS PEROXISOME BIOGENESIS	Q9Y5Y5	Peroxisomal membrane protein PEX16
601539	DISORDERS PEROXISOME BIOGENESIS	P40855	Peroxisomal biogenesis factor 19
601539	DISORDERS PEROXISOME BIOGENESIS	O43933	Peroxisome biogenesis factor 1
601539	DISORDERS PEROXISOME BIOGENESIS	Q7Z412	Peroxisome assembly protein 26
601539	DISORDERS PEROXISOME BIOGENESIS	P28328	Peroxisome assembly factor 1
601539	DISORDERS PEROXISOME BIOGENESIS	P56589	Peroxisomal biogenesis factor 3
601539	DISORDERS PEROXISOME BIOGENESIS	O00628	Peroxisomal targeting signal 2 receptor
601539	DISORDERS NEURAL TUBE DEFECTS,	Q13608	Peroxisome assembly factor 2
601634	FOLATE-SENSITIVE NEURAL TUBE DEFECTS,	P11586	C-1-tetrahydrofolate synthase, cytoplasmic
601634	FOLATE-SENSITIVE NEURAL TUBE DEFECTS,	Q99707	Methionine synthase
601634	FOLATE-SENSITIVE NEURAL TUBE DEFECTS,	P42898	Methylenetetrahydrofolate reductase
601634	FOLATE-SENSITIVE	Q9UBK8	Methionine synthase reductase, mitochondrial
601665	OBESITY LEANNESS	O00253	Agouti-related protein
601665	OBESITY LEANNESS	P41159	Leptin
601665	OBESITY LEANNESS	P32245	Melanocortin receptor 4
601665	OBESITY LEANNESS	P37231	Peroxisome proliferator-activated receptor gamma
601665	OBESITY LEANNESS	Q15466	Nuclear receptor subfamily 0 group B member 2
601665	OBESITY LEANNESS	P55916	Mitochondrial uncoupling protein 3
601665	OBESITY LEANNESS TRICHOThIODYSTROPHY,	P01189	Corticotropin-lipotropin
601675	PHOTOSENSITIVE TRICHOThIODYSTROPHY,	P19447	TFIIP basal transcription factor complex helicase XPB subunit
601675	PHOTOSENSITIVE TRICHOThIODYSTROPHY,	Q6ZY4	General transcription factor IIH subunit 5
601675	PHOTOSENSITIVE	P18074	TFIIP basal transcription factor complex helicase subunit
603174	HOMOCYSTEINEMIA	Q99707	Methionine synthase
603174	HOMOCYSTEINEMIA	Q9Y4U1	Methylmalonic aciduria and homocystinuria type C protein
603174	HOMOCYSTEINEMIA	P42898	Methylenetetrahydrofolate reductase
603174	HOMOCYSTEINEMIA PSEUDOhypoparathyroidism,	P35520	Cystathione beta-synthase
603233	TYPE IB PSEUDOhypoparathyroidism,	P84996	Protein ALEX
603233	TYPE IB PSEUDOhypoparathyroidism,	Q5JWF2	Guanine nucleotide-binding protein G(s) subunit alpha isoforms XLas
603233	TYPE IB	P63092	Guanine nucleotide-binding protein G(s) subunit alpha isoforms short

	PSEUDOHYPOPARATHYROIDISM, 603233 TYPE IB PSEUDOHYPOPARATHYROIDISM, 603233 TYPE IB	O95467 O14662	Neuroendocrine secretory protein 55 Syntaxin-16
603554	OMENN SYNDROME	Q96SD1	Protein artemis
603554	OMENN SYNDROME	P15918	V(DJ) recombination-activating protein 1
603554	OMENN SYNDROME	P55895	V(DJ) recombination-activating protein 2
603896	OVARIOLEUKODYSTROPHY	Q14232	Translation initiation factor eIF-2B subunit alpha
603896	OVARIOLEUKODYSTROPHY	P49770	Translation initiation factor eIF-2B subunit beta
603896	OVARIOLEUKODYSTROPHY	Q9UI10	Translation initiation factor eIF-2B subunit delta
603896	OVARIOLEUKODYSTROPHY	Q13144	Translation initiation factor eIF-2B subunit epsilon
603896	OVARIOLEUKODYSTROPHY CATARACT, AUTOSOMAL DOMINO	Q9NR50	Translation initiation factor eIF-2B subunit gamma
604219	MatchT CATARACT, AUTOSOMAL DOMINO	Q13515	Phakinin
604219	MatchT CATARACT, AUTOSOMAL DOMINO	P43320	Beta-crystallin B2
604219	MatchT CATARACT, AUTOSOMAL DOMINO	P07315	Gamma-crystallin C
604219	MatchT CATARACT, AUTOSOMAL DOMINO	P07320	Gamma-crystallin D
604219	MatchT	P02489	Alpha-crystallin A chain
604229	PETERS ANOMALY	Q16678	Cytochrome P450 1B1
604229	PETERS ANOMALY	Q12948	Forkhead box protein C1
604229	PETERS ANOMALY	P26367	Paired box protein Pax-6
604229	PETERS ANOMALY	Q99697	Pituitary homeobox 2
604229	PETERS ANOMALY	P61812	Transforming growth factor beta-2
604229	PETERS ANOMALY GENERALIZED EPILEPSY WITH	Q9UKV0	Histone deacetylase 9
604233	FEBRILE SEIZURES PLUS GENERALIZED EPILEPSY WITH	P35498	Sodium channel protein type 1 subunit alpha
604233	FEBRILE SEIZURES PLUS GENERALIZED EPILEPSY WITH	Q07699	Sodium channel subunit beta-1
604233	FEBRILE SEIZURES PLUS GENERALIZED EPILEPSY WITH	Q99250	Sodium channel protein type 2 subunit alpha
604233	FEBRILE SEIZURES PLUS SHORT STATURE, IDIOPATHIC,	P18507	Gamma-aminobutyric acid receptor subunit gamma-2
604271	AUTOSOMAL SHORT STATURE, IDIOPATHIC,	P10912	Growth hormone receptor
604271	AUTOSOMAL SHORT STATURE, IDIOPATHIC,	P01241	Somatotropin
604271	AUTOSOMAL PROTOCOLADHERIN-BETA GENE	Q92847	Growth hormone secretagogue receptor type 1
604967	CLUSTER PROTOCOLADHERIN-BETA GENE	Q9Y5F3	Protocadherin beta-1
604967	CLUSTER PROTOCOLADHERIN-BETA GENE	Q9Y5E7	Protocadherin beta-2
604967	CLUSTER PROTOCOLADHERIN-BETA GENE	Q9Y5E6	Protocadherin beta-3
604967	CLUSTER PROTOCOLADHERIN-BETA GENE	Q9Y5E5	Protocadherin beta-4
604967	CLUSTER PROTOCOLADHERIN-BETA GENE	Q9Y5E4	Protocadherin beta-5
604967	CLUSTER PROTOCOLADHERIN-BETA GENE	Q9Y5E3	Protocadherin beta-6
604967	CLUSTER PROTOCOLADHERIN-BETA GENE	Q9Y5E2	Protocadherin beta-7
604967	CLUSTER	Q9UN66	Protocadherin beta-8

	PROTOCADHERIN-BETA GENE		
604967	CLUSTER PROTOCADHERIN-BETA GENE	Q9Y5E1	Protocadherin beta-9
604967	CLUSTER PROTOCADHERIN-BETA GENE	Q9UN67	Protocadherin beta-10
604967	CLUSTER PROTOCADHERIN-BETA GENE	Q9Y5F1	Protocadherin beta-12
604967	CLUSTER PROTOCADHERIN-BETA GENE	Q9Y5F0	Protocadherin beta-13
604967	CLUSTER PROTOCADHERIN-BETA GENE	Q9Y5E9	Protocadherin beta-14
604967	CLUSTER PROTOCADHERIN-BETA GENE	Q9Y5E8	Protocadherin beta-15
604967	CLUSTER PROTOCADHERIN-BETA GENE	Q9NRJ7	Protocadherin beta-16
604967	CLUSTER RENAL CELL CARCINOMA,	Q9Y5F2	Protocadherin beta-11
605074	PAPILLARY RENAL CELL CARCINOMA,	Q9BZE9	Tether containing UBX domain for GLUT4
605074	PAPILLARY RENAL CELL CARCINOMA,	Q92733	Proline-rich protein PRCC
605074	PAPILLARY RENAL CELL CARCINOMA,	P19532	Transcription factor E3
605074	PAPILLARY RENAL CELL CARCINOMA,	P08581	Hepatocyte growth factor receptor
605899	GLYCINE ENCEPHALOPATHY	P23378	Glycine dehydrogenase [decarboxylating], mitochondrial
605899	GLYCINE ENCEPHALOPATHY	P48728	Aminomethyltransferase, mitochondrial
605899	GLYCINE ENCEPHALOPATHY MATURITY-ONSET DIABETES OF	P23434	Glycine cleavage system H protein, mitochondrial
606391	THE YOUNG MATURITY-ONSET DIABETES OF	P19835	Bile salt-activated lipase
606391	THE YOUNG MATURITY-ONSET DIABETES OF	P20823	Hepatocyte nuclear factor 1-alpha
606391	THE YOUNG MATURITY-ONSET DIABETES OF	P35680	Hepatocyte nuclear factor 1-beta
606391	THE YOUNG MATURITY-ONSET DIABETES OF	P41235	Hepatocyte nuclear factor 4-alpha
606391	THE YOUNG MATURITY-ONSET DIABETES OF	P35557	Glucokinase
606391	THE YOUNG MATURITY-ONSET DIABETES OF	Q13562	Neurogenic differentiation factor 1
606391	THE YOUNG	O14901	Krueppel-like factor 11
606904	JUVENILE MYOCLONIC EPILEPSY	O00305	Voltage-dependent L-type calcium channel subunit beta-4
606904	JUVENILE MYOCLONIC EPILEPSY	Q5JVL4	EF-hand domain-containing protein 1
606904	JUVENILE MYOCLONIC EPILEPSY	P14867	Gamma-aminobutyric acid receptor subunit alpha-1
607748	FAMILIAL HYPERCHOLANEMIA	P07099	Epoxide hydrolase 1
607748	FAMILIAL HYPERCHOLANEMIA	Q9UDY2	Tight junction protein ZO-2
607748	FAMILIAL HYPERCHOLANEMIA JUVENILE MYELOMONOCYTIC	Q14032	Bile acid-CoA:amino acid N-acyltransferase
607785	LEUKEMIA JUVENILE MYELOMONOCYTIC	Q06124	Tyrosine-protein phosphatase non-receptor type 11
607785	LEUKEMIA JUVENILE MYELOMONOCYTIC	P01116	GTPase KRas
607785	LEUKEMIA JUVENILE MYELOMONOCYTIC	P01111	GTPase NRas
607785	LEUKEMIA JUVENILE MYELOMONOCYTIC	Q9UNA1	Rho GTPase-activating protein 26
607785	LEUKEMIA	P21359	Neurofibromin
608089	ENDOMETRIAL CANCER	P12830	Epithelial cadherin
608089	ENDOMETRIAL CANCER	P40692	DNA mismatch repair protein Mlh1

608089	ENDOMETRIAL CANCER	P43246	DNA mismatch repair protein Msh2
608089	ENDOMETRIAL CANCER	P20585	DNA mismatch repair protein Msh3
608089	ENDOMETRIAL CANCER	P52701	DNA mismatch repair protein Msh6
608089	ENDOMETRIAL CANCER MYASTHENIC SYNDROME, CONGENITAL, FAST-CHANNEL	P60484	Phosphatidylinositol-3,4,5-trisphosphate 3-phosphatase and dual-specificity protein phosphatase PTEN
608930	CONGENITAL, FAST-CHANNEL MYASTHENIC SYNDROME,	P02708	Acetylcholine receptor subunit alpha
608930	CONGENITAL, FAST-CHANNEL MYASTHENIC SYNDROME,	Q04844	Acetylcholine receptor subunit epsilon
608930	CONGENITAL, FAST-CHANNEL MYASTHENIC SYNDROME, CONGENITAL, ASSOCIATED WITH ACETYLCHOLINE RECEPTOR DEFICIENCY	Q07001	Acetylcholine receptor subunit delta
608931	MYASTHENIC SYNDROME, CONGENITAL, ASSOCIATED WITH ACETYLCHOLINE RECEPTOR	P11230	Acetylcholine receptor subunit beta
608931	DEFICIENCY MYASTHENIC SYNDROME, CONGENITAL, ASSOCIATED WITH ACETYLCHOLINE RECEPTOR	Q04844	Acetylcholine receptor subunit epsilon
608931	DEFICIENCY MYASTHENIC SYNDROME, CONGENITAL, ASSOCIATED WITH ACETYLCHOLINE RECEPTOR	Q13702	43 kDa receptor-associated protein of the synapse
608931	DEFICIENCY SEVERE COMBINED	O15146	Muscle, skeletal receptor tyrosine protein kinase
608971	IMMUNODEFICIENCY SEVERE COMBINED	P04234	T-cell surface glycoprotein CD3 delta chain
608971	IMMUNODEFICIENCY SEVERE COMBINED	P16871	Interleukin-7 receptor subunit alpha
608971	IMMUNODEFICIENCY SUSCEPTIBILITY TO HUMAN	P08575	Leukocyte common antigen
609423	IMMUNODEFICIENCY VIRUS TYPE 1 SUSCEPTIBILITY TO HUMAN	P51681	C-C chemokine receptor type 5
609423	IMMUNODEFICIENCY VIRUS TYPE 1 SUSCEPTIBILITY TO HUMAN	P49238	CX3C chemokine receptor 1
609423	IMMUNODEFICIENCY VIRUS TYPE 1 ABDOMINAL BODY FAT	P41597	C-C chemokine receptor type 2
609830	DISTRIBUTION ABDOMINAL BODY FAT	P37231	Peroxisome proliferator-activated receptor gamma
609830	DISTRIBUTION ABDOMINAL BODY FAT	P18031	Tyrosine-protein phosphatase non-receptor type 1
609830	DISTRIBUTION SUSCEPTIBILITY TO HEPATITIS B	P01189	Corticotropin-lipotropin
610424	VIRUS SUSCEPTIBILITY TO HEPATITIS B	P01903	HLA class II histocompatibility antigen, DR alpha chain
610424	VIRUS SUSCEPTIBILITY TO HEPATITIS B	P16410	Cytotoxic T-lymphocyte protein 4
610424	VIRUS SUSCEPTIBILITY TO HEPATITIS B	Q08334	Interleukin-10 receptor beta chain
610424	VIRUS SUSCEPTIBILITY TO HEPATITIS B	P48551	Interferon-alpha/beta receptor beta chain
610424	VIRUS SUSCEPTIBILITY TO HEPATITIS B	P11226	Mannose-binding protein C
610424	VIRUS	P01375	Tumor necrosis factor

References

- [1] T. F. Smith and M. S. Waterman, "Identification of common molecular subsequences," *J Mol Biol*, vol. 147, pp. 195-7, Mar 25 1981.
- [2] S. B. Needleman and C. D. Wunsch, "A general method applicable to the search for similarities in the amino acid sequence of two proteins," *J Mol Biol*, vol. 48, pp. 443-53, Mar 1970.
- [3] O. Gotoh, "An improved algorithm for matching biological sequences," *J Mol Biol*, vol. 162, pp. 705-8, Dec 15 1982.
- [4] S. F. Altschul and B. W. Erickson, "Optimal sequence alignment using affine gap costs," *Bull Math Biol*, vol. 48, pp. 603-16, 1986.
- [5] D. J. Lipman, S. F. Altschul, and J. D. Kececioglu, "A tool for multiple sequence alignment," *Proc Natl Acad Sci U S A*, vol. 86, pp. 4412-5, Jun 1989.
- [6] W. R. Pearson and D. J. Lipman, "Improved tools for biological sequence comparison," *Proc Natl Acad Sci U S A*, vol. 85, pp. 2444-8, Apr 1988.
- [7] J. D. Thompson, D. G. Higgins, and T. J. Gibson, "CLUSTAL W: improving the sensitivity of progressive multiple sequence alignment through sequence weighting, position-specific gap penalties and weight matrix choice," *Nucleic Acids Res*, vol. 22, pp. 4673-80, Nov 11 1994.
- [8] C. Notredame, D. G. Higgins, and J. Heringa, "T-Coffee: A novel method for fast and accurate multiple sequence alignment," *J Mol Biol*, vol. 302, pp. 205-17, Sep 8 2000.
- [9] R. C. Edgar, "MUSCLE: multiple sequence alignment with high accuracy and high throughput," *Nucleic Acids Res*, vol. 32, pp. 1792-7, 2004.
- [10] C. Grasso and C. Lee, "Combining partial order alignment and progressive multiple sequence alignment increases alignment speed and scalability to very large alignment problems," *Bioinformatics*, vol. 20, pp. 1546-56, Jul 10 2004.
- [11] R. Hughey and A. Krogh, "Hidden Markov models for sequence analysis: extension and analysis of the basic method," *Comput Appl Biosci*, vol. 12, pp. 95-107, Apr 1996.
- [12] S. R. Eddy, "A probabilistic model of local sequence alignment that simplifies statistical significance estimation," *PLoS Comput Biol*, vol. 4, p. e1000069, May 2008.

- [13] S. F. Altschul, W. Gish, W. Miller, E. W. Myers, and D. J. Lipman, "Basic local alignment search tool," *J Mol Biol*, vol. 215, pp. 403-10, Oct 5 1990.
- [14] L. Holm and C. Sander, "Mapping the protein universe," *Science*, vol. 273, pp. 595-603, Aug 2 1996.
- [15] I. N. Shindyalov and P. E. Bourne, "Protein structure alignment by incremental combinatorial extension (CE) of the optimal path," *Protein Eng*, vol. 11, pp. 739-47, Sep 1998.
- [16] A. Guerler and E. W. Knapp, "Novel protein folds and their nonsequential structural analogs," *Protein Sci*, vol. 17, pp. 1374-82, Aug 2008.
- [17] A. R. Ortiz, C. E. Strauss, and O. Olmea, "MAMMOTH (matching molecular models obtained from theory): an automated method for model comparison," *Protein Sci*, vol. 11, pp. 2606-21, Nov 2002.
- [18] R. Mosca and T. R. Schneider, "RAPIDO: a web server for the alignment of protein structures in the presence of conformational changes," *Nucleic Acids Res*, vol. 36, pp. W42-6, Jul 1 2008.
- [19] F. Teichert, U. Bastolla, and M. Porto, "SABERTOOTH: protein structural alignment based on a vectorial structure representation," *BMC Bioinformatics*, vol. 8, p. 425, 2007.
- [20] W. R. Taylor, T. P. Flores, and C. A. Orengo, "Multiple protein structure alignment," *Protein Sci*, vol. 3, pp. 1858-70, Oct 1994.
- [21] E. Krissinel and K. Henrick, "Secondary-structure matching (SSM), a new tool for fast protein structure alignment in three dimensions," *Acta Crystallogr D Biol Crystallogr*, vol. 60, pp. 2256-68, Dec 2004.
- [22] Y. Zhang and J. Skolnick, "TM-align: a protein structure alignment algorithm based on the TM-score," *Nucleic Acids Res*, vol. 33, pp. 2302-9, 2005.
- [23] S. A. Canny, Y. Cruz, M. R. Southern, and P. R. Griffin, "PubChem promiscuity: a web resource for gathering compound promiscuity data from PubChem," *Bioinformatics*, vol. 28, pp. 140-1, Jan 1 2012.
- [24] Y. Wang, E. Bolton, S. Dracheva, K. Karapetyan, B. A. Shoemaker, T. O. Suzek, *et al.*, "An overview of the PubChem BioAssay resource," *Nucleic Acids Res*, vol. 38, pp. D255-66, Jan 2010.

- [25] S. Gunther, M. Kuhn, M. Dunkel, M. Campillos, C. Senger, E. Petsalaki, *et al.*, "SuperTarget and Matador: resources for exploring drug-target relationships," *Nucleic Acids Res*, vol. 36, pp. D919-22, Jan 2008.
- [26] M. Campillos, M. Kuhn, A. C. Gavin, L. J. Jensen, and P. Bork, "Drug target identification using side-effect similarity," *Science*, vol. 321, pp. 263-6, Jul 11 2008.
- [27] D. B. Allison, X. Cui, G. P. Page, and M. Sabripour, "Microarray data analysis: from disarray to consolidation and consensus," *Nat Rev Genet*, vol. 7, pp. 55-65, Jan 2006.
- [28] T. Mehta, M. Tanik, and D. B. Allison, "Towards sound epistemological foundations of statistical methods for high-dimensional biology," *Nat Genet*, vol. 36, pp. 943-7, Sep 2004.
- [29] H. K. Lee, A. K. Hsu, J. Sajdak, J. Qin, and P. Pavlidis, "Coexpression analysis of human genes across many microarray data sets," *Genome Res*, vol. 14, pp. 1085-94, Jun 2004.
- [30] D. Eisenberg, E. M. Marcotte, I. Xenarios, and T. O. Yeates, "Protein function in the post-genomic era," *Nature*, vol. 405, pp. 823-6, Jun 15 2000.
- [31] M. R. Trusheim, B. Burgess, S. X. Hu, T. Long, S. D. Averbuch, A. A. Flynn, *et al.*, "Quantifying factors for the success of stratified medicine," *Nat Rev Drug Discov*, vol. 10, pp. 817-33, 2011.
- [32] Z. Dezso, Y. Nikolsky, T. Nikolskaya, J. Miller, D. Cherba, C. Webb, *et al.*, "Identifying disease-specific genes based on their topological significance in protein networks," *BMC Syst Biol*, vol. 3, p. 36, 2009.
- [33] J. B. Gibbs, "Mechanism-based target identification and drug discovery in cancer research," *Science*, vol. 287, pp. 1969-73, Mar 17 2000.
- [34] K. A. Pattin and J. H. Moore, "Role for protein-protein interaction databases in human genetics," *Expert Rev Proteomics*, vol. 6, pp. 647-59, Dec 2009.
- [35] P. Imming, C. Sinning, and A. Meyer, "Drugs, their targets and the nature and number of drug targets," *Nat Rev Drug Discov*, vol. 5, pp. 821-34, Oct 2006.
- [36] D. C. Liebler and F. P. Guengerich, "Elucidating mechanisms of drug-induced toxicity," *Nat Rev Drug Discov*, vol. 4, pp. 410-20, May 2005.

- [37] H. Najmabadi, H. Hu, M. Garshasbi, T. Zemojtel, S. S. Abedini, W. Chen, *et al.*, "Deep sequencing reveals 50 novel genes for recessive cognitive disorders," *Nature*, vol. 478, pp. 57-63, Oct 6 2011.
- [38] M. G. Tektonidou and M. M. Ward, "Validation of new biomarkers in systemic autoimmune diseases," *Nat Rev Rheumatol*, Nov 1 2011.
- [39] E. C. Butcher, "Can cell systems biology rescue drug discovery?," *Nat Rev Drug Discov*, vol. 4, pp. 461-7, Jun 2005.
- [40] J. Drews, "Strategic trends in the drug industry," *Drug Discovery Today*, vol. 8, pp. 411-420, May 1 2003.
- [41] J. A. DiMasi, R. W. Hansen, and H. G. Grabowski, "The price of innovation: new estimates of drug development costs," *Journal of Health Economics*, vol. 22, pp. 151-185, Mar 2003.
- [42] CBO. (2006, January 20). Research and Development in the Pharmaceutical Industry. A *CBO Study*. Available: <http://www.cbo.gov/ftpdocs/76xx/doc7615/10-02-DrugR-D.pdf>
- [43] C. P. Adams and V. V. Brantner, "Estimating the cost of new drug development: Is it really \$802 million?," *Health Affairs*, vol. 25, pp. 420-428, Mar-Apr 2006.
- [44] E. A. Czerepak and S. Ryser, "Drug approvals and failures: implications for alliances," *Nature Reviews Drug Discovery*, vol. 7, pp. 197-198, Mar 2008.
- [45] K. Wester, A. K. Jonsson, O. Spigset, H. Druid, and S. Hagg, "Incidence of fatal adverse drug reactions: a population based study," *British Journal of Clinical Pharmacology*, vol. 65, pp. 573-579, Apr 2008.
- [46] J. Lazarou, B. H. Pomeranz, and P. N. Corey, "Incidence of adverse drug reactions in hospitalized patients - A meta-analysis of prospective studies," *Jama-Journal of the American Medical Association*, vol. 279, pp. 1200-1205, Apr 15 1998.
- [47] J. T. Hanlon, C. F. Pieper, E. R. Hajjar, R. J. Sloane, C. I. Lindblad, C. M. Ruby, *et al.*, "Incidence and predictors of all and preventable adverse drug reactions in frail elderly persons after hospital stay," *Journals of Gerontology Series a-Biological Sciences and Medical Sciences*, vol. 61, pp. 511-515, May 2006.

- [48] A. E. Lobley, T. Nugent, C. A. Orengo, and D. T. Jones, "FFPred: an integrated feature-based function prediction server for vertebrate proteomes," *Nucleic Acids Res*, vol. 36, pp. W297-302, Jul 1 2008.
- [49] E. D. Pleasance, R. K. Cheetham, P. J. Stephens, D. J. McBride, S. J. Humphray, C. D. Greenman, *et al.*, "A comprehensive catalogue of somatic mutations from a human cancer genome," *Nature*, vol. 463, pp. 191-6, Jan 14 2010.
- [50] M. R. Stratton, P. J. Campbell, and P. A. Futreal, "The cancer genome," *Nature*, vol. 458, pp. 719-24, Apr 9 2009.
- [51] M. Williams, "Target validation," *Curr Opin Pharmacol*, vol. 3, pp. 571-7, Oct 2003.
- [52] M. Rask-Andersen, M. S. Almen, and H. B. Schioth, "Trends in the exploitation of novel drug targets," *Nat Rev Drug Discov*, vol. 10, pp. 579-90, Aug 2011.
- [53] B. P. Zambrowicz and A. T. Sands, "Knockouts model the 100 best-selling drugs--will they model the next 100?," *Nat Rev Drug Discov*, vol. 2, pp. 38-51, Jan 2003.
- [54] T. Takenaka, "Classical vs reverse pharmacology in drug discovery," *BJU Int*, vol. 88 Suppl 2, pp. 7-10; discussion 49-50, Sep 2001.
- [55] C. Smith, "Drug target identification: a question of biology," *Nature*, vol. 428, pp. 225-31, Mar 11 2004.
- [56] G. J. Crowther, D. Shanmugam, S. J. Carmona, M. A. Doyle, C. Hertz-Fowler, M. Berriman, *et al.*, "Identification of attractive drug targets in neglected-disease pathogens using an in silico approach," *PLoS Negl Trop Dis*, vol. 4, p. e804, 2010.
- [57] C. R. Caffrey, A. Rohwer, F. Oellien, R. J. Marhofer, S. Braschi, G. Oliveira, *et al.*, "A comparative chemogenomics strategy to predict potential drug targets in the metazoan pathogen, *Schistosoma mansoni*," *PLoS One*, vol. 4, p. e4413, 2009.
- [58] A. Schlicker and M. Albrecht, "FunSimMat: a comprehensive functional similarity database," *Nucleic Acids Res*, vol. 36, pp. D434-9, Jan 2008.
- [59] A. Schlicker, F. S. Domingues, J. Rahnenfuhrer, and T. Lengauer, "A new measure for functional similarity of gene products based on Gene Ontology," *BMC Bioinformatics*, vol. 7, p. 302, 2006.

- [60] A. Schlicker, T. Lengauer, and M. Albrecht, "Improving disease gene prioritization using the semantic similarity of Gene Ontology terms," *Bioinformatics*, vol. 26, pp. i561-7, Sep 15 2010.
- [61] C. Pesquita, D. Faria, H. Bastos, A. E. Ferreira, A. O. Falcao, and F. M. Couto, "Metrics for GO based protein semantic similarity: a systematic evaluation," *BMC Bioinformatics*, vol. 9 Suppl 5, p. S4, 2008.
- [62] G. Lerman and B. E. Shakhnovich, "Defining functional distance using manifold embeddings of gene ontology annotations," *Proc Natl Acad Sci U S A*, vol. 104, pp. 11334-9, Jul 3 2007.
- [63] F. M. Couto, M. Silva, and P. M. Coutinho, "Semantic similarity over the gene ontology: family correlation and selecting disjunctive ancestors," presented at the Proceedings of the 14th ACM international conference on Information and knowledge management, Bremen, Germany, 2005.
- [64] F. M. Couto, M. J. Silva, and P. M. Coutinho, "Measuring semantic similarity between Gene Ontology terms," *Data & Knowledge Engineering*, vol. 61, pp. 137-152, 2007.
- [65] A. del Pozo, F. Pazos, and A. Valencia, "Defining functional distances over gene ontology," *BMC Bioinformatics*, vol. 9, p. 50, 2008.
- [66] S. Benabderahmane, M. Smail-Tabbone, O. Poch, A. Napoli, and M. D. Devignes, "IntelliGO: a new vector-based semantic similarity measure including annotation origin," *BMC Bioinformatics*, vol. 11, p. 588, 2010.
- [67] Y. R. Cho, W. Hwang, M. Ramanathan, and A. Zhang, "Semantic integration to identify overlapping functional modules in protein interaction networks," *BMC Bioinformatics*, vol. 8, p. 265, 2007.
- [68] X. Guo, R. Liu, C. D. Shriver, H. Hu, and M. N. Lieberman, "Assessing semantic similarity measures for the characterization of human regulatory pathways," *Bioinformatics*, vol. 22, pp. 967-73, Apr 15 2006.
- [69] P. W. Lord, R. D. Stevens, A. Brass, and C. A. Goble, "Investigating semantic similarity measures across the Gene Ontology: the relationship between sequence and annotation," *Bioinformatics*, vol. 19, pp. 1275-83, Jul 1 2003.

- [70] P. W. Lord, R. D. Stevens, A. Brass, and C. A. Goble, "Semantic similarity measures as tools for exploring the gene ontology," *Pac Symp Biocomput*, pp. 601-12, 2003.
- [71] M. Mistry and P. Pavlidis, "Gene Ontology term overlap as a measure of gene functional similarity," *BMC Bioinformatics*, vol. 9, p. 327, 2008.
- [72] C. Posse, A. Sanfilippo, B. Gopalan, R. Riensche, N. Beagley, and B. Baddeley, "Cross-Ontological Analytics: Combining Associative and Hierarchical Relations in the Gene Ontologies to Assess Gene Product Similarity," in *Computational Science – ICCS 2006*. vol. 3992, V. Alexandrov, G. van Albada, P. Sloot, and J. Dongarra, Eds., ed: Springer Berlin / Heidelberg, 2006, pp. 871-878-878.
- [73] J. Z. Wang, Z. Du, R. Payattakool, P. S. Yu, and C. F. Chen, "A new method to measure the semantic similarity of GO terms," *Bioinformatics*, vol. 23, pp. 1274-81, May 15 2007.
- [74] H. Wu, Z. Su, F. Mao, V. Olman, and Y. Xu, "Prediction of functional modules based on comparative genome analysis and Gene Ontology application," *Nucleic Acids Res*, vol. 33, pp. 2822-37, 2005.
- [75] X. Wu, L. Zhu, J. Guo, D. Y. Zhang, and K. Lin, "Prediction of yeast protein-protein interaction network: insights from the Gene Ontology and annotations," *Nucleic Acids Res*, vol. 34, pp. 2137-50, 2006.
- [76] H. Yu, L. Gao, K. Tu, and Z. Guo, "Broadly predicting specific gene functions with expression similarity and taxonomy similarity," *Gene*, vol. 352, pp. 75-81, Jun 6 2005.
- [77] M. Ashburner, C. A. Ball, J. A. Blake, D. Botstein, H. Butler, J. M. Cherry, *et al.*, "Gene ontology: tool for the unification of biology. The Gene Ontology Consortium," *Nat Genet*, vol. 25, pp. 25-9, May 2000.
- [78] B. Smith, J. Williams, and S. Schulze-Kremer, "The ontology of the gene ontology," *AMIA Annu Symp Proc*, pp. 609-13, 2003.
- [79] Y. Tao, L. Sam, J. Li, C. Friedman, and Y. A. Lussier, "Information theory applied to the sparse gene ontology annotation network to predict novel gene function," *Bioinformatics*, vol. 23, pp. i529-38, Jul 1 2007.
- [80] UniProt, "Ongoing and future developments at the Universal Protein Resource," *Nucleic Acids Res*, vol. 39, pp. D214-9, Jan 2011.

- [81] H. Mcwilliam, F. Valentin, M. Goujon, W. Z. Li, M. Narayanasamy, J. Martin, *et al.*, "Web services at the European Bioinformatics Institute-2009," *Nucleic Acids Research*, vol. 37, pp. W6-W10, Jul 1 2009.
- [82] Y. Arita, S. Nishimura, A. Matsuyama, Y. Yashiroda, T. Usui, C. Boone, *et al.*, "Microarray-based target identification using drug hypersensitive fission yeast expressing ORFeome," *Mol Biosyst*, vol. 7, pp. 1463-72, May 2011.
- [83] M. T. Dittrich, G. W. Klau, A. Rosenwald, T. Dandekar, and T. Muller, "Identifying functional modules in protein-protein interaction networks: an integrated exact approach," *Bioinformatics*, vol. 24, pp. i223-31, Jul 1 2008.
- [84] O. Bodenreider, M. Aubry, and A. Burgun, "Non-lexical approaches to identifying associative relations in the gene ontology," *Pac Symp Biocomput*, pp. 91-102, 2005.
- [85] Y. R. Cho and A. Zhang, "Identification of functional hubs and modules by converting interactome networks into hierarchical ordering of proteins," *BMC Bioinformatics*, vol. 11 Suppl 3, p. S3, 2010.
- [86] R. A. Craig and L. Liao, "Phylogenetic tree information aids supervised learning for predicting protein-protein interaction based on distance matrices," *BMC Bioinformatics*, vol. 8, p. 6, 2007.
- [87] J. L. Sevilla, V. Segura, A. Podhorski, E. Guruceaga, J. M. Mato, L. A. Martinez-Cruz, *et al.*, "Correlation between gene expression and GO semantic similarity," *IEEE/ACM Trans Comput Biol Bioinform*, vol. 2, pp. 330-8, Oct-Dec 2005.
- [88] A. Lewin and I. C. Grieve, "Grouping Gene Ontology terms to improve the assessment of gene set enrichment in microarray data," *BMC Bioinformatics*, vol. 7, p. 426, 2006.
- [89] R. Jansen, H. Yu, D. Greenbaum, Y. Kluger, N. J. Krogan, S. Chung, *et al.*, "A Bayesian networks approach for predicting protein-protein interactions from genomic data," *Science*, vol. 302, pp. 449-53, Oct 17 2003.
- [90] P. Resnik, "Using Information Content to Evaluate Semantic Similarity in a Taxonomy," *In Proceedings of the 14th International Joint Conference on Artificial Intelligence*, pp. 448-453, 1995.
- [91] D. Lin, "An Information-Theoretic Definition of Similarity," in *In Proceedings of the 15th International Conference on Machine Learning*, 1998, pp. 296-304.

- [92] B. Rost, "Enzyme function less conserved than anticipated," *J Mol Biol*, vol. 318, pp. 595-608, Apr 26 2002.
- [93] S. E. Brenner, "Errors in genome annotation," *Trends Genet*, vol. 15, pp. 132-3, Apr 1999.
- [94] D. Devos and A. Valencia, "Practical limits of function prediction," *Proteins*, vol. 41, pp. 98-107, Oct 1 2000.
- [95] R. Gentleman. (2010). *Visualizing and Distances Using GO*. Available: <http://www.bioconductor.org/packages/release/bioc/vignettes/GOstats/inst/doc/GOvis.pdf>
- [96] A. G. Murzin, S. E. Brenner, T. Hubbard, and C. Chothia, "SCOP: a structural classification of proteins database for the investigation of sequences and structures," *J Mol Biol*, vol. 247, pp. 536-40, Apr 7 1995.
- [97] S. Hunter, P. Jones, A. Mitchell, R. Apweiler, T. K. Attwood, A. Bateman, *et al.*, "InterPro in 2011: new developments in the family and domain prediction database," *Nucleic Acids Res*, vol. 40, pp. D306-D312, Jan 2012.
- [98] J. J. Jiang and D. W. Conrath, "Semantic Similarity Based on Corpus Statistics and Lexical Taxonomy," in *International Conference Research on Computational Linguistics (ROCLING X)*, 1997, p. 9008.
- [99] R. M. Riensche, B. L. Baddeley, A. P. Sanfilippo, C. Posse, and B. Gopalan, "XOA: Web-Enabled Cross-Ontological Analytics," in *Services, 2007 IEEE Congress on*, 2007, pp. 99-105.
- [100] A. Sanfilippo, C. Posse, B. Gopalan, R. Riensche, N. Beagley, B. Baddeley, *et al.*, "Combining Hierarchical and Associative Gene Ontology Relations With Textual Evidence in Estimating Gene and Gene Product Similarity," *NanoBioscience, IEEE Transactions on*, vol. 6, pp. 51-59, 2007.
- [101] P. Ye, B. D. Peyser, X. Pan, J. D. Boeke, F. A. Spencer, and J. S. Bader, "Gene function prediction from congruent synthetic lethal interactions in yeast," *Mol Syst Biol*, vol. 1, p. 2005 0026, 2005.
- [102] V. Pekar and S. Staab, "Taxonomy learning: factoring the structure of a taxonomy into a semantic classification decision," in *Proceedings of the Nineteenth Conference on Computational Linguistics*, 2002, pp. 786-792.

- [103] A. Nagar and H. Al-Mubaid, "Using path length measure for gene clustering based on similarity of annotation terms," in *Computers and Communications, 2008. ISCC 2008. IEEE Symposium on*, 2008, pp. 637-642.
- [104] D. P. Huttenlocher, G. A. Klanderman, and W. J. Rucklidge, "Comparing Images Using the Hausdorff Distance," *Ieee Transactions on Pattern Analysis and Machine Intelligence*, vol. 15, pp. 850-863, Sep 1993.
- [105] X. X. Chi and J. Y. Hou, "An iterative approach of protein function prediction," *Bmc Bioinformatics*, vol. 12, Nov 10 2011.
- [106] P. Khatri and S. Draghici, "Ontological analysis of gene expression data: current tools, limitations, and open problems," *Bioinformatics*, vol. 21, pp. 3587-3595, Sep 15 2005.
- [107] S. Y. Rhee, V. Wood, K. Dolinski, and S. Draghici, "Use and misuse of the gene ontology annotations," *Nature Reviews Genetics*, vol. 9, pp. 509-515, Jul 2008.
- [108] P. Khatri, B. Done, A. Rao, A. Done, and S. Draghici, "A semantic analysis of the annotations of the human genome," *Bioinformatics*, vol. 21, pp. 3416-21, Aug 15 2005.
- [109] A. Nagar and H. Al-Mubaid, "A New Path Length Measure Based on GO for Gene Similarity with Evaluation using SGD Pathways," in *Computer-Based Medical Systems, 2008. CBMS '08. 21st IEEE International Symposium on*, 2008, pp. 590-595.
- [110] M. Y. Galperin, D. R. Walker, and E. V. Koonin, "Analogous enzymes: independent inventions in enzyme evolution," *Genome Res*, vol. 8, pp. 779-90, Aug 1998.
- [111] D. Devos and A. Valencia, "Intrinsic errors in genome annotation," *Trends Genet*, vol. 17, pp. 429-31, Aug 2001.
- [112] R. D. Sleator and P. Walsh, "An overview of in silico protein function prediction," *Arch Microbiol*, vol. 192, pp. 151-5, Mar 2010.
- [113] B. Stein, "Principles of hash-based text retrieval," in *Proceedings of the 30th annual international ACM SIGIR conference*, Amsterdam, Netherlands, 2007.
- [114] X. W. Chen, J. C. Jeong, and P. Dermeyer, "KUPS: constructing datasets of interacting and non-interacting protein pairs with associated attributions," *Nucleic Acids Res*, Oct 15 2010.

- [115] J. Ling, B. R. So, S. S. Yadavalli, H. Roy, S. Shoji, K. Fredrick, *et al.*, "Resampling and editing of mischarged tRNA prior to translation elongation," *Mol Cell*, vol. 33, pp. 654-60, Mar 13 2009.
- [116] H. S. Zaher and R. Green, "Fidelity at the Molecular Level: Lessons from Protein Synthesis," *Cell*, vol. 136, pp. 746-762, Feb 20 2009.
- [117] E. N. Kersh, A. S. Shaw, and P. M. Allen, "Fidelity of T cell activation through multistep T cell receptor zeta phosphorylation," *Science*, vol. 281, pp. 572-575, Jul 24 1998.
- [118] T. Xu, L. F. Du, and Y. Zhou, "Evaluation of GO-based functional similarity measures using *S. cerevisiae* protein interaction and expression profile data," *BMC Bioinformatics*, vol. 9, Nov 6 2008.
- [119] C. Chothia, J. Gough, C. Vogel, and S. A. Teichmann, "Evolution of the protein repertoire," *Science*, vol. 300, pp. 1701-3, Jun 13 2003.
- [120] B. Long, P. S. Yu, and Z. Zhang, "A General Model for Multiple View Unsupervised Learning," in *In Proceedings of the 2008 SIAM International Conference on Data Mining*, Atlanta, Georgia, USA, 2008, pp. 822-833.
- [121] S. Rüping and T. Scheffer, "Learning With Multiple Views," in *Proceedings of the ICML 2005 Workshop*, Bonn, Germany, 2005.
- [122] A. Andreeva, D. Howorth, J. M. Chandonia, S. E. Brenner, T. J. Hubbard, C. Chothia, *et al.*, "Data growth and its impact on the SCOP database: new developments," *Nucleic Acids Res*, vol. 36, pp. D419-25, Jan 2008.
- [123] C. A. Orengo, A. D. Michie, S. Jones, D. T. Jones, M. B. Swindells, and J. M. Thornton, "CATH--a hierachic classification of protein domain structures," *Structure*, vol. 5, pp. 1093-108, Aug 15 1997.
- [124] S. Hunter, P. Jones, A. Mitchell, R. Apweiler, T. K. Attwood, A. Bateman, *et al.*, "InterPro in 2011: new developments in the family and domain prediction database," *Nucleic Acids Research*, vol. 40, pp. D306-D312, Jan 2012.
- [125] H. M. Berman, J. Westbrook, Z. Feng, G. Gilliland, T. N. Bhat, H. Weissig, *et al.*, "The Protein Data Bank," *Nucleic Acids Research*, vol. 28, pp. 235-242, Jan 1 2000.

- [126] E. M. Marcotte, M. Pellegrini, H. L. Ng, D. W. Rice, T. O. Yeates, and D. Eisenberg, "Detecting protein function and protein-protein interactions from genome sequences," *Science*, vol. 285, pp. 751-3, Jul 30 1999.
- [127] S. Letovsky and S. Kasif, "Predicting protein function from protein/protein interaction data: a probabilistic approach," *Bioinformatics*, vol. 19, pp. i197-i204, Jul 2003.
- [128] A. Vazquez, A. Flammini, A. Maritan, and A. Vespignani, "Global protein function prediction from protein-protein interaction networks," *Nat Biotechnol*, vol. 21, pp. 697-700, Jun 2003.
- [129] J. Muller and A. Hemphill, "Drug Target Identification in Intracellular and Extracellular Protozoan Parasites," *Curr Top Med Chem*, May 26 2011.
- [130] X. W. Chen, J. C. Jeong, and P. Dermeyer, "KUPS: constructing datasets of interacting and non-interacting protein pairs with associated attributions," *Nucleic Acids Res*, vol. 39, pp. D750-4, Jan 2011.
- [131] D. Wilson, R. Pethica, Y. D. Zhou, C. Talbot, C. Vogel, M. Madera, *et al.*, "SUPERFAMILY-sophisticated comparative genomics, data mining, visualization and phylogeny," *Nucleic Acids Research*, vol. 37, pp. D380-D386, Jan 2009.
- [132] D. Lee, O. Redfern, and C. Orengo, "Predicting protein function from sequence and structure," *Nat Rev Mol Cell Biol*, vol. 8, pp. 995-1005, Dec 2007.
- [133] L. Stein, "Genome annotation: from sequence to biology," *Nat Rev Genet*, vol. 2, pp. 493-503, Jul 2001.
- [134] Y. Loewenstein, D. Raimondo, O. C. Redfern, J. Watson, D. Frishman, M. Linial, *et al.*, "Protein function annotation by homology-based inference," *Genome Biol*, vol. 10, p. 207, 2009.
- [135] J. M. Chandonia, G. Hon, N. S. Walker, L. Lo Conte, P. Koehl, M. Levitt, *et al.*, "The ASTRAL Compendium in 2004," *Nucleic Acids Res*, vol. 32, pp. D189-92, Jan 1 2004.
- [136] C. Camacho, G. Coulouris, V. Avagyan, N. Ma, J. Papadopoulos, K. Bealer, *et al.*, "BLAST+: architecture and applications," *BMC Bioinformatics*, vol. 10, p. 421, 2009.
- [137] M. Pellegrini, E. M. Marcotte, M. J. Thompson, D. Eisenberg, and T. O. Yeates, "Assigning protein functions by comparative genome analysis: protein phylogenetic profiles," *Proc Natl Acad Sci U S A*, vol. 96, pp. 4285-8, Apr 13 1999.

- [138] C. Chothia and A. M. Lesk, "The Relation between the Divergence of Sequence and Structure in Proteins," *Embo Journal*, vol. 5, pp. 823-826, Apr 1986.
- [139] H. Hasegawa and L. Holm, "Advances and pitfalls of protein structural alignment," *Curr Opin Struct Biol*, vol. 19, pp. 341-8, Jun 2009.
- [140] T. J. Ley, E. R. Mardis, L. Ding, B. Fulton, M. D. McLellan, K. Chen, *et al.*, "DNA sequencing of a cytogenetically normal acute myeloid leukaemia genome," *Nature*, vol. 456, pp. 66-72, Nov 6 2008.
- [141] X. W. Chen and J. C. Jeong, "Sequence-based prediction of protein interaction sites with an integrative method," *Bioinformatics*, vol. 25, pp. 585-91, Mar 1 2009.
- [142] R. R. Crichton and M. Charlotteaux-Wauters, "Iron transport and storage," *Eur J Biochem*, vol. 164, pp. 485-506, May 4 1987.
- [143] E. C. Theil, "Ferritin: structure, gene regulation, and cellular function in animals, plants, and microorganisms," *Annu Rev Biochem*, vol. 56, pp. 289-315, 1987.
- [144] J. E. Dutton, L. J. Rogers, B. G. Haslett, I. A. H. Takruri, J. T. Gleaves, and D. Boulter, "Comparative Studies on the Properties of Two Ferredoxins from *Pisum sativum L.*," *Journal of Experimental Botany*, vol. 31, pp. 379-391, April 1, 1980 1980.
- [145] J. R. Mason and R. Cammack, "The electron-transport proteins of hydroxylating bacterial dioxygenases," *Annu Rev Microbiol*, vol. 46, pp. 277-305, 1992.
- [146] L. Hedstrom, "Serine protease mechanism and specificity," *Chem Rev*, vol. 102, pp. 4501-24, Dec 2002.
- [147] N. D. Rawlings and A. J. Barrett, "Families of serine peptidases," *Methods Enzymol*, vol. 244, pp. 19-61, 1994.
- [148] E. S. Alnemri, D. J. Livingston, D. W. Nicholson, G. Salvesen, N. A. Thornberry, W. W. Wong, *et al.*, "Human ICE/CED-3 protease nomenclature," *Cell*, vol. 87, p. 171, Oct 18 1996.
- [149] E. A. Stura, G. G. Fieser, and I. A. Wilson, "Crystallization of Antibodies and Antibody-Antigen Complexes," *ImmunoMethods*, vol. 3, pp. 164-179, 1993.
- [150] M. G. Marinus and N. R. Morris, "Isolation of deoxyribonucleic acid methylase mutants of *Escherichia coli* K-12," *J Bacteriol*, vol. 114, pp. 1143-50, Jun 1973.

- [151] M. R. Badger and G. D. Price, "The Role of Carbonic-Anhydrase in Photosynthesis," *Annual Review of Plant Physiology and Plant Molecular Biology*, vol. 45, pp. 369-392, 1994.
- [152] K. H. Liu, J. J. E. Dore, M. P. Roberts, R. Krishnan, F. M. Hopkins, and J. D. Godkin, "Expression and Cellular-Localization of Retinol-Binding Protein Messenger-Ribonucleic-Acid in Bovine Blastocysts and Extraembryonic Membranes," *Biology of Reproduction*, vol. 49, pp. 393-400, Aug 1993.
- [153] J. Hurwitz, "The discovery of RNA polymerase," *J Biol Chem*, vol. 280, pp. 42477-85, Dec 30 2005.
- [154] S. Takahashi and T. Koyama, "Structure and function of cis-prenyl chain elongating enzymes," *Chem Rec*, vol. 6, pp. 194-205, 2006.
- [155] A. E. Chung and J. H. Law, "Cyclopropane Fatty Acid Synthetase: Partial Purification and Properties," *Biochemistry*, vol. 3, pp. 967-74, Jul 1964.
- [156] P. Dinadayala, F. Laval, C. Raynaud, A. Lemassu, M. A. Laneelle, G. Laneelle, *et al.*, "Tracking the putative biosynthetic precursors of oxygenated mycolates of *Mycobacterium tuberculosis*. Structural analysis of fatty acids of a mutant strain devoid of methoxy- and ketomycolates," *J Biol Chem*, vol. 278, pp. 7310-9, Feb 28 2003.
- [157] A. Hamosh, A. F. Scott, J. S. Amberger, C. A. Bocchini, and V. A. McKusick, "Online Mendelian Inheritance in Man (OMIM), a knowledgebase of human genes and genetic disorders," *Nucleic Acids Res*, vol. 33, pp. D514-7, Jan 1 2005.
- [158] H. J. Bandelt, Q. P. Kong, W. Parson, and A. Salas, "More evidence for non-maternal inheritance of mitochondrial DNA?," *J Med Genet*, vol. 42, pp. 957-60, Dec 2005.
- [159] M. Pronicki, E. Matyja, D. Piekutowska-Abramczuk, T. Szymanska-Debinska, A. Karkucsinska-Wieckowska, E. Karczmarewicz, *et al.*, "Light and electron microscopy characteristics of the muscle of patients with SURF1 gene mutations associated with Leigh disease," *Journal of Clinical Pathology*, vol. 61, pp. 460-466, Apr 2008.
- [160] M. Hirano and S. G. Pavlakis, "Mitochondrial myopathy, encephalopathy, lactic acidosis, and strokelike episodes (MELAS): current concepts," *J Child Neurol*, vol. 9, pp. 4-13, Jan 1994.

- [161] O. Gimm, M. Armanios, H. Dziema, H. P. Neumann, and C. Eng, "Somatic and occult germ-line mutations in SDHD, a mitochondrial complex II gene, in nonfamilial pheochromocytoma," *Cancer Res*, vol. 60, pp. 6822-5, Dec 15 2000.
- [162] D. Cotesta, C. Caliumi, P. Alo, L. Petramala, M. G. Reale, R. Masciangelo, *et al.*, "High plasma levels of human chromogranin A and adrenomedullin in patients with pheochromocytoma," *Tumori*, vol. 91, pp. 53-8, Jan-Feb 2005.
- [163] R. McFarland, D. M. Kirby, K. J. Fowler, A. Ohtake, M. T. Ryan, D. J. Amor, *et al.*, "De novo mutations in the mitochondrial ND3 gene as a cause of infantile mitochondrial encephalopathy and complex I deficiency.,," *American Journal of Human Genetics*, vol. 73, pp. 462-462, Nov 2003.
- [164] A. D. Sheftel, O. Stehling, A. J. Pierik, H. P. Elsasser, U. Muhlenhoff, H. Webert, *et al.*, "Humans possess two mitochondrial ferredoxins, Fdx1 and Fdx2, with distinct roles in steroidogenesis, heme, and Fe/S cluster biosynthesis," *Proc Natl Acad Sci U S A*, vol. 107, pp. 11775-80, Jun 29 2010.
- [165] S. J. Hoefs, C. E. Dieteren, F. Distelmaier, R. J. Janssen, A. Epplen, H. G. Swarts, *et al.*, "NDUFA2 complex I mutation leads to Leigh disease," *American Journal of Human Genetics*, vol. 82, pp. 1306-15, Jun 2008.
- [166] J. L. Loeffen, R. H. Triepels, L. P. van den Heuvel, M. Schuelke, C. A. Buskens, R. J. Smeets, *et al.*, "cDNA of eight nuclear encoded subunits of NADH:ubiquinone oxidoreductase: human complex I cDNA characterization completed," *Biochem Biophys Res Commun*, vol. 253, pp. 415-22, Dec 18 1998.
- [167] M. Bugiani, F. Invernizzi, S. Alberio, E. Briem, E. Lamantea, F. Carrara, *et al.*, "Clinical and molecular findings in children with complex I deficiency," *Biochim Biophys Acta*, vol. 1659, pp. 136-47, Dec 6 2004.
- [168] E. Ostergaard, R. J. Rodenburg, M. van den Brand, L. L. Thomsen, M. Duno, M. Batbayli, *et al.*, "Respiratory chain complex I deficiency due to NDUFA12 mutations as a new cause of Leigh syndrome," *Journal of Medical Genetics*, vol. 48, pp. 737-740, Nov 2011.
- [169] H. Lu and X. M. Cao, "GRIM-19 is essential for maintenance of mitochondrial membrane potential," *Molecular Biology of the Cell*, vol. 19, pp. 1893-1902, May 2008.

- [170] M. P. Puissegur, N. M. Mazure, T. Bertero, L. Pradelli, S. Grosso, K. Robbe-Sermesant, *et al.*, "miR-210 is overexpressed in late stages of lung cancer and mediates mitochondrial alterations associated with modulation of HIF-1 activity," *Cell Death and Differentiation*, vol. 18, pp. 465-478, Mar 2011.
- [171] T. Marui, I. Funatogawa, S. Koishi, K. Yamamoto, H. Matsumoto, O. Hashimoto, *et al.*, "The NADH-ubiquinone oxidoreductase 1 alpha subcomplex 5 (NDUFA5) gene variants are associated with autism," *Acta Psychiatrica Scandinavica*, vol. 123, pp. 118-124, Feb 2011.
- [172] G. D. Mellick, P. A. Silburn, J. A. Prince, and A. J. Brookes, "A novel screen for nuclear mitochondrial gene associations with Parkinson's disease," *Journal of Neural Transmission*, vol. 111, pp. 191-199, Feb 2004.
- [173] M. Gu, J. M. Cooper, J. W. Taanman, and A. H. V. Schapira, "Mitochondrial DNA transmission of the mitochondrial defect in Parkinson's disease," *Annals of Neurology*, vol. 44, pp. 177-186, Aug 1998.
- [174] R. H. Swerdlow, J. K. Parks, S. W. Miller, J. B. Tuttle, P. A. Trimmer, J. P. Sheehan, *et al.*, "Origin and functional consequences of the complex I defect in Parkinson's disease," *Annals of Neurology*, vol. 40, pp. 663-671, Oct 1996.
- [175] B. J. C. van den Bosch, M. Gerards, W. Sluiter, A. P. A. Stegmann, E. L. C. Jongen, D. M. E. I. Hellebrekers, *et al.*, "Defective NDUFA9 as a novel cause of neonatally fatal complex I disease," *Journal of Medical Genetics*, vol. 49, pp. 10-15, Jan 2012.
- [176] R. Janssen, J. Smeitink, R. Smeets, and L. van Den Heuvel, "CIA30 complex I assembly factor: a candidate for human complex I deficiency?," *Hum Genet*, vol. 110, pp. 264-70, Mar 2002.
- [177] E. Fassone, J. W. Taanman, I. P. Hargreaves, N. J. Sebire, M. A. Cleary, M. Burch, *et al.*, "Mutations in the mitochondrial complex I assembly factor NDUFAF1 cause fatal infantile hypertrophic cardiomyopathy," *J Med Genet*, vol. 48, pp. 691-7, Oct 2011.
- [178] S. E. Calvo, A. G. Compton, S. G. Hershman, S. C. Lim, D. S. Lieber, E. J. Tucker, *et al.*, "Molecular diagnosis of infantile mitochondrial disease with targeted next-generation sequencing," *Sci Transl Med*, vol. 4, p. 118ra10, Jan 25 2012.

- [179] T. B. Haack, F. Madignier, M. Herzer, E. Lamantea, K. Danhauser, F. Invernizzi, *et al.*, "Mutation screening of 75 candidate genes in 152 complex I deficiency cases identifies pathogenic variants in 16 genes including NDUFB9," *Journal of Medical Genetics*, vol. 49, pp. 83-89, Feb 2012.
- [180] R. Szklarczyk, B. F. J. Wanschers, S. B. Nabuurs, J. Nouws, L. G. Nijtmans, and M. A. Huynen, "NDUFB7 and NDUFA8 are located at the intermembrane surface of complex I," *Fefs Letters*, vol. 585, pp. 737-743, Mar 9 2011.
- [181] S. Loublier, A. Bayot, M. Rak, R. El-Khoury, P. Benit, and P. Rustin, "The NDUFB6 subunit of the mitochondrial respiratory chain complex I is required for electron transfer activity: A proof of principle study on stable and controlled RNA interference in human cell lines," *Biochemical and Biophysical Research Communications*, vol. 414, pp. 367-372, Oct 22 2011.
- [182] C. Ugalde, R. J. Janssen, L. P. van den Heuvel, J. A. Smeitink, and L. G. Nijtmans, "Differences in assembly or stability of complex I and other mitochondrial OXPHOS complexes in inherited complex I deficiency," *Hum Mol Genet*, vol. 13, pp. 659-67, Mar 15 2004.
- [183] D. M. Kirby, R. Salemi, C. Sugiana, A. Ohtake, L. Parry, K. M. Bell, *et al.*, "NDUFS6 mutations are a novel cause of lethal neonatal mitochondrial complex I deficiency," *J Clin Invest*, vol. 114, pp. 837-45, Sep 2004.
- [184] S. Granata, G. Zaza, S. Simone, G. Villani, D. Latorre, P. Pontrelli, *et al.*, "Mitochondrial dysregulation and oxidative stress in patients with chronic kidney disease," *Bmc Genomics*, vol. 10, Aug 21 2009.
- [185] Y. A. Su, J. Wu, L. Zhang, Q. Y. Zhang, D. M. Su, P. He, *et al.*, "Dysregulated Mitochondrial Genes and Networks with Drug Targets in Postmortem Brain of Patients with Posttraumatic Stress Disorder (PTSD) Revealed by Human Mitochondria-Focused cDNA Microarrays," *International Journal of Biological Sciences*, vol. 4, pp. 223-235, 2008.
- [186] E. J. Tucker, S. G. Hershman, C. Kohrer, C. A. Belcher-Timme, J. Patel, O. A. Goldberger, *et al.*, "Mutations in MTFMT underlie a human disorder of formylation causing impaired mitochondrial translation," *Cell Metab*, vol. 14, pp. 428-34, Sep 7 2011.

- [187] M. E. Smoot, K. Ono, J. Ruscheinski, P. L. Wang, and T. Ideker, "Cytoscape 2.8: new features for data integration and network visualization," *Bioinformatics*, vol. 27, pp. 431-2, Feb 1 2011.
- [188] D. Jaquet, J. Leger, C. Levy-Marchal, J. F. Oury, and P. Czernichow, "Ontogeny of leptin in human fetuses and newborns: effect of intrauterine growth retardation on serum leptin concentrations," *J Clin Endocrinol Metab*, vol. 83, pp. 1243-6, Apr 1998.
- [189] L. A. Tartaglia, M. Dembski, X. Weng, N. Deng, J. Culpepper, R. Devos, *et al.*, "Identification and expression cloning of a leptin receptor, OB-R," *Cell*, vol. 83, pp. 1263-71, Dec 29 1995.
- [190] R. S. Jackson, J. W. Creemers, S. Ohagi, M. L. Raffin-Sanson, L. Sanders, C. T. Montague, *et al.*, "Obesity and impaired prohormone processing associated with mutations in the human prohormone convertase 1 gene," *Nat Genet*, vol. 16, pp. 303-6, Jul 1997.
- [191] L. Yaswen, N. Diehl, M. B. Brennan, and U. Hochgeschwender, "Obesity in the mouse model of pro-opiomelanocortin deficiency responds to peripheral melanocortin," *Nat Med*, vol. 5, pp. 1066-70, Sep 1999.
- [192] W. H. Dietz, "Health consequences of obesity in youth: childhood predictors of adult disease," *Pediatrics*, vol. 101, pp. 518-25, Mar 1998.
- [193] H. Hampel, N. S. Abraham, and H. B. El-Serag, "Meta-analysis: obesity and the risk for gastroesophageal reflux disease and its complications," *Ann Intern Med*, vol. 143, pp. 199-211, Aug 2 2005.
- [194] D. L. Roberts, C. Dive, and A. G. Renahan, "Biological mechanisms linking obesity and cancer risk: new perspectives," *Annu Rev Med*, vol. 61, pp. 301-16, 2010.
- [195] E. E. Calle and M. J. Thun, "Obesity and cancer," *Oncogene*, vol. 23, pp. 6365-78, Aug 23 2004.
- [196] H. Masuya, Y. Makita, N. Kobayashi, K. Nishikata, Y. Yoshida, Y. Mochizuki, *et al.*, "The RIKEN integrated database of mammals," *Nucleic Acids Res*, vol. 39, pp. D861-70, Jan 2011.

- [197] I. E. Scheffer and S. F. Berkovic, "Generalized epilepsy with febrile seizures plus. A genetic disorder with heterogeneous clinical phenotypes," *Brain*, vol. 120 (Pt 3), pp. 479-90, Mar 1997.
- [198] R. Singh, I. E. Scheffer, K. Crossland, and S. F. Berkovic, "Generalized epilepsy with febrile seizures plus: a common childhood-onset genetic epilepsy syndrome," *Annals of Neurology*, vol. 45, pp. 75-81, Jan 1999.
- [199] L. Zinman, E. Ng, and V. Bril, "IV immunoglobulin in patients with myasthenia gravis: a randomized controlled trial," *Neurology*, vol. 68, pp. 837-41, Mar 13 2007.
- [200] M. Giraud, R. Taubert, C. Vandiedonck, X. Ke, M. Levi-Strauss, F. Pagani, *et al.*, "An IRF8-binding promoter variant and AIRE control CHRNA1 promiscuous expression in thymus," *Nature*, vol. 448, pp. 934-7, Aug 23 2007.
- [201] H. J. Garchon, F. Djabiri, J. P. Viard, P. Gajdos, and J. F. Bach, "Involvement of human muscle acetylcholine receptor alpha-subunit gene (CHRNA) in susceptibility to myasthenia gravis," *Proc Natl Acad Sci U S A*, vol. 91, pp. 4668-72, May 24 1994.
- [202] H. L. Wang, M. Milone, K. Ohno, X. M. Shen, A. Tsujino, A. P. Batocchi, *et al.*, "Acetylcholine receptor M3 domain: stereochemical and volume contributions to channel gating," *Nat Neurosci*, vol. 2, pp. 226-33, Mar 1999.
- [203] A. Masuda, X. M. Shen, M. Ito, T. Matsuura, A. G. Engel, and K. Ohno, "hnRNP H enhances skipping of a nonfunctional exon P3A in CHRNA1 and a mutation disrupting its binding causes congenital myasthenic syndrome," *Hum Mol Genet*, vol. 17, pp. 4022-35, Dec 15 2008.
- [204] O. Uchitel, A. G. Engel, T. J. Walls, A. Nagel, M. Z. Atassi, and V. Bril, "Congenital myasthenic syndromes: II. Syndrome attributed to abnormal interaction of acetylcholine with its receptor," *Muscle Nerve*, vol. 16, pp. 1293-301, Dec 1993.
- [205] K. Ohno, H. L. Wang, M. Milone, N. Bren, J. M. Brengman, S. Nakano, *et al.*, "Congenital myasthenic syndrome caused by decreased agonist binding affinity due to a mutation in the acetylcholine receptor epsilon subunit," *Neuron*, vol. 17, pp. 157-70, Jul 1996.

- [206] R. Croxen, C. Hatton, C. Shelley, M. Brydson, G. Chauplannaz, H. Oosterhuis, *et al.*, "Recessive inheritance and variable penetrance of slow-channel congenital myasthenic syndromes," *Neurology*, vol. 59, pp. 162-8, Jul 23 2002.
- [207] A. G. Engel, K. Ohno, M. Milone, H. L. Wang, S. Nakano, C. Bouzat, *et al.*, "New mutations in acetylcholine receptor subunit genes reveal heterogeneity in the slow-channel congenital myasthenic syndrome," *Hum Mol Genet*, vol. 5, pp. 1217-27, Sep 1996.
- [208] C. M. Gomez, R. Maselli, J. Gammack, J. Lasalde, S. Tamamizu, D. R. Cornblath, *et al.*, "A beta-subunit mutation in the acetylcholine receptor channel gate causes severe slow-channel syndrome," *Annals of Neurology*, vol. 39, pp. 712-23, Jun 1996.
- [209] C. M. Gomez, R. A. Maselli, B. P. Vohra, M. Navedo, J. R. Stiles, P. Charnet, *et al.*, "Novel delta subunit mutation in slow-channel syndrome causes severe weakness by novel mechanisms," *Annals of Neurology*, vol. 51, pp. 102-12, Jan 2002.
- [210] E. Hund, R. P. Linke, F. Willig, and A. Grau, "Transthyretin-associated neuropathic amyloidosis. Pathogenesis and treatment," *Neurology*, vol. 56, pp. 431-5, Feb 27 2001.
- [211] J. N. Buxbaum and N. Reixach, "Transthyretin: the servant of many masters," *Cell Mol Life Sci*, vol. 66, pp. 3095-101, Oct 2009.
- [212] M. A. Gertz and R. A. Kyle, "Myopathy in primary systemic amyloidosis," *J Neurol Neurosurg Psychiatry*, vol. 60, pp. 655-60, Jun 1996.
- [213] J. Keith, Z. Afshar-Ghotli, R. Roussev, B. Ernst, B. Young, and J. M. Bilbao, "Myopathy as the initial manifestation of primary amyloidosis," *Can J Neurol Sci*, vol. 38, pp. 161-4, Jan 2011.
- [214] Y. Friedman, J. T. Paul, J. Turley, L. N. Hazrati, and D. Munoz, "Axial myopathy due to primary amyloidosis," *Muscle Nerve*, vol. 36, pp. 542-6, Oct 2007.
- [215] D. Karacostas, M. Soumpourou, I. Mavromatis, G. Karkavelas, I. Poulios, and I. Milonas, "Isolated myopathy as the initial manifestation of primary systemic amyloidosis," *J Neurol*, vol. 252, pp. 853-4, Jul 2005.
- [216] P. Bielefeld, L. Leveque, A. Turcu, L. Popitean, E. Justrabo, and J. F. Besancenot, "[Myopathy revealing AL amyloidosis]," *Presse Med*, vol. 31, p. 361, Mar 2 2002.

- [217] N. Nadkarni, M. Freimer, and J. R. Mendell, "Amyloidosis causing a progressive myopathy," *Muscle Nerve*, vol. 18, pp. 1016-8, Sep 1995.
- [218] H. Tuomaala, M. Karppa, H. Tuominen, and A. M. Remes, "Amyloid myopathy: a diagnostic challenge," *Neurol Int*, vol. 1, p. e7, 2009.
- [219] D. Petrey, M. Fischer, and B. Honig, "Structural relationships among proteins with different global topologies and their implications for function annotation strategies," *Proceedings of the National Academy of Sciences of the United States of America*, vol. 106, pp. 17377-17382, Oct 13 2009.
- [220] H. Y. Yu, N. M. Luscombe, H. X. Lu, X. W. Zhu, Y. Xia, J. D. J. Han, *et al.*, "Annotation transfer between genomes: Protein-protein interologs and protein-DNA regulogs," *Genome Research*, vol. 14, pp. 1107-1118, Jun 2004.
- [221] D. Petrey and B. Honig, "Is protein classification necessary? Toward alternative approaches to function annotation," *Current Opinion in Structural Biology*, vol. 19, pp. 363-368, Jun 2009.
- [222] M. Osadchy and R. Kolodny, "Maps of protein structure space reveal a fundamental relationship between protein structure and function," *Proc Natl Acad Sci U S A*, vol. 108, pp. 12301-6, Jul 26 2011.
- [223] M. A. Yildirim, K. I. Goh, M. E. Cusick, A. L. Barabasi, and M. Vidal, "Drug-target network," *Nat Biotechnol*, vol. 25, pp. 1119-26, Oct 2007.
- [224] T. U. Consortium, "The Universal Protein Resource (UniProt) in 2010," *Nucleic Acids Res*, vol. 38, pp. D142-8, Jan 2010.